UNIVERSITY OF SOUTHAMPTON

NATURAL AND ENVIRONMENTAL SCIENCES

Ocean and Earth Sciences

Expanding the radioanalysts toolbox: using the latest generation plasma mass spectrometers for nuclear waste characterisation

by

Benjamin Colin Russell

Thesis for the degree of Doctor of Philosophy

June_2014

UNIVERSITY OF SOUTHAMPTON

ABSTRACT

NATURAL AND ENVIRONMENTAL SCIENCES

Ocean and Earth Sciences

Thesis for the degree of Doctor of Philosophy

EXPANDING THE RADIOANALYSTS TOOLBOX: USING THE LATEST GENERATION PLASMA MASS SPECTROMETERS FOR NUCLEAR WASTE CHARACTERISATION

Benjamin Colin Russell

This project investigates the application of sector field inductively coupled mass spectrometry (ICP-SFMS) in low-level radionuclide detection in environmental samples and low-level nuclear waste. The aim was to develop robust and sensitive procedures for measuring medium-long lived emitters of interest to various Nuclear Decommissioning Authority (NDA) sites. ICP-SFMS has been investigated for the measurement of the significant fission product radionuclides of caesium (^{135}Cs and ^{137}Cs) and strontium (^{90}Sr). In the case of some shorter-lived radionuclides such as ^{90}Sr, ICP-SFMS can achieve sensitivities that rival existing radiometric techniques, whilst offering a significant improvement in the speed of analysis. Additionally, long-lived low abundance radionuclides such as ^{135}Cs are not detectable using radiometric techniques, but can be quantified by ICP-SFMS, which is important given their major contribution to the long-term radiological risk associated with deep geological disposal. Measurement of ^{135}Cs also enables measurement of the ^{135}Cs/^{137}Cs ratio, which varies with the source of nuclear contamination, and therefore can provide a powerful forensic tool compared to radiometric ^{137}Cs detection alone.

ICP-SFMS has been proven to achieve high sensitivities that will enable low-level radionuclide detection. In order to reach these sensitivities, it is critical to ensure removal of interfering elements that otherwise significantly impact the accuracy of measured values. This led to the development of novel and efficient chemical separation procedures that achieve both a high analyte recovery, and effective decontamination of interferences, which have been proven to be effective for a range of sample matrices including seawater and sediments. The combination of imaginative sample preparation procedures and use of new generation ICP-SFMS offer a streamlining of the process that will contribute to faster more sensitive assessment and clean-up of nuclear sites. This will lead to a reduction in analytical timescales and reduce the demand on existing analytical facilities, benefitting site operators and the NDA.

Table of Contents

List of tables

List of figures

DECLARATION OF AUTHORSHIP

I, Benjamin C. Russell..... [please print name]

declare that this thesis and the work presented in it are my own and has been generated by me as the result of my own original research.

[title of thesis] .....

.....

I confirm that:

1. This work was done wholly or mainly while in candidature for a research degree at this University;
2. Where any part of this thesis has previously been submitted for a degree or any other qualification at this University or any other institution, this has been clearly stated;
3. Where I have consulted the published work of others, this is always clearly attributed;
4. Where I have quoted from the work of others, the source is always given. With the exception of such quotations, this thesis is entirely my own work;
5. I have acknowledged all main sources of help;
6. Where the thesis is based on work done by myself jointly with others, I have made clear exactly what was done by others and what I have contributed myself;
7. [Delete as appropriate] None of this work has been published before submission [or] Parts of this work have been published as: [please list references below]:

Signed:.....

Date:.....

Acknowledgements

First of all, thank you to GAU Radioanalytical and the Nuclear Decommissioning Authority for funding this project.

I would like to thank my academic supervisors. Ian Croudace and Phil Warwick were terrific in answering the multitude of questions I threw at them about anything related to PhD life. They were always approachable, friendly, patient, and willing to take as much time as was necessary to make sure I was happy and fully understood whatever query I was presenting them with. Thanks also to Rex Taylor, who was very helpful with any instrument-based issues, and in helping to establish the clean laboratory side of the research. I would also like to thank my industrial supervisor Martin Dutton, in particular for his work that allowed me to attend industrial conferences and events.

Thank you to Andy Milton for all his assistance in the instrument lab. He was willing to take as much time as was necessary to show me how to use the instrumentation for myself, which I am very grateful for. I would also like to thank Matt Cooper and Agnus Michaelik for their assistance (often at no notice) in both the instrument and clean laboratories. Thank you also to everyone at GAU, in particular Pawel Gaca for help in learning about a range of radiochemical techniques. Finally, I would like to thank Mike Zubkov and Polly Hill for their help in the build up to and during the JR271 Research Cruise, which was an extraordinary opportunity.

List of Abbreviations

ACM	Actively Cooled Membrane
AMP	Ammonium molybdophosphate
AMS	Accelerator mass spectrometry
ASG	Ammonium molybdophosphate loaded on silica gel
BCB	1,3-calix[4]bis-*o*-benzo-crown-6
BOBCalixC6	Calix[4]arene-bis-(tert-octylbenzo-crown-6)
CC	Collision cell
CE	Capillary electrophoresis
CTD	Conductivity temperature density
GD	Glow discharge
DFR	Dounreay Fast Reactor
DRC	Dynamic reaction cell
EPMA	Electron probe micro analysis
ESA	Electrostatic analyser
ETV	Electrothermal vaporisation
FCC	Face centered cubic
GM	Geiger Muller
HEPA	High-efficiency particulate air
HETP	Height equivalent to a theoretical plate
HLW	High level waste
HpGe	High purity germanium

ICP-MS	Inductively coupled plasma mass spectrometry
ICP-SFMS	Inductively coupled plasma sector field mass spectrometry
ICP-QMS	Inductively coupled plasma quadrupole mass spectrometry
KCoFC	Potassium cobalt hexacyannoferrate
KNiFC	Potassium nickel hexacyannoferrate
KSCN	Potassium thiocyanate
LSC	Liquid scintillation counting
MAC	Medium active concentrate
MC-ICP-MS	Multi-collector inductively coupled plasma mass spectrometry
MODB	Methyloctyl-2-di-methyl-butanemide
MTR	Materials Test Reactor
NAA	Neutron activation analysis
NDA	Nuclear Decommissioning Authority
NMR	Nuclear magnetic resonance
NPP	Nuclear Power Plant
PAN	Polyacrylonitrile
PFA	Perfluoroalkoxy alkane
PTFE	Polytetrafluoroethylene
RF	Radio frequency
RIMS	Resonance ionisation mass spectrometry
RPQ	Retarding potential quadrupole lens filter
SEM	Secondary electron multiplier (ICP-MS detector)
	Scanning electron microscope (examination of surface morphology)

SIXEP	Sellafield Ion Exchange Effluent Plant
TIMS	Thermal ionisation mass spectrometry
XRD	X-ray diffraction
WD-XRF	Wavelength dispersive X-ray fluorescence

Introduction

i. Rationale

Decommissioning samples at nuclear sites are varied and require efficient and effective methods to prepare them for analysis. Some existing conventional methods are slow, laborious and require multistage sample dissolution and chemical purification stages to isolate the key radionuclides. The combination of imaginative sample preparation procedures and use of new generation sector field inductively coupled plasma mass spectrometers (ICP-SFMS) offer a streamlining of the process that will contribute to faster more sensitive assessment and clean-up of nuclear sites. Such procedures contribute to the analytical armoury to facilitate effective waste characterisation.

The aim of this research is to develop robust and sensitive procedures (incorporating sample digestion, separation and measurement using ICP-SFMS) for measuring medium-long lived emitters of interest to various Nuclear Decommissioning Authority (NDA) sites in connection with waste characterisation and environmental monitoring. The research will contribute to an increased sample throughput and more rapid characterisation of radionuclides in land remediation and waste sentencing. This will lead to a reduction in analytical timescales and reduce the demand on existing analytical facilities, benefitting site operators and the NDA.

ii. Measurement of radionuclides

Radionuclides are measurable using both radiometric and mass spectrometric techniques. The former measures the product of nuclear rearrangement, where as mass spectrometry measures the concentration of the radionuclide itself. Since nuclear arrangement occurs in a predictable way, it is possible to interrelate the two methods (Lariviere et al. 2006). Radioactive decay occurs at a constant decay rate ‘A’, specific for each radioisotope Equation 1:

$$A=N\lambda \qquad (1)$$

Where N is the number of radioactive atoms, and λ is the decay constant, or fraction of atoms undergoing rearrangement per unit time (t^{-1}), or fraction of atoms undergoing rearrangement per unit time. If λ is known for a radioisotope, the activity and number of atoms can be linked. The number of radioactive atoms (N) is proportional to the mass of the analyte (m) with respect to molar mass (MM) and Avogadro's number (N_A) (Equation 2):

$$N = \frac{N_A \times m}{MM} \qquad (2)$$

Substituting Equation 1 into Equation 2 gives:

$$m = \frac{A \times MM}{N_A \times \lambda} \qquad (3)$$

Given that half life ($t_{1/2}$) is a more common way of expressing nuclear arrangement than the decay constant, Equation 3 can be rearranged given that $\lambda = (\ln 2)/ t_{1/2}$:

$$m = \frac{A \times MM \times t_{1/2}}{Ln2 \times N_A} \qquad (4)$$

If half-life is expressed in seconds, activity in Becquerels (Bq), and molar mass in g/mol, then the analyte mass is represented in grams. Mass can also be expressed as a concentration e.g. g/g if activity is expressed as a concentration e.g. Bq/g. (Lariviere et al. 2006). Equation 4 shows that for an equivalent activity, the number of radioactive atoms in a sample is proportional to analyte molar mass and half-life (Lariviere et al. 2006). Traditionally, mass spectrometry has focused on detection of long-lived, low

activity radionuclides, as the detection limits for shorter-lived radionuclides are typically several orders of magnitude higher than is achievable by radiometric techniques. This project investigates the capabilities of the latest generation ICP-SFMS, and its implications for low-level measurement of medium and long-lived radionuclides.

iii. Instrumentation

The capabilities of ICP-SFMS for low level radionuclide detection are investigated using a Thermo Element XR (Figure 1). Double focusing of the ion beam is achieved by initially focusing ions according to their mass to charge ratio through a sector magnetic field, followed by energy focusing in an Electro-Static Analyser (ESA). A single Faraday detector and dual mode Secondary Electron Multiplier (SEM) make up the detection system, with a linear dynamic range of 12 orders of magnitude. The Element XR is capable of changing between three fixed resolution, with an increase in resolution focusing the ion beam over a narrower mass range, which can achieve a reduction or elimination of spectral interferences (Thermo Scientific, 2008). The instrumental setup is highly flexible, and has a significant impact on the sensitivity and extent of interference separation achievable.

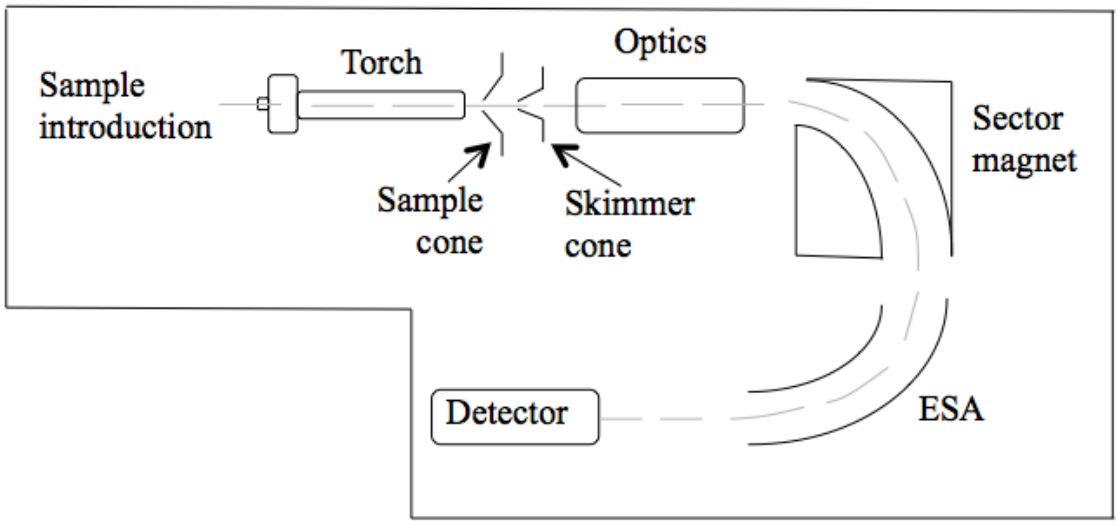

Figure 1. Schematic of the Thermo Element XR ICP-SFMS

iv. Thesis Outline

This project is divided into two sections. The first five chapters focus on the detection of long-lived low abundance radionuclides, specifically caesium-135, a high yield fission product with a half-life of 2.5 million years. Detection of this radionuclide is difficult using radiometric techniques, however measurement is important given its significant contribution to the long-term nuclear waste repository. In addition, accurate detection enables measurement of the $^{135}Cs/^{137}Cs$ ratio, which varies depending on the source of nuclear contamination, and therefore has the potential to be a powerful forensic tool.

Chapter 1 reviews previous measurements of ^{135}Cs and ^{137}Cs, and identifies isobaric barium interferences (^{135}Ba and ^{137}Ba) and peak tailing of stable ^{133}Cs as critical factors impacting detection of these radionuclides. *Chapter 2* describes the development of a method for low-level detection of $^{135}Cs/^{137}Cs$, with a procedure incorporating digestion, chemical separation and quantification by ICP-SFMS. The advances in instrumental performance demonstrated enable detection of radionuclides at extremely low levels. It is also shown that, at these concentrations, the extent of Ba decontamination has a significant impact on the sensitivities achievable. The removal of Ba prior to quantification is investigated further in *Chapter 3*, with the development of a novel calixarene extraction chromatography procedure. The material developed shows a high Cs selectivity and effective Ba decontamination, whilst the straightforward extraction and elution of Cs is well suited towards ICP-SFMS procedures.

The methodology developed was investigated further for two applications that demonstrate the impact of interfering elements on ICP-SFMS procedures. Firstly, *Chapter 4* presents a modification of the chemical separation procedure to successfully extract Cs from high volume seawater samples in the North Atlantic and Arctic Oceans. This environment has been contaminated by multiple sources of anthropogenic nuclear activity, including atmospheric fallout from nuclear weapons testing and the Chernobyl incident, and is therefore a suitable application for investigating the variation in $^{135}Cs/^{137}Cs$ values. Whilst the instrumental sensitivity was sufficient to enable detection of these samples, the concentration of Ba inherently present in the reagents and the general laboratory environment exceeded the $^{135}Cs/^{137}Cs$ concentration in the final

sample. As a result the detection limit of the method was not able to match the instrument capabilities.

A salt marsh in close proximity to the Sellafield fuel reprocessing facility, UK, is investigated in *Chapter 5*. The vertical sediment core collected shows a good chronological record of aqueous discharges from the Sellafield site since operations began in the early 1950's, whilst the known discharge history and site activity represented a good application for measurement of $^{135}Cs/^{137}Cs$. Chemical separation effectively removed Ba from the sediment, however the high concentration of stable ^{133}Cs led to a tailing effect that impacted the measurement of ^{135}Cs. The ability to remove this tail is a function of the instrument used, and measurement of $^{135}Cs/^{137}Cs$ in sediment samples requires either mathematical correction of the tailing effect, or quantification using an instrument with an improved ability to remove tailing effects.

The final two chapters of this project investigate the ability of ICP-SFMS to compete with existing radiometric techniques in the detection of medium-lived radionuclides. Specifically, strontium-90 (half life 30 years) is a major component of spent nuclear fuel and nuclear waste, and is therefore of significant interest with regards to waste management and environmental protection. Highly sensitive measurement of ^{90}Sr using radiometric techniques often requires a long total procedural time. Although ICP-MS is a more rapid technique, this has traditionally been at the expense of analyte sensitivity. *Chapter 6* reviews ICP-MS procedures and the sensitivities achievable compared to radiometric techniques, with accurate detection dependent on separation of ^{90}Sr from an isobaric zirconium interference (^{90}Zr), tailing from stable ^{88}Sr, and multiple polyatomic interferences formed by reactions of elements with gases in the plasma. The capability of the Element XR for detection of ^{90}Sr is investigated in *Chapter 7*, which demonstrates the versatility ICP-MS with regards to the instrumental setup, and the impact this has on the sensitivity achievable and extent of interference separation. An optimal instrumental procedure is developed that can be taken forward for low-level detection of ^{90}Sr in environmental samples.

Chapter 1: Determination of ^{135}Cs and ^{137}Cs in Environmental Samples: A Review

Abstract

High yield fission products ^{135}Cs and ^{137}Cs have entered the environment as a result of anthropogenic nuclear activities. Whilst ^{137}Cs is routinely measurable by gamma spectrometry, long-lived ^{135}Cs detection by radiometric methods is challenging; however measurement is important given its significance in long-term nuclear waste storage and disposal. Furthermore, the ^{135}Cs/ ^{137}Cs ratio varies with reactor, weapon and fuel type, and accurate measurement of this ratio can be used as a forensic tool to identify the source of nuclear contamination.

Detection of ^{135}Cs and ^{137}Cs is achievable by mass spectrometric techniques, in particular inductively coupled plasma mass spectrometry (ICP-MS). The critical issue is effective removal of barium to eliminate isobaric interferences arising from ^{135}Ba and ^{137}Ba. The extent of Ba decontamination can significantly impact the accuracy of ^{135}Cs/^{137}Cs values and detection limits achievable, particularly in the case of low-level environmental samples. This report summarises and compares the analytical procedures developed for determination of ^{135}Cs/^{137}Cs, with particular focus on ICP-MS and the methods applied to separation of Cs from Ba.

1.1 Introduction

High yield fission products ^{135}Cs and ^{137}Cs (Table 1.1) are present in environmental samples due to releases from nuclear power plants and reprocessing sites, nuclear accidents, and fallout from atmospheric weapons testing (Chao and Tseng, 1996). Whilst ^{137}Cs is established as an important radionuclide in radiation protection, environmental monitoring and waste disposal (Moreno et al. 1999), ^{135}Cs is a long-lived radioisotope with a comparatively low radiation risk, however is a significant contributor to the long term radiological risk associated with deep geological disposal. Furthermore, the ^{135}Cs/^{137}Cs ratio varies with reactor, weapon and fuel type, and therefore can be used as a forensic tool to identify the source of radioactive contamination (Lee et al. 1993; Chao and Tseng, 1996; Taylor et al. 2008; Russell et al. 2014 (A)).

Radioisotope	Half life (years)	^{235}U fission yield (%)	Specific activity (Bq/g)
^{135}Cs	2.3×10^{6}	6.58	4.09×10^{7}
^{137}Cs	30.2	6.22	3.20×10^{12}

Table 1.1. Properties of ^{135}Cs and ^{137}Cs

Caesium-137 decays by beta emission to short-lived metastable isomer ^{137m}Ba, with maximum energies of 514 keV (94.4 %) and 1175 keV (5.4 %). This is immediately accompanied by gamma ray emission of 661.7 keV (85.1 %) to return ^{137m}Ba to the ground state (Moreno et al. 1999). Detection is therefore achievable using beta counting or gamma spectrometry. The latter is favoured because of the high abundance gamma ray, little self-absorption as a result of high decay energy, minimal contamination in sample preparation, and direct, highly sensitive sample measurement. A HPGe well detector can readily achieve a detection limit of ~50 mBq (for a 20g sample counted for half a day), which is suitable for many environmental samples (Hou and Roos, 2008). Caesium-135 decays with a maximum beta particle energy of 269keV, and gamma ray

emission at a maximum energy of 268.2 keV (15.5 %). Measurement by beta counting is restricted by any ^{137}Cs also present in the sample with a radioactivity concentration that is typically 5 orders of magnitude higher. Furthermore, the low specific activity of ^{135}Cs (43 mBq/ng) and low counting efficiency of gamma spectrometry makes radiometric measurement of ^{135}Cs challenging (Hou and Roos, 2008).

Measurement of ^{135}Cs by mass spectrometry offers a considerable advantage because of the larger atom population compared with radioactive decays (its long half-life leading to a low specific activity). Resonance ionisation mass spectrometry (RIMS) (Karam et al. 2002, Pibida et al. 2004), thermal ionisation mass spectrometry (TIMS) (Lee et al. 1993; Delmore et al. 2011; Snyder et al. 2012), and most frequently ICP-MS (Table 1.2) (Alonso et al. 1995; Meeks et al. 1998; Moreno et al. 1999; Song et al. 2001; Granet et al. 2008; Taylor et al. 2008; Liezers et al. 2009; Russell et al. 2014 (A); Ohno and Muramatsu, 2014; Zheng et al. 2014) have been applied to ^{135}Cs/^{137}Cs measurement. Radionuclide measurement by ICP-MS has traditionally focused on the longer-lived, low activity nuclides, as the technique was unable to match the sensitivities achievable by radiometric methods for shorter-lived radionuclides such as ^{90}Sr and ^{137}Cs (Lariviere et al. 2006; Hou and Roos, 2008; Vajda and Kim 2010). Recently developed instruments now provide improved sensitivity and offer the prospect of measuring both shorter and longer-lived radionuclides, enabling quantification at ultra-low concentrations (Figure 1.1). Such improvements expand the options available for environmental, contaminated land and nuclear waste assessments and even nuclear forensics. The primary challenge for mass spectrometric measurement is removal of isobaric interferences from naturally occurring ^{135}Ba and ^{137}Ba (isotopic abundances 6.6% and 11.2%, respectively).

1.1.1 Environmental sources of ^{135}Cs and ^{137}Cs

The most significant source of radiocaesium is regular releases from operations at nuclear power plants and fuel reprocessing sites. For example, at the Sellafield reprocessing facility, Cumbria, UK, atmospheric and marine discharges of ^{137}Cs peaked from 1974-1978, with aqueous discharges exceeding 4000 TBq/yr, compared to 4 TBq in 2012 (Figure 1.2) (Gray et al. 1995; SEPA, 2012). Peak values were attributed to corrosion of Magnox fuel elements in the storage ponds, which were brought under control initially through the use of zeolite absorbers in the ponds, and then from 1985

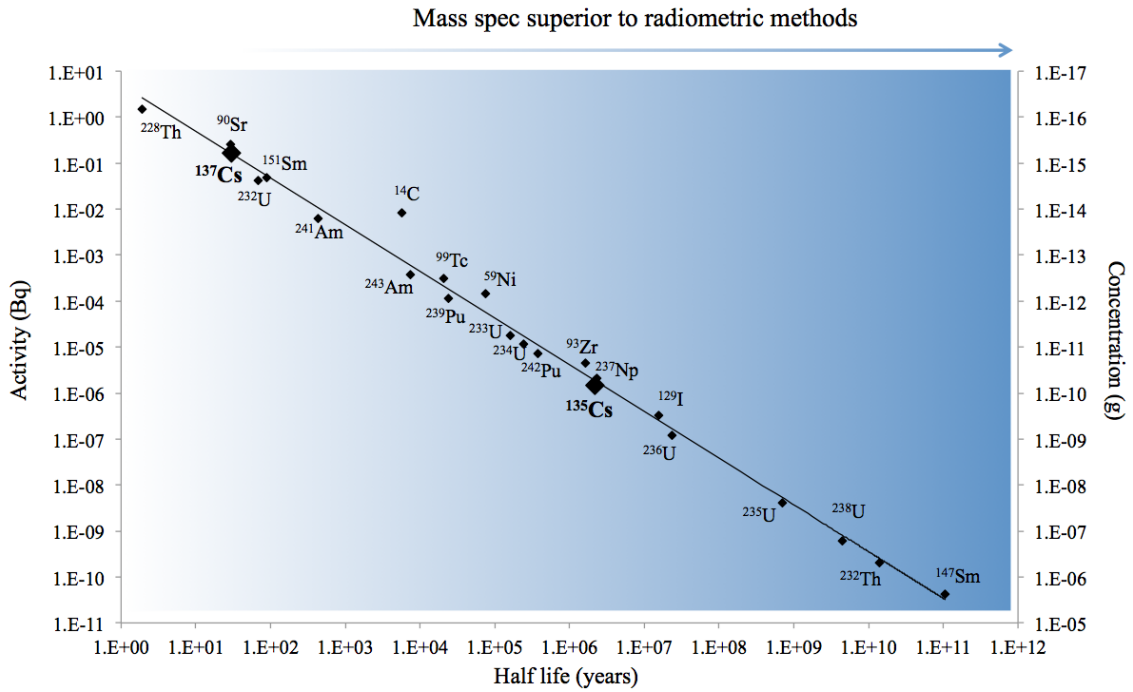

Figure 1.1. Half-life versus minimum detectable activity and concentration of selected radionuclides. Highlighted radionuclides (diamonds) reflect those that potentially benefit from advances in ICP-MS sensitivity. Activity and concentration values correspond to detection limits of 0.05 Bq/kg and 5 pg/kg, respectively

when the operation of the site ion-exchange effluent plant (SIXEP) began (Hunt et al. 2013). A second reprocessing facility responsible for marine discharges around the UK is La Hague, France, with a peak annual ^{137}Cs discharge of 243 TBq in 1971, compared to 2 TBq in 1996 (Warneke, 2002). Additionally, milling, cropping and reprocessing operations at the Dounreay Fast Reactor (DFR) and Materials Test Reactor (MTR) sites on the North coast of Scotland led to the production of sand-sized (up to several mm diameter) 'hot particles' that predominantly consisted of ^{137}Cs and ^{90}Sr (Dennis et al. 2007). Whilst the majority of waste produced was dealt with at licensed disposal and storage facilities on site, some particles were accidentally released into the sites low level liquid effluent system and into the marine environment. The number of hot particles in sediments around Dounreay has been estimated at up to 50,000, with activities of 1.4-5.5 MBq measured (Dennis et al. 2007; Charles and Harrison, 2007).

Table 1.2. A summary of analytical methods for measurement of ^{135}Cs and ^{137}Cs

Ref	Sample	Chemical separation	Measurement	Recovery	LOD ^{137}Cs
Lee (1993)	Coastal sediment	Cation exchange: AG50Wx8	TIMS	>90 %	
Alonso (1995)	Spent nuclear fuel pellets, solutions	Cation exchange: CG3+CS3	ICP-QMS	-	
Chao (1996)	Radioactive waste	AMP Cation exchange: Amberlite 200	NAA	-	
Meeks (1998)	Waste tank sludges and supernates	$Ba(OH)_2$ precipitation using ammonium hydroxide	ICP-QMS	-	209 ng/L
Moreno (1999)	High activity waste, spent fuel	On-line cation exchange comparing multiple resins	ICP-QMS	-	16 ng/L
Song (2001)	^{137}Cs standard	ETV sample introduction	ETV-ICP-MS	96-99 %	0.2 ng/L
Karam (2002)	Freshwater lake sediment	AMP	RIMS, TIMS	70 %	
Pibida (2004)	Nuclear fuel burn up samples	Extraction chromatography with Eichrom TRU resin; AMP	RIMS, TIMS	82 %	0.2 ng/L

Ref	Sample	Chemical separation	Measurement	Recovery	LOD ^{137}Cs
Granet (2008)	Spent fuel pellets	Anion exchange: AG50Wx4; HPLC with interchim uptisphere SCX	DRC-MC-ICP-MS	-	
Taylor (2008)	Soil and sediment	AMP; Anion exchange: AG-MP; On-line cation exchange: CS12A	DRC-ICP-QMS	-	0.2 ng/L
Pitois (2008)	Simulated spent fuel	Capillary electrophoresis sample introduction	CE-ICP-QMS CE-ICP-SFMS	-	6000 ng/L 4 ng/L (^{133}Cs)
Isnard (2009)	Spent fuel	Anion exchange: AG1x4 HPLC with interchim uptisphere SCX	TIMS, MC-ICP-MS	-	
Liezers (2009)	Spiked groundwater	On-line cation exchange with CG3	ICP-QMS	-	0.9 pg/L
Delmore (2011)	Reactor effluents	AMP-PAN; Anion exchange: AG1x8 Cation exchange: AG50Wx8	TIMS	-	
Ohno (2014)	Rainwater	-	ICP-QQQ-MS		0.27 ng/L

Ref	Sample	Chemical separation	Measurement	Recovery	LOD ^{137}Cs
Zheng (2014)	Environmental samples	AMP Anion exchange: AGMP-1M Cation exchange: AG50Wx8	ICP-QQQ-MS		
Russell (2014(A))	^{137}Cs standard	AMP Cation exchange: AG50Wx8 Extraction chromatography (Sr-resin)	ICP-SFMS	>85%	0.05 ng/L

Weapons test facilities are a further source of ^{137}Cs contamination (Table 1.3). The majority of aboveground testing occurred in the Northern hemisphere between the late 1940's and early 1960's. Depending on the size and power of the explosion, radioactive debris is partitioned into the troposphere and stratosphere, with fallout primarily detected in the hemisphere of origin (Warneke et al. 2002). Environmental radiocaesium contamination has also been produced following nuclear accidents, in particular at the Chernobyl nuclear power plant (NPP) in 1986, and at the Fukushima Daiichi NPP in 2011. An estimated 42.5 TBq of ^{137}Cs was released into the environment following the Chernobyl accident (UNSCEAR, 2000), with initial deposition in Scandinavia, Belgium, the Netherlands and Great Britain, extending to southern and central Europe (Warneke et al. 2002). More recently, the accident at Fukushima following a magnitude 9 earthquake and resulting tsunami led to estimated atmospheric $^{134+137}Cs$ releases ranging from 10-13 PBq (Buessleler et al. 2011; Bailly Du Bois et al. 2012). In addition, Fukushima represented the largest known release of radioactivity into the sea (Bailly Du Bois et al. 2012), with a total estimated ^{137}Cs activity of 12-41 PBq by mid-July 2011 (Stohl et al. 2012).

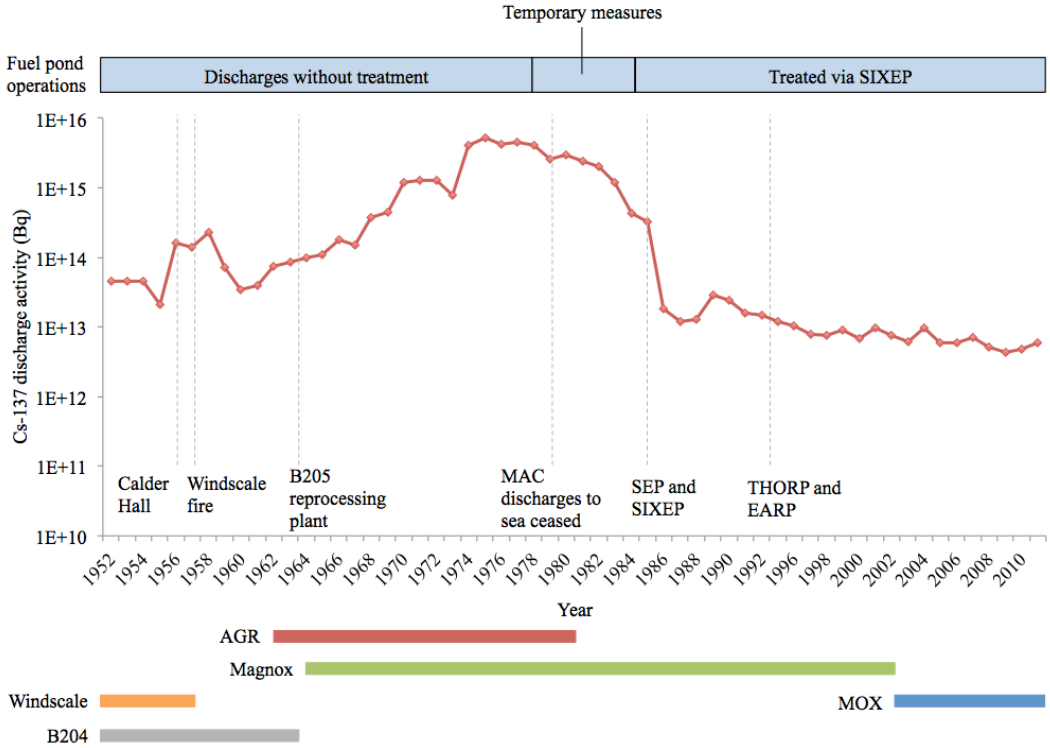

Figure 1.2. Annual aqueous ^{137}Cs discharges from the Sellafield reprocessing site, and major changes in site operations. Discharge data from Gray et al. (1995) and RIFE reports (SEPA, 2012)

Source	Number of tests, location	^{137}Cs inventory (TBq)
Northern hemisphere	350, atmospheric	9.0×10^{5}
Nevada Test Site	828, underground	7.4×10^{4}
French Polynesia	50 atmospheric, 160 underground	1.1×10^{4}

Table 1.3. Caesium-137 inventory at nuclear weapon test sites (Hu et al. 2010)

1.1.2 Environmental concentration of ^{135}Cs and ^{137}Cs

The ^{137}Cs activity in beach sediments along the Cumbrian coast range from 39-450 Bq/kg, with typical values of 1-35 Bq/kg in sands and muds on the coast of Northern Ireland (SEPA, 2012). Marine plants and animals around Sellafield are monitored as

part of the Food Standards Agency national monitoring program (Table 1.4), as these represent the primary route for ^{137}Cs uptake into the food chain.

Sample type	^{137}Cs activity concentration (Bq/kg)
Cod	0.61
Skates/rays	2.00
Lobsters	0.15
Scallops	0.29
Milk	<0.20
Mushrooms	0.26*
Onions	0.05*
Grass	2.7^{+}
Soil	65^{+}
Rabbit	1.4*
Sheep muscle	0.91*$^{+}$

Table 1.4. Environmental concentrations of ^{137}Cs in animals and plants near the Sellafield reprocessing site, measured in 2011. *Total ^{134}Cs+^{137}Cs. $^{+}$Maximum activity detected from Radioactivity in Food and the Environment (RIFE) report 17 (2012). (SEPA, 2012)

In England and Wales, the average activities in rainwater are on the order of ~1x10^{-5} Bq/m^3, with values of 1x10^{-6} Bq/m^3 in rivers and lakes (SEPA, 2012). In 2011, the ^{137}Cs activity in the Irish Sea was generally <3x10^{-5} Bq/m^3, with slightly elevated values in the Eastern Irish Sea (~1.2x10^{-4} Bq/m^3) closer to the Sellafield site (SEPA, 2012). In the seas surrounding Japan, values decreased from a few tens of Bq/m^3 in the early 1960's (as a result of atmospheric weapons test fallout) to 1-4 Bq/m^3 in 2010, due to a combination of ocean mixing and ^{137}Cs decay (Buesseler et al. 2011, Bailly Du Bois et al. 2012). Following the Fukushima accident, Buesseler et al. (2011) recorded peak

^{137}Cs activities of ~4x10^{7} Bq/m^{3} in discharge channels north and south of the Daiichi NPP at the end of March 2011, dropping to ~25,000 Bq/m^{3} by the end of July 2011. Caesium-137 has been detected in marine biota, however dose calculations suggest minimal impact to biota or humans as a result of direct exposure in ocean waters, with doses dominated by naturally occurring radionuclides ^{210}Po and ^{40}K.

Typical surface water values in oceans in the Southern hemisphere are <1 Bq/m^{3} because of lower input from atmospheric weapons testing, compared to ~3-5 Bq/m^{3} in oceans in the Northern hemisphere (Aarkrog, 1994; Kershaw and Baxter, 1995). Additional inputs of ^{137}Cs detected in the Northern hemisphere include reprocessing facilities, fallout from the Chernobyl accident and disposals of solid and liquid wastes into rivers that drain into the Arctic Ocean (Table 1.5) (Aarkrog, 1994; Dahlgaard, 1995; Kershaw and Baxter, 1995; Nies et al. 1999; Heldal and Varskog, 2002; Hu et al. 2010).

1.1.3 Environmental behaviour of ^{135}Cs and ^{137}Cs

Direct discharges from Sellafield are transported northwards out of the Irish Sea, before entering the North Sea, with further northward transport through the Norwegian Sea to the Arctic Ocean and Greenland Sea (Jefferies et al. 1973; Kershaw et al. 1995). The transit time for ^{137}Cs between discharge from Sellafield and detection in the Greenland Sea is approximately 10 years, with higher activities measured along the East coast of Greenland representing a signature of older and higher aqueous discharges (Chapter 4, page 61-79) (Aarkrog, 1994; Kershaw and Baxter, 1995; Dahlgaard, 1995; Dahlgaard et al. 2005).

The ^{137}Cs activity concentration in the seas around Japan reduced by a factor of ~10,000 within several months of the Fukushima accident, due to rapid horizontal and vertical mixing (Buesseler et al. 2011). A significant part of ^{137}Cs is expected to bind to suspended particles, leading to contamination by deposition on the seafloor. In the short time since the Fukushima accident, activity has not been able to penetrate to greater depths, however over a longer period this is expected be a significant source of contamination (Buesseler et al. 2011).

Source	^{137}Cs (PBq)
Global fallout	4
Runoff of global fallout	1
Sellafield discharges	10-15
USSR river discharges	1-5
Chernobyl	1-5
Total	**17-30**

Table 1.5. Estimate of ^{137}Cs in the Arctic Ocean from multiple sources (Aarkgrog, 1994)

In soils, ^{137}Cs is generally immobilised at the surface, with an approximately exponential decline in activity concentration with depth (Livens and Loveland, 1988). Retention is particularly strong in clay-rich samples, as layer-type silicate minerals bind Cs by either electrostatic interactions, or stronger bonds through partial sharing of electrons between Cs^{+} and ligand sites of the clay mineral (Bostick et al. 2002). Outer sphere complexes are formed by electrostatic interactions of hydrated Cs with anionic surfaces in the interlayer or basal plane, and also dissociated edge hydroxyl groups. Inner sphere complexes are formed by electronic bonding within the interlayer, at external basal sites or frayed edge sites (Bostick et al. 2002). Strong surface retention means ^{137}Cs can be used as a tracer to investigate soil migration, with multiple factors affecting Cs mobility (Table 1.6) (Livens and Loveland, 1988). This strong binding at the surface means Cs redistribution into the environment is likely to be the result of physical processes associated with erosion, transport and deposition (Owens et al. 1996). Remobilisation of Sellafield-contaminated sediments on the Irish Sea bed has occurred in response to the reduction in aqueous discharges from the site, and has been acting as a source of ^{137}Cs since the 1980's (Gray, 1995). An estimated 300 TBq ^{137}Cs was remobilised in the tidal area around Sellafield from 1989-2009, and in 2012 was

responsible for an activity of ~6 TBq, effectively doubling the input from direct aqueous discharges (Hunt, 2013).

Reduced mobility	Increased mobility
Micaceous minerals	Vermiculite, montmorillonite and kaolin minerals
Free carbonates	High ammonium content
pH 4-7	pH >9
Low organic matter	High organic matter
	Low potassium

Table 1.6. Summary of factors affecting Cs mobility in soils (Livens and Loveland, 1988)

1.1.4 Variation in $^{135}Cs/^{137}Cs$

The average fission yield $^{135}Cs/^{137}Cs$ value is 1.01 at the time of production (Ketterer and Szechenyi, 2008), with variation in isotope ratios originating from ^{135}Xe and ^{137}Xe fission products in the ^{135}Cs and ^{137}Cs decay chains (Equations 1.1 and 1.2). Xenon-135 is a potent neutron poison (neutron capture cross section $2x10^6$ barns) that can transmute to ^{136}Xe, reducing the production of ^{135}Cs, whereas there is no such competing reaction for ^{137}Xe affecting the ^{137}Cs yield (Hou and Roos, 2008; Taylor et al. 2008). The time of neutron irradiation therefore has a significant impact on the $^{135}Cs/^{137}Cs$ ratio (Figure 1.3).

$$^{135}Te \xrightarrow[19.2s]{(\beta,\gamma)} {}^{135}I \xrightarrow[6.61h]{(\beta,\gamma)} {}^{135}Xe \xrightarrow{(\beta,\gamma)\ 9.1h} {}^{135}Cs \xrightarrow[2.3x10^6a]{(\beta)} {}^{135}Ba_{(stable)} \qquad (1.1)$$

$$^{135}Xe \xrightarrow{Neutron\ capture} {}^{136}Xe$$

$$^{137}Te \xrightarrow[4s]{(\beta,\gamma)} {}^{137}I \xrightarrow[24.5s]{(\beta,\gamma)} {}^{137}Xe \xrightarrow[3.82m]{(\beta,\gamma)} {}^{137}Cs \xrightarrow[30.2a]{(\beta)} {}^{137}Ba_{(stable)} \qquad (1.2)$$

The average $^{135}Cs/^{137}Cs$ value for global weapons fallout is 2.25 (Lee et al. 1993; Karam et al. 2002, Snyder et al. 2012) due to little ^{135}Xe at the time of high neutron flux (Betti, 1997). By comparison, in a nuclear reactor, more depleted values are expected because of long-term exposure to a high neutron flux, and ^{136}Xe produced by neutron capture by ^{135}Xe will compete with ^{135}Cs production (Betti, 1997; Taylor et al. 2008). Isotope ratios range from 0.41-1.56 for reactor effluent and waste, with an average value of 0.99 (Chao and Tseng, 1996; Taylor et al. 2008; Delmore et al. 2011). This is a greater variation than for any other source, which may be the result of changes in operating conditions and fuel type over a reactors lifetime (Taylor et al. 2008). Depleted $^{135}Cs/^{137}Cs$ values measured in samples near the Chernobyl site reflect a high neutron

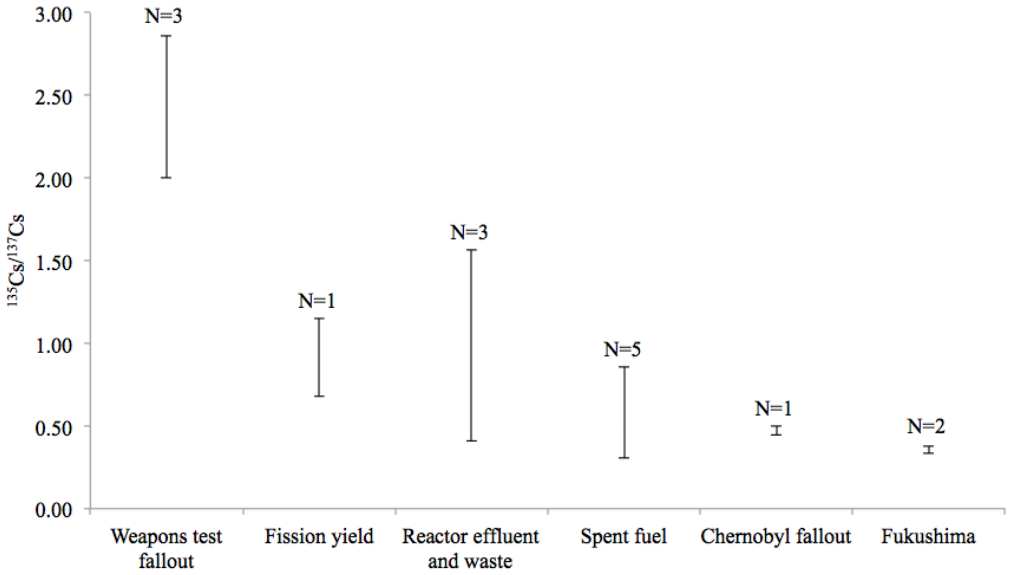

Figure 1.3. Summary of $^{135}Cs/^{137}Cs$ atom ratios for a range of sources measured by mass spectrometry. Weapons fallout values have not been decay corrected

flux at the time of production, with a corrected value at the time of the accident in 1986 of 0.28-0.32 (Taylor et al. 2008). Depleted ratios were also measured in rainwater following the Fukushima accident, with an average $^{135}Cs/^{137}Cs$ value of 0.37 (Ohno and Muramatsu, 2014). Isotope ratios were also measured in environmental samples collected in the 20-50km zone around the Fukushima Daiichi NPP, with values ranging from 0.33-0.38 (Zheng et al. 2014). The source of contamination was determined by

comparing the values in environmental samples with those in a spent fuel pool and damaged reactors, which suggested that environmental contamination was mainly a result of releases from the Unit 2 reactor, with negligible contribution as a result of fission product release from the spent fuel pool.

Accurate measurement of $^{135}Cs/^{137}Cs$ ratios can distinguish between different sources of contamination, which in turn will improve modelling of the dispersion of anthropogenic radioactivity. The absence of a certified $^{135}Cs/^{137}Cs$ reference material prevents direct comparison between studies, with published ratios for ^{137}Cs standards ranging from 0.66-1.96 (Lee et al. 1993; Chao and Tseng, 1996; Ketterer and Szcechenyi, 2008; Taylor et al. 2008; Russell et al. 2014 (A)). Furthermore, the high variation in values measured makes it challenging to determine how effective $^{135}Cs/^{137}Cs$ measurement is as a forensic tool, and knowledge of source conditions would be beneficial in constraining variations between sites. Isotope ratio values can potentially support similar approaches applied to uranium and plutonium isotopes by Warneke et al. 2002 and Lindahl et al. 2010. For example, ^{240}Pu is produced by neutron capture of ^{239}Pu, therefore $^{240}Pu/^{239}Pu$ also varies between reactor type (0.23-0.67) and weapon production (0.01-0.07) (Warneke et al. 2002). For a high neutron flux, $^{240}Pu/^{239}Pu$ is expected to increase as $^{135}Cs/^{137}Cs$ decreases (Taylor et al. 2008).

1.2 Analytical Methods for Determination of ^{135}Cs and ^{137}Cs in the Environment

Measurement of $^{135}Cs/^{137}Cs$ has been applied to a range of solid and aqueous samples. Prior to quantification, solid samples are digested, followed by separation of Cs from isobaric Ba interferences using chemical and/or instrument based procedures.

1.2.1 Sample digestion

For solid samples, a sufficient amount is dried, ground, and sieved to get a homogeneous and representative sample for analysis. Ashing of the sample decomposes organic matter, with temperatures up to 500^0C reported with no loss of Cs (Taylor et al. 2008). Digestion techniques include HNO_3: HF (Lee et al. 1993), aqua regia (Karam et al. 2002), and lithium borate fusion (Taylor et al. 2008). In clay-rich samples, more aggressive fusion techniques are required to achieve a quantitative recovery, as acid

leaching struggles to fully liberate Cs (Russell et al. 2014 (A) (Chapter 2.3.1. page 33-35)). Spent fuel samples have been digested using HNO_3 (Pitois et al. 2008), aqua regia (Alonso et al. 1995), closed vessel microwave digestion (Meeks et al. 1998), and lithium metaborate fusion (Delmore et al. 2011).

1.2.2 Chemical separation

Ion exchange is the dominant technique with regards to radiocaesium separation. A number of materials have been developed for ^{137}Cs separation (Table 1.7) (Marsh et al. 1994; Dozol et al. 1999), with the aim of combining decontamination of interferences with high analyte recovery. The majority of materials focus on separation of Cs from fission products, and alkali metals (specifically Na and K). For mass spectrometric measurement, an additional factor to consider is the chemical stability of materials (Dozol et al. 1999), which can make quantitative recovery of Cs from the material and subsequent quantification challenging. This section therefore focuses on separation procedures that have been or can potentially be applied to mass spectrometric determination of ^{135}Cs and ^{137}Cs.

1.2.2.1 Ammonium molybdophosphate (AMP)

AMP $[(NH_4)_3PMo_{12}O_{40}]$ is an inorganic ion exchanger that has been successfully applied to ^{135}Cs and ^{137}Cs separation prior to ICP-MS quantification (Taylor et al. 2008; Russell et al. 2014 (A); Zheng et al. 2014), as well as ^{137}Cs isolation from sea and fresh waters, acidic nuclear wastes, and solid materials including spent fuel, soils and sediments (Marsh et al. 1994; Gaur, 1996; Tranter et al. 2002).

The phosphomolybdate ion $(PMo_{12}O_{40})^{3-}$ is a hollow sphere composed of 12 octahedral MoO_6 groups and a central PO_4 group, with ammonium ions ($3NH_4^+$) and associated water molecules located between these negative ion spheres. Separation is based on exchange of Cs^+ with NH_4^+ ions (Equation 1.3). The reaction is rapid, and highly selective under acidic conditions, with >95 % recoveries and a distribution coefficient (K_d) of 10^4 mL/g routinely achievable (Mimura et al. 2001). The highest selectivity is observed in ~1-3 M HNO_3, as only monovalent cations (particularly Cs) can stably pack into the molybdophosphoric acid lattice and form an insoluble compound. Under weaker acid and neutral conditions, there is a reduction in selectivity, with AMP acting

as a generic ion exchanger (Chapter 2.3.2, page 35) (Morgan and Arkell, 1963; Smit and Robb, 1964).

$$[NH_4^+]_x + Cs^+ \rightleftharpoons NH_4^+ + [Cs]_x \quad (1.3)$$

Where X is the ion sorbed onto AMP

The mechanical properties of the fine powder crystalline structure of AMP is often modified by impregnation onto an inert support material, such as silica gel (Baker et al. 1975), asbestos (Morgan and Arkell, 1964), and polyacrylonitrile (PAN) (Sebesta and Stefula, 1990; Tranter et al. 2002) (Appendix A, page 147). In batch separations, small quantities (~50-100 mg/10 mL sample), are mixed with the sample, followed by separation by centrifuging and/or filtration (Karam et al. 2002; Taylor et al. 2008; Russell et al. 2014 (A), Zheng et al. 2014). The interaction time with AMP ranges from several minutes (Karam et al. 2002) to 1 hour (Taylor et al. 2008), with a similar recovery across this timescale. Longer reaction times can negatively impact ^{137}Cs recovery as a result of displacement with other ions, or AMP degradation (Marsh et al. 1994). Chromatographic separations have been applied to high volume aqueous samples, including seawater (Chapter 4.1.1, page 64) (Molero et al. 1995; Gaur, 1996; Aoyama et al. 2000; Bombard et al. 2013), which despite the high ionic strength does not impact AMP performance.

Solid AMP+Cs has been successfully dissolved in alkali solutions including NaOH (Chao and Tseng, 1996), NH_4OH (Pibida et al. 2004), or NH_4NO_3 (Delmore et al. 2011). Distribution coefficient values for Cs decreases in the order $H^+ > Na^+ > K^+ > NH_4^+$, which relates to the decreasing size of hydrated cations, implying that NH_4-based solutions are most effective for dissolution (Mimura et al. 2001).

Inorganic ion exchanger	K_d Cs (cm^3/g)
Potassium nickel hexacyannoferrate (KNiFC)	$8.5x10^4$
Potassium cobalt hexacyannoferrate (KCoFC)	$1.1x10^2$
Ammonium phosphotungstate trihydrate (AWP)	$1.3x10^4$
Ammonium molybdophosphate (AMP)	$9.5x10^3$
Ferrierite	2.5
Synthetic mordenite	8.5
Natural mordenite	$3.5x10^2$
Clinoptilolite	$2.3x10^2$
Crystalline silicotitanate	$1.9x10^5$ *

Table 1.7. Cs distribution coefficient values for a range of ion exchange materials in 3M HNO_3. *0.1M HNO_3 (Mimura et al. 1997 A; Ramendik et al. 2001)

1.2.2.2 Insoluble hexacyannoferrates

Transition metal hexacyanoferrates show rapid, selective and quantitative separation of ^{137}Cs (Watari et al. 1967; Lehto et al. 1992; Mimura et al. 1997A; Mardan et al. 1999; Clearfield, 2000; Moon et al. 2004). A frequently used material is potassium nickel hexacyannoferrate (KNiFC), which has been effectively used in batch and chromatographic separation of ^{137}Cs from samples including nuclear waste and large volume aqueous solutions (Gaur, 1996; Mimura et al. 1997A; Ismail et al. 1998; Mimura et al. 1999A; Kamenik and Sebesta, 2003; Nilchi et al. 2006; Du et al. 2013; Bombard et al. 2013; Okamura et al. 2014). As with AMP, the exchanger is commonly precipitated onto an inert support material e.g. colloidal silica or PAN (Gaur, 1996; Bombard et al. 2013). The K_d for Cs decreases with increasing concentrations of K and NH_4, with the linear decrease at NH_4 concentrations greater than 0.1M, suggesting Cs uptake is a cation exchange reaction, and that NH_4-based alkali solutions can effectively elute Cs (Mimura et al. 1997 B; Mimura et al. 1997 C; Mimura et al. 1999 B). KNiFC

has achieved quantitative separation of ^{137}Cs in neutral, acidic and alkaline solutions, with the highest chemical and thermal stability in neutral or slightly acidic conditions (Bombard et al. 2013; Ismail et al. 1998).

KNiFC has been reported to achieve K_d values one order of magnitude higher than AMP (Mimura et al. 1997 A). A 25 mL KNiFC-PAN column achieved 93% ^{137}Cs recovery from a 100 L acidified seawater sample at a flow rate of 300 mL/min, compared to 89% recovery using 25 mL AMP-PAN (Bombard et al. 2013). However, KNiFC has not been applied to a mass spectrometry-based procedure, with little information on the ability to quantitatively elute Cs, or the Ba decontamination factors achievable (Appendix B, page 151).

1.2.2.3 Ion exchange chromatography

The ion exchange procedure is based on interactions between the mobile phase and functional groups bonded to the support material, with quality of analysis determined by the chromatographic conditions and choice of a suitable stationary phase (Moreno et al. 1999). The Ba decontamination factor required to recover accurate $^{135}Cs/^{137}Cs$ isotopic composition varies with sample type, therefore ion exchange chromatography has been used as a single separation stage (Lee et al. 1993; Moreno et al. 1999; Ketterer and Szechenyi, 2008), or in multi-stage separations (Table 1.2) (Chao and Tseng, 1996; Taylor et al. 2008; Russell et al. 2008; Delmore et al. 2011; Snyder et al. 2012; Zheng et al. 2014). Ion exchange chromatography is a versatile, sensitive and selective technique, however potential disadvantages are long elution times and the large volumes of acids and resin required (Betti, 1997; Moreno et al. 1999; Spry et al. 2000).

Strong acid cation exchange resin, specifically Bio Rad AG50W, has been applied to ^{135}Cs and ^{137}Cs separation (Lee et al. 1993; Russell et al. 2014 (A); Delmore et al. 2011; Shiho et al. 2011). Bio Rad AG50W is composed of sulphonic acid functional groups covalently bonded to a styrene divinylbenzene co-polymer lattice. Cs elution has been achieved with 0.3-2M HCl (Lee et al. 1993; Delmore et al. 2011; Snyder et al. 2012), and 1 M HNO_3 (Shiho et al. 2011; Russell et al. 2014(A)) (Chapter 2.3.2. page 35-36)).

Moreno et al. (1999) investigated a number of Dowex ion exchangers, of which CS5 resin using a 1 M HNO_3 eluent gave the most effective separation. This was determined from the precision of $^{134}Cs/^{137}Cs$ ratios measured by gamma spectrometry, and the

accuracy of ion chromatography-ICP-MS measurement of $^{133}Cs/^{135}Cs$ and $^{135}Cs/^{137}Cs$, which was compared to values obtained by KORIGEN code calculations (a package that calculates fuel depletion during irradiation and decay). Precision and accuracy values of 2.5% and 5% were achieved, respectively. Dionex CS5 is a high-resolution column with both anion and cation exchange capacity (sulphonic acid and quaternary ammonium functional groups), with Cs effectively eluted in 0.03-1 M HNO_3 (Alonso et al. 1995).

1.2.2.4 Extraction chromatography

Extraction chromatography combines the ease of use of ion exchange with the selectivity of solvent extraction (Horwitz, 1998). Calixarenes are macrocyclic extractants that have been extensively applied to ^{137}Cs separation, for example from acidic nitrate solutions (Horwitz et al. 1996), acidic liquid waste (Grunder et al. 1999), spent nuclear fuel (Riddle et al. 2005) and Savannah River Site tank wastes (Bonnesen et al. 1998).

Calixarenes are made up of phenolic units (C_6H_5OH) linked by methylene groups (CH_2^+) (Dozol et al. 1999). Rotation around this group allows the formation of a number of conformations and unique cavities, and therefore selectivity towards different ions (Appendix F, page 169) (Ikeda and Shinkai, 1997; Thuery et al. 2000). Calix[4]arenes in the 1,3 alternate conformation with bis-crown-6 ethers show the highest selectivity, as the crown-6 cavity size (1.70 Å) is complimentary towards the ionic radius of Cs (1.67 Å), giving Cs/Na and Cs/K separation factors exceeding 10^4 and 10^2, respectively (Bonnesen et al. 1998; Sachleben et al. 1999; Haverlock et al. 2000; Leonard et al. 2001; Riddle et al. 2005).

The general method for extraction of Cs (Equation 1.4, (Asfari et al. 1995)) is to contact equal volumes of organic (calixarene) and aqueous (HNO_3) phases at 25^0C, followed by centrifuging and measurement of ^{137}Cs in the two phases by gamma spectrometry. Contact time has ranged from 1 minute (Bonnesen et al. 1998) to 12 hours (Ikeda and Shinkai, 1999). Caesium has been retained on the solid phase at 1-4 M HNO_3, with elution achieved in <0.05 M HNO_3 or Milli-Q water (due to the low K_d for Cs), or 6-8M (because of competitive extraction of HNO_3) (Asfari et al. 1995; Kim et al. 1998; Dozol et al. 1999). Chromatographic separation has been successfully applied by impregnation of the calixarene onto inert materials including Amberlite XAD-7 (Sigma Aldrich)

(Dietz et al. 2006), SiO_2 particles (Zhang et al. 2009, and 2010), and pre-filter resin material (Triskem International) (Chapter 3.2.3, page 48) (Russell et al. 2014(B)).

$$Cs^{+}_{(aq)} + NO_3^{-}{}_{(aq)} + X_{(org)} + nH_2O_{(aq)} \rightleftharpoons [CsX]^{+} \cdot [NO_3^{-} \cdot nH_2O]_{org} \qquad (1.4)$$

Where X is the calixarene

Calixarenes offer straightforward extraction and elution of Cs, and the limited number and volume of reagents may reduce Ba contamination introduced during the procedure. Extraction chromatography resins are expensive, but are often regarded as an economically and technically justifiable option (Boll et al. 1997). As with insoluble hexacyannoferrates, calixarenes have yet to be applied to a mass spectrometric procedure for $^{135}Cs/^{137}Cs$ separation from Ba interferences (Chapter 3, page 43-59) (Russell et al. 2014 (B)).

Depending on the decontamination factors required, a multi-stage chemical separation procedure is often required. However, this increases the number and volume of reagents used and risks a higher Ba procedural blank concentration, which has a significant impact on the detection limits achievable for low-level $^{135}Cs/^{137}Cs$ measurement (Chapter 2.3.3. page 39-40) (Russell et al. 2014(A)).

1.2.3 Radiometric detection

Direct measurement of ^{135}Cs by radiometric techniques is challenging, however neutron activation analysis (NAA) has been applied to detection of ^{135}Cs by gamma spectrometry of the activated product ^{136}Cs (Stamm, 1973; Chao and Tseng, 1996).

1.2.3.1 Neutron activation analysis (NAA)

Caesium-135 has a thermal neutron capture cross section of 9 barns, and its activated product ^{136}Cs ($t_{1/2}$ = 16 days), formed through (n, γ) reaction, emits gamma rays at energies of 818, 1048 and 1235 keV (Stamm, 1973). Chao and Tseng (1996) separated ^{135}Cs from fission and activation products in radioactive wastes using AMP, which was then dissolved in NaOH and immobilised on a cation exchange column for irradiation.

The main gamma emitters detected were ^{134}Cs, ^{136}Cs, and ^{137}Cs. An earlier study by Stamm (1973) did not include AMP separation, leading to detection of other peaks (namely ^{22}Na) and thus increasing the limit of detection.

Whilst NAA avoids isobaric Ba interferences, the detection limit is affected by the concentration of ^{133}Cs, its activated product ^{134}Cs, and ^{137}Cs (Hou and Roos, 2008). For a sample with a 1:1:1 ratio of ^{133}Cs:^{135}Cs:^{137}Cs, a detection limit of 10^{-12} g of ^{135}Cs has been reported (Chao and Tseng, 1996). NAA has focused on radioactive waste samples with high ^{135}Cs, ^{137}Cs concentration, and applying a similar procedure to environmental samples would be challenging, given the short half-life of ^{136}Cs, and the need to irradiate samples in order to form this activated product.

1.2.4 Mass spectrometric detection

Mass spectrometry, primarily ICP-MS, is an effective technique for measurement of ^{135}Cs/^{137}Cs, with the extent of separation from isobaric Ba interferences a critical factor in the detection limits achievable. Measurements must also not be affected by tailing from naturally occurring ^{133}Cs (natural abundance 100 %) on ^{135}Cs, which, depending on the sample matrix, requires an abundance sensitivity of ~1x10^{9} (Lee et al. 1993).

1.2.4.1 ICP-MS

Caesium-135 and ^{137}Cs quantification has been achieved using quadrupole (ICP-QMS) (Alonso et al. 1995; Meeks et al. 1998; Moreno et al. 1999; Song et al. 2001), and sector field (ICP-SFMS) instruments (Pitois et al. 2008; Russell et al. 2014(A)), with the latter offering greater sensitivity, albeit at a higher cost. A procedure recently developed by Russell et al. (2014(A)) using ICP-SFMS achieved an instrumental detection limit of 1 pg/L for stable ^{133}Cs. This compared to a method detection limit of 50 pg/L for ^{135}Cs and ^{137}Cs in environmental samples as a result of Ba contamination introduced during the separation procedure (Chapter 2, page 27-42).

The sample introduction system affects analyte sensitivity, transport efficiency and sample uptake, and for higher activity samples is contained in a glovebox (Alonso et al. 1995; Moreno et al. 1999). Traditional concentric and cross flow nebulisers suffer from high sample uptake rates (up to ~1 mL/min) and poor introduction efficiency (<1 %) (Taylor et al., 2008). Analytical sensitivity is improved through the use of more efficient

micro-concentric (Isnard et al. 2009), direct injection or desolvating nebulisers (Liezers et al. 2009; Russell et al. 2014(A)) that can achieve up to 100 % analyte transport efficiency and a sample uptake rate as low as 50 µL/min.

Sample introduction can also be applied as a further Cs purification stage. For example, an electrothermal vaporisation (ETV) system using an appropriate chemical modifier can discriminate against Ba, based on selective volatisation of Cs. Song et al. (2001) investigated 12 chemical modifiers and determined potassium thiocyanate (KSCN) to be the most effective with regards to Cs signal enhancement and Ba separation. A volatilisation temperature of 1100^0C was used for vaporisation of Cs in a 10^4 excess of Ba, with a Ba signal increase at mass 135 of only 1 %. The detection limit of ^{135}Cs was calculated as 0.2 ng/L. Advantages of ETV-ICP-MS include limited sample preparation and high introduction efficiency (70-100 %). However, without prior chemical separation this procedure could struggle to achieve ^{135}Cs and ^{137}Cs purification in samples such as soils and sediments, where a greater Ba decontamination factor (up to 10^{12}) is required.

Capillary electrophoresis (CE-ICP-MS) has achieved ^{135}Cs/^{137}Cs measurement in spent nuclear fuel samples, with interfering Ba^{2+} having a shorter migration time in the capillary than Cs^+, based on faster movement as a result of its higher charge (Pitois et al. 2008). The procedure uses low microlitre sample volumes and nanolitre scale sample injection, with ^{133}Cs detection limits of 6,000 ng/L and 4 ng/L using ICP-QMS and ICP-SFMS, respectively. The speed and effectiveness of separation compares favourably to ion exchange based procedures, and applying this to environmental samples would be beneficial in determining the extent of Ba decontamination achievable.

Online chromatographic separation can minimise reagent volumes, achieve a more efficient Ba separation and thus improve the detection limits achievable (Alonso, 1995; Moreno et al. 1999; Taylor et al. 2008; Pitois et al. 2008; Liezers et al. 2009). For example, Liezers et al. (2009) achieved a ^{135}Cs and ^{137}Cs detection limit of 2 pg/L and 1 pg/L, respectively, using on-line chromatographic separation with a CG3 IonPac guard column (Dionex, USA), which was effectively applied to measurement of ^{135}Cs/^{137}Cs in a spiked groundwater matrix.

Instruments equipped with a collision cell (CC) or dynamic reaction cell (DRC) have been applied to Cs separation (Granet et al. 2008; Taylor et al. 2008). The aim is to use

an appropriate gas to react with Ba and convert it to a non-interfering product, whilst having little or no impact on Cs (Amr and Abdel-Lateef, 2010), with N_2O (Granet et al. 2008), and CH_3Cl (Taylor et al. 2008) used as reactive gases. For example, the reaction between Ba and N_2O to form BaO is exothermic (-236.8 kJ/mol); whereas the reaction with Cs is thermodynamically unfavourable (+106.3 kJ/mol) (Granet et al. 2008). Kinetic data from Lavrov et al. (2004) supports this, indicating the reaction for Ba has an efficiency of 32 %, compared to 0.01 % for Cs.

A recently developed triple quadrupole instrument (Agilent 8800) equipped with a quadrupole mass filter in front of an octopole reaction cell and second quadrupole mass filter in an MS/MS configuration, was applied to $^{135}Cs/^{137}Cs$ detection in environmental samples following the Fukushima accident (Ohno and Muramatsu, 2014; Zheng et al. 2014). In rainwater samples, using N_2O as a reactive gas, a Cs detection limit of 10 pg/L was achieved in a Ba-free solution, compared to 100 pg/L and 270 pg/L ng/L for ^{135}Cs and ^{137}Cs, respectively, in solutions containing 100 µg/L Ba. These values are higher than the instrumental and method detection limits achievable using ICP-SFMS. However, the reaction cell can suppress the Ba signal by a factor of 10^4 (Zheng et al. 2014), and therefore depending on the sample matrix, no chemical separation is required, significantly reducing the total procedural time compared to the extensive chemical separation using sector field instruments. In addition, the theoretical abundance sensitivity is 10^{-14}, which is superior to any other ICP-MS (Zheng et al. 2014).

Time independent fractionation is an issue affecting accurate isotope ratio measurements by ICP-MS. One cause of this is space charge effects, as lighter ions are deflected to a greater extent than heavier ions during ion extraction (Isnard et al. 2009). The absence of a $^{135}Cs/^{137}Cs$ certified reference material makes accurate mass bias correction challenging, and restricts the ability to compare results between studies (Taylor et al. 2008). Isnard et al. (2009) applied a sample standard bracketing technique using natural isotopes of tin (^{121}Sb, ^{123}Sb) and europium (^{151}Eu, ^{153}Eu) to correct for mass bias, as the average mass of these isotopes is close to that of ^{137}Cs. Barium-138 (natural abundance 71.7%) has been used to assess the effectiveness of separation at masses 135 and 137, however any interference correction will reduce the accuracy of $^{135}Cs/^{137}Cs$ values (Chapter 2.3.3. page 39-40). Caesium-137 values can be verified by

gamma spectrometry, however if a significant correction is required this will not validate the ^{135}Cs result (Meeks et al. 1998).

1.2.4.2 Thermal ionisation mass spectrometry (TIMS)

Measurement of ^{135}Cs/^{137}Cs by TIMS is affected by time-dependent isotopic fractionation, as lighter isotopes are preferentially evaporated from the filament. This can be corrected by measuring ^{133}Cs/^{137}Cs and ^{135}Cs/^{137}Cs ratios during the analysis, with Isnard et al. (2009) recording a relative bias ranging from 0.5-1.5%, and a relative standard deviation better than 0.1% for all isotope ratios measured.

Peak tailing from ^{133}Cs can lead to substantial statistical errors if not effectively removed by an appropriate instrumental setup (Delmore et al. 2011). Lee et al. (1993) was the first to develop a procedure for measuring ^{135}Cs/^{137}Cs in environmental samples using TIMS. The instrument was equipped with a retarding potential quadrupole lens filter (RPQ) that acted as an energy and directional filter to remove ^{133}Cs ions scattered in the tail (Table 1.8).

The isotopic fractionation affecting TIMS and ICP-MS, as well as the absence of a certified reference material to verify accuracy of ^{135}Cs/^{137}Cs measurements, lead to Isnard (2009) comparing the two techniques for uranium oxide and mixed oxide fuel samples. The agreement between the two approaches was good, with a relative difference on ^{133}Cs/^{137}Cs and ^{135}Cs/^{137}Cs ratios ranging from 0.2% to 0.5%.

1.2.4.3 Resonance ionisation mass spectrometry (RIMS)

In RIMS analysis, the solid or liquid sample is vaporised and atomised by an atomic beam source, for example by applying a gradually increasing electrical current in a graphite furnace (Karam et al. 2002). Selectivity towards Cs is maximised by tuning one or more lasers to the appropriate wavelength required for excited states, followed by ionisation using an argon ion laser (Hou and Roos, 2008). Laser tuning can achieve excellent separation from Ba interferences, and because of the high ionisation efficiency, high transmission and low background, detection limits up to 10^{-18}g are achievable (Pibida et al. 2004). The absence of a commercially available instrument is the primary limitation to this approach (Hou and Roos, 2008). In addition, optimisation of instrument efficiency and chemical preparation is time-consuming compared to other mass spectrometric approaches (Pibida et al. 2004).

Reference	Modification	$^{135}Cs/^{133}Cs$ quantified	Transmission efficiency (%)
Lee et al. (1993)	RPQ	$1x10^{-9}$	20
Chen et al. (2008)	Modified RPQ II	$1.5x10^{-10}$	80
Chen et al. (2008)	Unmodified RPQ II	$1x10^{-8}$	90

Table 1.8. Impact of TIMS instrumental setup on ^{133}Cs peak tailing removal

1.3 Conclusions

Caesium-135 and ^{137}Cs are high yield fission products, whose presence in the environment is a result of anthropogenic nuclear activities. Caesium-137 is of major importance in decommissioning, environmental monitoring and radiation safety, whereas ^{135}Cs is a major contributor to the long-term radiological risk associated with deep geological disposal. Advances in mass spectrometry (specifically ICP-MS) have put the technique at a stage where it can accurately detect low-level environmental concentrations of ^{135}Cs and ^{137}Cs. This also enables the measurement of $^{135}Cs/^{137}Cs$ values that can be used to identify the source of radioactive contamination, and therefore has the potential to be a powerful forensic tool in environmental studies. To date $^{135}Cs/^{137}Cs$ ratios measured have been a series of isolated studies, with the absence of a certified reference material and inconclusive evidence over the site history being limiting factors in comparing variations between, and even within sites. The capability of $^{135}Cs/^{137}Cs$ as a forensic tool would be better understood if applied at a location where the source of contamination was well constrained, such as a site contaminated by long-term discharges from a reactor or reprocessing facility.

ICP-SFMS is a highly sensitive technique, however, the detection limits achievable are strongly controlled by the extent of chemical separation of isobaric Ba interferences, and contamination introduced during the separation procedure, as opposed to the

capabilities of the instrument. AMP and/or ion exchange chromatography are the most common separation methods, whilst alternative exchange materials (namely KNiFC and calixarenes) are also potentially suitable. Coupling the separation stage online to the instrument reduces contamination by minimising reagent volumes and analyst exposure, for example through ion exchange, electro thermal vaporisation or capillary electrophoresis. Alternatively, instruments equipped with a collision or reaction cell potentially eliminate the need for chemical separation prior to sample introduction, however these instruments struggle to match the sensitivity of sector field instruments.

Chapter 2: Determination of Precise $^{135}Cs/^{137}Cs$ in Environmental Samples Using Sector Field Inductively Coupled Plasma Mass Spectrometry

Abstract

Recent advances in sector field inductively coupled plasma mass spectrometry (ICP-SFMS) have led to significant sensitivity enhancements that expand the range of radionuclides measurable by ICP-MS. The increasing capability and performance of modern ICP-MS now allows analysis of medium-lived radionuclides previously undertaken using radiometric methods. A Thermo Element XR ICP-SFMS equipped with a Jet Interface, X-skimmer cone and an Aridus II desolvating sample introduction system was configured to achieve sensitivities up to 80,000 counts for a 1 ng/L ^{133}Cs solution, providing a detection limit of 1 pg/L. In order to extend this approach to environmental samples it has been necessary to develop an effective chemical separation scheme and to use ultra-pure reagents. A procedure incorporating digestion, chemical separation and quantification by ICP-SFMS is presented for detection of the significant fission product radionuclides of caesium (^{135}Cs and ^{137}Cs) at concentrations found in environmental and low level waste samples. This in turn enables measurement of the $^{135}Cs/^{137}Cs$ ratio, which varies with the source of nuclear contamination, and can therefore provide a powerful dating and forensic tool compared to radiometric detection of ^{137}Cs alone. A detection limit in sediment samples of 0.05 ng/kg has been achieved for ^{135}Cs and ^{137}Cs, corresponding to 2.0×10^{-3} mBq/kg and 160 mBq/kg, respectively. The critical issue is ensuring removal of barium to eliminate isobaric interferences arising from ^{135}Ba and ^{137}Ba. The ability to reliably measure $^{135}Cs/^{137}Cs$ using a high specification laboratory ICP-SFMS now enables characterisation of waste materials destined for nuclear waste repositories as well as extending options in environmental geochemical and nuclear forensics studies.

2.1 Introduction

Radionuclide measurement by ICP-MS has traditionally focused on the longer-lived, low activity nuclides (Lariviere et al. 2006; Hou and Roos, 2008), as the technique was unable to match the sensitivities achievable by radiometric methods for shorter-lived radionuclides such as ^{90}Sr and ^{137}Cs (Lariviere et al. 2006; Vajda and Kim, 2010). Recent developments in sector field ICP-MS now provide significantly improved sensitivity and offer the prospect of effectively measuring both shorter and longer-lived radionuclides, at ultra-low concentrations (Figure 1.1, page 4). These improvements are important and expand the options available for environmental, contaminated land and nuclear waste assessments and even nuclear forensics.

This study focuses on method developments to enable quantification of ^{137}Cs ($t_{1/2}$ = 30y) and ^{135}Cs ($t_{1/2} = 2.10^6$ y; Table 1.1, page 2). Both radionuclides are high yield fission products that have been or are released into the environment from nuclear power plants, reprocessing sites; nuclear accidents and atmospheric weapons test fallout (Chao and Tseng, 1996; Hou and Roos, 2008; Taylor et al. 2008). Caesium-137 is typically measured using gamma spectrometry in radiation protection, environmental monitoring and waste characterisation fields (Moreno et al. 1999; Song et al. 2001; Hou and Roos, 2008). Caesium-135 is not currently considered to be radiologically significant, but is a major contributor to the long-term radionuclide inventory of deep geological repositories. Furthermore, the $^{135}Cs/^{137}Cs$ ratio varies with reactor, weapon and fuel type (Figure 1.3, page 13), and can potentially be used as a forensic tool to identify the source of radioactive contamination (Chao and Tseng, 1996; Taylor et al. 2008).

Variations in $^{135}Cs/^{137}Cs$ originate from ^{135}Xe and ^{137}Xe fission products in the ^{135}Cs and ^{137}Cs decay chains (Equation 2.1 and 2.2). Xenon-135 is a potent neutron poison (neutron capture cross section 2.7 x 10^6 barns) that can transmute to ^{136}Xe, reducing the fission yield of ^{135}Cs, however there is no such competing reaction for ^{137}Xe affecting the ^{137}Cs yield (Taylor et al. 2008; Liezers et al. 2009). The time of neutron irradiation therefore has a significant impact on $^{135}Cs/^{137}Cs$. For example, in a nuclear reactor, there is long-term exposure to a high neutron flux, and ^{136}Xe produced by neutron capture by ^{135}Xe will compete with ^{135}Cs production from ^{135}Xe beta decay (Betti, 1997; Taylor et al. 2008). By comparison, a nuclear weapon forms relatively more ^{135}Cs, as there is little

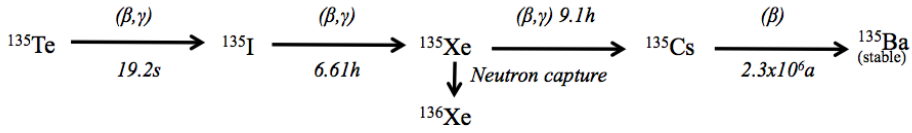

(2.1)

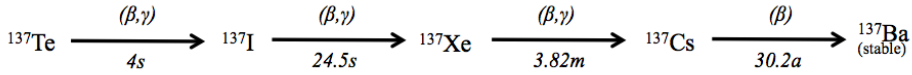

(2.2)

^{135}Xe existing at the time of the relatively transient but high neutron flux (Betti, 1997). Accurate measurement can distinguish between different sources of contamination, which in turn will improve the modeling of anthropogenic radionuclide dispersion. Similar insights have been obtained using ^{134}Cs/^{137}Cs ratios, but application is limited by the relatively short half-life of ^{134}Cs (2.06 y) (Moreno et al. 1999; Molero et al. 1999; Merz et al. 2013). Measurement of ^{135}Cs/^{137}Cs is considerably less restricted, and can be a powerful tool in the field of nuclear forensics. In environmental studies this will provide significantly more information than detection of ^{137}Cs alone, and can build on analogous studies involving U and Pu isotopes that have already provided valuable insights (Warneke et al. 2002 and Lindahl et al. 2010).

Whilst ^{137}Cs is commonly measured using high resolution gamma spectrometry, radiometric detection of ^{135}Cs is considerably more challenging, since it is a pure beta emitter with a relatively low specific activity (4.1×10^7 Bq/g). The nuclide also exists in the presence of ^{137}Cs, which has an activity concentration that is 5 orders of magnitude higher. Mass spectrometry has been successfully applied to ^{135}Cs measurement; with ICP-MS the most frequently used approach (Table 1.2, page 5). The primary challenge is removal of isobaric ^{135}Ba and ^{137}Ba interferences, with isotopic abundances of 6.6% and 11.2%, respectively. The resolution required to separate these isobars from ^{135}Cs and ^{137}Cs is greater than high resolution ICP-MS can achieve (R=10,000) (Thermo Scientific, 2008), therefore complete chemical separation prior to measurement is critical in achieving accurate ^{135}Cs and ^{137}Cs measurements. In addition, depending on the sample matrix, high concentrations of stable ^{133}Cs (100 % isotopic abundance) can lead to peak tailing on ^{135}Cs and impact the detection limits achievable (Lee et al. 1993; Taylor et al. 2008).

The most frequently used chemical separation procedure utilises ammonium molybdophosphate (AMP) and/or ion exchange chromatography (Lee et al. 1993; Chao and Tseng, 1996; Granet et al. 2008; Ketterer and Szechenyi, 2008; Taylor et al. 2008; Isnard et al, 2009; Liezers et al. 2009; Asai et al. 2011; Delmore et al. 2011; Snyder et al. 2012; Zheng et al. 2014). AMP ($[NH_4]_3PMo_{12}O_{40}$) is an inorganic ion exchanger that has been applied to ^{137}Cs separation / pre-concentration from sea and fresh waters, acidic nuclear wastes, and solid materials including spent fuel, soils and sediments (Marsh et al. 1994; Gaur, 1996; Clearfield, 2000). The structure consists of phosphomolybdate ions $(PMo_{12}O_{40})^{3-}$ surrounded by ammonium ions ($3NH_4^+$) that can exchange with Cs^+ (Gaur, 1996; Clearfield, 2000; Mimura et al. 2001; Tranter et al. 2002). The reaction is highly selective towards Cs, with K_d values of around 10^4 cm^3/g routinely achievable (Mimura et al. 2001). Anion and cation exchange chromatography has been used in both single stage (Alonso, 1995; Moreno et al. 1999; Ketterer and Szechenyi, 2008; Asai et al. 2011) and multi-stage separations (Chao and Tseng, 1996; Taylor et al. 2008; Delmore et al. 2011; Snyder et al. 2012). Strong acid cation exchange resin, specifically Bio-Rad AG50W, has frequently been applied to ^{135}Cs and ^{137}Cs separation (Lee et al. 1993; Delmore et al. 2011; Shiho et al. 2011; Zheng et al. 2014), with Cs elution achieved using both HCl (Lee et al. 1993; Ketterer and Szechenyi, 2008; Delmore et al. 2011; Snyder et al. 2012) and HNO_3 (Asai et al. 2011; Shiho et al. 2011).

Extending the application of ^{135}Cs measurements for environmental and nuclear forensics studies is dependent on the development of robust techniques for ultra-low level measurement of ^{135}Cs. This paper reports a state-of-the-art ICP-SFMS study for low-level measurement of ^{135}Cs and ^{137}Cs through a combination of a highly efficient chemical separation of interfering elements along with improvements in ICP-SFMS sensitivity. The method now permits a high specification laboratory instrument to be used for a range of applications in the fields of nuclear and environmental forensics and nuclear waste characterisation and demonstrates the extended range of nuclides that can now be effectively measured by mass spectrometry.

2.2 Experimental

2.2.1 Reagents and materials

Stable Cs and Ba standard solutions were prepared from 1000mg/L elemental stock solutions (Inorganic Ventures) in 0.1 % HNO_3 (v/v). Teflon sub-boiled HNO_3, sub-boiled HCl and high purity de-ionised water (resistivity higher than 18.2 MΩ) produced from a Q-Pod Millipore System (Merck) were used throughout.

In order to minimise introduction of Ba during the procedure, digestion and chemical separation steps were carried out in a Class 100 workstation contained in a Class 1000 clean laboratory. Vials, pipette tips and columns were cleaned in 10 % HNO_3 for at least 24 hours prior to use. Heavy duty PFA jars with lids (Savillex, USA) were used for digestion. Similar open jars were used to collect the Cs fraction following cation exchange. PFA jars were cleaned before and after use using 50 % HCl (v/v) at 100^0C for 24 hours, followed by 50 % HNO_3 (v/v) at 100^0C for 24 hours. Cation exchange chromatography was performed in a HEPA cabinet. The resin was soaked overnight in 6M HNO_3, loaded onto the column and then conditioned with 40mL 6M HNO_3 to elute residual Ba (concentrations range from 5-10 µg/L). This cleaning step had no notable impact on the performance of the column with regards to Cs separation / purification.

2.2.2 Digestion and separation of Cs

Aqua regia acid leaching, lithium metaborate fusion (Fluxana, Germany) and sodium hydroxide sintering (Analytical reagent grade, Fisher chemicals, UK) were evaluated as digestion techniques for Cs dissolution using an Irish Sea marine sediment (contaminated with Sellafield-derived radionuclides), having a ^{137}Cs concentration of ~0.34 pg/g (1.1 Bq/g) and Ba concentration of ~380 µg/g. Recovery of ^{137}Cs was assessed by gamma spectrometry (Table 2.1). For borate fusion, 5 g of sediment and 5 g lithium metaborate are mixed in a Pt-Au 5 % crucible and heated at 950^0C for 10 minutes using a Vulcan flame fusion system (Fluxana, Germany). The resulting melt is poured into a PTFE beaker containing Milli-Q water to form a frothy glass. The water is decanted, replaced with 8 M HNO_3, and then transferred to an ultrasonic bath for 30 minutes to accelerate the digestion and dissolution of the frothy glass. The mixture is

then left on a hot plate at 80^0C with a PTFE magnetic stirrer for 4 hours and finally vacuum filtered.

For aqua regia acid leaching, 5 g of sediment is added to a PFA jar, followed by addition of 100 mL *aqua regia* to the sediment in 10 mL increments, allowing any effervescence to subside before adding the next fraction. The sample is then transferred to a hot plate at 80^0C with a PTFE magnetic stirrer at 300 rpm for 4 hours. The contents of the beaker are then centrifuged for 5 minutes at 4500 rpm, and the supernatant transferred to a clean PFA jar and evaporated to dryness.

For sodium hydroxide sintering, 5 g sediment is transferred to a quartz crucible, followed by addition of 10 mL 6M NaOH. The sample is evaporated to dryness by heating with an infrared lamp, and then ignited at 450^0C for 4 hours. After cooling, 10ml Milli-Q water is added to the ignited sample, and then transferred to a hot plate at 80^0C, with regular stirring until all solid material is liberated from the base of the beaker. The contents of the beaker are transferred to a centrifuge tube and centrifuged for 10 minutes at 4500 rpm. The supernatant is transferred to a clean PFA jar and evaporated to dryness. The effectiveness of a double NaOH sinter, and acid leaching followed by NaOH sintering were also investigated.

Cation exchange chromatography and AMP separation were investigated using Milli-Q water, acidic solutions and digested sediment samples spiked with natural or radioactive Cs and Ba standards. An AMP-based separation medium was prepared by loading AMP onto inert silica gel support material (Phase Separations Ltd, UK) following the method described by Baker (1975) (Appendix D, page 165). The effect of AMP mass, interaction time and HNO_3 concentration on Cs recovery and selectivity was assessed. For the combined separation procedure, AMP+Cs dissolution prior to cation exchange was tested using analytical reagent grade ammonium hydroxide and sodium hydroxide (Fisher Chemicals, UK). Uptake of Cs and separation from interfering species by cation exchange chromatography (AG 50-WX8, 8 % cross-linked, 100-200 mesh, Bio-Rad laboratories, USA) was assessed at 1-4 M HCl and HNO_3 concentrations for a 3x0.7 cm column.

2.2.3 Instrumentation

Low-level ^{135}Cs and ^{137}Cs measurements were performed using a Thermo Element XR ICP-SFMS based at the Waterfront Campus, University of Southampton. Ions are focused according to their mass to charge ratio through a sector magnetic field, followed by energy focusing in an Electro-Static Analyser (ESA). A single Faraday detector and dual mode Secondary Electron Multiplier (SEM) make up the detection system, with a linear dynamic range of $>10^{12}$ (Thermo Scientific, 2008).

The instrument can be equipped with the Jet interface (consisting of a high capacity dry interface pump and specially designed Jet sample cone) and X-skimmer cone, which was specifically developed for Thermo ICP-SFMS. When combined with a desolvating sample introduction system, this setup can yield significant improvements in sensitivity (Thermo Scientific, 2011). The impact of the Jet interface and a Cetac Aridus II desolvating unit on sensitivity was determined using 0.01-10 ng/L stable ^{133}Cs standards.

For digestion and chemical separation procedures, samples spiked with radioactive Cs (mixed ^{135,137}Cs) and ^{133}Ba standards were counted as concentrates following separation using a Canberra well-type HPGe detector with an efficiency of 10% at 662 keV (corresponding to the gamma photopeak energy for ^{137}Cs/^{137m}Ba). Analysis of the energy spectra and calculation of radionuclide activity was performed using Fitzpeaks software (JF Computing, Stanford in the Vale, UK). Samples spiked with natural Cs and Ba standards were assessed using the Thermo-Scientific X-series II bench-top ICP-QMS.

2.3 Results and Discussion

2.3.1 Sample digestion

Lithium borate fusion (metaborate, tetraborate or mixtures) has been shown to be one of the best and most rapid opening-out techniques for environmental materials (silicates, carbonates, oxides etc., Croudace et al. 1998). No significant volatilisation of Cs during the borate fusion procedure was observed (Table 2.1), as the Cs becomes largely

trapped in the borate melt. The filtered solution is retained for chemical separation. The solid residual phase contains boric acid, which does not sorb Cs.

Digestion method	^{137}Cs recovery (%)	Time to completion (hrs)
Aqua regia acid leach and filtration/centrifug	78 ± 3	4
Acid leaching in ultrasonic bath + Evap	80 ± 6	2
Lithium metaborate fusion & digestion	100 ± 6	5
Single attack NaOH sinter in silica crucible	90 ± 9	5
Double attack NaOH sinter in silica crucible	100±10	10
Acid leach + NaOH sinter	100 ± 9	10

Table 2.1. Caesium-137 recovery from a Sellafield-contaminated Irish Sea sediment using various digestion methods (estimated time for the full process)

Alternative, though inferior, methods for sample digestion investigated included double NaOH sintering and *aqua regia* acid leaching followed by evaporation and NaOH sintering. A single NaOH sinter using 5 mL 6M NaOH achieved a Cs recovery of 76±7%, increasing to 90±9% when the volume was increased to 10 mL. A unique feature of sintering is that it acts as a separation stage for Cs from actinide elements, as ^{241}Am present in the sediment was retained in the solid hydroxide phase.

A consistent Cs recovery of 78±3% was achieved by acid leaching, with no additional Cs recovered following repeated leaching of the solid residue, or increased contact time (up to 24 hours). This implies that a component of the Cs is being effectively retained in the sediment, which is most likely through retention in clay minerals. A 100% recovery of ^{241}Am, which shows no such affinity for clay minerals, is evidence for this partial retention mechanism. Layer-type silicate minerals are the major sorbents in soil that bind Cs by electrostatic interactions, or stronger bonds through partial electron sharing between Cs and ligand sites of the clay mineral (Bostick et al. 2002). The mineralogical associations of Cs means recovery using *aqua regia* leaching is likely to vary

significantly between sample types; and for clay-rich samples borate fusion is a more suitable technique.

2.3.2 Chemical separation

Recoveries of >95% and K_d for Cs of ~1x10^4 mL/g are achievable using AMP. Selectivity towards Cs reduces as HNO_3 concentration decreases, leading to sorption of other ions including Ba, with K_d increasing from <1 mL/g in 1M HNO_3 to ~50 mL/g in Milli-Q water. At lower acid concentrations, AMP acts as a generic ion exchanger, where as in 1-4 M HNO_3 only monovalent cations (particularly Cs) can stably pack into the molybdophosphoric acid lattice (Morgan and Arkell, 1964; Smit and Robb, 1963). K_d values decrease at >4 M HNO_3, indicative of H^+ ion competition with Cs for sorption sites (Miller et al. 1997; Tranter et al. 2002).

Caesium uptake reached a maximum after approximately 60 minutes contact time, with no evidence of desorption, AMP degradation or uptake of other ions observed after 24 hours. Contact times of five minutes have been previously used (Karam et al. 2002); however, in this study Cs was detected in the filtered solution at contact times of less than 30 minutes. AMP was effectively dissolved in either 4 M NaOH or 4 M NH_4OH. Of these, NH_4OH is theoretically more effective, as the K_d for Cs decreases in the order of H^+>Na^+>K^+>NH_4^+, which relates to the decreasing size of hydrated cations (Mimura et al. 2001).

There was no significant difference in Cs recovery over an AMP mass range of 100-1000 mg/10 mL solution, with the lower value of 100 mg more in line with previous investigations (Karam et al. 2002; Taylor et al. 2008). The filter materials tested achieved a Cs recovery of ~85%, with the remainder retained on the filter paper. This value improved to ~90% when the alkali solution was left to interact with AMP for several minutes before filtering.

The elution profiles for Cs and Ba at 1-4 M acid concentrations for a 3x0.7 cm cation exchange column were determined (Figure 2.1). A lower wash volume and higher Cs recovery was achieved for HNO_3 compared to HCl. However, above 2 M HNO_3 Ba and Cs were detected in the same wash fractions, and at 4 M HNO_3 the elution profiles are

almost indistinguishable. By comparison, a good separation of Cs can be achieved in 1-3 M HCl, although Ba was detected in the Cs fraction at 4 M HCl. The more rapid elution of Ba in HNO_3 than HCl is due to alkaline earth elements forming a univalent cationic ion-pair complex of the form $Ba(II)NO_3^+$ (Croudace and Marshall, 1991).

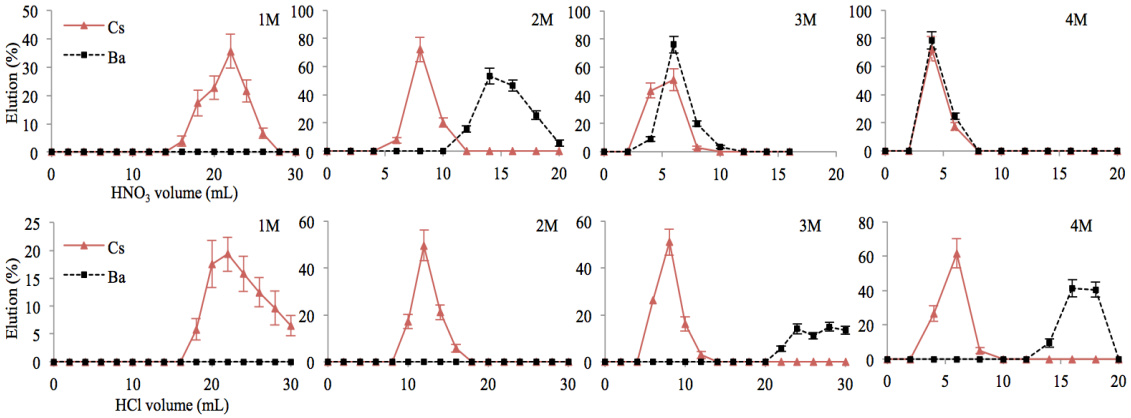

Figure 2.1. Elution profiles for Cs and Ba in 1-4M HNO_3 and 1-4M HCl from a 3x0.7 cm DOWEX AG50 W-X8 cation exchange column

Caesium is loaded directly onto a cation exchange column from the alkaline AMP digest. Removal of residual alkaline solution entrained in the column is required prior to the acid wash, which was achieved using a 30 mL Milli-Q water wash, which also removes remaining dissolved AMP from the column. Molybdenum concentration declined to a maximum of 2 µg/L in the water washings compared with ~40 mg/L in the original alkali load fraction, with < 2 % of the Cs detected in the water washings.

The AMP and cation exchange separation procedure can routinely achieve >85 % Cs recovery and a decontamination from Ba of up to 8 orders of magnitude. However, for more complex sample matrices such as soils or sediment, a final stage clean up is generally required. The use of Sr-resin (Triskem International) for the separation of Cs from Ba has not previously been investigated; however in ~3 M HNO_3 Sr-resin is known to exhibit good retention of Ba (Triskem International, 2013). Results from Sr-resin column tests showed a distribution coefficient for Cs of <10 mL/g in 1-3 M HNO_3, compared to 120-130 mL/g for Ba under the same conditions. Given the low level environmental concentrations aiming to be measured, Sr-resin is very suitable for final removal of Ba. A further advantage is that it is possible to combine the Sr-resin with the

cation exchange resin in a single column (Figure 2.2). A 30 mL 1M HNO_3 wash quantitatively elutes Cs from a column consisting of 3x0.7 cm cation exchange resin overlying a 0.5 cm plug of Sr resin, whilst residual Ba eluted from the cation exchange resin is retained on the Sr resin until the wash volume exceeds 40 mL. This approach minimises the number and volume of reagents used compared to two separate columns, improving the Ba procedural blank concentration. Finally, the procedure reduced the boron content of the Cs fraction by a factor of 10^5-10^6 in samples digested by borate fusion, with typical B concentrations of 30-60 µg/L in final Cs fraction.

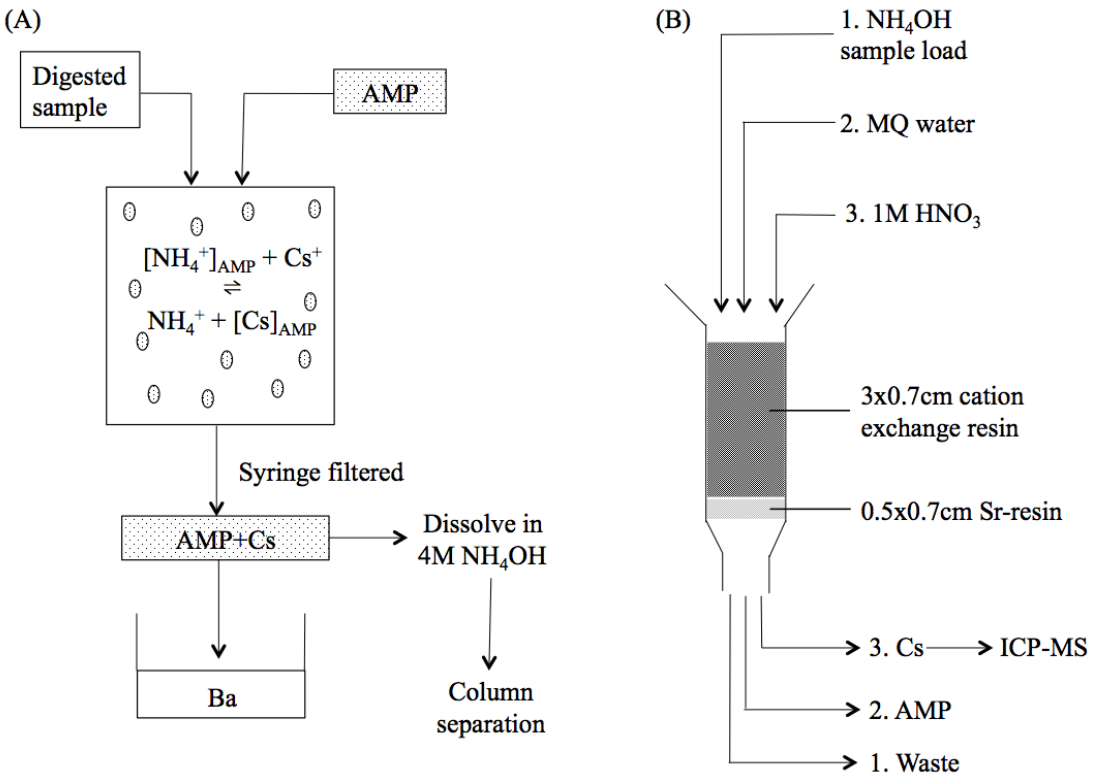

Figure 2.2. Summary of chemical separation procedure for ^{135}Cs, ^{137}Cs, incorporating (A) AMP and (B) cation exchange and extraction chromatography

2.3.3 Quantification

The optimal instrumental setup (Table 2.2) uses a combination of the Cetac Aridus II desolvating sample introduction system and the Jet interface. With this setup Cs sensitivity is around 20,000 counts per ng/L, compared to 700 counts per ng/L when operating with a PC^3 Peltier-cooled cyclonic spray chamber (Elemental Scientific), Self-

Aspirating Nebuliser, H-Skimmer and standard nickel sample cones, and a Pfeiffer Duo 5 rotary pump. The improvement agrees well with data quoted by the manufacturer, who recorded 20,000 counts for a 1 ng/L Indium-115 standard when operating with the Jet interface, X-skimmer cone and either the Aridus or Apex Q (Elemental Scientific) Desolvating Sample Introduction Systems, compared to 1,000 cps in standard setup (Thermo Scientific, 2011).

The sensitivities shown represent instrument tuning in standard mode only, with no additional tuning when components were changed; therefore, these values are only an estimate of the improvements achievable. Further tuning with the optimal setup described can consistently produce sensitivities of ~30,000 counts per ng/L, and a maximum of 80,000 counts per ng/L, corresponding to a detection limit of 1 pg/L (calculated as the concentration of 3 times the standard deviation of the background at mass 133). The Element XR ICP-SFMS is therefore capable of detection limits that can rival radiometric techniques for short-lived radionuclides such as ^{137}Cs (Table 2.2).

Detection method	^{133}Cs sensitivity (counts/ng/L)	LOD (ng/L)		LOD (mBq/L)	
		^{133}Cs	^{137}Cs	^{135}Cs	^{137}Cs
ICP-SFMS- Standard*	720±26	0.02			
ICP-SFMS- Aridus II + Jet Interface + X-skimmer (initial)	20,050±164	0.004			
ICP-SFMS- Aridus II + Jet interface + X-skimmer (maximum)	82,033±790	0.001	0.05	2.1×10^{-3}	160
Gamma spectrometry			0.001		3.2

Table 2.2. Detection limits achievable with ^{133}Cs standards, and for a radioactive standard solution by ICP-SFMS compared to radiometric techniques

Repeat measurements of a ^{137}Cs standard solution (AEA Technology QSA) with a Ba concentration of approximately 5 mg/L was used to determine the validity of the separation and ICP-SFMS procedure described in this study. At a concentration of 1 ng/L, the average ^{135}Cs/^{137}Cs value was 0.97±0.05 (n=8). The absence of a certified ^{135}Cs/^{137}Cs reference material prevents direct comparison between studies, with published ratios for ^{137}Cs standards ranging from 0.66-1.96 (Lee et al. 1993; Chao and Tseng, 1996; Taylor et al. 2008). Sensitivities measured for ^{135}Cs, ranging from 18,300-19,300 counts per ng/L, are in good agreement with the average ^{133}Cs sensitivity (20,500 counts) over the same runs (Figure 2.3A). At a ^{137}Cs concentration of 2.5 ng/L, gamma spectrometry and ICP-MS results are in good agreement (2.45±0.28 ng/L and 2.53±0.14 ng/L for ICP-SFMS and gamma spectrometry, respectively) (Figure 2.3B). At 0.1 ng/L, there is an increased discrepancy between the two techniques (0.11±0.04 ng/L for ICP-SFMS and 0.19±0.04 ng/L for gamma spectrometry) due to the weaker signal and relative increase in ^{137}Ba contribution.

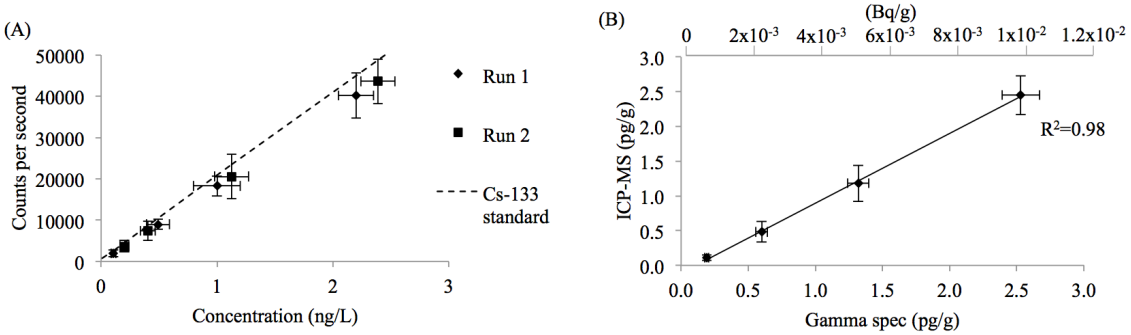

Figure 2.3. (A) Caesium-135 measured following peak correction using the natural ^{135}Ba/^{138}Ba isotope ratio. (B) Comparison of ICP-MS and gamma spectrometry measurements for ^{137}Cs standard solution. Points in (A) and (B) represent an average of 4 repeat runs

Barium derived from the sample and the reagents used in the chemical separation procedure is the primary limitation to the detection limits achievable, as opposed to the capability of the instrument itself. The extent of Ba separation can be monitored and corrected for using ^{138}Ba (natural abundance 71.7%) and known ^{135}Ba/^{138}Ba and ^{137}Ba/^{138}Ba ratios. However any correction will increase the uncertainty in measured values, and will have a more significant impact with increasing contamination and lower radiocaesium concentrations (Figure 2.4). The accuracy of this correction is also

dependent on accounting for instrumental mass bias, which is a drawback to the ICP-MS technique. The absence of a standard material with a certified $^{135}Cs/^{137}Cs$ value makes mass bias correction challenging (Taylor et al. 2008; Isnard et al. 2009). A linear correction was applied based on repeated measurements of stable $^{135}Ba/^{138}Ba$ and $^{137}Ba/^{138}Ba$ values in Cs-free solutions on the day of measurement using the equation $t=m*(1+\Delta Mf)$, where t and m are the true and measured ratios, respectively, ΔM is the difference in mass of the two isotopes, and f is the mass bias correction factor. Given the instrumental sensitivity, a linear correction was considered to be acceptable rather than exponential or power laws.

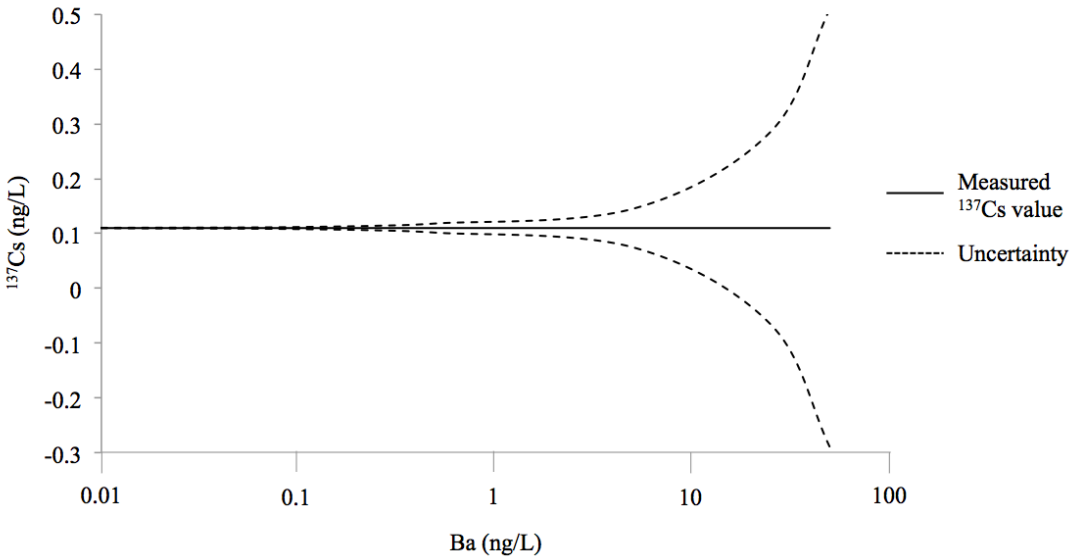

Figure 2.4. Impact of Ba procedural concentration on the measurement precision of a 0.1 ng/L ^{137}Cs solution

Correcting for Ba decontamination means the optimal detection limit (1 pg/L) is lower than has been achieved for ^{135}Cs and ^{137}Cs (average 0.05 ng/L over the run data presented in Figure 2.3) (Table 2.2). The LOD for real samples is calculated as the concentration of 3 times the standard deviation of the background at masses 135 and 137 in the procedural blank. Developing thorough cleaning procedures for resins, columns and labware, and use of high purity reagents significantly reduced the Ba procedural blank from 40-50 ng/L to 3-5 ng/L for Sellafield-contaminated Irish Sea sediment (Appendix C, page 159-163). The difficulty in reducing this value further suggests Ba is present as a result of general environmental contamination, with

minimum concentrations of 1.9±0.1 ng/L, 1.0±0.1 ng/L and 0.7±0.04 ng/L measured in sub-boiled HNO_3, Milli-Q water and 2% HNO_3, respectively. Coupling the chemical separation online with ICP-SFMS (Alonso, 1995; Moreno et al. 1999; Song et al. 2001; Pitois et al. 2008; Taylor et al. 2008; Liezers et al. 2009) may reduce the procedural blank further by minimising reagent volumes and achieving a more efficient Cs/Ba separation. Alternatively, a separation technique that can elute Cs in dilute HNO_3 would enable direct sample introduction, reducing the procedural time and therefore environmental Ba contamination.

The procedure developed demonstrates an advance in the sensitivities achievable for ICP-MS measurement of $^{135}Cs/^{137}Cs$ in environmental samples, with the instrument capable of reaching a detection limit to as low as 1 pg/L. The methodology developed enables low-level measurement of $^{135}Cs/^{137}Cs$, which has the potential to be a powerful forensic tool in identifying the source of radioactive contamination compared to measurement of ^{137}Cs alone.

2.4 Conclusions

The method presented provides precise determination of $^{135}Cs/^{137}Cs$ using ICP-SFMS at concentrations representative of environmental samples. These medium (^{137}Cs) and long-lived (^{135}Cs) fissionogenic radionuclides are of growing importance in waste characterisation at nuclear sites and repositories where they contribute to long-term radionuclide inventory. They are of additional interest as the environmental $^{135}Cs/^{137}Cs$ signature reflects contributions from one or more sources (variations in reactor type, fuel burn-up, weapons' characteristics) and accurate measurement can therefore be applied to nuclear forensics to identify the source of radioactive contamination and as a dating tool in some circumstances.

Detection at low levels has been achieved by development of a robust procedure incorporating digestion of solid samples, chemical separation and quantification by ICP-SFMS. The Thermo Element XR combined with the CETAC Aridus II desolvating sample introduction system and Jet interface can achieve up to 80,000 counts for a 1 ng/L ^{133}Cs solution, a 100-fold increase compared to the standard instrument setup. In the current method the best detection limit achieved for a pure ^{133}Cs standard solution is

1 pg/L, which puts ICP-SFMS in a position where it can rival radiometric techniques in terms of sensitivities achievable for short-lived radionuclides such as ^{137}Cs.

The main factor affecting the ultra low-level measurement of ^{135}Cs and ^{137}Cs is the concentration of isobaric ^{135}Ba and ^{137}Ba contamination in the measurement solution. This necessitates a correction using natural Ba isotope ratios, leading to increasing uncertainty with decreasing ^{135}Cs and ^{137}Cs concentration. A future aim is to further reduce this contamination, as the ICP-SPMS instrumental detection limits for pure Cs are two orders of magnitude lower than are practically measurable in sediment samples (because of residual Ba contamination). Sample preparation has focused on minimising the number and volume of reagents used, and has been performed using the cleanest possible conditions and reagents. At the low levels being aimed for, the Ba concentration inherently present in the reagents is often higher than that of ^{135}Cs and ^{137}Cs in the samples.

The sensitivities achieved are applicable to measurement of the key fissionogenic Cs isotopes in environmental samples, and the methodology developed can be extended further. For example, other long-lived, low abundance radionuclides such as ^{59}Ni and ^{93}Zr (activation and fission products, respectively) are not detectable by radiometric techniques, but like ^{135}Cs will contribute to the long-term radionuclide inventory of any geological repository. Furthermore, ^{90}Sr is a medium-lived radionuclide of significant interest with regards to waste disposal and environmental monitoring. Traditionally, ICP-MS has offered reduced analytical time for ^{90}Sr compared to radiometric techniques at the expense of sensitivity. The analytical development described involving instrumental setup offered in this study may provide the improvement in sensitivity that can make ICP-MS a realistic alternative for routine analysis of ^{90}Sr. This combined with a higher sample throughput, offers more rapid assessment and clean up of nuclear sites, and with potential economic benefits.

Chapter 3: Calixarene-based Extraction Chromatographic Separation of ^{135}Cs and ^{137}Cs Prior to ICP-MS Analysis

Abstract

Radioactive caesium isotopes ^{135}Cs and ^{137}Cs are high yield fission products that have entered the environment as a result of anthropogenic nuclear activities. Advances in the sensitivities achievable by sector field inductively coupled plasma mass spectrometry (ICP-SFMS) offer the prospect of measuring both shorter and longer-lived radionuclides, thus expanding options for environmental and contaminated land assessment. Accurate detection will also enable measurement of ^{135}Cs/^{137}Cs ratios, which can be used as a forensic tool in determining the source of nuclear contamination.

The critical requirement for accurate ^{135}Cs and ^{137}Cs detection is the effective chemical separation of isobaric interferences from ^{135}Ba and ^{137}Ba prior to sample introduction. A number of exchange materials can effectively extract Cs; however, non-quantitative elution of Cs from these exchangers makes subsequent ICP-MS quantification challenging. A novel extraction chromatographic resin has been developed by dissolving Calix[4]arene-bis-(tert-octylbenzo-crown-6) (BOBCalixC6) in octanol and loading onto pre-filter resin material. Preparation of the material takes less than 1 hour, and at an optimal concentration of 3 M HNO_3 shows high selectivity towards Cs, which is effectively eluted in 0.05 M HNO_3. The procedure developed shows high Cs selectivity and Ba decontamination in solutions containing alkali metals, fission products, as well as a saltmarsh sediment contaminated by aqueous discharges from a nuclear fuel reprocessing facility. Repeated tests suggest the resin can be re-used up to 4 times, which is significant given the high cost of BOBCalixC6. For low-level ICP-SFMS quantification, more complex sample matrices benefit from a cation exchange chromatography pre-separation stage, which improves the performance of BOBCalixC6 with regards to Cs recovery and Ba decontamination.

3.1 Introduction

High yield fission products ^{135}Cs and ^{137}Cs have entered the environment from nuclear power generation and reprocessing, nuclear accidents and atmospheric weapons' test fallout (Chao and Tseng, 1996; Hou and Roos, 2008, Taylor et al. 2008). Caesium-135 (half-life 2.5×10^6 years) is not frequently investigated but is a major contributor to the long term radiological risk associated with deep geological disposal. In contrast, ^{137}Cs (half-life 30.1 years) is routinely measured in radiation protection, environmental monitoring and waste characterisation (Moreno et al. 1999; Song et al. 2001; Hou and Roos, 2008). Caesium-137 is commonly measured using high-resolution gamma spectrometry, whilst radiometric detection of ^{135}Cs is considerably more challenging, since it is a pure beta emitter with a low specific activity and always associated with ^{137}Cs, which has an activity concentration that is 5 orders of magnitude higher. Mass spectrometry has been successfully applied to ^{135}Cs measurement; with ICP-MS the most frequently used approach (Alonso et al. 1995; Meeks et al. 1998; Moreno et al. 1999; Song et al. 2001; Granet et al. 2008; Taylor et al. 2008; Liezers et al. 2009; Russell et al. 2014; Ohno and Muramatsu, 2014; Zheng et al. 2014). Furthermore, accurate measurement of ^{135}Cs/^{137}Cs ratios is of interest to nuclear forensics, which may utilise the variability of ^{135}Cs/^{137}Cs ratios associated with the source of contamination (Lee et al. 1993; Chao and Tseng, 1996; Taylor et al. 2008; Russell et al. 2014).

The primary challenge in ICP-MS measurement is removal of isobaric interferences from naturally occurring ^{135}Ba and ^{137}Ba prior to measurement. There has been extensive development of exchange materials for radiocaesium isolation, primarily focusing on ^{137}Cs separation from other fission products and alkali metals (Table 1.7, page 17) (Marsh et al. 1994; Gaur, 1996; Dozol et al. 1999). A limit to some of these materials with regards to ICP-MS measurement is the non-quantitative elution of Cs (Dozol et al. 1999). For example, ammonium molybdophosphate (AMP) has been used as an initial ^{135}Cs/^{137}Cs separation stage for ICP-MS-based procedures (Taylor et al. 2008; Russell et al. 2014). The drawback to this technique is that dissolution of the material and liberation of Cs requires an alkaline solution (Chao and Tseng, 1996; Pibida et al. 2004; Karam et al. 2002; Taylor et al. 2008; Delmore et al. 2011; Russell et al. 2014), necessitating additional separation prior to quantification. This lengthens the procedure, introduces additional reagents, and increases potential Ba contamination,

thus impacting the precision of low-level $^{135}Cs/^{137}Cs$ measurements. Ion exchange chromatography has also been applied to ^{135}Cs and ^{137}Cs separation; with Cs elution achieved using both HCl (Lee et al. 1993; Delmore et al. 2011; Snyder et al. 2012) and HNO_3, (Shiho et al. 2011; Russell et al. 2014(A)). The drawback to this technique with regards to Ba contamination is that high reagent and resin volumes are often required in order to achieve an effective separation. For ICP-MS procedures, a combination of high Cs selectivity and straightforward back-extraction is desirable.

Calixarenes are macrocyclic extractants (Ikeda and Shinkai, 1997; Dozol et al. 1999; Mohapatra et al. 2006) that are potentially well suited to Cs separation prior to ICP-MS quantification, and have been widely applied to^{137}Cs isolation from a range of samples including acidic nitrate solutions, acidic liquid waste, spent nuclear fuel, and Savannah River Site tank wastes (Horwitz et al. 1996; Bonnesen et al. 1998; Grunder et al. 1999; Riddle et al. 2005). Caesium purification has previously focused on separation from fission products and alkali metal ions, specifically Na and K. Calix[4]arenes in the 1,3 alternate conformation with bis-crown-6 ethers, for example BOBCalixC6 (calix[4]arene-bis-(tert-octylbenzo-crown-6)) (Figure 3.1) show the highest Cs selectivity (Bonnesen et al. 1998; Sachleben et al. 1999; Haverlock et al. 2000; Leonard et al. 2001; Riddle et al. 2005). This is due to the crown-6 cavity size (1.70Å) being matched closely to the Cs ionic radius (1.67 Å), giving Cs/Na and Cs/K separation factors exceeding 10^4 and 10^2, respectively (Asfari et al. 1995; Casnati et al. 1995; Lamare et al. 1999; Sachleben et al. 1999; Haverlock et al. 2000; Thuery et al. 2000; Zhang et al. 2009). However, there are no data published on Cs/Ba separation factors.

The general procedure for calixarene-based ^{137}Cs extraction (Equation 3.1 (Mohapatra et al. 2006)) is to mix equal volumes of organic and aqueous phases, separate the phases by centrifugation and then measure ^{137}Cs in the two phases by gamma spectrometry. Contact times range from one minute (Bonnesen et al. 1998; Riddle et al. 2005), to 12 hours (Ikeda and Shinkai, 1997), and the reaction temperature is often controlled, as higher distribution ratios have been recorded at lower temperatures (Bonnesen et al. 1998; Riddle et al. 2005). Caesium has been successfully extracted from ~2-4 M HNO_3, with back-extraction achieved using either ~0.05 M HNO_3 or water due to the low distribution coefficient (K_d) for Cs under these conditions, or using 6-8M HNO_3 due to competitive extraction of HNO_3 (Asfari et al. 1995; Kim et al. 1998; Dozol et al. 1999). Dilute HNO_3 is preferential to water, as the latter can form cloudy phases following

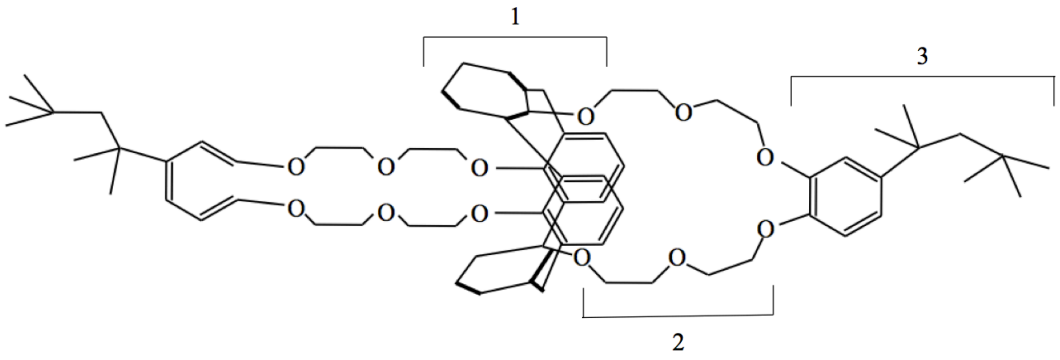

Figure 3.1. Structure of Calix-4-arene-bis-(tert-octylbenzo-crown-6) (BOBCalixC6)

1. Calix-4-arene (4 phenolic units linked by methylene groups) in the 1,3 alternate conformation; 2. Crown-6 extractant; 3. Octyl-benzo group

interaction, whereas the minimal ionic strength provided by dilute HNO_3 can prevent this third phase formation. Other additives have been used to improve performance compared to using HNO_3 alone, including non-radioactive $CsNO_3$, NaOH, and alkylamine (Bonnesen et al. 1998; Leonard et al. 2001; Riddle et al. 2005; Mohapatra et al. 2006).

$$Cs^{+}_{(aq)} + NO_3^{-}{}_{(aq)} + X_{(org)} + nH_2O_{(aq)} \rightleftharpoons [CsX]^{+} \cdot [NO_3^{-} \cdot nH_2O]_{org} \qquad (3.1)$$

Where X is the calixarene

There are fewer examples of calixarene-based chromatographic separation procedures, which can offer rapid adsorption and elution, higher separation factors, improved mechanical strength and better resistance and stability to HNO_3 and temperature than batch procedures, providing the binding characteristics and selectivity of the calixarene can be preserved (Dietz et al. 2006; Zhang et al. 2009; Zhang and Hu, 2010; Xiao et al. 2014). Dietz et al. (2006) was the first to develop an extraction chromatography procedure, impregnating 1,3-calix[bis]-*o*-benzo-crown-6 onto an inert polymeric substrate (Amberlite XAD-7, Sigma Aldrich). The material showed high selectivity towards Cs in 0.05 M HNO_3, which was successfully eluted in 6 M HNO_3. The Cs recovery decreased in solutions with >0.01 M K concentrations, whilst the mechanical

strength, adsorption capacity, and resistance to acids and irradiation were low when considering Cs separation from high level waste solutions (Xiao et al. 2014). Further procedures have been developed through impregnation of a calix[4]arene-crown-6 into the pores of SiO_2-P particles, where P is a styrene-divinylbenzene copolymer (Zhang et al. 2009; Zhang and Hu, 2010). With this setup Cs has been effectively separated from acidic solutions containing fission and non-fission products found in high-level waste solutions.

Previous chromatographic procedures involved lengthy and complex preparation procedures, with a focus on ^{137}Cs separation from nuclear waste samples. This study presents the development of a novel extraction chromatographic resin using Calix[4]arene-bis-(tert-octylbenzo-crown-6; BOB-calixC6). The procedure developed is straightforward and rapid, both in terms of synthesis, and the separation procedure for isolating ^{135}Cs and ^{137}Cs from isobaric ^{135}Ba and ^{137}Ba interferences to enable accurate low-level ICP-SFMS detection.

3.2 Characterisation of chromatographic materials

3.2.1 Instrumentation

Mass spectrometric measurement of Cs and Ba were performed using a Thermo-Scientific X-series II bench-top ICP-QMS. Radiometric measurements of Cs (mixed ^{135,137}Cs) and ^{133}Ba tracers were performed using a Canberra well-type HPGe detector having 10% efficiency at 662 keV gamma energy for ^{137}Cs (^{137m}Ba). Analysis of the energy spectra and calculation of radionuclide activity was performed using Fitzpeaks software (JF Computing, Stanford in the Vale, UK).

3.2.2 Reagents and materials

Stable Cs and Ba standard solutions were prepared from 1000mg/L elemental stock solutions (Inorganic Ventures) in 0.1 % HNO_3 (v/v). Teflon sub-boiled HNO_3, sub-boiled HCl and high purity de-ionised water (resistivity higher than 18.2 MΩ) produced from a Q-Pod Millipore System (Merck) were used throughout. For more complex sample matrices, cation exchange chromatography (Dowex AG50W-x8, BioRad, USA) was investigated as an initial clean-up stage prior to the calixarene separation.

3.2.3 Preparation of chromatographic materials

BOBCalixC6, sold as MacroLig 209R, was supplied from IBC Advanced Technologies (American Fork, Utah, USA). Octanol (HPLC grade, Aldrich, UK) was selected as a suitable diluent based on its previous use in chromatographic separation (Zhang et al. 2009), and suitable dielectric constant value (Table 3.1) (Appendix F, page 169-172). A 0.02 M solution was prepared by diluting 0.116 g BOBCalixC6 in 5 g 1-octanol.

Three grams of BOBCalixC6/octanol was mixed with 2 g hydrophilic, macroporous, acrylic polymeric pre-filter resin (100-150 μm, Triskem International) drop-wise with constant stirring to prevent clumping and to ensure even distribution of the extractant on the resin material. Up to 4 g of BOBCalixC6/octanol can be added to 2 g of pre-filter resin, however for testing purposes, 3 g of material was added to 2 g of pre-filter resin. Following this, Milli-Q water was added drop-wise to form a paste. Adding water too rapidly leads to poor dispersion of the chromatographic material in the aqueous medium, which ultimately impacts on the column performance. The slurried material was loaded into a 0.5 cm diameter column to a depth of 4 cm. The total time to create this material is <1 hour, with each batch producing 5 columns.

Diluent	Dielectric constant	D_{Cs}
Nitrobenzene	34.8	5.2
Dichloromethane	16.7	3.9
1-octanol	10.4	2.9
1-decanol	8.1	2.75
Chloroform	4.8	0.62
Toluene	2.4	0.3
Benzene	2.2	0.31
n-dodecane	2	7.5×10^{-4}

Table 3.1. Properties of diluents for a 4.8×10^{-3} M calix[4]arene-bis(crown-6) at 298 K (Mohapatra et al. 2006)

3.2.4 Characterisation of BOBCalixC6 column

BOBCalixC6 was characterised for Cs capacity and efficiency of separation from other elements, primarily Ba, as well as fission products and other gamma-emitting radionuclides. The stages investigated were sample load, extraction of other ions, elution of Cs, and regeneration/reuse of the resin material. The laboratory temperature was maintained at ~18^0C, but was not accurately monitored. The procedure focused on the effect of HNO_3 concentration only, with no additional modifying chemicals used.

A blank column was prepared by loading 3 g octanol onto 2 g pre-filter resin. This was mixed with Milli-Q water and loaded onto a 0.5 cm x 4 cm column. A 5 mL 1 M HNO_3 solution spiked with 5 Bq ^{137}Cs was loaded onto the column, followed by a 10 mL 1 M HNO_3 wash. 75±4% of the Cs was recovered in the sample load, with 99±3% in the combined load and wash fractions, showing that octanol and pre-filter resin do not show an affinity for Cs.

Caesium load, elution characteristics and K_d values were determined for columns with a starting BOBCalixC6 concentration of 0.02 M. Caesium load and contaminant elution conditions were assessed using HNO_3 concentrations ranging from 1 to 4 M. Initial Cs elution was performed using 0.05 M HNO_3, with a final column stripping stage (to remove residual Cs) using $5x10^{-4}$ M HNO_3. No Cs breakthrough was observed in 3 M HNO_3 for load and extraction volumes up to 5 mL (Figure 3.2), with a K_d of 5,300 mL/g. By comparison, 16.7 %, 1.3 % and 32.6 % Cs was detected following 5 mL load and extraction volumes at 1 M, 2 M and 4 M HNO_3 concentrations, respectively, with K_d values of 56, 829 and 26 mL/g, respectively. A concentration of 0.05 M HNO_3 quantitatively eluted Cs from the column, with a K_d value of <1 mL/g. Caesium elution is therefore achievable in ≥4 M HNO_3, and dilute HNO_3 (≤0.05 M HNO_3), with the latter offering the advantage of immediate ICP-MS sample introduction without further sample treatment.

The effect of BOBCalixC6 concentration on Cs separation from Ba was determined by loading a 100 µg/L standard solution in 5 mL 3 M HNO_3, followed by 5x1 mL 3 M HNO_3 column washings and 10 mL 0.05 M HNO_3 elution with BOBCalixC6 concentrations of 0.01 M and 0.02 M. At both concentrations (Figure 3.3), Ba is eluted in the load and wash stages. However, at 0.01 M, 5.5 % Cs was also detected in the

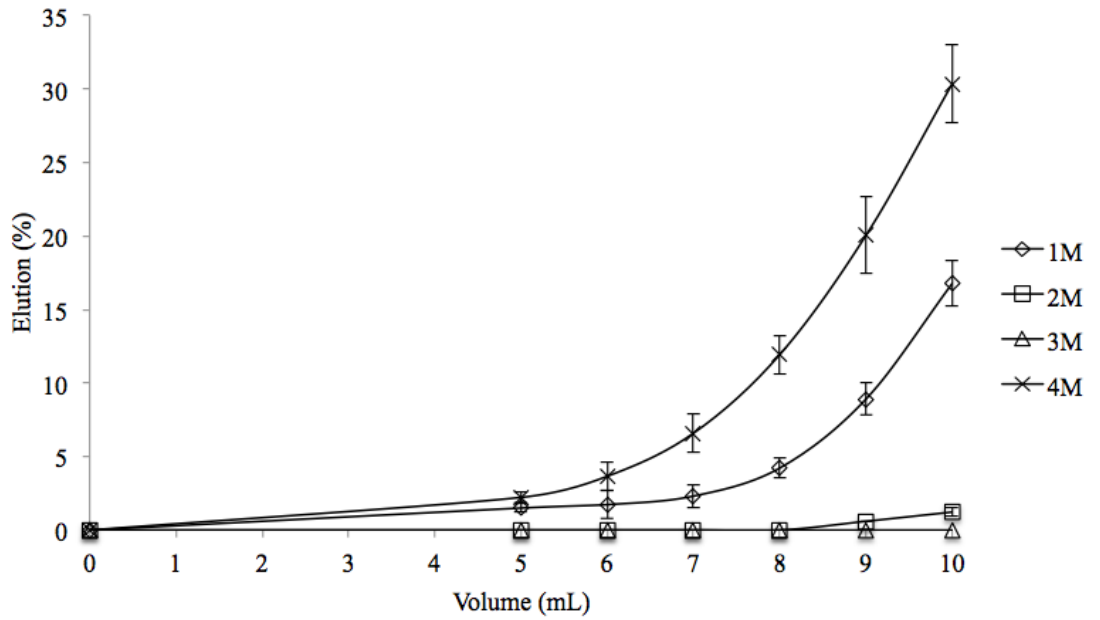

Figure 3.2. Effect of nitric acid concentration on the Cs elution from 0.02M BOBCalix C6 following a 5mL sample load

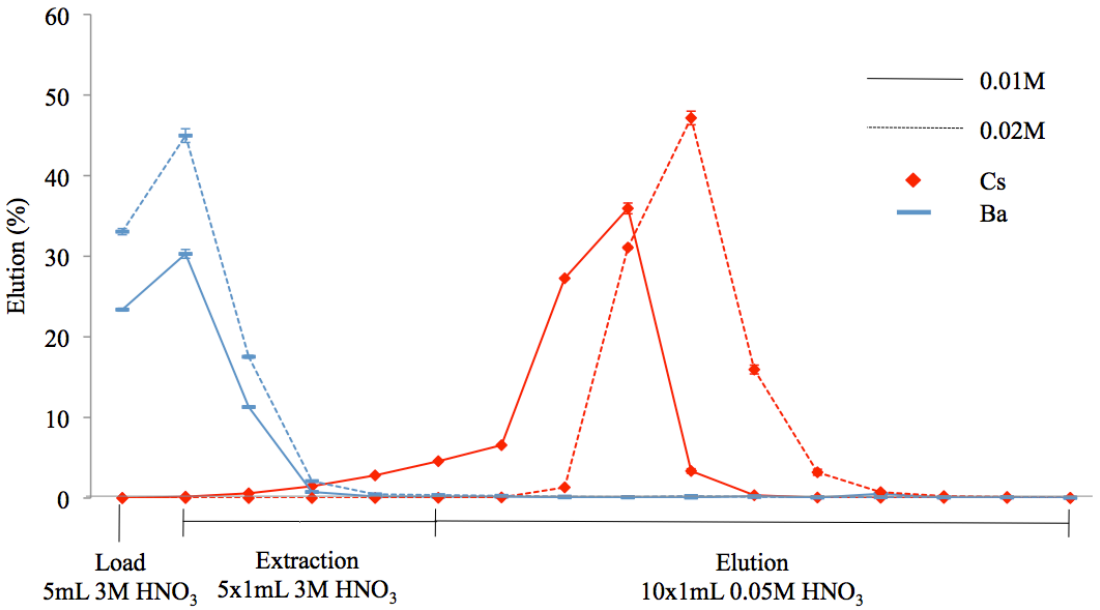

Figure 3.3. Comparison of Cs and Ba elution profiles for 0.01 and 0.02M BOBCalixC6 concentrations

column washing stage, compared to <0.1 % at 0.02 M. This higher concentration requires an elution volume of 7 mL 0.05 M HNO_3 to elute Cs, compared to 5 mL for 0.01 M BOBCalixC6. The high cost of BOBCalixC6 necessitates minimising the concentration used, however for effective retention of Cs in the load and extraction stages, a 0.02 M BOBCalixC6 concentration was chosen for subsequent use.

The decontamination factors of Ba, alkali metals and fission products were determined from a 100 µg/L multi-element solution (Figure 3.4). Rubidium showed a low decontamination factor of 30±1, with values of other elements ranging from 880+40 (Magnesium) to 12,500+500 (Yttrium). The Rb value is in line with other studies (Zhang and Hu, 2010), and is due to the ionic radius (1.52 Å) being close to that of Cs (1.67 Å) and therefore the calixarene cavity (1.70 Å). The results for other alkali metals support this, with a decreasing decontamination factor in the order Li>Na>K>Rb>Cs, corresponding to an increasing ionic radius and disparity with the calixarene cavity size. The partial retention displayed by Rb did not impact the recovery of Cs, and would not affect ICP-MS quantification of $^{135}Cs/^{137}Cs$.

The Ba decontamination factor (2,940±80) indicates that the calixarene method is capable of effective Cs / Ba separation. This is beneficial to low-level $^{135}Cs/^{137}Cs$ measurements, where Ba present in the materials and reagents used will increase the procedural blank concentration, which impacts the accuracy of $^{135}Cs/^{137}Cs$ measurements by ICP-MS. A previous chemical separation procedure consisting of AMP followed by cation exchange chromatography achieved a minimum Ba procedural blank concentration of 5 ng/L, corresponding to a detection limit (calculated as the concentration of 3 times the standard deviation of the blank at masses 135 and 137) of 0.05 ng/L for both ^{135}Cs and ^{137}Cs (equivalent to $2.1x10^{-6}$ and 0.2 Bq/L, respectively) (Russell et al. 2014(A)). The eluted Cs fraction following cation exchange must be evaporated to dryness and then brought up in dilute HNO_3 for ICP-MS measurement. For low-level measurements, this evaporation stage introduces an additional source of Ba contamination, which can be removed by the addition of a calixarene separation stage that allows immediate ICP-MS measurement of the eluted Cs fraction in 0.05M HNO_3. By reducing the calixarene column length from 4 cm to 2 cm, and the load volume from 5 mL to 0.5 mL 3 M HNO_3, Ba was eluted in 5 mL 3 M HNO_3, whilst Cs was eluted in 3 mL 0.05 M HNO_3. Limiting the elution volume reduced the extent of sample dilution, and achieved a Ba procedural blank of 2 ng/L, improving the detection

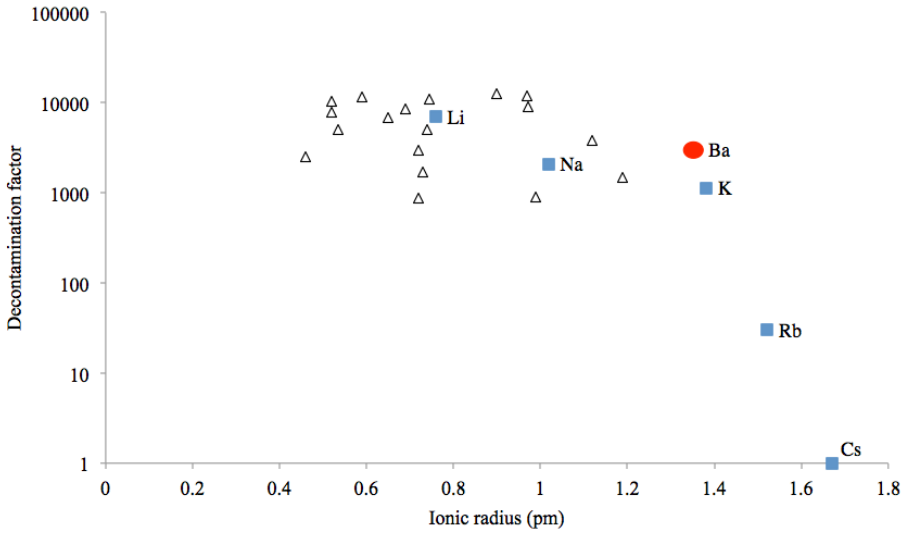

Element	Decontamination factor
Li	7113±288
Na	2067±80
K	1135±123
Rb	30±0.61
Cs	1±0.09
Mg	878±42
Ca	905±103
Sr	3815±107
Ba	2940±84
Mn	2485±97
Cr	10362±318
Al	4987±306
V	11459±383
Mo	6790±256
Ni	8519±530
Zr	3013±117
Cu	1686±66
Zn	5101±185
Co	11006±1355
Y	12494±849
Cd	12039±908
Pb	1495±62
Th	9059±427
U	7854±207

Figure 3.4. Decontamination factor of multiple elements from a 0.02 M BOBCalixC6 column. Alkali metals are highlighted in blue to show the negative correlation between ionic radius and decontamination factor

limit to 0.02 ng/L for ^{135}Cs and ^{137}Cs (equivalent to 8.2×10^{-7} and 0.06 Bq/L, respectively).

The Cs capacity was determined by loading increasing quantities of stable Cs in 3M HNO_3. The Cs concentration was determined by ICP-QMS, which was used to calculate the amount retained on the column, with a calculated value of ~25 µg Cs (Figure 3.5). The saturation curve was also used to further characterise the BOBCalixC6 column (Figure 3.6 and Table 3.2) (Braun and Ghersini, 1975). Free column volume (V_m) was determined by successively loading 1 µg/L Ba in 3 M HNO_3 in 100 µl increments; with V_m the volume at which the Ba concentration eluted was equal to that in the 1 µg/L standard (V_m = 1.8 mL). The height equivalent to a theoretical plate (HETP) was calculated by dividing the length of the column in mm by the number of theoretical plates (17) (calculation in Table 3.2). This gave a value of 2.4 mm. A lower HETP value indicates higher column efficiency, as more theoretical plates are contained in a given length of column. The HETP value calculated for BOBCalixC6 is higher than a chromatographic setup using 1,3-calix[4]bis-o-benzo-crown-6 (BC6B) (HETP=0.5 mm) (Table 3.3). Directly comparing HETP values can only be used to give a general trend, due to variation in experimental conditions between studies such as temperature, flow

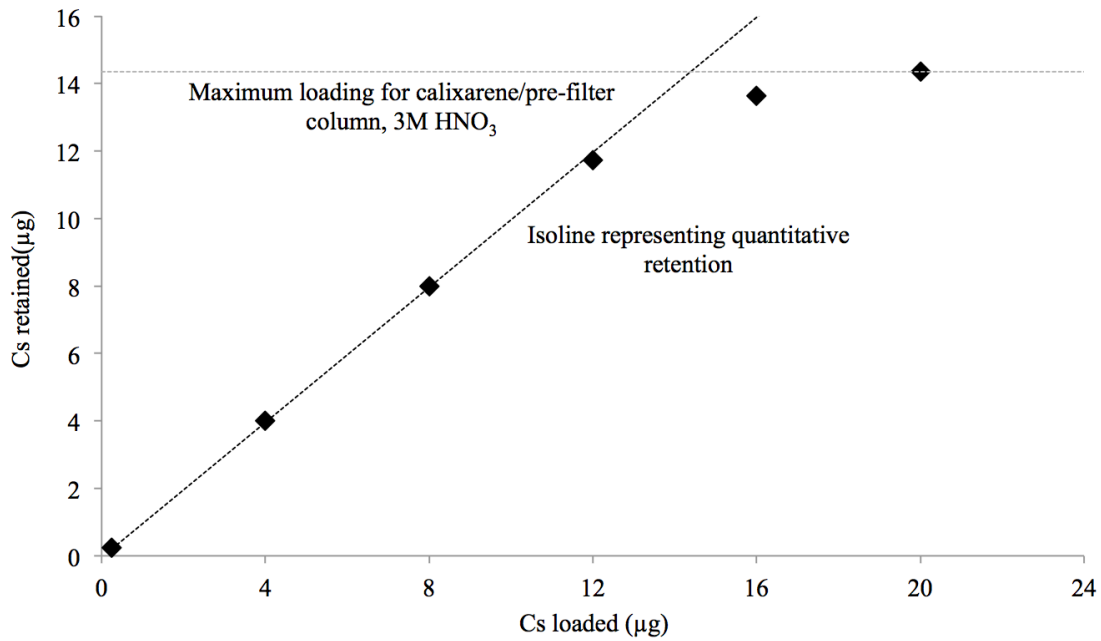

Figure 3.5. Cs recovery vs. initial loading on a 4x0.5 cm 3:2 (w/w) BOBCalixC6-octanol/pre-filter column from 3 M HNO_3. Plot adapted from Warwick and Croudace (2006)

rate, and migration distance (Braun and Ghersini, 1975), as well as the methods used to calculate the HETP and number of theoretical plates (Braun and Ghersini, 1975; Agilent, 2012). Despite the moderate capacity and column efficiency, the procedure developed is proven to be highly selective towards Cs over multiple elements, primarily isobaric Ba interferences, with a final stage calixarene separation effectively reducing the Ba procedural blank concentration for existing procedures, improving the detection limits of ICP-SFMS with regards to low-level $^{135}Cs/^{137}Cs$ measurements.

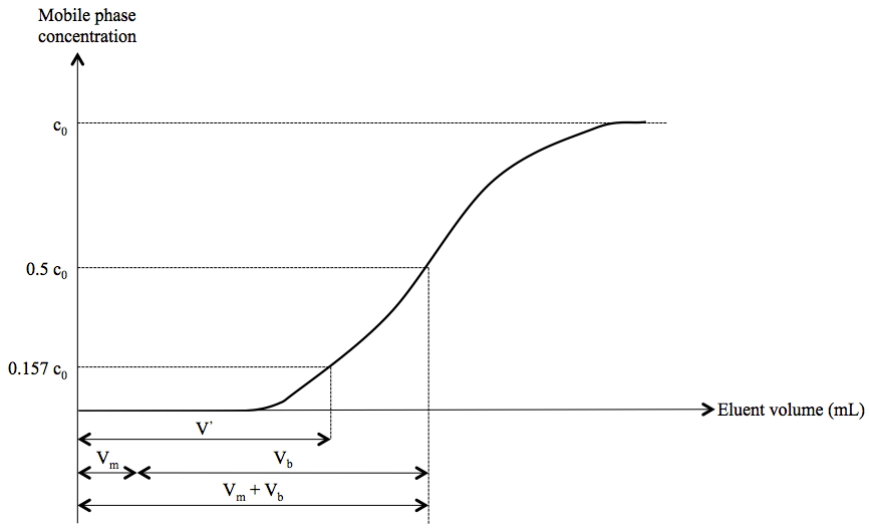

Figure 3.6. Evaluation of Cs breakthrough curve. Terms are defined in Table 3.2. Adapted from Braun and Ghersini (1975)

Parameter	Definition	Value
V_m	Free column volume (mL)	1.8
V_s	Stationary phase volume (mL)	0.6
V_b	Breakthrough volume (mL)	25.7
V_{mb}	Total breakthrough volume (mL)	27.5
	$=V_m+V_b$	
V'	Eluent volume when the concentration of the eluent reaches 0.157 C_0	23
C_0	Initial concentration	
D	Concentration distribution ratio	44.6
	$= V_b/V_s$	
N	Number of theoretical plates of the bed	17.0
	$= V_{mb} \times V'/(V_{mb} - V')^2$	

Table 3.2. Properties of the BOBCalixC6 chromatographic material determined from the Cs saturation curve (Figure 3.6) (Braun and Ghersini, 1975)

Reference	Dietz et al. (2006)	This study
Stationary phase	0.05 M BC6B in 1,2 dichloroethane	0.02 M BOBCalixC6 in 1-octanol
Support	Amberchrom CG-71m	Eichrom pre-filter resin
Particle diameter	50-100 µm	100-150 µm
Preparation time	Several days	<1 hour
V_s, mL/mL of bed	0.1	0.6
FCV	0.7	1.8
V_s/Vm	0.1	0.3
Number of theoretical plates	40	17
HETP	0.5	2.4

Table 3.3. Comparison of the characteristics of Cs-selective extraction chromatographic materials

3.3 Application to sediment samples

The performance of the separation procedure was assessed using a sediment core sample collected from the Ravenglass salt marsh, Cumbria, UK, in September 2012. This site has been contaminated with ^{137}Cs arising from authorised aqueous discharges from the Sellafield reprocessing site, and represents a good test for the applicability of the BOBCalixC6 procedure. Sediments were digested with *aqua regia* for 4 hours, with an average Ba concentration in the sediment leachate of 43.2±0.5 mg/L.

Three separation procedures were then investigated on the sediment leachate (Figure 3.7):

(i) BOBCalixC6 only;
(ii) Cation exchange + BOBCalixC6;
(iii) 2 x cation exchange + BOBCalixC6

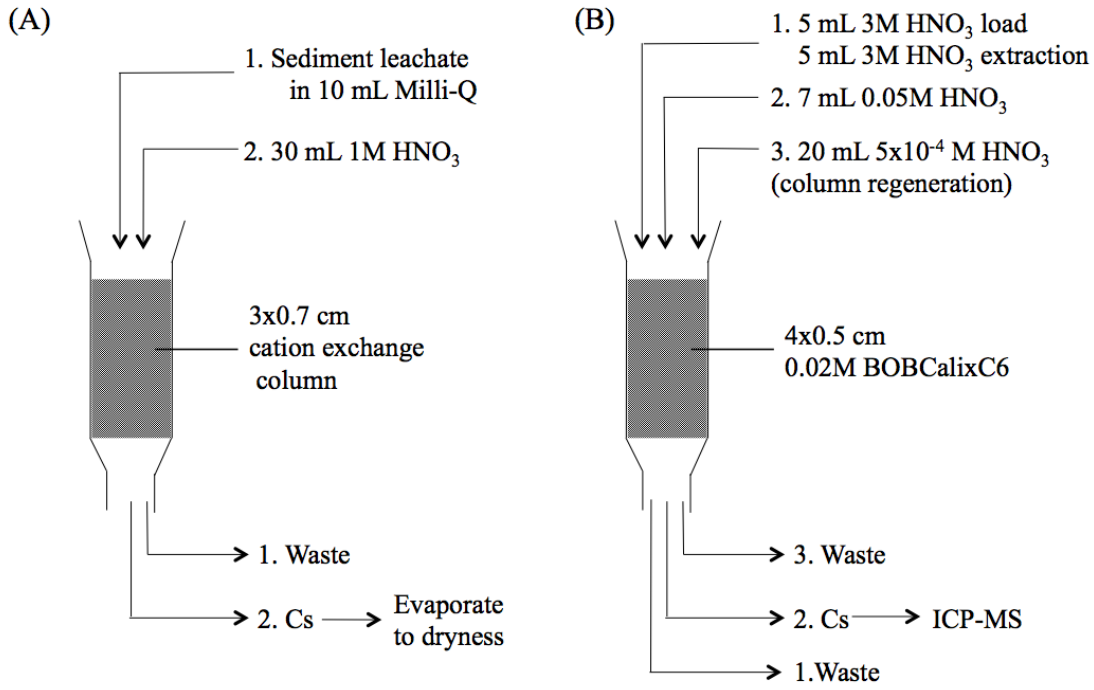

Figure 3.7. Summary of separation procedures for ^{135}Cs and ^{137}Cs, incorporating (A) Cation exchange chromatography and (B) BOBCalixC6 extraction chromatography

An initial cation exchange separation was investigated to determine if the sediment matrix impacted the performance of BOBCalixC6. Following the $5x10^{-4}$ M HNO_3 resin wash, the column in procedure (i) was loaded with second sediment leachate to determine the potential for re-using the material. Recovery for all procedures was determined by gamma spectrometry as the percentage of ^{137}Cs recovered from the sediment leachate (Table 3.4).

3.3.1 Caesium-137 recovery

The ^{137}Cs recovery for procedure (i) was 90±6 and 90±7 % for the 1st and 2nd cyles, respectively. Following the first cycle, 2.3±0.7 % of Cs remained on the column following the wash, which was eluted with a further 20 mL $5x10^{-4}$ M HNO_3 prior to loading of the second leachate sample (giving a total Cs recovery of 102±6%). The total recovery in the 2nd cycle was comparable at 95±6%. This implies BOBCalixC6 is capable of dealing with a complex sample matrix, and that the material can potentially be re-used, although a column wash of 40 mL $5x10^{-4}$ M HNO_3 is required between samples, compared to 20 mL used for standard solutions.

Procedure	Cation exchange (CE) (%)		Calixarene (BCB6) (%)				Total (%)
	1	2	Wash	Elution	Regen	Resin	
(i) BCB6	-	-	1.0±0.4	89.7±6.1	8.7±1.4	2.3±0.7	101.7±6.4
(i) BCB6 Repeat	-	-	0.7±0.3	89.5±6.6	4.6±0.9	≤0.1	94.8±6.3
(iii) CE +BCB6	84.9 ±6	-	≤0.1	75.2±5.7	3±0.7	≤0.1	78.2±4.5
(iii) 2xCE +BCB6	84.6 ±6.6	78.6± 5.2	≤0.1	76.3±3.9	≤0.1	≤0.1	76.3±3.9

Table 3.4. Percentage ^{137}Cs recovery from multiple BOBCalixC6 separation procedures from an Irish Sea sediment sample

The ^{137}Cs recovery was lower for procedures (ii) and (iii), with values of 75±6 % and 76±4%, respectively. However, this increases to 86±7 % and 97±6 % if calculated as the recovery from the cation exchange stage, rather than from the sediment leachate. In addition, no ^{137}Cs was recovered for procedures (ii) and (iii) in the load stage or on retained resin material after washing, and in procedure (iii) no ^{137}Cs was detected in the regeneration fraction. This compares to ^{137}Cs detection in all fractions for procedure (i). This suggests a double cation exchange separation benefits the performance of BOBCalixC6, with the limitation of procedures (ii) and (iii) being recovery of Cs by cation exchange.

3.3.2 Use of recycled BOBCalixC6

Following the sediment leachate test, the BOBCalixC6 resin was counted for 12 hours by gamma spectrometry to ensure resin clean-up had been effective. Residual ^{137}Cs activities were below the detection limits, equivalent to 0.07 % of the total activity

loaded onto the resin. Following this, the BOBCalixC6 columns from the 3 procedures described were subjected to repeated loading of a 100 µg/L Cs+Ba standard solution to further test the potential of re-using the material (Table 3.5).

The Cs recovery and Ba decontamination achieved by BOBCalixC6 did not change significantly over the 3 runs for any of the procedures, and is comparable to results from a previously unused resin column (Table 3.5). The average Cs recovery ranged from 96.1±2.2 % to 98.8±2.7 % for the elution stage and ≤1.0 % to 3.7±0.1 % for the extraction stage. After 3 runs, the maximum Cs detected in the column wash was 0.3 %.

Cs	Unused BOBCalix C6 (%)	BOBCalix C6 only (%)	Cation exchange + BOBCalixC6 (%)	2 x cation exchange + BOBCalixC6 (%)
Load	≤0.2	≤0.2	≤0.2	≤0.2
Wash	1.6±0.1	2.5±0.1	3.7±0.1	1.0±0.1
Elution	98.1±1.5	97.2±3.4	96.1±2.2	98.8±2.7
Regeneration	≤0.2	≤0.2	≤0.2	≤0.2
Ba	**Unused BOBCalix C6 (%)**	**BOBCalix C6 only (%)**	**Cation exchange+ BOBCalixC6 (%)**	**2xcation exchange+ BOBCalixC6 (%)**
Load+ Wash	97.6±1.0	96.1±1.5	96.4±1.4	97.8±1.4
Elution	2.2±0.1	3.7±0.2	3.3±0.2	2.1±0.2
Regeneration	≤0.2	≤0.2	≤0.2	≤0.2

Table 3.5. Average performance of BOBCalixC6 from 3x loading of a 100 µg/L Cs and Ba solution. Other than the unused BOBCalixC6, the resins had previously been used in ^{137}Cs separation from Cumbrian saltmarsh sediment

The BOBCalixC6 column used in procedure (iii) achieved an average Ba recovery of 97.8±1.4 % in the load+ extraction, and 2.1±0.2 % in the elution fraction. This is comparable to the 97.6±1.0 % and 2.2±0.1 % achieved from a previously unused BOBCalixC6 column. By comparison, the average Ba recovery from procedure (i) and (ii) was marginally lower in the load+ extraction (96.1±1.5 % and 96.4±1.4 %, respectively) and higher in the elution fraction (3.7±0.2 % and 3.3±0.2 %, respectively). A single or double cation exchange separation therefore slightly improves the performance of BOBCalixC6 with regards to Cs recovery and decontamination of isobaric Ba interferences. This may be significant for ultra-low level ICP-SFMS quantification, where decontamination of Ba is the primary factor affecting accuracy and precision of $^{135}Cs/^{137}Cs$ values.

3.4 Conclusions

A novel extraction chromatographic separation procedure has been developed for separation of ^{135}Cs and ^{137}Cs, by dissolving BOBCalixC6 in octanol and loading onto pre-filter resin. Preparation of the material is rapid and straightforward, and the separation is cleaner and more efficient than batch-based calixarene procedures. Caesium extraction in 3 M HNO_3 and elution in 0.05 M HNO_3 has been effective in multi-element solutions and salt marsh sediment contaminated by a nearby fuel-reprocessing site. Straightforward extraction and elution of Cs, combined with effective decontamination of isobaric ^{135}Ba and ^{137}Ba interferences, is beneficial to ICP-SFMS quantification, which combined with advances in instrumental sensitivity will enable determination of $^{135}Cs/^{137}Cs$ values, which can potentially be used as a forensic tool to identify the source of radioactive contamination.

Reuse of the material has been successfully proven by repeat loading of ^{137}Cs-containing saltmarsh sediment and stable Cs solutions, with average recoveries of 90 % and 97 %, respectively. This is significant given the high cost of BOBCalixC6, which is a limitation to calixarene-based procedures. Results suggest isolation of ^{137}Cs from alkali metals and fission products can be achieved with chromatographic BOBCalixC6 separation alone. For low-level ICP-SFMS detection of ^{135}Cs and ^{137}Cs, more complex sample matrices may benefit from an initial cation exchange chromatography separation. This additional step offers improved BOBCalixC6 performance with regards to Cs elution and Ba decontamination.

Chapter 4: Measurement of ^{135}Cs and ^{137}Cs in the North Atlantic and Arctic Oceans

Abstract

The North Atlantic and Arctic Oceans have been contaminated by inputs of radioactive caesium isotopes from multiple sources, including atmospheric weapons test fallout and discharges from reprocessing facilities. Past measurements have focused on detection of ^{137}Cs, however recent advances in the sensitivities achievable by sector field inductively coupled plasma mass spectrometry (ICP-SFMS) have expanded measurement options, enabling detection of long-lived low abundance radionuclides including ^{135}Cs. This in turn permits the measurement of ^{135}Cs/^{137}Cs ratios, which varies depending on the source of nuclear contamination, and therefore offers a potentially powerful tool in nuclear forensics, providing more information than measurement of ^{137}Cs alone.

A procedure is presented for detection of ^{135}Cs/^{137}Cs in seawater samples in the North Atlantic and Arctic Oceans, incorporating chemical separation and ICP-SFMS detection. Caesium was initially extracted from seawater using ammonium molybdophosphate supported on silica gel (ASG), followed by further chemical separation by cation exchange and extraction chromatography, with quantification by gamma spectrometry and ICP-SFMS. The spatial distribution of ^{137}Cs activities detected by gamma spectrometry is in agreement with previous studies, with the highest activities around the East coast of Greenland reflecting older discharges from the Sellafield reprocessing site. A Thermo Element XR ICP-SFMS equipped with the Jet Interface, X-skimmer cone and Aridus II desolvating sample introduction system was set up to achieve sensitivities of up to 80,000 counts for a 1 ng/L ^{133}Cs solution, providing a detection limit of 1 pg/L. Achieving these detection limits for seawater samples is restricted by isobaric interferences arising from ^{135}Ba and ^{137}Ba, with a minimum method detection limit of 49 pg/L, which is higher than the expected range of concentrations in seawater samples (10-41 pg/L). Accelerator mass spectrometry (AMS) offers a highly sensitive mass spectrometric technique that may be applicable to detection of ^{135}Cs/^{137}Cs in seawater samples, however the complexities of optimising the instrumental setup compared to ICP-SFMS must be considered.

4.1 Introduction

The inventory of radiocaesium isotopes in the North Atlantic and Arctic Oceans has been increased by anthropogenic inputs from multiple sources, with previous studies primarily focusing on detection of ^{137}Cs (Table 1.5, page 11). Direct fallout from atmospheric weapons testing was once the dominant source of ^{137}Cs in Polar regions (Aarkrog, 1994; Kershaw and Baxter, 1995), with ~2 % of the fallout deposition a result of runoff from the land (Aarkrog 1994; Livingston et al. 1984; Cochran et al. 1995; Dahlgaard 1995). Secondly, the Chernobyl incident in 1986 was responsible for the release of approximately 100 PBq ^{137}Cs into the atmosphere, with ~1-5 PBq deposited into the Arctic Ocean, either from fallout, or outflow from the heavily contaminated Baltic and North Seas (Dahlgaard, 1995; Kershaw and Baxter, 1995; Nies et al. 1999). The high initial contamination of the Baltic Sea combined with the restricted outflow means it remains a long-term ^{137}Cs source (Kershaw and Baxter, 1995). In 1991, Chernobyl was estimated to be responsible for 50 % of ^{137}Cs in the North Sea, compared to 1-2 % in the Arctic Basin (Kershaw and Baxter, 1995). A further source of contamination is disposals of solid and liquid waste from Russian nuclear facilities into the Ob and Yenisey rivers, which drain into the Eastern Arctic Ocean, specifically the Barents and Kara Seas (Nies et al. 1999; Heldal and Varskog, 2002; Hu et al. 2010). For example, plutonium production at the Chelyabinsk Site discharged radioactive waste into the Techa River, a tributary of the Ob (Aarkrog, 1994), with more than 95 % of the total waste discharged between 1950 and 1951. The majority of ^{137}Cs released (~10 PBq) from the facility was retained in sediments close to the site (Kershaw and Baxter, 1995), as well as in reservoirs and by-pass canals at the upper reaches of the Techa River (Aarkrog, 1994).

Aqueous discharges from the Sellafield reprocessing facility, Cumbria, UK represent an on-going source of radiocaesium. Discharges peaked at 4-5 PBq per year in the mid-1970's, resulting in an Arctic Ocean ^{137}Cs 'pulse' in the late 1970's and early 1980's (Aarkrog et al. 1988; Kershaw and Baxter, 1995). Since then, releases from the site have reduced significantly (3.6×10^{-3} PBq in 2012 (SEPA, 2012)), but can still be detected and quantified (Kershaw et al. 1995). On-going discharges have led to significant deposition of ^{137}Cs in Irish Sea sediments, which now act as a continuing source of contamination by desorbing into the water column in response to the reduction in Sellafield discharges

(Kershaw and Baxter, 1995; Hunt et al. 2013). Discharges from a second reprocessing site at La Hague, France, are comparatively low, with the total contribution to the Arctic estimated as 2.3 % of the contribution from Sellafield (Kershaw and Baxter, 1995).

The transport of discharges from the Sellafield site (Figure 4.1) has led to widespread detection of ^{137}Cs, with particularly elevated activities observed in waters of polar origin along the east coast of Greenland. These higher signals represent ^{137}Cs from earlier, higher Sellafield discharges entering the Arctic, and then exiting via the East Greenland current (Aarkrog et al. 1988; Dahlgaard, 1995; Kershaw et al. 1995; Kershaw et al. 1997; Dahlgaard et al. 2004).

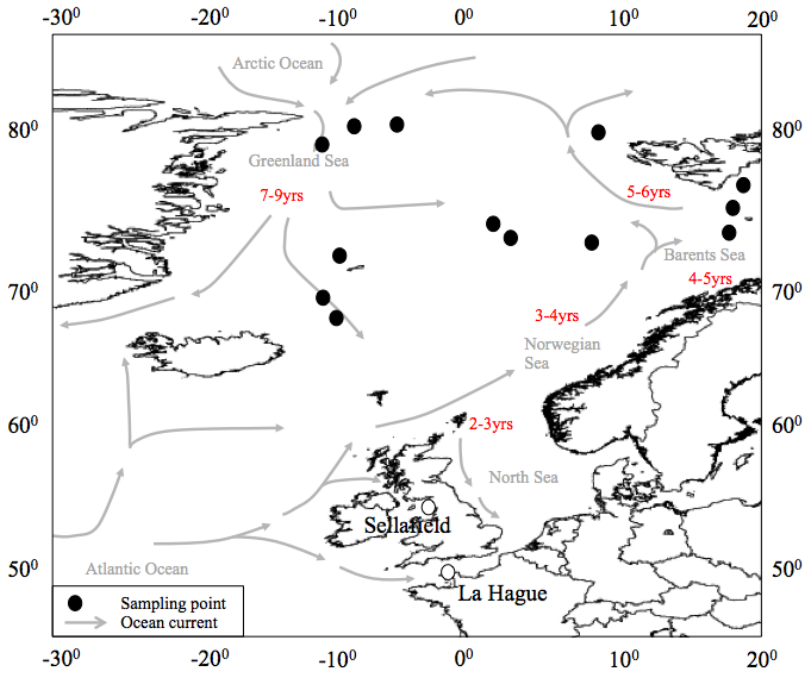

Figure 4.1. Map of the North Atlantic and Arctic Oceans, outlining major ocean currents, estimated transport times for aqueous Sellafield discharges (Kershaw and Baxter, 1995), and sampling locations during the JR271 Cruise

Multiple techniques have been applied to estimate the total activity of radionuclides in the Arctic region, with the primary issue being discrepancies between estimated and real values (Aarkrog, 1994). There are a number of uncertainties related to estimating transit times, including low spatial and temporal resolution, selecting an appropriate background level and from this determining what constitutes a signal, variation in water

transport rates, and assuming a steady state of a certain discharge characteristic over a given time period, such as a specific isotope ratio (Kershaw and Baxter, 1995). Considering the distances over which radionuclides are transported, it is not expected that there will be a perfect match between the initial production of a signal, and detection years later (Kershaw and Baxter, 1995).

4.1.1 Measurement of ^{137}Cs in seawater

The conservative behaviour of ^{137}Cs in seawater, combined with routine detection by gamma spectrometry, makes it a suitable tracer for ocean circulation patterns and assessing the fate of radionuclides discharged into the marine environment (Jefferies et al. 1973). Separation of ^{137}Cs from seawater has been successfully achieved using inorganic ion exchangers (Table 4.1), most commonly ammonium molybdophosphate (AMP) ($(NH_4)_3PMo_{12}O_{40}$), as well as insoluble hexacyannoferrates (Baker, 1975; Jefferies et al. 1973; Smith et al. 1990; Kershaw and Baxter, 1995; Kershaw et al. 1995; Gaur, 1996). AMP is unaffected by the high ionic strength of seawater, with a ^{137}Cs recovery of 94-99 %, and a distribution coefficient (K_d) of ~1500 mL/g (Molero et al. 1995; Gaur, 1996; Aoyama et al. 2000), however dissolution of AMP can occur if seawater is not first acidified to pH 1-2 (Baker, 1975; Kershaw and Baxter, 1995; Molero et al. 1995; Aoyama et al. 2000). Chromatographic separation is the most efficient approach for high volume (typically 20-100 L) samples, which requires binding of fine-grained crystalline AMP with an inert support material, such as colloidal silica, polyacrylonitrile (PAN), and in some early studies, asbestos (Morgan and Arkell, 1963; Sebesta and Stefula, 1990; Kershaw and Baxter, 1995; Kershaw et al. 1997; Miller et al. 1997; Todd et al. 2002; Tranter et al. 2002).

4.1.2 Isotope ratio measurements

Measurement of isotope ratios can give insights into the source of contamination, ocean transport patterns, and the transit times of radionuclides (Table 4.2) (Bowen et al. 1974; Dahlgaard, 1995; Kershaw et al. 1995; Aarkrog et al. 1999; Dahlgaard et al. 2004). For example, measurement of the ^{137}Cs/^{90}Sr ratio has been used to indicate the source of contamination, with a value of ~1.5 representing the global fallout value in Atlantic water (Bowen et al. 1974; Dahlgaard, 1995; Kershaw et al. 1995; Aarkrog et al. 1999), compared to values approximately four times higher than this indicative of Sellafield

Reference	Sample volume (L)	Pre-treatment	Exchange material
Baker (1975)	50	Acidify and filter	ASG column, 10g
Livingston et al. (1984)			Cupric ferrocyanide column
Smith et al. (1990)	100		2xpotassium cobalt hexacyannoferrate (KCFC) column
Kershaw and Baxter (1995)	50	Acidify and filter	ASG column, 8g
Molero et al. (1995)	60-100L	Acidify, add CsCl carrier	0.5g AMP per 1L sample Batch separation, 2hr contact time, leave to stand overnight
Aoyama et al. (2000)	20-100	Acidify, add CsCl carrier	AMP, 4g Batch separation, 6-24hr contact time

Table 4.1. Procedures for separation of ^{137}Cs from seawater

discharges (Dahlgaard, 1995). Since 1986, isotope ratio values of 5-6 have also been attributed to fallout from Chernobyl, with particularly elevated values seen in waters surrounding the Faroe Islands and South Greenland (Kershaw and Baxter, 1995; Dahlgaard et al. 2004).

The background of ^{137}Cs from weapons test fallout has previously been suggested as a potential limitation of using it as a tracer, encouraging measurement of other isotopes such as the activation product ^{134}Cs, with activities of 0.009-0.1 Bq/m^3 measured in surface waters in Greenland in 1982-85 (Aarkrog et al. 1988). The ^{134}Cs/^{137}Cs ratio has been measured in Sellafield discharges (Jefferies et al. 1973), with the change of value

in relation to distance from discharge point being used as an estimate of transit times (Jefferies et al. 1973). A transfer factor can also be calculated to demonstrate the transport of reprocessing wastes to other regions, expressed as the measured concentration of a radionuclide in seawater (Bq/m^3) as a proportion of the Sellafield discharge (PBq/year) (Aarkrog et al. 1988; Kershaw and Baxter, 1995). However, this measurement assumes no other source of radionuclide other than the one under consideration (Aarkrog et al. 1988).

Ratio	1960	1970	1980	1990
$^{137}Cs/^{134}Cs$	10	25	80	>200
$^{137}Cs/^{90}Sr$	1.8	3.8	7	7
$^{238}U/^{239,240}Pu$	0.05	0.1	0.23	0.23

Table 4.2. Measurement of radioisotope ratios in seawater samples (Kershaw and Baxter, 1995)

Variations in chemical behaviour and half-life of radionuclides can lead to differences in transport, and therefore in the reliability of isotope ratios measured. In the case of $^{134}Cs/^{137}Cs$, applications are restricted by the short half-life of ^{134}Cs (2.1 yrs). Recent advances in the sensitivities achievable by ICP-SFMS have expanded measurement options to enable detection of long-lived low abundance radionuclides, including ^{135}Cs (half-life $2.5x10^6$ yrs). This allows measurement of the $^{135}Cs/^{137}Cs$ ratio, which varies depending on the source of nuclear contamination, and therefore has the potential to be a powerful forensic tool (Lee et al. 1993; Taylor et al. 2008; Ohno and Muramatsu, 2014; Zheng et al. 2014). Given the multiple contamination sources, accurate measurement of this ratio would be beneficial in developing understanding of ocean circulation patterns and the fate of radionuclides in this region compared to previous measurements of ^{137}Cs alone. The primary challenge is removal of isobaric ^{135}Ba and ^{137}Ba interferences (6.6 % and 11.2 % abundance, respectively), which significantly impacts the detection limits achievable in the case of low-level detection. A procedure is described for detection of $^{135}Cs/^{137}Cs$ in North Atlantic and Arctic Ocean waters,

incorporating chemical separation by AMP, cation exchange and extraction chromatography, and quantification by gamma spectrometry and ICP-SFMS.

4.2 Experimental

4.2.1 Extraction of ^{137}Cs from seawater

ASG resin was prepared by loading AMP onto inert silica gel support material (Phase Separations Ltd, UK) following the method described by Baker (1975) (Appendix D, page 165). To test ASG performance prior to collection of real samples, 1 L of seawater was acidified to pH 1 with 1 mL concentrated HNO_3 (Fisher Chemicals, analytical reagent grade) and spiked with a ^{137}Cs standard (AEA Technology QSA) to obtain a starting activity of approximately 1 Bq/L. One gram of ASG resin was added to the spiked seawater and left mixing for 1 hour with a PTFE magnetic stirrer, followed by vacuum filtration through a 0.22 μm PTFE filter. The filtrate was evaporated to dryness, and then made up in 20 mL 1 M HNO_3, transferred to a 22 mL polythene scintillation vial, and counted for one hour by gamma spectrometry using a Canberra HPGe well detector having 10% efficiency at 662 keV gamma energy for ^{137}Cs (^{137m}Ba). Analysis of the energy spectra and calculation of ^{137}Cs activity was performed by Fitzpeaks software (JF Computing, Stanford in the Vale, UK). The average ^{137}Cs recovery by ASG from 3 repeat procedures was 93.7±4.7 %, with a K_d of 1,620 mL/g.

Seawater samples were collected from multiple sites in the North Atlantic and Arctic Oceans (Figure 4.1) during the JR271 Cruise aboard the RRS James Clark Ross in June and July 2012. Seawater was collected from 20 L Niskin bottles mounted on a stainless steel Conductivity Temperature Density (CTD) profiler, and stored in 20 L high-density polyethylene (HDPE) carboys. Approximately 20 L of seawater was pumped through a 47 mm diameter Whatman polycarbonate filter (10 μm pore size) using a Wetson Marlow 323 peristaltic pump. Filtered seawater was acidified to pH 1 by adding 1 mL concentrated HNO_3 per litre of seawater and mixed thoroughly. Ten grams of dried ASG resin was mixed with distilled water (Ultra High Pressure water system, Elgastat polishing unit), loaded onto a 10 cm long x 1.4 cm diameter cartridge and sealed with a polypropylene cap. Distilled water was pumped through the resin until the sample was loaded to prevent the resin from drying out. Acidified seawater was pumped through cartridges at a maximum rate of 3 L/hr, with higher flow rates causing breakthrough of

ASG and visible discoloration of the resin (Figure 4.2(A)). A small loss of seawater was observed by leaking from the sealing cap, which could be prevented by securing the cap with a clamp (Pike et al. 2013). The efficiency of ASG was assessed by measurement of the stable ^{133}Cs concentration in seawater, with a separate 20 mL sample collected at each site prior to sample processing. The recovery was calculated as the difference in ^{133}Cs concentration in untreated seawater compared to that recovered by ASG resin.

At each site a sample was taken from two depth ranges (0-25 m and 100-500 m) so as to ascertain any differences in recorded activities. Between samples, carboys were washed four times with distilled water, and the tubing pumped through with 2 L-distilled water. Following the cruise, ASG resin was dried at 60^{0}C for 24 hrs, and then transferred to 22 mL polythene scintillation vials and counted for 24 hrs using a Canberra HPGe well detector. Results were normalised for an ASG resin mass of 10 g and the maximum sample volume collected (22 L), with a detection limit equivalent to 0.5-0.7 Bq/m^3.

Dissolution of ASG resin and Cs separation by cation exchange chromatography (AG 50-WX8, 8 % cross-linked, 100-200 mesh, Bio-Rad laboratories, USA) prior to ICP-SFMS measurement was initially investigated using a ^{137}Cs standard (AEA Technology QSA), with recovery assessed by gamma spectrometry. In order to minimise the Ba procedural blank concentration, a final clean-up procedure was applied using calixarene extraction chromatography ((bis-crown calix[4]arene (BOBCalixC6), IBC Advanced Technologies, Utah, USA) using a procedure developed by Russell et al. (2014(B)) (Chapter 3, page 43-60). To further minimise environmental Ba contamination, cation exchange and extraction chromatography work was carried out in a clean laboratory using high purity reagents and thorough cleaning procedures for non-disposable labware (Appendix C, page 159-163).

4.2.2 Instrumentation

Stable ^{133}Cs and low-level ^{135}Cs and ^{137}Cs measurements were acquired using a Thermo Element 2 XR ICP-SFMS. For low-level measurements the instrument was equipped with the Jet interface (consisting of a high capacity dry interface pump and specially designed Jet sampler cone) and X-skimmer cone. When combined with a Cetac Aridus II desolvating sample introduction system, this setup can yield significant improvements in sensitivity (Thermo Scientific, 2010). The instrument sensitivity was assessed by

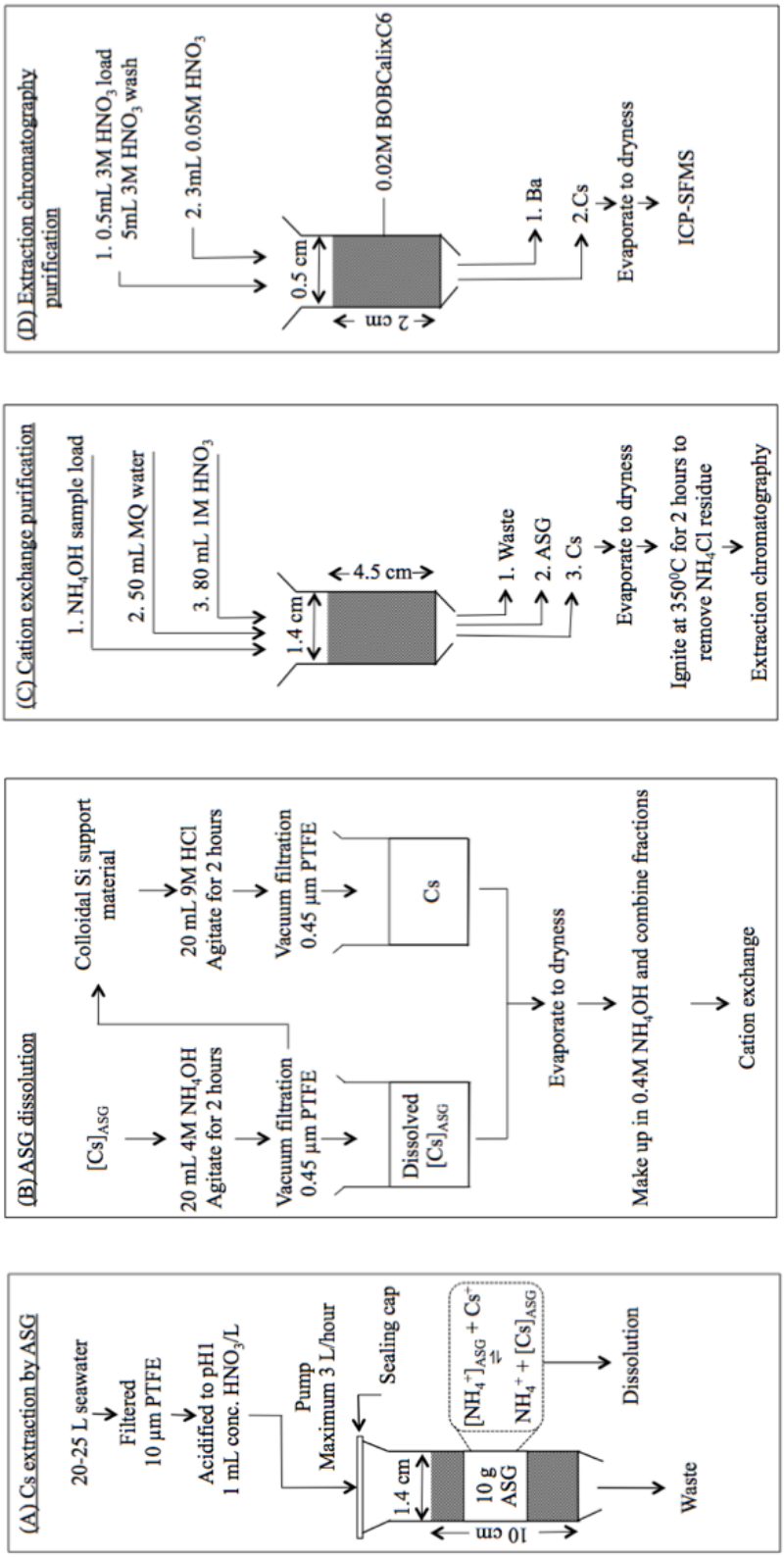

Figure 4.2. (A) Extraction of ^{135}Cs and ^{137}Cs from seawater using ASG resin, and subsequent purification for ICP-SFMS measurement, incorporating (B) ASG dissolution; (C) Cation exchange chromatography; (D) Calixarene extraction chromatography

measuring 0.001-10 ng/L stable ^{133}Cs solutions prepared from 1000 mg/L elemental stock solutions (Inorganic Ventures) in 0.1 % HNO_3 (v/v). Teflon sub-boiled HNO_3 and high purity de-ionised water (resistivity higher than 18.2 MΩ) produced from a Q-Pod Millipore System (Merck, UK) were used throughout.

4.3 Results and Discussion

4.3.1 Filtering

Caesium-137 was not detected in filter papers at any site after 24 hours counting by gamma spectrometry. A recent study investigating seawater contaminated by the accident at the Fukushima Daiichi Nuclear Power Plant accident detected <0.1 % of the total $^{134+137}Cs$ activity from a 1 μm diameter filter (Pike et al. 2013), consistent with the soluble nature of Cs in seawater (Jefferies et al. 1973; Bailly du Bois et al. 2012; Buesseler et al. 2012). Despite this, the filtration stage was important in reducing the pressure on ASG resin, particularly for seawater taken at 0-20 m depths with high particle content, which required several filter paper changes for a 20-25 L sample. Prior to sampling from the CTD, the performance of ASG was assessed using the ships underway supply at a depth of approximately 5 m. For unfiltered samples, there was a visible discolouration of the resin column and a considerably slower flow rate, however it is unknown whether ^{137}Cs recovery was affected compared to filtered samples.

4.3.2 Gamma spectrometry of ^{137}Cs

Results from gamma spectrometry (Figure 4.3(A) and 4.3(B)) for the 2 depth ranges investigated are based on a 100% recovery of ^{137}Cs by ASG (see section 4.3.5). Counting uncertainties were high, ranging from 19-50 %, which could be improved by extending the count time to longer than 24 hours. There is a weak correlation between the activities measured at both depth ranges (Figure 4.4), both of which recorded an average activity of 1.9±0.5 Bq/m^3 (Table 4.3). If this similarity had been known whilst on-board, samples from the two depths could have been combined for each site to maximise the sample volume and improve the likelihood of ^{137}Cs detection. Measurements at >500 m depths was not possible in this study, but for future investigations would be desirable for getting a broader understanding of ^{137}Cs distribution.

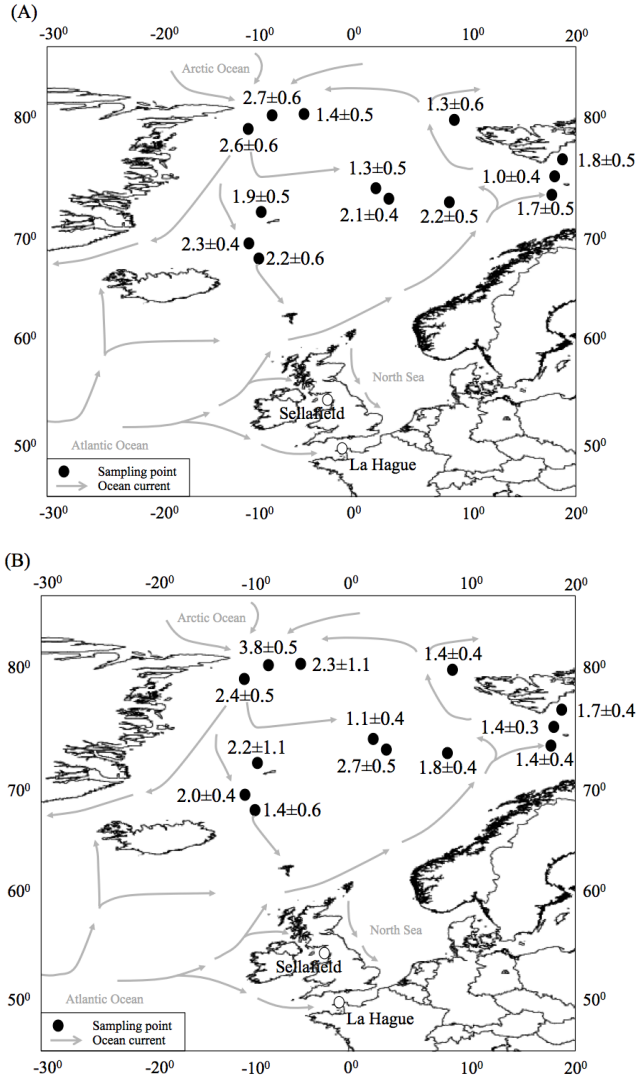

Figure 4.3. ^{137}Cs activities (Bq/m^3) in seawater samples at 0-20 m (A) and 80-500 m (B) sampling depths following 24-hour counting of ASG resin by gamma spectrometry

Sampling depth range (m)	Minimum detected activity (Bq/m^3)	Maximum activity (Bq/m^3)	Average activity (Bq/m^3)
0-20	1.0±0.4	2.7±0.6	1.9±0.5
80-500	1.1±0.4	3.8±0.5	2.0±0.5

Table 4.3. Summary of ^{137}Cs activities in seawater samples at different sampling depths

As with previous studies, the highest activities were measured along the east coast of Greenland, representing ^{137}Cs from older, higher Sellafield discharges. Measurements of ^{137}Cs activity in the North Atlantic and Arctic Oceans have been found dating back to 1962 (Table 4.4), with a general reduction in the measured activity in more recent studies. This is likely to be a result of ^{137}Cs decay, and mixing of inputs from Chernobyl and atmospheric weapons test fallout, as well as a reduction in discharges from the Sellafield site. The activities in this study are lower than any previously recorded value, with an average activity of 1.9±0.5 Bq/m^3. The average activity of samples taken around the East Coast of Greenland (2.8±0.5 Bq/m^3) are comparable with those from a more recent study of Greenland surface waters (3.5 Bq/m^3) (Dahlgaard et al. 2004), but are significantly lower than the average value of 23.0 Bq/m^3 recorded between 1962 and 1980 (Aarkrog et al. 1999).

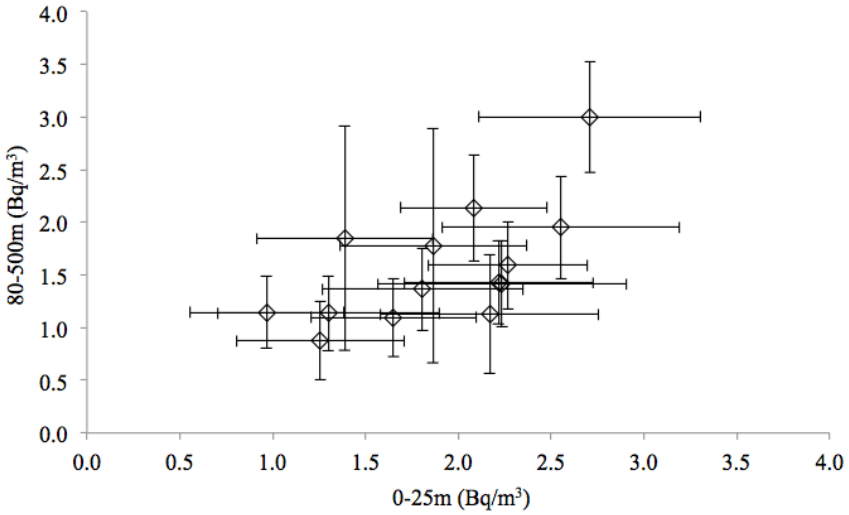

Figure 4.4. Comparison of ^{137}Cs activities measured by gamma spectrometry over 0-20 m and 80-500 m depth ranges (R^2 = 0.49)

Measurement of samples on-board would have given an early indication of the effectiveness of ASG performance, which would have allowed modifications to the procedure if required. However, this would have been challenging given the low activities being investigated. Preliminary sample analysis has been achieved using a sodium iodide detector for seawater off the coast of Japan following the incident at the Fukushima Daiichi nuclear power plant, however this was carried out to evaluate

Reference	Location	Sampling date	Depth	^{137}Cs range (Bq/m^3)	Mean ^{137}Cs (Bq/m^3)
Smith et al. (1990)	Norwegian Sea	1982	Surface water	3.7-26.9	11.3
Aarkrog et al. (1999)	Greenland	1970-79	0-100 m	3.2-9.7	6.4
		1980-89		3.5-7.4	5.2
		1990-97		3.6-7.1	5.1
Aarkrog et al. (1999)	East Greenland Current	1962-80			23.0
		1980-1997			2.4
Nies et al. (1999)	Arctic Ocean	1995	Surface	2.1-4.9	3.1
Dahlgaard et al. (2004)	Greenland	1999	Surface water	1.8-5.5	3.5
Heldal and Varskog (2002)	Spitsbergen-Bear Island	1998-99	Surface sediments	<0.5-9.3 Bq/kg	4.0 Bq/kg
This study	North Atlantic, Arctic Ocean	2012	0-500 m	<0.5-3.8	1.9
This study	East Greenland current	2012	0-500 m	2.5-3.8	2.8

Table 4.4. Summary of ^{137}Cs activities measured in the North Atlantic and Arctic Ocean.

exposure levels to personnel and the ship, with activities of >300 Bq/m^3 recorded (Pike et al. 2013). The results in this study also represents measurement at a single point in time, which can be compared to previous investigations; however, the application of isotope ratio measurements is limited, with repeat sampling over a greater depth range desirable. In addition, measurement of marine sediments are a potential indicator of past, present and future contamination (Heldal and Varskog, 2002). Variation in sedimentation rates, and remobilisation of contaminated sediments must be considered, as well as strong retention of ^{137}Cs in areas with a high proportion of clay particles (Heldal and Varskog, 2002). Sediment core sampling has been applied to plutonium isotope ratio analysis, which can potentially support $^{135}Cs/^{137}Cs$ work, as the $^{239}Pu/^{240}Pu$ ratio also varies depending on the source of nuclear contamination and has been effectively measured in environmental samples (Warneke, Croudace et al. 2002; Taylor, Evans et al. 2008).

4.3.3 Dissolution of ASG

To determine a procedure for effectively dissolving ASG, 10 g of material was mixed with 30 mL 0.1 M HNO_3 spiked with 5 Bq ^{137}Cs and shaken for 1 hour. This was dried overnight at 60^0C to form a powder representative of the cruise samples collected. The dried powder was then combined with 20 mL 4M NH_4OH, which has been proven to effectively dissolve ASG (Russell et al. 2014(A)) (Chapter 2.3.2. page 35). After centrifuging for 5 minutes at 4,500 rpm (Eppendorf centrifuge 5702), a colourless solution was produced, overlying a gelatinous layer of colloidal silica support material. The silica gel layer was then vacuum filtered through a 0.22 μm PTFE filter. Following this, a few drops of 2 % HNO_3 was added to the dried silica, with yellow colouration indicating incomplete dissolution of ASG. Repeated filtration with NH_4OH was applied until no yellow colouring was seen upon addition of 2 % HNO_3. A consistent recovery of 70-75 % was achieved by mixing 20 mL 4 M NH_4OH with ASG on a roller for 2 hours (Luckham Multimix Major), followed by centrifugation and vacuum filtration (Figure 4.2(B)). The solid colloidal silica was then subjected to repeated mixing and vacuum filtration using 20 mL 9 M HCl, improving the ^{137}Cs recovery to 79-90 %. The liquid fractions from the 2 stages were evaporated to dryness, and combined in 5 mL 0.4 M NH_4OH to redissolve AMP+Cs prior to cation exchange.

Colloidal silica is an effective support material for AMP in chromatographic separations; however, it has also been applied to the immobilisation of radionculides (including ^{137}Cs) in groundwater and freshwater samples (Noell et al. 1998; Hakem et al. 2004), which may account for the difficulty in achieving a high ^{137}Cs recovery from ASG resin. An investigation into the aggregation of colloidal silica in the presence of alkali chlorides revealed that Cs is capable of forming large, abundant and stable aggregates (Johnson et al. 2008). The higher selectivity towards Cs is attributed to ion size, as larger ions sorb more favourably on the silica surface. Secondly, Cs ions are the least hydrated of the alkali cations, and can sorb more closely to the surface than more hydrated ions, such as Li and Na. (Johnson et al. 2008). Whilst ASG can be dissolved in alkali solution, the high mass of material used in this study may be impacting the recovery, which is significant in the case of low-level ^{135}Cs and ^{137}Cs measurements.

4.3.4 Cation exchange and extraction chromatography separation

The cation exchange procedure (Figure 4.2C) was modified from a method developed by Russell et al. 2014(A) (Figure 2.2(B), page 37) to account for the high ionic content of seawater, which can reduce the performance of ICP-SFMS (see section 4.3.5). Dissolved ASG bound with ^{137}Cs was loaded in 0.4M NH_4OH onto a 4.5 cm long x 1.4 cm diameter cation exchange column, previously conditioned with 30 mL 0.4 M NH_4OH. Neutralisation of the resin between alkali loading and Cs elution in HNO_3 was achieved by a 50 mL Milli-Q water wash, which also removes AMP from the column. A ^{137}Cs recovery of >95 % was achieved by elution in 80 mL 1M HNO_3, whilst Ba was retained on the column. The losses of ^{137}Cs in the sample load, Milli-Q wash, and resin material post Cs-elution was <5 %.

Eluted Cs was evaporated to dryness, leaving a visible white residue, which readily dissolved in 2 % HNO_3 for ICP-MS sample introduction. However, this solid material led to blockage in the heated spray chamber of the Aridus II desolvating sample introduction system, therefore had to be removed prior to sample introduction. Investigation of the residue by Micro X-ray fluorescence (XRF) (EDAX Eagle III Microanalysis) and ion chromatography (Metrohm 861 Advanced Compact IC with a Metrosep A Supp 5 Column) detected a high chloride and ammonium ion content, respectively, suggesting the residue was ammonium chloride (NH_4Cl), possibly from a combination of NH_4OH and HCl applied to the dissolution of ASG resin. Ammonium

chloride decomposes at 338^0C, and therefore was removed by transferring the solid material to a borosilicate glass beaker and heating in a furnace (KF Thermosave, Stoke-on-Trent, UK), with the temperature increased gradually to a maximum of 350^0C, and then left at this temperature for 30 minutes. There was no loss of Cs from the sample, with ignition temperatures of up to 500^0C previously applied to solid samples with no loss of analyte (Taylor et al. 2008).

Evaporation and ignition of the Cs fraction following cation exchange chromatography necessitated a final separation stage to minimise the Ba concentration prior to ICP-SFMS introduction. This was achieved using a calixarane-based extraction chromatographic procedure developed by Russell et al. 2014(B) (Chapter 3, page 43-60) (Figure 4.2(D)). Calixarenes are macrocyclic extractants that show a high Cs selectivity, and have been extensively applied to separation of ^{137}Cs from nuclear waste solutions (Bonnesen et al. 1998; Grunder et al. 1999; Leonard et al. 2001; Riddle et al. 2005; Mohapatra et al. 2006). In short, the calixarene extractant (Calix-4-arene-bis-(tert-octylbenzo-crown-6) is dissolved in octanol and combined with pre-filter resin material (Triskem International). The resulting powder is slurried with water and then loaded onto a 2 cm long x 0.5 cm diameter column. Caesium is retained on the resin in 3 M HNO_3, and eluted in 0.05 M HNO_3. This rapid and straightforward technique is capable of a Ba decontamination factor of $2.9x10^3$. For simulated cruise samples, the ^{137}Cs recovery from ASG dissolution, cation exchange and extraction chromatography ranged from 72.2±3.6 % to 81.2±4.1 %, with retention by colloidal silica being the most significant loss. The efficiency of ASG in extracting Cs from seawater is not included in these calculations.

4.3.5 ICP-SFMS measurement

Measuring the stable ^{133}Cs seawater concentration as a measure of ASG recovery is a simplified method that eliminates the need for spiking with a stable Cs carrier (Morgan and Arkell, 1963; Molero et al. 1995; Aoyama et al. 2000; Pike et al. 2013). As well as the tests carried out prior to the cruise, an indicator of ASG efficiency was determined by running samples at two sites through two ASG cartridges in tandem. In both cases ^{137}Cs was detected in the first cartridge only, with an activity of <0.5 Bq/m^3 in the second cartridge based on the detection limit from gamma spectrometry.

To assess ASG recovery, a 50x dilution of seawater samples was spiked with a 1 µg/L indium internal standard to correct for instrument drift. Samples were analysed using an Element XR ICP-SFMS equipped with a PC^3 sample inlet system (Elemental Scientific), self-aspirating nebuliser, H-Skimmer and standard nickel sample cones, and a Pfeiffer Duo 5 rotary pump. Stable ^{133}Cs concentrations were determined by running 0.1-100 ng/L standard solutions, prepared in 2 % HNO_3 (v/v). Changing from standard solutions in a 2 % HNO_3 matrix to diluted seawater samples will affect the instrument response; therefore, sample uptake was repeated four times to condition the instrument with the sample matrix, with analysis performed following the fifth uptake. Despite the dilution, the instrument sensitivity dropped by 25 % during the 30-sample run as a result of the high ionic content of seawater, with visible deposits left on both the sample and skimmer cones. For actual samples, the extensive chemical separation procedure described should minimise the ionic content of the final sample, however the addition of an internal standard can assess this more accurately.

Four of the samples collected during the cruise returned a ^{137}Cs activity below the detection limit (0.5 Bq/m^3) following a 24-hour count time. Given the successful detection of ^{137}Cs in all other samples, it is unclear why these results occurred. The only common factor is that the 26 samples that successfully detected ^{137}Cs were collected from the CTD, where as samples with activities below the detection limit were obtained from the ships constant underway supply. These four samples were taken forward to assess the Ba decontamination factor achievable, and the performance of ASG resin. Despite the low ^{137}Cs activity, the stable ^{133}Cs concentration was successfully detected using the same instrumental setup as described for untreated seawater samples, with the average ASG recovery calculated as 75.0±2.8 %. The ASG recovery achieved is lower than the 93.7±4.7 % achieved prior to the cruise, which was determined from batch separation for a smaller volume (1 L) of seawater. This initial test was only applied as an indicator of the effectiveness of ASG, given that the material was prepared in house. Factors in chromatographic separation such as the high volume of seawater processed, degradation of the resin, formation of air bubbles in the cartridge, pumping rate, and storage conditions prior to further treatment may be responsible for the reduced recovery seen. As an alternative, commercially available AMP-PAN (Triskem international) can recover 88.1±3.3 % Cs from a 100 L seawater sample, and at a maximum flow rate of 18 L/hr, compared to 3 L/hr in this study (Bombard et al. 2013).

Furthermore, the PAN support material shows no uptake of Cs, which would likely lead to an improved chemical recovery compared to colloidal silica gel support material (Sebesta and Stefula, 1990; Nilchi et al. 2006).

Assuming a 1:1 ^{135}Cs:^{137}Cs ratio, the predicted ^{135}Cs concentrations range from 10-41 pg/L in a 500 µL solution. The combination of the Cetac Aridus II Desolvating Sample Introduction System, Jet interface and X-skimmer cone can achieve a Cs sensitivity of up to 80,000 counts per ng/L, corresponding to a detection limit of 1 pg/L (calculated as the concentration of 3 times the standard deviation of the background at mass 133). It has been challenging to repeatedly achieve this optimal sensitivity, with a more consistent value of ~40,000 counts per ng/L, and a detection limit of 2 pg/L. However, this sensitivity means ICP-SFMS is capable of measuring low-level $^{135}Cs/^{137}Cs$ values in seawater samples.

The concentration of isobaric Ba interferences in untreated seawater ranged from 3.3-8.2 µg/L, necessitating a decontamination factor of 10^5 prior to sample introduction. This is achievable by a combination of ASG and cation exchange chromatography, however environmental contamination introduced during the procedure is the primary challenge that determines whether the method detection limit can match the capabilities of the instrument. Barium introduced by evaporation and ignition of the Cs fraction following cation exchange chromatography was effectively reduced by a factor of 700-1,020 by calixarene separation. Despite this, a minimum Ba blank concentration of 5.0 ng/L was measured from simulated cruise samples, and samples collected from the ships underway supply. This corresponds to a method detection limit of 48.8 pg/L, calculated as the concentration of 3 times the standard deviation of the background in the procedural blank at masses 135 and 137. This value is higher than the predicted concentration in seawater samples, and prevents accurate detection of $^{135}Cs/^{137}Cs$ values. A reduction in the procedural blank concentration of one order of magnitude to 0.5 ng/L is required to achieve the desired method detection limit of 10.0 pg/L. Repeat calixarene separation stages did not improve the procedural blank, suggesting environmental contamination from the laboratory environment is acting as a source of Ba. Direct sample introduction of the eluted Cs fraction from the calixarene without evaporation can reduce the method detection limit to 20pg/L (Chapter 3.2.4, page 51), however the 3 mL elution volume reduces the predicted ^{135}Cs concentration range to 1.7-6.9 pg/L, which is at the limit of the instrumental capabilities. At these ultra-low

levels the Ba concentration in the reagents used are higher than the $^{135}Cs/^{137}Cs$ content in the final samples, with an average Ba concentration during this study of 700 pg/L in the 2% HNO_3 blank solution. An improvement can potentially be achieved by operating chromatographic procedures online with the ICP-SFMS, as this can deliver a more efficient separation, whilst also minimising reagent volumes (Alonso et al. 1995; Moreno et al. 1999; Taylor et al. 2008; Pitois et al. 2008; Liezers et al. 2009).

An alternative analytical technique under consideration for these samples is accelerator mass spectrometry (AMS), which is capable of sub fg/L detection limits (Becker, 2005). Suppression of isobaric interferences can be achieved through the inability of some elements to form negative ions during the sputtering process, however AMS is limited by high cost and complex analysis (Becker 2005; Zoriy et al. 2005; Kutschera, 2013), with no known application for detection of $^{135}Cs/^{137}Cs$. AMS does not offer the analytical flexibility of ICP-MS, as a number of inter-related parameters must be considered for developing a procedure for measurement of a new isotope. With regards to sample preparation, an improvement in Ba separation has been achieved using on-line chemistry, by combining a fluoride ion source target (to enhance anion production) with radio-frequency guided ion reaction cells, with NO_2 as a reactive gas (Eliades et al. 2013). The preferential formation of CsF_2^- over BaF_2^- in combination with the reaction cell achieved a Ba decontamination factor of ~$2x10^5$. A high amount of stable ^{133}Cs is used as a sputtering source, however this is likely to be free of ^{135}Cs and ^{137}Cs, and it may also be possible to incorporate ^{134}Cs as a yield tracer. Alternatively, the primary beam can be generated using a rubidium source to eliminate the risk of Cs contamination.

4.4 Conclusions

The inventory of radioactive caesium isotopes in the North Atlantic and Arctic Ocean has been increased by inputs from multiple sources, including atmospheric weapons test fallout, and aqueous discharges from reprocessing facilities. Past measurement has primarily focused on ^{137}Cs, however advances in the sensitivities achievable by ICP-SFMS enable detection of long-lived, low abundance radionuclides, such as ^{135}Cs. This permits the measurement of $^{135}Cs/^{137}Cs$ ratios, which varies with the source of contamination and can therefore provide a powerful tool in the field of nuclear forensics.

An Element XR ICP-SFMS equipped with the Jet interface and X-skimmer cone can detect concentrations down to 1 pg/L, enabling low-level detection of $^{135}Cs/^{137}Cs$, which is applicable to measurement of seawater samples in the North Atlantic and Arctic Oceans. To be able to achieve these detection limits in real samples, extensive chemical separation and ultra-clean working conditions have been developed to minimise interferences arising from isobaric ^{135}Ba and ^{137}Ba. Caesium was initially extracted from seawater using AMP supported on colloidal silica (ASG resin), followed by dissolution of the resin, and further purification of Cs by cation exchange and extraction chromatography. The chemical recovery ranged from 71.2-82.2%, with the retention of Cs by the silica support material being the most significant source of analyte loss.

The minimum Ba procedural blank concentration achieved by the separation procedure described was 5.0 ng/L, which is equivalent to a detection limit of 48.8 pg/L. This is higher than the predicted concentration of ^{135}Cs in seawater samples, ranging from 10-41 pg/L. Without further reduction in the Ba procedural blank to ≤0.5 ng/L, it is not possible to perform accurate measurement of $^{135}Cs/^{137}Cs$ in seawater samples by ICP-SFMS. Whilst this measurement technique is capable of low-level detection of radionuclides in environmental samples, the primary limitation is minimising isobaric interferences inherently present in the reagents and labware used. An alternative approach being considered for seawater samples is AMS, which is capable of sub fg/L detection limits. AMS does not offer the analytical flexibility of ICP-SFMS, and is not considered a viable alternative for routine analysis, given the extensive instrument development time to enable measurement of $^{135}Cs/^{137}Cs$.

The spatial distribution of ^{137}Cs activities measured by gamma spectrometry are in agreement with previous investigations, with the highest activities measured on the East coast of Greenland, reflecting earlier, higher discharges from the Sellafield reprocessing site. With regards to measurement of isotopic ratios, $^{135}Cs/^{137}Cs$ is suitable for North Atlantic and Arctic Ocean samples, which have been contaminated by multiple anthropogenic activities. In addition, the long half-life of ^{135}Cs means measurements are not restricted in the same way as $^{134}Cs/^{137}Cs$. However, this study shows measurement at a single point in time, and future studies would benefit from repeated measurements at similar locations over a greater depth range, as well as in seafloor sediments.

Chapter 5: Measurement of $^{135}Cs/^{137}Cs$ in a salt marsh sediment core

Abstract

The improvements in sensitivity achievable by inductively coupled plasma sector field mass spectrometry (ICP-SFMS) has expanded the range of medium and long lived radionuclides measurable using this technique. A procedure is presented (incorporating digestion, chemical separation and quantification) for low-level detection of ^{135}Cs and ^{137}Cs in a saltmarsh sediment core that shows a good record of authorised aqueous discharges from the Sellafield reprocessing site since operations began in the early 1950's. This in turn will enable measurement of the $^{135}Cs/^{137}Cs$ ratio, which varies depending on the source of nuclear contamination, and therefore has the potential to be a powerful tool in the field of nuclear forensics. Measurement of this ratio at a site with known discharge history and source of contamination is a more robust assessment of the $^{135}Cs/^{137}Cs$ ratio compared to isolated applications that represent values at a single point in time. The critical factors in achieving accurate measurements are removal of isobaric barium interferences ^{135}Ba and ^{137}Ba, and peak tailing from stable ^{133}Cs.

An Element XR ICP-SFMS equipped with the Jet interface, X-skimmer cone and Aridus II desolvating sample introduction system achieved an instrumental detection limit of 2.4 pg/L. Despite the successful purification of Cs from Ba following chemical separation, at the low levels being investigated, Ba contamination introduced during the procedure resulted in a method detection limit of ~50pg/L. This clean-up is sufficient for measuring $^{135}Cs/^{137}Cs$ in the sediment core, based on a ^{137}Cs concentration of 0.09-2.1 ng/L measured by gamma spectrometry. The primary limitation preventing accurate detection of ^{135}Cs is a tailing effect from the high concentration of stable ^{133}Cs, which requires an abundance sensitivity of 10^6-10^8. This is greater than the value achievable using the Element XR, and to measure sediment samples using this instrument would require a correction for the tailing effect of ^{133}Cs. This is likely to increase the uncertainty in the measured values, given that a separate correction must also be applied to account for Ba contamination. Alternatively, the successful separation and recovery of ^{135}Cs and ^{137}Cs from sediment samples can be quantified using an instrument with improved abundance sensitivity.

5.1 Introduction

The advance in sensitivities achievable by ICP-SFMS has expanded the range of radionuclides measurable using this technique, including the significant fission product radionuclides of caesium ^{135}Cs and ^{137}Cs ($t_{1/2}$ = 2.1^{6} y and 30 y, respectively). Such advances enable the measurement of the ^{135}Cs/^{137}Cs ratio, which varies depending on the source of nuclear contamination (Lee et al. 1993; Taylor et al. 2008; Ohno and Muramatsu, 2013; Russell et al. 2014 (A); Zheng et al. 2014), and thus can provide a powerful forensic tool compared to measurement of ^{137}Cs alone. Accurate measurement also offers an advantage over measurement of the ^{134}Cs/^{137}Cs activity ratio, which is limited by the relatively short half-life of ^{134}Cs (2.06 years). Aside from nuclear forensics, the ability to accurately measure medium-lived and long-lived low abundance radionuclides by ICP-SFMS has significant implications for characterisation of low level waste at nuclear facilities, which could be of benefit with regards to more rapid assessment and clean-up of nuclear sites, which will bring with it significant economic benefits.

A number of previous ^{135}Cs/^{137}Cs applications have been limited to a series of isolated case studies (Table 1.2, page 5), with isotopic ratios representing a value at a single point in time. The applicability of ^{135}Cs/^{137}Cs as a forensic tool can be further assessed with an application to a site with a well-recorded historical record of contamination, rather than measurement at a single point in time. One possibility is a location in close proximity to the Sellafield reprocessing facility in Cumbria, UK, where authorised discharges into the Irish Sea since 1952 have been monitored (Figure 1.2, page 8). Routine detection of ^{137}Cs by gamma spectrometry means the activities released are well known, with peak discharges recorded in the mid to late 1970's. Subsequent changes in site operations have reduced the activity of discharges, including storage of Medium Active Concentrate (MAC) from 1980, and the opening of the Sellafield Ion Exchange Effluent Plant (SIXEP) in 1985, which removed solids and soluble material from pond water, significantly reducing radiocaesium and radiostrontium activities (Gray, 1995; Hunt et al. 2013).

The investigation of historical Sellafield discharges is facilitated by nearby flat-lying saltmarshes bordering the Irish Sea, which have been proven to produce a chronological record of past discharges (Warwick, 1999; Morris et al. 2000; Wigley, 2000; Thomson et al. 2001; Finnegan et al. 2009). The surface of the marsh tends to track the tidal mean high water, with growth of the marsh through trapping of material by vegetation (Thomson et al. 2001). If contaminated sediment is deposited in an area of net accretion, it is possible to achieve a chronological record of past discharges with depth. Caesium behaves conservatively in seawater, however the high concentration of suspended matter in the Irish Sea (50-150mg/L) means a considerable amount of Cs discharged becomes associated with the solid phase (Jefferies et al. 1973; Hunt et al. 2013). Ungrazed salt marshes bordering the Irish Sea have a high accumulation rate (~1cm/year) and minimal post-depositional mixing, with the marsh stabilised and covered by the root system of pioneering plant species. By comparison, the adjacent mudflats undergo extensive post-depositional mixing through tidal action and bioturbation, which destroys any chronological record, whilst seabed sediments are hampered by low accumulation rates. Aside from aqueous discharges, additional sources of contamination arise from fallout of atmospheric Sellafield discharges, nuclear weapons testing, and the Chernobyl accident. However, at a saltmarsh located in close proximity to the Sellafield site, the contributions from sources other than aqueous discharges are insignificant (Gray, 1995).

The critical factor determining the accurate measurement of $^{135}Cs/^{137}Cs$ in low-level environmental samples is effective removal of isobaric interferences arising from naturally occurring ^{135}Ba and ^{137}Ba (isotopic abundance 6.6% and 11.2%, respectively). Furthermore, peak tailing from high concentrations of stable ^{133}Cs (isotopic abundance 100%) may impact detection of ^{135}Cs in environmental samples (Lee et al. 1993; Taylor et al. 2008; Snyder et al. 2011). Given that ICP-SFMS is of increasing importance in the fields of low-level nuclear waste characterisation, environmental monitoring and nuclear forensics, it is important to establish the applicability and limitations of this technique in environmental samples. This study describes a procedure incorporating digestion, chemical separation and quantification using ICP-SFMS for a saltmarsh sediment core with a chronological record of discharges from the Sellafield reprocessing site.

5.2 Methodology

5.2.1 Sample collection and storage

The Wyre salt marsh is located on the North Lanchashire coastline, approximately 60 km southeast of Sellafield (Figure 5.1). A sediment core was manually collected at low tide near the front of the marsh, which is regularly inundated, but is not easily accessible and therefore unlikely to be disturbed by livestock and the public. The core was collected using a Russian corer, consisting of a 30cm long steel chamber, blade and handlebar. The corer was manually driven into the sediment with a 'closed' blade, and then rotated 180^0 using the handlebar to trap a 30 cm section of undisturbed sediment. For 30-60 cm depth, an extension to the handlebar was added to reach the required depth and to remove sediment from the core. The core was placed in a halved PVC tube and wrapped in cling film to prevent it from drying out. Within 24 hours of collection, the core was transported back to the National Oceanography Centre, Southampton, and stored at 4^0C until processing. The halved core was cut into 1 cm subsamples, with any large organic detritus such as roots removed. Sediment samples were freeze-dried, ground into a fine powder and mixed to form a homogenous sample.

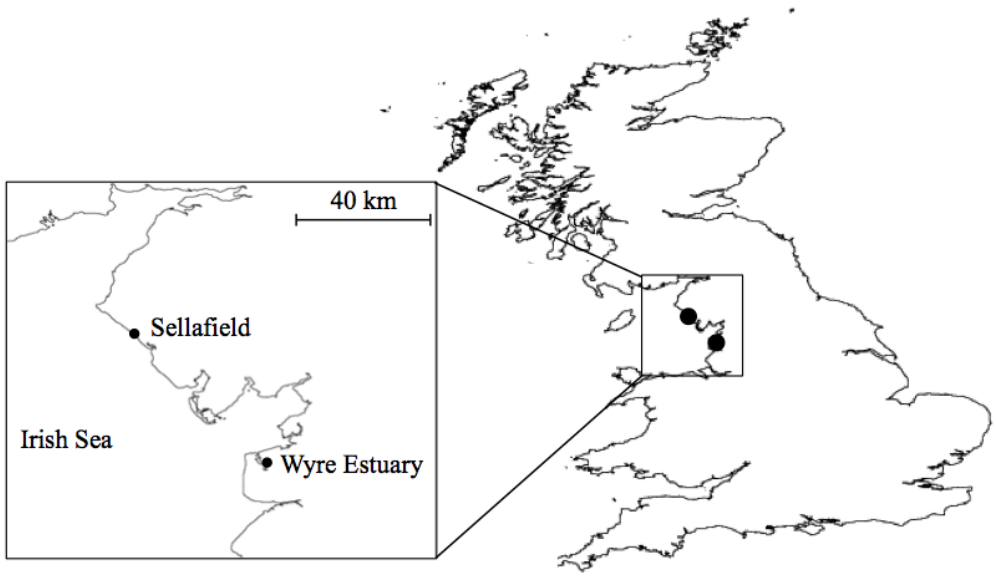

Figure 5.1. Location of the Sellafield reprocessing site and Wyre Estuary from which a vertical sediment core was collected

5.2.2 Gamma spectrometry

The ^{137}Cs activity of each 1 cm sample was measured using a Canberra well-type HPGe detector with an efficiency of 10% at 662 keV (corresponding to the gamma photopeak energy for $^{137}Cs/^{137m}Ba$). Analysis of the energy spectra and calculation of radionuclide activity was performed using Fitzpeaks software (JF Computing, Stanford in the Vale, UK). Approximately 20 g of each sample was transferred to a 22 mL plastic scintillation vials and counted for approximately 5 hours, with a detection limit on the order of 1Bq/kg.

5.2.3 X-ray fluorescence spectrometry

The concentration of major and trace elements was measured using a wavelength dispersive X-ray fluorescence spectrometer (WD-XRF) (Philips Magix-Pro). Approximately 10g of sediment was formed into a solid pellet using a HERZOG HP40 hydraulic press. No binding agent was added owing to the high clay content of the samples. The Ba concentration in sediment samples ranged from 323.4-363.6 mg/kg.

5.2.4 Digestion, chemical separation and quantification

5.2.4.1 Reagents and materials

Stable Cs and Ba standard solutions were prepared from 1000 mg/L elemental stock solutions (Inorganic Ventures) in 0.1% HNO_3 (v/v). Teflon sub-boiled HNO_3, sub-boiled HCl and high purity de-ionised water (resistivity higher than 18.2 MΩ) produced from a Q-Pod Millipore System (Merck) were used throughout.

Digestion and chemical separation were taken from the procedures developed by Russell et al. 2014(A and B) (Chapter 2.3 page 33-37, and Chapter 3.2.4 page 49-55). In short, 5g of sediment was digested by aqua regia acid leaching, followed by a three-stage chemical separation incorporating ammonium molybdophosphate (AMP), a single chromatographic column consisting of cation exchange resin (Dowex AG50 W-X8) overlying Sr-resin (Triskem International), and a final stage extraction chromatography clean-up using a calixarene (calix[4]arene-bis-(tert-octylbenzo-crown-6) (BOBCalixC6)) (Figure 5.2). Caesium is eluted from the calixarene in 0.05M HNO_3, therefore stable Cs and Ba standards were prepared at the same concentration to prevent

any variation in instrument performance. To minimise environmental Ba contamination, chemical separation procedures were carried out in a class 100 work bench in a class 1000 clean laboratory, with thorough cleaning procedures applied to resins and non-disposable labware (Appendix C, page 159-164).

5.2.4.2 Instrumentation

The chemical recovery was assessed from the ^{137}Cs activity measured following each stage by gamma spectrometry, compared to the starting activity in the sediment sample. Low-level ^{135}Cs and ^{137}Cs measurements were performed using a Thermo Element XR ICP-SFMS. The instrument was fitted with the Jet interface (consisting of a high capacity dry interface pump and Jet sample cone) and X-skimmer cone, combined with a Cetac Aridus II desolvating unit with an uptake rate of 100 μL/min from a C-flow PFA-100 nebuliser. Instrumental sensitivity was determined from repeat measurements of 0.01-10 ng/L stable ^{133}Cs standard solutions, whilst 0.1-50 ng/L stable Ba standards were run in order to apply a correction for instrumental mass bias, and interference correction in the case of sample contamination.

5.3 Results and Discussion

5.3.1 Digestion and chemical separation

The vertical ^{137}Cs sediment core profile shows a resemblance to the Sellafield aqueous discharge record (Figure 5.3A and B) Nine sampling depths were selected from various points of the core (Table 5.1 and Figure 5.3A) for ICP-SFMS analysis, representative of the range of ^{137}Cs activities measured by gamma spectrometry. The ^{137}Cs recovery (Table 5.2) following acid leaching ranged from 64.5-78.0%. It has been shown that acid leaching struggles to fully liberate Cs from a sediment matrix, particularly in clay-rich samples (Chapter 2.3.1. page 33-35) (Bostick et al. 2002). By comparison, lithium metaborate fusion has been proven to achieve a quantitative recovery of ^{137}Cs and other radionuclides from multiple sample matrices, including sediments (Croudace et al. 1998; Taylor et al. 2008; Russell et al. 2014(A)). Low-level lithium and boron isotope ratio research using the same ICP-SFMS as this study prevented the application of borate fusion. The chemical separation procedure described can achieve a boron decontamination factor of 10^6-10^7, which for the instrument used in this study is

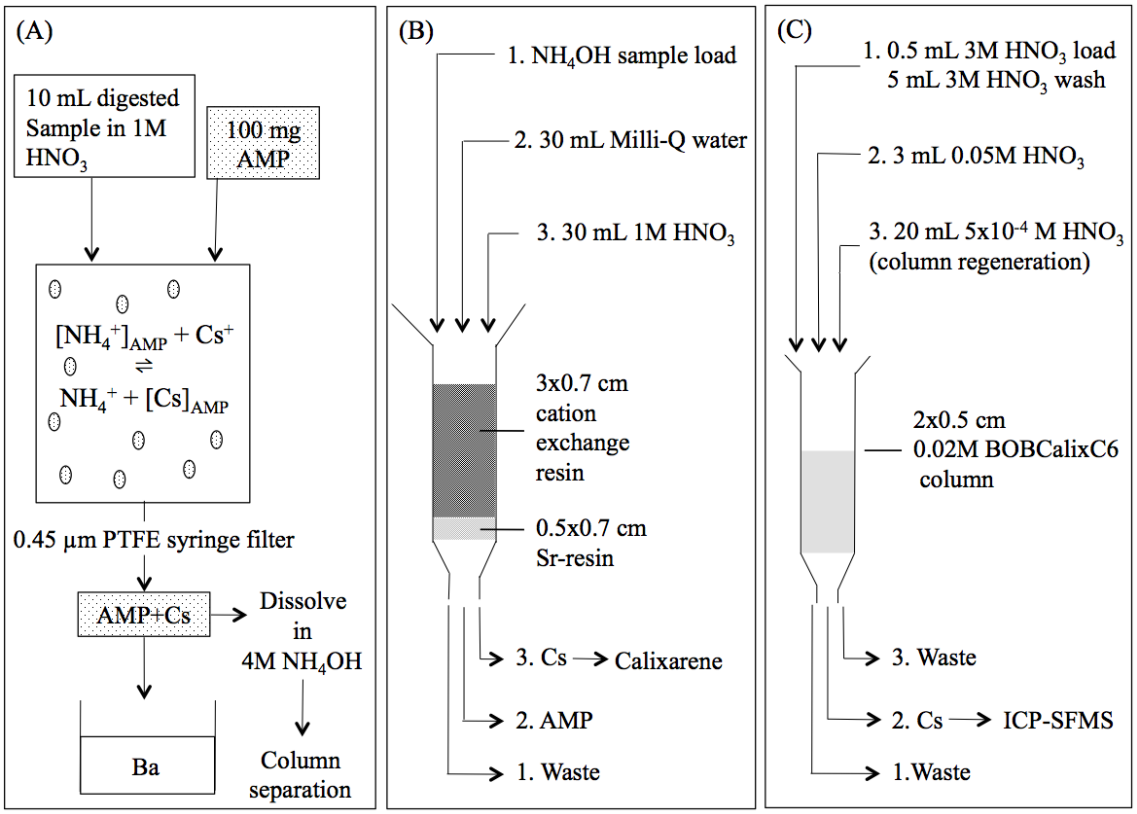

Figure 5.2. Chemical separation procedure for saltmarsh sediment samples, incorporating (A) AMP; (B) Combined cation exchange and Sr-resin extraction chromatography; (C) Calixarene-extraction chromatography

insufficient to prevent the risk of contamination, with a decontamination factor of 10^{10}-10^{12} required, given the high starting concentrations of lithium and boron in the digested sample. Aqua regia acid leaching was therefore applied as a straightforward alternative with minimal risk of instrument contamination.

AMP recovered 87.8-91.7% of ^{137}Cs from the sediment leachate, with the remaining activity detected on the syringe filter unit. The combined cation-exchange/Sr-resin column recovered >96% ^{137}Cs from the AMP stage, with <4% detected in the sample load, Milli-Q wash and on the resin post-Cs elution following a count time of 4 hours.

The calixarene separation stage can achieve a Ba decontamination factor of 2.9×10^3, and a ^{137}Cs recovery of 90% from Wyre sediment leachate samples without prior chemical separation (Chapter 3.3. page 55-57) (Russell et al. 2014(B)). However, in this study, the calixarene was ineffective, with ^{137}Cs recovered in the sample load and extraction stages for all samples, and a recovery of <4% in the 3mL 0.05M HNO_3 wash.

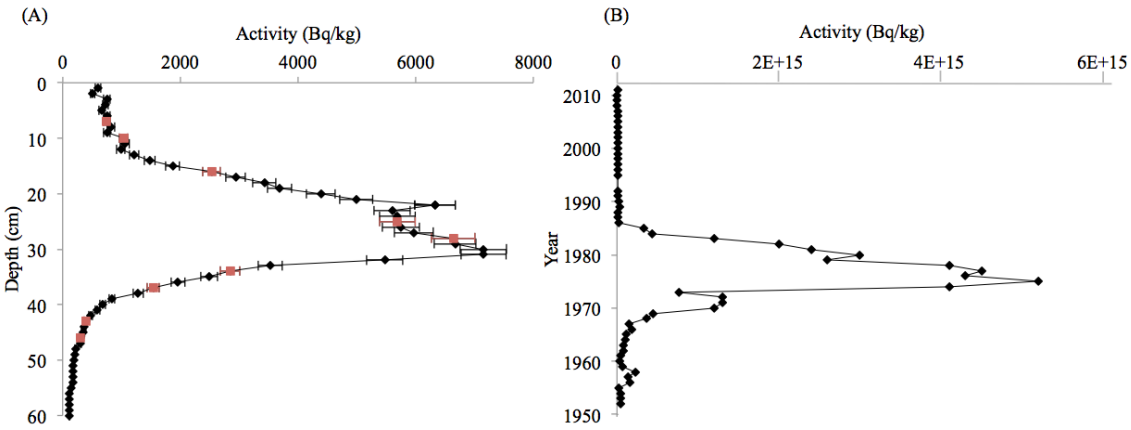

Figure 5.3. Caesium-137 activity in (A) Wyre sediment core in Bq/kg dry weight and (B) Authorised aqueous discharges from the Sellafield reprocessing site. Values in red in (A) represent those taken forward for ICP-SFMS analysis (see Table 5.1). Results have not been decay-corrected

Depth (cm)	^{137}Cs (Bq/kg)	^{137}Cs (pg/g)
7	750±60.8	0.23
10	1,038±72.7	0.32
16	2,530±147	0.79
25	5,690±302	1.78
28	6,640±365	2.08
34	2,850±165	0.89
37	1,540±102	0.48
43	393±23.2	0.12
46	295±26.5	0.09

Table 5.1. Caesium-137 activity in salt marsh sediment samples selected for ICP-SFMS analysis

There was no improvement in performance when repeated for a larger 4cm long x 0.5cm diameter column. Given the extensive testing of the calixarene, it is unlikely that the sample matrix was a limiting factor. The high cost of the calixarene led to the development of a stage to regenerate the resin and allow repeated use. A 20 mL $5x10^{-4}$M HNO_3 wash successfully removed residual activity and contamination from the column, with quantitative recovery of Cs achieved with up to 4 repeated uses. However, with each usage there is likely to be a gradual loss of extractant from the resin. Given the low concentration of the calixarene (0.02M), a loss of extractant may account for the poor performance of the calixarene in this study. Further evidence for this is a recovery of >95% ^{137}Cs when a sample was loaded onto a column containing pre-filter resin support material (Triskem International) and no calixarene. In the case of low-level radionuclide detection, it is recommended that new resin be applied to all samples to achieve optimal Cs recovery and Ba decontamination, however this would be a costly option.

Procedure stage	Average recovery (range) (%)
Digestion	72.1 (64.5-78.0)
AMP filter + filtrate	89.1 (87.8-91.7)
Cation exchange + extraction chromatography:	
Sample load	<4
Milli-Q water	<4
Remaining on resin post-Cs elution	<4

Table 5.2. Sources of analyte loss in digestion and chemical separation of sediment samples based on gamma spectrometry of ^{137}Cs. Detection criteria based on a 4-count time

5.3.2 ICP-SFMS measurement

Repeat measurement of stable ^{133}Cs solutions (0.01-10 ng/L) on the day of measurement returned a sensitivity of ~42,000 counts for a 1 ng/L solution, with good linearity

(R^2=1.00), and an instrumental detection limit of 2.4 pg/L (calculated as the concentration of 3 times the standard deviation of the background at mass 133). The abundance sensitivity was determined from a 25 µg/L ^{133}Cs standard solution, with a value of 3.7x10^{-5} at low mass resolution (R=300), calculated as the signal intensity at mass 135, divided by the signal at mass 133. This value was calculated using a PC^3 sample inlet system (Elemental Scientific), and standard nickel sample and skimmer cones. This 'standard' instrument setup achieved a sensitivity of 1,300 counts for a 1 ng/L solution, and a detection limit of 15.0 pg/L, highlighting the improvement in sensitivity achievable when operating with the Jet interface.

A linear mass bias correction was applied based on repeated measurements of a 10 ng/L stable Ba solution on the day of measurement (Figure 5.4) using the equation t=m*(1+ΔMf), where t and m are the true and measured ratios, respectively, ΔM is the difference in mass of the 2 isotopes, and f is the mass bias correction factor (Appendix E. page 167). The overall precision of repeated measurements (n=10) of ^{135}Ba/^{138}Ba and ^{137}Ba/^{138}Ba was within 0.4% and 0.3%, respectively. The Ba concentration following chemical separation was assessed from the ^{138}Ba signal, with values ranging from 20.2 ng/L to 53.6 ng/L. An interference correction was calculated using Equation 5.1:

$$(^{135}\text{Ba and } ^{137}\text{Ba})_c = {}^{138}\text{Ba}_m \times (^{135}\text{Ba and } ^{137}\text{Ba})/{}^{138}\text{Ba}_t \qquad (5.1)$$

Where $(^{135}\text{Ba and } ^{137}\text{Ba})_c$ is the calculated value, $^{38}\text{Ba}_m$ is the measured value, and $(^{135}\text{Ba and } ^{137}\text{Ba})/{}^{138}\text{Ba}_t$ is the true isotope ratio based on isotopic abundances. Prior to this, a further correction was applied at mass 138 to account for the presence of lanthanum-138 (0.1% abundance) and cerium-138 (0.3% abundance). The contribution of these elements was minimal because of effective removal by chemical separation prior to sample introduction, and the low isotopic abundances. Any residual signal was corrected for using high abundance isotopes at lanthanum-139 (99.9% abundance) and cerium-140 (88.5% abundance).

A final stage calixarene separation is capable of reducing the Ba procedural blank concentration to a minimum value of 2 ng/L, corresponding to a method detection limit of 10 pg/L (calculated as the concentration of 3 times the standard deviation of the

background at masses 135 and 137) (Russell et al. 2014(B)) (Chapter 3.2.4. page 51) In this study, the calixarene did not provide optimal Ba decontamination, with an average

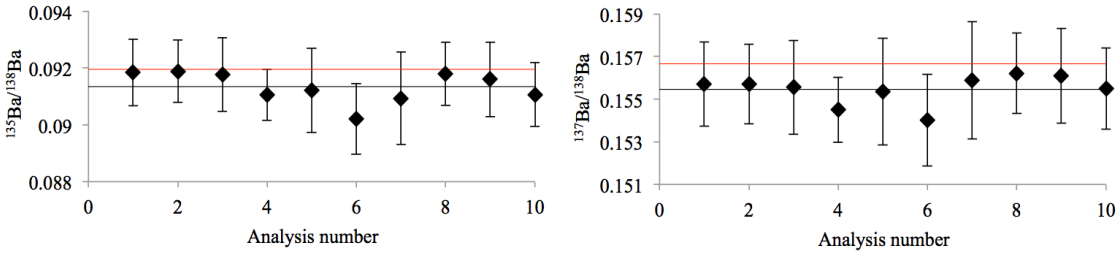

Figure 5.4. $^{135}Ba/^{138}Ba$ and $^{137}Ba/^{138}Ba$ ratios determined from repeat measurement of a 10ng/L stable Ba standard. Solid black and red lines represent the average measured and true ratio, respectively. Error bars are the combined uncertainty in the measured values of the two isotopes.

method procedural blank concentration of 52.1 pg/L. To further determine the extent of environmental Ba contamination, separate procedural blank samples were evaporated to dryness overnight following calixarene separation, and then made up in 3 mL 0.05M HNO_3 for sample introduction. The Ba concentration in evaporated samples was higher than non-evaporated samples by a factor of up to 2.4. This highlights the importance of direct sample introduction in order to minimise contamination in the case of low-level environmental samples, even when operating under clean laboratory conditions (Appendix C, page 159-164). If the sample must be evaporated to dryness to concentrate the analyte up in a smaller volume, the evaporation time must be minimised. Alternatively, online chromatographic separation can reduce contamination, as well as minimising reagent volumes and improving the efficiency of Cs/Ba separation (Alonso, 1995; Moreno et al. 1999; Pitois et al. 2008; Taylor et al. 2008; Liezers et al. 2009).

The stable ^{133}Cs concentration in the final fraction was initially determined by running the samples using a quadrupole ICP-MS (Thermo X-series II). Assuming a 100% recovery of ^{137}Cs, and a 1:1 ^{135}Cs:^{137}Cs ratio, the $^{135}Cs/^{133}Cs$ value in sediment samples ranged from $1.0x10^{-6}$ – $2.2x10^{-8}$, which exceeds the abundance sensitivity of the Element XR. In some cases, a neighbouring peak can be removed by sample pre-treatment, for example tailing of ^{238}U on ^{239}Pu. In this case the tailing is caused by a

stable isotope of the radioanalyte of interest, and will be retained through the chemical clean-up stages (Lariviere et al. 2006). For sediment samples, tailing of ^{133}Cs can therefore be considered the primary factor affecting the detection limits achievable, as opposed to isobaric Ba interferences, which are effectively removed by the separation procedure described. It is recommended that samples are pre-screened for ^{133}Cs and ^{137}Cs concentration by ICP-MS and gamma spectrometry, respectively, prior to analysis to determine the potential impact of peak tailing.

5.3.3 Resolving the tailing effect

The most significant cause of peak tailing is collisions of ions with residual gas molecules (Boulyga et al. 2006). This ion scattering leads to a loss in kinetic energy and/or change in direction of motion (Thermo Scientific, 2011). Relatively poor values have been recorded for ICP-MS compared to other mass spectrometric techniques, as the ion source operates at atmospheric pressure, leading to a relatively high residual gas pressure in the mass analyser (Boulyga et al. 2006).

The abundance sensitivity required to overcome the tailing effect of ^{133}Cs for measurement of ^{135}Cs in environmental samples has been reported as 10^{-8} to 10^{-9} (Lee et al. 1993; Delmore et al. 2011). By comparison, analysis of $^{135}Cs/^{137}Cs$ in spent fuel samples (Moreno et al. 1999; Pitois et al. 2007; Granet et al. 2008; Isnard et al. 2009), as well as other sample matrixes including groundwater (Liezers et al. 2009) and rainwater (Ohno and Muramatsu, 2014) have not considered peak tailing to be a limiting factor. Detection of $^{135}Cs/^{137}Cs$ has been determined in soil and sediment samples using an ICP-QMS equipped with a dynamic reaction cell (Elan DRC II (Perkin Elmer)), with Ba removed by a combination of chemical separation, and CH_3Cl reactive gas in the DRC (Taylor et al. 2008). The theoretical abundance sensitivity of this instrument is 10^{-10} (Perkin Elmer, 2004) (Table 5.3). The study by Taylor et al. (2008) did not give a measured value, and it is therefore assumed that the abundance sensitivity of the instrument was sufficient to eliminate the tailing effect.

Operating at a higher mass resolution and narrowing the ion energy beam (Lariviere et al. 2006) can improve abundance sensitivity of ICP-SFMS. The 25 µg/L Cs standard used to calculate the abundance sensitivity at low mass resolution was re-run at medium mass resolution (R=4000), improving the abundance sensitivity to $2.9x10^{-6}$.

Instrument	Abundance sensitivity	References
ICP-SFMS (Thermo Element XR)	10^{-5} (low resolution)	This study
	10^{-6} (medium resolution)	
ICP-DRC-MS (Perkin Elmer DRC II)	$<10^{-10}$ (theoretical)	Taylor et al. (2008)
TIMS (Finnegan MAT262Q)	10^{-10}	Lee et al. (1993)
ICP-QQQ-MS (Agilent 8800)	10^{-14} (theoretical)	Ohno and Muramatsu (2013)
		Zheng et al. (2014)

Table 5.3. Abundance sensitivity values for different instruments applied to $^{135}Cs/^{137}Cs$ detection

Operating at high resolution (R=10,000) can improve this value further (Vonderheide et al. 2004), however the concern is a reduction in instrumental sensitivity by a further order of magnitude compared to medium mass resolution. The reduction in tailing effect is not sufficient to enable detection of ^{135}Cs in the sediment samples in this study.

Providing there is a stable spread of ion energy and stable vacuum conditions, the tailing effect can potentially be corrected for (Thirlwall, 2001; Chu et al. 2002). The tailing effect is proportional to analyser vacuum, with improved vacuum conditions reducing the number of collisions with residual gas molecules (Chu et al. 2002). The accuracy of this correction will be improved by measurement of a monoisotopic (or close to monoisotopic) ion beam close to the mass of the analyte of interest, with no interfering peaks at masses either side of this. Previous applications include ^{89}Y for Sr correction, and ^{209}Bi for Pb correction (Thirlwall, 2001; Chu et al. 2002). Measuring the ion beam over short mass intervals (e.g. 0.1 mass units) will improve the accuracy of the mass tailing correction. The tailing effect can be significant several mass units away on instruments using a Faraday detector, and in the case of electron multipliers without an energy filter can be greater still (Thirlwall, 2001). Equation 5.2 can be applied to quantitatively measure the tail present under a peak (Thirlwall, 2001; Chu et al. 2002).

$$^{N}X_{corr} = {}^{N}X_{meas} - ({}^{N+1}X_{.T-1} + {}^{N+2}X_{.T-2} + {}^{N+3}X_{.T-3}) - ({}^{N-1}X_{.T1} + {}^{N-2}X_{.T2} + {}^{N-3}X_{.T3}) \qquad (5.2)$$

Where ^{N}X is the isotope of interest, and T_y is the proportional tail at $_y$ units e.g. +0.000001 for a tail of $1x10^{-6}$). Accurately quantifying the tailing effect for ^{135}Cs using ^{133}Cs is challenging because of the presence of Xenon in the plasma gas, with isotopes at masses 131, 132 and 134 (21.2%, 26.9% and 10.4% abundance, respectively). Given the challenges in removing Ba, it is also possible that ^{132}Ba (0.1% abundance) and ^{134}Ba (2.4% abundance) may also contribute to the signal. An alternative is to prepare a pure solution of praseodymium-141 (100% abundance), with tailing quantified over a mass range of 138-144. Over this range the presence of ^{138}Ba (71.7% abundance) may impact the low mass tailing correction at 3 mass units from the major peak. A final consideration is that, in low-level environmental samples, it has been shown that increased Ba contamination has a significant effect on the uncertainty of measured values (Russell et al. 2014(A) (Figure 2.4, page 40)), and this will be increased further with an additional tailing correction.

An alternative to correcting for peak tailing is to use an instrument with improved abundance sensitivity. Measurement of ^{135}Cs in sediment samples using thermal ionisation mass spectrometry (TIMS) equipped with a retarding potential quadrupole lens filter (RPQ) effectively eliminated ^{133}Cs ions scattered in the tail, leading to detection of ^{135}Cs with an abundance of 10^{-9} that of ^{133}Cs (Lee et al. 1993). The Thermo Neptune multi-collector ICP-MS can also offer an improvement in abundance sensitivity over the single collector Element XR, with values of up to $2x10^{-10}$ achievable (Becker, 2005). The instrument is equipped with two retarding potential quadrupole lenses (RPQ) that act as energy and directional filters to remove ions with disturbed energy or angle (Thermo Scientific, 2011). Furthermore, the Neptune *Plus* MC-ICP-MS is equipped with the Jet interface, and therefore can achieve the high instrument sensitivities described in this study. This instrument is potentially the most suitable option for low-level detection of ^{135}Cs in samples with a high starting concentration of stable ^{133}Cs, as it combines the high instrumental sensitivity of sector field instruments with an improvement in abundance sensitivity.

The abundance sensitivity of quadrupole instruments is not significantly improved by increasing mass resolution, but can be enhanced by operating with a collision or

reaction cell (Boulyga et al. 2002). Collisions with gas atoms reduces the ion kinetic energy and increases the residence time in the mass analyser, which can lead to a greater rejection of ions of the incorrect mass (Boulyga et al. 2000; Boulyga et al. 2002). The recent introduction to the market of a triple quadrupole instrument (Agilent 8800) equipped with two tandem quadrupoles can theoretically achieve an abundance sensitivity of 10^{-14}, calculated as the product of each quadrupole achieving a value of 10^{-7} (Zheng et al. 2014). This has been applied to detection of ^{135}Cs and ^{137}Cs in litter, lichen and soil collected in the 20-50 km zone around the Fukushima Daiichi nuclear power plant, with ^{137}Cs values ranging from 11.5-4,649 Bq/g (3.6-1,452.8 ng/kg) (Zheng et al. 2014). Barium decontamination was achieved using a combination of chemical separation, and an octopole reaction cell, with N_2O reactive gas achieving a Ba decontamination factor of 10^4. No detection limit was given, however a previous study by Ohno and Muramatsu (2013) using the same instrument achieved a value of 0.01 ng/L for ^{135}Cs and ^{137}Cs in Ba-free solutions. Whilst this is higher than the instrumental capabilities of ICP-SFMS, the sensitivity is sufficient for measurement of $^{135}Cs/^{137}Cs$ in the salt marsh sediment core sample in this study. The additional advantage is that the environmental Ba contamination introduced during chemical separation can potentially be removed using the octopole reaction cell. This potentially removes the need to use high purity resins and reagents and operating under ultra-clean laboratory conditions, which is not always practicable or economical.

5.4 Conclusions

The sensitivity achievable by new generation ICP-SFMS permits the low-level detection of a range of medium-long lived radionuclides, including the significant fission product radionuclides of caesium (^{135}Cs and ^{137}Cs). This in turn enables measurement of the $^{135}Cs/^{137}Cs$ ratio, which varies depending on the source of nuclear contamination, and therefore has the potential to be a powerful forensic tool. A number of applications to date have been constrained to isolated case studies, and a more comprehensive assessment of $^{135}Cs/^{137}Cs$ would be through application to a location with known historical activity and source of contamination. This study presents the measurement of $^{135}Cs/^{137}Cs$ from a salt marsh sediment core that shows a chronological record of aqueous discharges from the Sellafield reprocessing facility since operations began in the early 1950's.

The critical factors in achieving accurate detection are the removal of isobaric interferences arising from stable barium isotopes ^{135}Ba and ^{137}Ba, and peak tailing of stable ^{133}Cs. A thermo Element XR equipped with the Jet interface, X-skimmer cone and Aridus II desolvating sample introduction system routinely achieved an instrumental detection limit of 2.4 pg/L. The ability to match this detection limit was restricted by Ba contamination, with a triple stage chemical separation procedure effectively reducing the Ba concentration from ~350 mg/L in the sediment, to 20.2 - 53.6 ng/L in the final sample, resulting in an average method detection limit of 52.1 pg/L. The final stage calixarene extraction chromatography separation can improve this value to as low as 10 pg/L, however in this study this was ineffective. This is most likely because of repeated use of the resin leading to gradual loss of extractant from the material. Previously unused resin is preferable for achieving optimal Cs recovery and Ba decontamination, however this incurs a high expense.

The primary issue restricting measurement of ^{135}Cs/^{137}Cs in sediment samples is peak tailing from the high concentration of stable ^{133}Cs in sediment samples. The abundance sensitivity of the Element XR at low mass resolution ($3.7x10^{-5}$) is insufficient to resolve the ^{135}Cs/^{137}Cs value of $1.0x10^{-6}$ - $2.2x10^{-8}$ in sediment samples. Operating at medium mass resolution improved the abundance sensitivity to $2.9x10^{-6}$, therefore if the Element XR is to be applied to sediment samples, the tailing effect must be accurately quantified. Given that a correction for Ba contamination is already applied, a further tailing correction is likely to lead to high uncertainties in measured values in the case of low level concentrations. An alternative is to use an instrument with higher abundance sensitivity. Such instruments include the Agilent 8800 triple quadrupole instrument, or the Neptune Plus multi-collector instrument, the latter of which combines a high abundance sensitivity with the instrumental sensitivity of the JET interface described in this study. Other than the sediment core described, additional cores collected from two other sites in close proximity to the Sellafield site are available, which combined could provide the strongest measure to date of the applicability of ^{135}Cs/^{137}Cs as a forensic tool. This study highlights the flexibility of ICP-MS with regards to the strengths and limitations offered by different instruments. The Element XR combined with the Jet interface can achieve extremely low detection limits. However, in order to achieve these values in environmental samples a highly efficient chemical separation procedure is

required. In addition, the relatively low abundance sensitivity is a limitation to this instrument with regards to samples with a high initial stable ^{133}Cs concentration.

Chapter 6: Reviewing ICP-MS as a Technique for Measurement of ^{90}Sr in Environmental Samples

Abstract

Strontium-90 is a radioisotope of significant interest with regards to nuclear waste management, radioecology, environmental monitoring and protection. Highly sensitive measurement is achievable by radiometric techniques, however this often requires a long total procedural time (2-3 weeks) to allow for ingrowth of Yttrium-90 decay product, and establishment of secular equilibrium with ^{90}Sr. Mass spectrometric techniques, in particular inductively coupled plasma mass spectrometry (ICP-MS), are also applicable to ^{90}Sr detection, which offers a reduction in the total procedural time compared to radiometric procedures. However, this has traditionally been at the expense of sensitivity, limiting applications to higher activity samples. The critical factor in ICP-MS detection is removal of the isobaric interference from stable ^{90}Zr, as well as peak tailing of ^{88}Sr, which can significantly impact the detection limits achievable, particularly in the case of low-level environmental samples.

Recent advances in the sensitivities achievable by ICP-MS potentially put this technique in a position where it can compete with the detection limits offered by radiometric techniques, whilst offering a higher sample throughput. This report summarises the analytical procedures developed for determination of ^{90}Sr, focusing on ICP-MS and its validity as a technique for routine measurement.

6.1 Introduction

The high levels of ^{90}Sr detected in environmental and nuclear waste samples make this radionuclide of high importance in nuclear waste management, environmental monitoring and radiation protection (Rodriguez et al. 1996; Vonderheide et al. 2004; Becker, 2005; Lariviere et al. 2006; Grinberg et al. 2007; Hou and Roos, 2008; Amr and Abdel-Lateef 2010). Strontium-90 is a mobile element, and can accumulate in soils and plants via precipitation and ion exchange mechanisms (Zoriy et al. 2005; Grinberg et al. 2007; Vajda and Kim, 2010), as well as in bones and teeth if inhaled or ingested, because of its similar chemical properties to calcium. Approximately 20-30% of ^{90}Sr ingested is deposited in bone, increasing the risk of leukaemia and bone cancer (Rodriguez et al. 1996; Brun et al. 2002; Vonderheide et al. 2004; Jakopi and Benedik, 2005; Zoriy et al. 2005).

Strontium-90 is a beta-emitting radionuclide with a half-life of 28.8 years (Equation 6.1) with measurement achievable through radiometric or mass spectrometric (most commonly ICP-MS) techniques. ICP-MS traditionally offers faster assessment and higher sample throughput than radiometric techniques; however, this is at the expense of sensitivity, limiting its application to higher activity samples. Recent advances in ICP-MS sensitivity means it can potentially rival the detection limits achievable by radiometric techniques for shorter-lived radionuclides such as ^{90}Sr, whilst still offering a significant reduction in the total procedural time. This would have significant implications for the nuclear industry in the assessment and clean up of reactor sites, for routine environmental monitoring, and when a rapid response is required following a nuclear accident (Sakama et al. 2013; Takagai et al. 2014).

$$^{90}Kr \xrightarrow[32s]{(\beta,\gamma)} {}^{90}Rb \xrightarrow[3m]{(\beta,\gamma)} {}^{90}Sr \xrightarrow[30a]{(\beta)} {}^{90}Y \xrightarrow[64h]{(\beta)} {}^{90}Zr_{(stable)} \qquad (6.1)$$

Interference separation prior to measurement is required for both radiometric and mass spectrometric techniques. Detection of ^{90}Sr by radiometric methods is affected by significant spectrum interferences due to the continuous nature of the energy distribution of beta emitting radionuclides, which cannot be resolved by beta counters (Vajda and Kim, 2010). Strontium-90 must therefore be separated from radioactive

isotopes of lead, polonium, plutonium, neptunium and potassium, as well as from alkali earth matrix components and radionuclides e.g. Barium-133, barium-140 and radium-226 (Vonderheide et al. 2004; Vajda and Kim, 2010).

The primary limitation affecting ICP-MS measurement of ^{90}Sr is the isobaric interference from stable ^{90}Zr (natural abundance 51.5%). The similarity in mass between ^{90}Sr (89.907738) and ^{90}Zr (89.904703) requires a mass resolution of ~30,000 for effective separation, which is beyond the capabilities of sector field instruments (ICP-SFMS) (maximum ~10,000) (Vonderheide et al. 2004). It is therefore critical to reduce the ^{90}Zr concentration to lower than that expected of ^{90}Sr prior to measurement (Feuerstein et al. 2008). The decontamination factor required is dependent on the sample; however, even in the highly ^{90}Sr-contaminated soils surrounding the Chernobyl Nuclear Power Plant, a ^{90}Zr decontamination factor of ~10^6 is still required (Grinberg et al. 2007; Feuerstein et al. 2008).

An additional interference affecting ICP-MS procedures is peak tailing from stable ^{88}Sr (natural abundance 82.6%), which is present at high concentrations in environmental samples (20-300 mg/kg in soils, 7-9 mg/L in seawater) (Zoriy et al. 2005; Hou and Roos, 2008; Feuerstein et al. 2008), and is a particular concern for low-level ^{90}Sr detection. Measurement techniques based on atom counting require a high isotopic selectivity (abundance sensitivity) to suppress the influence of stable isotopes (Zimmer et al. 1994). The abundance sensitivity is a property of the instrument used, with relatively poor values for ICP-MS because of high-energy ions produced in the plasma discharge. Chemical separation will retain both stable ^{88}Sr and ^{90}Sr prior to measurement; therefore, the tailing interference is potentially the primary limitation affecting detection of ^{90}Sr, rather than isobaric ^{90}Zr. Finally, molecular interferences (e.g. hydrides, oxides and argides) can arise from reactions of elements in the plasma, which are often not resolvable by ICP-SFMS (Table 6.1) (Lariviere et al. 2006).

The aim of this report is to summarise the mass spectrometric procedures applied to measurement of ^{90}Sr, focusing on ICP-MS. Chemical and instrumental separation techniques for the removal of interferences prior to detection are reviewed, as well as the detection limits achievable compared to radiometric techniques, to determine whether ICP-MS is applicable as a technique for routine low-level ^{90}Sr measurement.

Interference	Resolution required for separation
$^{52}Cr^{38}Ar$	19,987
$^{50}V^{40}Ar$	49,894
$^{54}Fe^{36}Ar$	155,548
$^{50}Ti^{40}Ar$	158,287
$^{38}Ar^{40}Ar^{12}C$	5,175
$^{89}Y^{1}H$	89
$^{180}W^{2}$	1,370
$^{180}Hf^{2}$	1,372
$^{58}Ni^{16}O_2$	2,315
$^{74}Ge^{16}O$	10,765
$^{74}Se^{16}O$	9,300
^{90}Zr	29,877

Table 6.1. Isobaric and polyatomic interferences affecting ICP-MS measurement of ^{90}Sr

6.2 Chemical Separation

Traditional chemical separation techniques focussed on separation of ^{90}Sr from alkali earth elements calcium and barium through the formation of precipitates, commonly nitrates, chromates, oxalates and sulphates (Sunderman and Townley, 1960). Separation from Ca can be achieved based on the greater solubility of $CaNO_3$ in fuming HNO_3. This is a simple, cheap method that can handle high amounts of sample; however,

handling of hazardous fuming HNO_3 is required, and the procedure may need repeating depending on the sample matrix (Horwitz et al. 1991; Brun et al. 2002; Vajda and Kim, 2010). Separation from Ba can be achieved by formation of a chromate precipitate in slightly acidic solution (~pH 5.5), whilst ^{90}Y can be successfully separated using ferric hydroxide (Vajda and Kim, 2010). Ion exchange chromatography is also applicable to Sr separation from alkaline earth elements and fission products (Sunderman and Townley, 1960; Vajda and Kim, 2010), as well as separation from uranium and plutonium in radioactive waste matrices (Isnard et al. 2006; Jäggi and Eikenberg, 2009). This is a well-suited technique to ^{90}Sr measurement in high activity samples; however, if applied to ICP-MS procedures, column conditioning is required prior to use to remove high concentrations of stable Sr that can be present in the resin (Vajda and Kim, 2010).

Extraction chromatography using commercially available Sr-spec resin (Triskem International and Eichrom Industries) is a rapid and straight forward technique, which has been extensively applied to separation of ^{90}Sr from both radiometric and mass spectrometric interferences. The material consists of an extractant (4,4'(5')-bis(*t*-butylcyclohexano)-18-crown-6) (Figure 6.1) diluted in octanol solution and sorbed on an inert polymeric support (Vajda and Kim, 2010). Strontium uptake increases with HNO_3 concentration, with peak retention at 8M HNO_3, and elution at concentrations below 0.05M HNO_3, or in Milli-Q water (Equation 6.2) (Horwitz et al. 1991). Samples containing high concentrations of potassium, ammonium, calcium and/or sodium nitrate, as well as stable Sr reduce ^{90}Sr recovery (Happel, 2008; Hou and Roos, 2008; Amr and Abdel-Lateef, 2010; Eichrom, 2013). The concentration of these elements (other than stable Sr) can be reduced by the application of a pre-concentration stage prior to Sr-resin, such as calcium oxalate precipitation. With regards to radiometric interferences, Ba retention on the resin increases with HNO_3 concentration up to a peak at 3M HNO_3, therefore is effectively eluted in 8M HNO_3 (Happel, 2008; Eichrom, 2013). In the actinide series, tetravalent Pu and Np show a high affinity for the resin. Oxalic acid can be used as a competitive complexing agent to elute actinide elements, with the addition of a 3M HNO_3/0.05M oxalic acid wash following loading of the sample in 8M HNO_3 (Happel, 2008; Maxwell et al. 2010; Eichrom, 2013).

$$Sr^{2+}_{(aq)} + Crown_{(org)} + 2NO_3^-{}_{(aq)} \rightleftharpoons Sr(Crown)(NO_3)_{2(org)} \qquad (6.2)$$

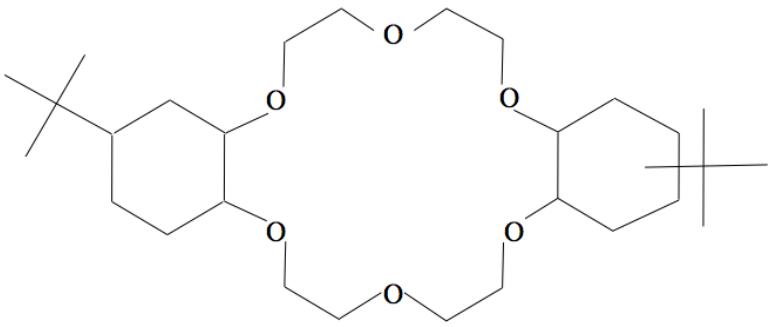

Figure 6.1. The extractant system in Sr-resin: (4,4'(5')-bis(*t*-butylcyclohexano)-18-crown-6)

There is less information regarding the effectiveness of Sr resin in removing isobaric and polyatomic interferences affecting ICP-MS measurement; however, the technique has been successfully applied to samples including sediments, urine and spent fuel (Vonderheide et al. 2004; Isnard et al. 2006; Grinberg et al. 2007; Taylor et al. 2007; Feuerstein et al. 2008; Takagai et al. 2014). Inherently high levels of natural Sr on the resin material (~1 ng/g) (Grinberg et al. 2007) may increase instrument background and hence the detection limit achievable, particularly for low-level environmental samples. This can be removed by pre-washing the resin with ≤0.05M HNO_3 or Milli-Q water. Despite the specificity of Sr-resin, at environmental concentrations the presence of residual Zr still impacts the accuracy of ^{90}Sr detection; therefore, repeated extraction chromatography and/or additional instrument-based separation may be required.

6.3 Measurement Techniques

6.3.1 Radiometric

Highly sensitive beta-counting techniques are applicable to detection of ^{90}Sr (Table 6.2). Detection is achieved through direct measurement of ^{90}Sr, or via ^{90}Y, a short-lived ($T_{1/2}$=2.7 days) beta-emitting daughter of ^{90}Sr (Hou and Roos, 2008; Vajda and Kim, 2010). Detection of ^{90}Y is often favoured owing to the high-energy electrons emitted by ^{90}Y (2.28 MeV) compared to those of ^{90}Sr (0.55 MeV). The overlapping spectra of these

two radionuclides can be resolved by calculating an ingrowth of ^{90}Y, or more commonly waiting for the establishment of secular equilibrium, which requires a waiting time of 2-3 weeks, followed by long count times in excess of 1,000 minutes, depending on the detection limits required (Taylor et al. 2007; Feuerstein et al. 2008; Tovedal et al. 2008; Vajda and Kim, 2010).

Technique	LOD
Gas ionisation detectors (proportional counters, GM counters)	1.0-7.2 fg
Cerenkov counting	2.0-5.9 fg
Liquid scintillation counters	1.9-5.9 fg

Table 6.2. Strontium-90 detection limits using radiometric techniques (Vonderheide et al. 2004; Zoriy et al. 2005; Lariviere et al. 2006; Vajda and Kim, 2010)

6.3.2 ICP-MS

ICP-MS is capable of further separation of Sr from isobaric and polyatomic interferences, with the most common techniques being a quadrupole instrument (ICP-QMS) equipped with a collision/reaction cell, or a sector field instrument (ICP-SFMS) operating at medium mass resolution (R=4,000-4,500) and cold plasma conditions (Table 6.3). These approaches are time and cost-effective compared to chemical separation for rapid monitoring of ^{90}Sr contamination, but often at the expense of analyte sensitivity (Vajda and Kim, 2010). A thorough chemical separation procedure potentially eliminates the need to compromise on analyte sensitivity, and any ^{90}Zr remaining at the measurement stage can be corrected using interference-free ^{91}Zr (natural abundance 11.2%), although this correction increases uncertainty in the measured value. The short measurement time (5-10 minutes per sample) means the concentration of ^{90}Y daughter product is negligible (~0.02% of the total intensity at

m/z=90 in nuclear fuel samples, compared to ~20% for ^{90}Zr) and will not interfere with ^{90}Sr determination (Isnard et al. 2006; Feuerstein et al. 2008).

Table 6.3. Summary of ICP-MS procedures for detection of ^{90}Sr

Reference	Instrument	Sample matrix	Digestion	Separation	LOD
Betti (1996)	GDMS	Environmental samples			0.01 ng/kg
Vonder-heide (2004)	ICP-QMS with collision cell, O_2 reaction gas	Urine	Acidification 60mL conc. HNO_3	Calcium phosphate precipitation Sr-resin Collision cell	2 ng/L (ICP-QMS) 0.4 pg/L (ICP-SFMS)
	SF-ICP-MS			Medium resolution, cold plasma	
Zoriy (2005)	SF-ICP-MS	Groundwater		Medium resolution, cold plasma	11 pg/L
Isnard (2006)	MC-ICP-MS collision cell	Uranium oxide and mixed oxide spent fuels		Sr resin Collision cell, O_2 reactive gas	
	TIMS				
Taylor (2007)	ICP-DRC-MS	Natural water, plant and sediment	Microwave	Water: cation exchange + Sr resin Plants: 2x Sr-resin Sediments: Sr resin, Toyopearl AF- chelate, Sr-resin	Sediments: 0.1 ng/kg Plant: 0.04 ng/kg Water: 3 pg/L

Reference	Instrument	Sample matrix	Digestion	Separation	LOD
Grinberg (2007)	ETV-ICP-MS with DRC	Environmental samples	Sediment samples: Microwave digestion: HNO_3:HF:$HClO_4$ (3:3:1) Biological samples: HNO_3	Sr resin ETV sample introduction DRC, O_2 reactive gas	1.8 ng/kg
Feuerstein (2008)	ICP-DRC-MS	Soils		Sr resin Collision cell, O_2 reactive gas	0.2 ng/kg
Amr (2010)	ICP-QMS with collision cell ICP-SFMS	Pottery	$HF:HClO_4$	ICP-QMS: collision cell, O_2 reactive gas ICP-SFMS: medium resolution, cold plasma	ICP-QMS: 0.9 ng/L ICP-SFMS: 0.01 ng/L
Sakama (2013)	ICP-DRC-MS	Water Soil	Microwave	On-line solid phase elution	0.6 ng/L
Takagai (2014)	ICP-DRC-MS	Soil	Microwave	On-line Sr resin DRC, O_2 reactive gas	0.8 pg/L

6.3.2.1 Isotope dilution

A limitation to applying radiometric standards as a yield tracer is that they are not aimed at ICP-MS analysis, and often consist of interfering elements at significantly higher concentrations than the isotope of interest (Granfors, 2013). An alternative is to apply a spike solution using a stable Sr isotope. For example, ^{86}Sr has been used as a yield

tracer at a similar concentration to that of ^{90}Sr (Granfors, 2013). Alternatively, Isnard et al. (2006) prepared a ^{84}Sr-^{235}U spike in order to measure $^{90}Sr/^{238}U$ by isotope dilution in uranium oxide and mixed oxide fuel samples using multi-collector ICP-MS equipped with a hexapole collision cell. Instrumental mass fractionation was corrected using a sample standard bracketing technique by measuring stable Sr isotopes $^{86}Sr/^{88}Sr$. The average mass of the two isotopes is the same as $^{84}Sr/^{90}Sr$, with analysis carried out using the same concentration of sample and standard. To validate the method, samples were also measured using thermal ionisation mass spectrometry (TIMS), with an average relative difference of <0.35% between the two techniques.

6.3.2.2 Sample introduction

Effective sample introduction can improve analyte sensitivity and/or interference removal. Direct measurement of solid samples using electrothermal vaporisation (ETV) or glow discharge (GD) mass spectrometry are straightforward, rapid techniques that also reduce the risk of sample loss and contamination (Betti et al. 1996; Grinberg et al. 2007; Resano et al. 2008).

ETV uses a hot surface, such as graphite, to vaporise samples for introduction to the plasma. This approach offers high analyte transport efficiency (20-80%) compared to solution nebulisation (2-5%), reduced oxide and hydride formation by solvent removal, low sample consumption (10-100 µL), and the ability to handle complex matrices (Grinberg et al. 2007). Grinberg et al. (2007) investigated separation of Sr from Zr and Y by using a commercial graphite tube in combination with ICP-QMS equipped with a dynamic reaction cell (DRC). The temperature of the graphite tube was limited to <2600^{0}C, which is lower than the boiling points of refractory elements Zr and Y (4,400^{0}C and 3,300^{0}C, respectively). Therefore, a homemade tungsten coil capable of operating at higher temperatures was also investigated, however a compromise had to be made between Sr sensitivity and interference separation using this approach. By comparison, Zr and Y effectively formed carbides using the commercial graphite tube, with a interfering signal equivalent of ~10% of that for 10 µg/kg Sr. ETV alone cannot achieve the Zr decontamination factor required in the majority of samples, but can be an effective separation stage following chemical clean-up and/or additional instrumental-based separation. ETV can also partially remove Fe and Ni that can form polyatomic interferences through reactions with oxygen in the reaction cell, however

chromatographic separation was deemed a more effective approach for removal of these elements. In the absence of Zr, ETV using a graphite tube achieved a Sr detection limit of 1.8 ng/kg, compared to 0.1 ng/kg using solution nebulisation. However, solution nebulisation cannot achieve interference separation, and in the presence of 100mg/kg Zr, the detection limit increased to 89 ng/kg, compared to 2.9 ng/kg using ETV.

Glow discharge forms a plasma by passing an electric current through a low-pressure gas (Betti et al. 1996). Gas ions and atoms strike the sample and knock atoms off the surface (sputtering), generating neutral particles that are ionised in the glow discharge plasma (Betti et al. 1996; Hou and Roos, 2008). Glow discharge mass spectrometry has been applied to ^{90}Sr measurement in certified samples of soil, sediment and vegetation (Betti et al. 1996). In order to prepare the samples, 500 mg of material was blended with a conductive high purity (99.999%) silver powder host matrix, and pressed into a disc using a hydraulic press. This technique was combined with the use of a secondary tantalum cathode, introduced during the analysis to obtain a stable discharge. This reduced sample dilution and contamination from silver impurities, which must always be considered at ultra-trace levels, despite using such a high purity powder. Glow discharge combined with a double focussing mass spectrometer operating at a mass resolution of 5,000 achieved a detection limit of 0.01 ng/L, with errors ranging from 9-30% compared to certified values (Betti et al. 1996). Interferences arising from the discharge gas and sample matrix could be removed by operating at a higher mass resolution, however this would reduce sensitivity and make this technique unsuitable for low-level analysis. In addition, the presence of ^{90}Zr means ^{90}Sr cannot be directly determined, with the contribution of isobaric interferences having to be calculated, thus increasing the uncertainty of the measured values.

Sample introduction also impacts the sensitivities achievable. For example, an Apex (Elemental Scientific) sample introduction system operating with a PFA nebuliser achieved superior Sr sensitivity and a lower uptake rate compared to a cyclonic spray chamber and ultrasonic nebuliser (Table 6.4) (Feuerstein et al. 2008) A desolvating sample introduction system such as a Cetac Aridus, or Apex equipped with an Actively Cooled Membrane (ACM) can offer a combination of high sensitivity, and a reduction in hydride and oxide-based polyatomic interferences by reducing the solvent load into the plasma (Amr and Abdel-Lateef, 2010).

Introduction system	Uptake rate (mL/min)	Sr sensitivity (counts per pg/L)
Apex + PFA nebuliser	0.1	129±2.6
Ultrasonic nebuliser	0.5	38±1.1
Cyclonic spray chamber + PFA nebuliser	0.9	4±0.6

Table 6.4. Sample uptake rate and Sr sensitivity for different sample introduction systems using DRC-ICP-MS (Feuerstein et al. 2008)

Chemical separation can be operated online with ICP-MS, which can reduce contamination, and minimise reagent volumes and total procedure time compared to offline procedures (Takagai et al. 2014). This approach is also advantageous when a rapid response is required, for example in the prompt assessment of contamination following the Fukushima accident in 2011 (Sakama et al. 2013; Takagai et al. 2014). A lab-on-valve based setup successfully removed 99.8% Zr using Sr-resin prior to DRC-ICP-MS (Takagai et al. 2014), whilst an automated solid phase elution (SPE) system coupled to DRC-ICP-MS reduced the chemical separation and analysis time by ~50% compared to offline separation (Sakama et al. 2013). The SPE setup used a GL Sciences InertSep ME-1 column for removal of alkali and alkali earth elements (including ^{90}Sr), which was followed by a UTEVA column (Eichrom Industries) for purification of plutonium.

6.3.2.3 Collision and reaction cells

Certain quadrupole instruments are equipped with either a collision or reaction cell, commonly positioned between the ion optics and the mass analyser (Epov et al. 2003). Operating with a collision cell can reduce the kinetic energy of interfering ions leaving the interface by injecting a gas such as argon or helium. By comparison, a reaction cell can eliminate isobaric and polyatomic interferences, providing the reaction gas has little or no interaction with the analyte of interest (Isnard et al. 2006). The kinetics of the reaction is also important, given the short contact time between the gas molecules and ions in the cell (Isnard et al. 2006). Using O_2 as the reaction gas, ^{90}Zr is oxidised to

$^{90}Zr^{16}O$, which can be observed at mass 106. Conversely, the same oxidation reaction with ^{90}Sr is not energetically favourable (Equation 6.3 and 6.4) and would require a stronger oxidant such as N_2O (Vonderheide et al. 2004), or a higher O_2 flow rate (Epov et al. 2003; Zoriy et al. 2005; Isnard et al. 2006; Hou and Roos 2008; Amr and Abdel-Lateef, 2010; Takagai et al. 2014).

$$Sr + O_2 \rightleftharpoons SrO + O \qquad \Delta Hr = 47.8 \text{ kcal/mol} \qquad (6.3)$$

$$Zr + O_2 \rightleftharpoons ZrO + O \qquad \Delta Hr = -88.7 \text{ kcal/mol} \qquad (6.4)$$

The most commonly applied reaction cell instrument is the Elan II DRC-ICP-MS (Perkin Elmer) (Epov et al. 2003; Grinberg et al. 2007; Taylor et al. 2007; Feuerstein et al. 2008; Takagai et al. 2014). The Bandpass tuning feature of this instrument offers mass discrimination against interfering by-products formed in the cell, whilst allowing analyte transmission. Interferences from molecular ions such as $^{50}Ti^{40}Ar$ and $^{50}Cr^{40}Ar$ are also suppressed (Hou and Roos, 2008). By comparison, a collision cell often operates with an energy filter to prevent newly formed interferences from leaving the cell. This can lead to an energy overlap between interferences and the analyte, which can increase the instrument background, reduce analyte signal and adversely impact detection limits (Perkin Elmer, 2004).

DRC-ICP-MS has been applied to detection of ^{90}Sr in soil samples in the vicinity of the Chernobyl nuclear power plant (Feuerstein et al. 2008). A Zr decontamination factor of $>10^7$ was achieved by a combination of Sr-resin and DRC-ICP-MS. The abundance sensitivity was calculated as $\sim 3 \times 10^{-9}$, which is superior to that achievable by ICP-SFMS (Table 6.5) with a detection limit of 4 pg/L for Zr-free solutions, increasing to 200 pg/L in digested soils. Strontium-90 has also been measured in soil contaminated by the accident at the Fukushima nuclear power plant, using on-line Sr-resin separation combined with DRC-ICP-MS, with a detection limit of 0.77 pg/L (Takagai et al. 2014). This study determined that, even if the efficiency of Zr removal in the cell reached 99.9%, the remaining signal would still interfere with ^{90}Sr detection.

Reference	Instrument	Abundance sensitivity
Vonderheide et al. (2004)	ICP-SFMS (low resolution)	10^{-5}
Vonderheide et al. (2004)	ICP-SFMS (medium resolution)	10^{-7}
Feuerstein et al. (2008)	ICP-DRC-MS	10^{-9}
Wendt et al. (1997)	RIMS	10^{-10}
Tumey et al. (2008)	AMS	10^{-15}

Table 6.5. Abundance sensitivity values measured to assess the impact of peak tailing of ^{88}Sr on ^{90}Sr

Taylor et al. (2007) measured ^{90}Sr by DRC-ICP-MS in samples collected from Perch Lake, Ontario, located downstream from an aquifer contaminated by discharges of radionuclides in the 1950's. The procedure achieved detection limits of 0.1 ng/kg, 0.04 ng/kg and 0.003 ng/L for sediments, plants and water, respectively. Iron and nickel oxide interferences formed from in-cell reactions were removed with Bandpass tuning (and initially by extraction chromatography for plant and sediment samples). The formation of these oxides is not believed to be thermodynamically favourable, and may have formed through oxygen atom transfer from residual water that is present either in the cell itself, or entrained in the gas cell lines. In-cell reactions with germanium-74 and selenium-74 were also observed, however these were successfully removed by extraction chromatography prior to sample introduction. There was a good agreement in the values measured for a standard reference material by Cerenkov counting and DRC-ICP-MS, with detection limits for the two techniques of 13.7 pg/kg and 97.7 pg/kg, respectively.

Collisions in the cell can reduce the ion kinetic energy, potentially improving the abundance sensitivity by increasing the residence time of ions in the mass analyser, thereby achieving better mass separation (Boulyga et al. 2002). If a high accelerating voltage (several hundred volts) is applied, ions are extracted more efficiently from the ICP to the quadrupole, further reducing peak tailing effects. This was not observed by

Feuerstein et al. (2008) using DRC-ICP-MS, as the low extraction potentials applied meant the energy of ions entering the mass analyser was low, thus limiting the impact of deceleration by collisions. Additionally, the collision gas increases pressure in the mass analyser, with residual gas ions leading to scattering of ions in the quadrupole. At higher gas flow rates this can have a negative impact on the abundance sensitivity.

6.3.2.4 Sector field instruments

The most common instrumental setup for ICP-SFMS detection of ^{90}Sr is to operate at cold plasma conditions (forward power = 650-750W) and medium mass resolution (R= 4,000-4,500) to improve Sr/Zr separation and abundance sensitivity, respectively (Table 6.3) (Vonderheide et al. 2004; Zoriy et al. 2005; Amr and Abdel-Lateef, 2010) (chapter 7.1, page 120-122). Operating under cold plasma conditions can suppress elements with a higher ionisation potential, which is applicable to separation of Sr (5.7eV) from Zr (6.8eV) (Vonderheide et al. 2004). Additionally, the formation of polyatomic argide-based interferences, including $^{50}Ti^{40}Ar$, $^{40}Ar^{50}Cr$ and $^{54}Fe^{36}Ar$, are also reduced (Zoriy et al. 2005).

Under cold plasma conditions, sensitivity is dependent on the sample matrix, with a potential increase in the formation of matrix-induced polyatomic ions. The potential loss in sensitivity is a result of the presence of an easily ionisable matrix constituent, variation in sample density and viscosity, or clogging of the cone orifice due to matrix salt deposition (Lariviere et al. 2006). Matrix effects can be minimised by chemical separation prior to sample introduction. In addition, a shielded plate between the torch and RF coil can increase sensitivity under cold plasma conditions by eliminating capacitive coupling between the plasma and the radio frequency (RF) coil, and therefore secondary discharge between the sampler and skimmer cones. The resulting narrower ion energy distribution improves transmission and sensitivity (Amr and Abdel-Lateef, 2010).

ICP-SFMS offers variable mass resolution, which can be used to improve the abundance sensitivity and minimise the tailing effect of stable ^{88}Sr (Vonderheide et al. 2004). The disadvantage is a reduction in instrument sensitivity due to reduced ion transmission (Epov et al. 2003; Taylor et al. 2007; Feuerstein et al. 2008). When a combination of medium mass resolution and cold plasma are applied, peak tailing of ^{88}Sr is considered the critical factor affecting accurate detection of ^{90}Sr (Zoriy et al.

2005). Abundance sensitivity values of $6x10^{-7}$ and $0.8x10^{-7}$ have been recorded when operating at medium resolution, which is an improvement of 2 orders of magnitude compared to low mass resolution (Vonderheide et al. 2004; Amr and Abdel-Lateef, 2010). Applications of ICP-SFMS include urine, groundwater and pottery (Vonderheide et al. 2004; Zoriy et al. 2005; Amr and Abdel-Lateef, 2010). In the case of urine samples, a detection limit of 0.4 pg/L was achieved for ICP-SFMS, compared to 2 ng/L for ICP-QMS operating with a collision cell (Platform, Micromass Ltd, Manchester, UK) (Vonderheide et al. 2004).

ICP-SFMS is a more costly and less frequently applied option than ICP-QMS (specifically DRC-ICP-MS) with regards to ^{90}Sr detection. Although the high instrumental sensitivity is beneficial to low-level detection, the relatively poor abundance sensitivity values in comparison to DRC-ICP-MS (Table 6.5) potentially restricts the applications of this technique. Instruments equipped with a collision/reaction cell have a lower sensitivity than ICP-SFMS, but can reduce the extent of, or even remove, the need for chemical separation, reducing the total procedural time and, in the case of higher activity samples, lower analyst exposure (Favre et al. 2007).

6.3.3 Alternatives mass spectrometric measurements

Resonance ionisation mass spectrometry (RIMS) vaporises solid or liquid samples using an atomic beam source, with one or more lasers tuned to specific wavelengths that ionise the element of interest (Hou and Roos, 2008). Compared to ICP-MS, RIMS offers improved isobaric suppression, abundance sensitivity, and instrument sensitivity (Zimmer et al. 1994; Wendt et al. 1997). This technique has been applied to ^{90}Sr detection in air samples collected in Munich following the Chernobyl accident (Zimmer et al. 1994). Following ashing and chemical separation, samples were transferred to a graphite tube furnace of the ion source. A detection limit of 4.0 fg was achieved using synthetic samples, with a statistical uncertainty of <25%. In a separate study, a simple and effective double resonance method was developed using two diode lasers (Wendt et al. 1997). A pyrolitic graphite-coated crucible was used for atomisation, with a maximum operating temperature of ~$2,400^0$C. Combined with a quadrupole mass analyser, this setup produced a detection limit of 0.8 fg, and an overall isotopic selectivity of greater than 10^{10} against stable Sr (Wendt et al. 1997).

Accelerator mass spectrometry (AMS) consists of a sample injector and an analyser mass spectrometer, which are linked together by a tandem accelerator (Hou and Roos, 2008). The sample is prepared as a solid target, and following sputtering is injected as a negative ion beam to the first mass analyser. The sample is then accelerated and converted to positive ions, to allow measurement by the second mass analyser. The stripping of electrons to form a positive ion beam can remove molecular interferences prior to detection, with AMS capable of radionuclide detection in the presence of an overwhelming stable isotope (abundance sensitivity ~10^{-15}) (Lariviere et al. 2006; Hou and Roos, 2008; Tumey et al. 2008).

AMS is limited by elements with small electron affinities, such as Sr (52 meV). This means that formation of anions in the sputter source is weak (Paul et al. 1997), and a molecular ion with an element of a higher electron affinity must be formed. Paul et al. (1997) achieved a detection limit of 7.9 fg for a groundwater sample by injecting ^{90}Sr as SrH_3^-. More recently, Eliades et al. (2013) used a fluoride ion source to improve Sr anion formation and isobar suppression. Targets were prepared by mixing the compound of interest with PbF_2 at a 1:5 ratio by volume. Using NO_2 gas, a reduction factor of ~$4x10^{-6}$ for ZrF_3^-/SrF_3^- was measured, with a theoretical detection efficiency of ~$6x10^{-16}$ for $^{90}Sr/Sr$. Tumey et al. (2008) achieved an instrumental detection limit of 0.02 fg, with a significantly higher method detection limit of 0.01 pg as a result of ^{90}Zr present in the sample holders. Replacing the aluminium target holders with high purity nickel holders, as well as redesigning of the detector to improve Sr/Zr discrimination, were suggested as approaches to improve the detection limit.

The detection limit for RIMS and AMS is superior to that of ICP-MS (Table 6.6), and comparable to GM counting and LSC. However, the high analytical expense, complex sample analysis and limited availability on the analytical market makes these techniques unsuitable for routine ^{90}Sr measurement (Wendt et al. 1997; Vonderheide et al. 2004; Becker, 2005; Zoriy et al. 2005; Hou and Roos, 2008; Tumey et al. 2008).

Reference	Detection method	Detection limit	Separation time	Count time
Chen et al. (2002)	GM counter	1.0 fg	1-2 d (+2-3 wks ingrowth time)	3-5 h
Suomela et al. (1993)	LSC by Cerenkov	2.0 fg	1-2 d (+2-3 wks ingrowth time)	2-3 h
Paul et al. (1997)	AMS	7.9 fg	6-8 h	0.5-1 h
Wendt et al. (1997)	RIMS	0.8 fg		0.5 h
Sakama et al. (2013)	ICP-DRC-MS	0.6 pg/mL	1 h*	5-10m
Zoriy et al. (2005)	ICP-SFMS	0.01 pg/mL	1-3 h	5-10m

Table 6.6. Comparison of radiometric and mass spectrometric techniques for detection of ^{90}Sr in water samples. *Estimated based on 50% reduction in preparation time compared to offline separation (Sakama et al. 2013)

6.4 Conclusions

Measurement of ^{90}Sr is achievable by both radiometric and mass spectrometric (most commonly ICP-MS) techniques. Radiometric techniques offer highly sensitive measurement, however the limitation is the need for mathematical calculation of ingrowth of the decay product ^{90}Y, or a waiting period of 2-3 weeks for secular equilibrium with ^{90}Sr to be reached. This can be followed by long counting times in order to reach the low detection limits required for environmental samples. The major advantage of ICP-MS is that there is no need to wait for ingrowth of daughter product ^{90}Y. This significantly reduces the total procedural time, allowing faster routine environmental monitoring and accident response, as well as potentially reducing the

total clean-up time at nuclear sites. However, ICP-MS struggles to rival the detection limits achievable by radiometric techniques due to interferences from isobaric ^{90}Zr, peak tailing of natural ^{88}Sr, and polyatomic interferences formed by reactions of elements in the plasma.

Radiometric and ICP-MS techniques both require removal of interferences prior to detection. The most common chemical separation procedure is extraction chromatography using Sr-resin, which is highly selective towards ^{90}Sr over both radiometric and ICP-MS interferences. A factor to consider in ICP-MS procedures is the presence of Zr in the resins and reagents used, which can increase the procedural blank concentration and the detection limits achievable. Decontamination of Zr can be improved through instrument-based separation, most commonly using DRC-ICP-MS with oxygen as the reactive gas. Alternatively, ICP-SFMS has been applied to ^{90}Sr detection, operating at medium mass resolution and cold plasma conditions in order to reduce ^{88}Sr and ^{90}Zr interferences, respectively. As yet, there is no known procedure that has relied solely on chemical separation of ^{90}Sr prior to ICP-SFMS detection. Such a procedure would allow operating at low mass resolution and 'hot' plasma conditions, which offers the highest instrumental sensitivity.

ICP-MS is currently considered to be a step forward in routine monitoring, and for higher activity samples the chemical and/or instrumental separation techniques described in this paper are effective. The limits of detection achievable are higher than existing radiometric techniques, however advances in the instrumental sensitivities achievable by ICP-SFMS, and flexibility with regards to the instrumental setup means the technique is worthy of further investigation to determine if it can be established as a realistic alternative to radiometric techniques for routine measurement of low level ^{90}Sr.

Chapter 7: Developing a Method for Detection of ^{90}Sr in Environmental Samples by Sector field Inductively Coupled Plasma Mass Spectrometry

Abstract

Advances in the sensitivities achievable by sector field inductively coupled plasma mass spectrometry (ICP-SFMS) enables the measurement of shorter-lived radionuclides such as ^{90}Sr at concentrations that can rival existing radiometric techniques, whilst offering a significant reduction in the total procedural time. This increased sample throughput is beneficial to rapid assessment and clean up of nuclear sites, as well as in routine environmental monitoring. In order to achieve these sensitivities, it is critical to eliminate the isobaric zirconium interference arising from ^{90}Zr, polyatomic interferences formed by reactions of multiple elements with gases in the plasma, and peak tailing from stable ^{88}Sr.

This study investigates the capability of ICP-SFMS for low-level detection of ^{90}Sr following interference removal by a combination of chemical purification (calcium oxalate precipitation and extraction chromatography), and instrument-based cold plasma separation. The chemical clean-up described is capable of a Zr decontamination factor of 10^5, which is insufficient in the case of low-level ^{90}Sr analysis. However, the inclusion of this stage is important in minimising the impact of matrix interferences, which impact the performance of ICP-SFMS, particularly when operating under cold plasma conditions. The instrument setup has a significant impact on sensitivity and the extent of Sr/Zr separation, with variations depending on the sample introduction system, and sample and skimmer cones used. The most sensitive setup investigated under 'hot' plasma conditions (forward power = 1200 W) was the Aridus II desolvating sample introduction system combined with the Jet interface and X-skimmer cone, with a detection limit of 15.9 pg/L. However, this setup does not benefit from cold plasma separation, and is dependent on chemical separation for removal of interferences. Under cold plasma conditions (~700 W), the Apex Q introduction system combined with a standard nickel sample cone and H-skimmer cone achieved the lowest detection limit of 4.5 pg/L at 650 W. Further improvements in sensitivity can be accomplished by a more comprehensive retuning of the instrument under cold plasma conditions. In addition,

operating at medium mass resolution can offer an improvement in the detection limit by improving the abundance sensitivity and minimising the impact of peak tailing from stable ^{88}Sr.

7.1 Introduction

High yield fission product ^{90}Sr is a major radionuclide in spent nuclear fuel and radioactive waste, with large amounts also produced during atmospheric weapons testing, as well as following the incidents at the Chernobyl and Fukushima Nuclear Power Plants. The relatively high levels of ^{90}Sr in environmental and nuclear waste samples make it an important radioisotope in waste management and environmental protection. Highly sensitive measurement is achievable by radiometric techniques, however these are affected by the spectral overlap of ^{90}Sr and its decay product ^{90}Y (Hou and Roos, 2008; Vajda and Kim, 2010). This necessitates the calculation of an ingrowth factor for ^{90}Y, or a waiting time of up to 3 weeks for radiochemical equilibrium to be established, as well as long counting times depending on the precision required (Taylor et al. 2007; Feuerstein et al. 2008; Hou and Roos, 2008; Vajda and Kim, 2010). The sensitivity achievable by new-generation ICP-SFMS can potentially rival the detection limits achievable by existing radiometric methods, with a significant reduction in the total procedural time, as ingrowth of ^{90}Y does not have to be considered. The higher sample throughput could lead to more rapid assessment and clean up of nuclear sites, which would offer significant economic benefits. This technique would also be applicable to routine environmental monitoring, and quick response following a nuclear accident.

Accurate detection of ^{90}Sr by ICP-MS is dependent on the removal of the isobaric interference from ^{90}Zr (51.5% abundance), peak tailing from naturally occurring ^{88}Sr (82.6% abundance), and multiple polyatomic interferences that can form from reactions of multiple elements in the plasma, most commonly with argon, oxygen and hydrogen (Table 6.1, page 102) (Zoriy et al. 2005; Lariviere et al. 2006). Decontamination of Zr and elements that can form polyatomic interferences can be achieved by chemical and/or instrument-based separation techniques. Extraction chromatography using commercial Sr-resin (Triskem International and Eichrom Industries) is a well-established technique for separation of ^{90}Sr from a range of sample matrices, including water, plants and sediments (Vonderheide et al. 2004; Isnard et al. 2006; Grinberg et al.

2007; Taylor et al. 2007; Feuerstein et al. 2008). The inclusion of an initial separation stage prior to Sr-resin increases the number and volume of reagents used, risking increased contamination, and a higher concentration of interfering elements in the procedural blank. However, direct loading of complex sample matrices can reduce the performance of Sr-resin and impact ^{90}Sr recovery (Eichrom, 2013), which may necessitate repeat procedures and/or the application of larger resin columns, increasing the analytical expense. To overcome this, formation of an insoluble compound or stable complex (Table 7.1) has been successfully applied to radiochemical procedures to separate ^{90}Sr from other alkali earth elements (Calcium and Barium) (Vajda and Kim, 2010). An initial separation stage may reduce the pressure on Sr-resin, and potentially improve the decontamination factor of interfering elements (Vajda and Kim, 2010).

Anion	Solubility in water (g/100 mL)
Carbonate	0.0011
Oxalate	0.0051
Fluoride	0.011
Sulphate	0.011
Chromate	0.12
Nitrate	70.9

Table 7.1. Solubility of common Sr salts (Vajda and Kim, 2010)

Previous procedures for detection of ^{90}Sr by ICP-SFMS have combined chemical clean-up with instrument-based separation using cold plasma conditions and medium mass resolution (Table 7.2) (Vonderheide et al. 2004; Zoriy et al. 2005; Amr and Abdel-Lateef, 2010). When operating under cold plasma conditions (RF= 650-850 W), the sensitivity is a function of ionisation potential (Tanner, 1995), with separation achieved

based on the higher first ionisation energy of Zr (6.6 eV) compared to Sr (5.7 eV) (Vonderheide et al. 2004). Cold plasma also reduces argide-based interferences, with a change in the instrument background spectrum from O, Ar and ArO, to O_2, N_2O, H_2O^+ and H_3O (Niu and Houk, 1996; Wollenweber et al. 1999). The reduction in background noise and improved ion transmission can improve the detection limit (Jakubowski et al. 1998; Wollenweber et al. 1999; Appelblad et al. 2000), with cold plasma conditions most frequently applied to measurement of low mass elements such as potassium, calcium and iron, which are affected by Ar and ArO interferences (Wollenweber et al. 1999; Murphy et al. 2002; Quemet et al. 2012; Lo et al. 2014). A reduction in forward power increases the vulnerability of the analysis to matrix effects, which originate from multiple sources in the instrument and can enhance, reduce or even have no impact on the analyte signal compared to a matrix-free solution (Agatemor and Beauchemin, 2011). The unpredictable nature of matrix interferences can be minimised by chemical separation prior to sample introduction.

The high concentration of stable ^{88}Sr in environmental samples (20-300 mg/kg in soils, 7-9 mg/L in seawater) can lead to a tailing effect at mass 90, which can impact the detection limits achievable for ^{90}Sr, particularly in the case of low-level analysis (Zoriy et al. 2005; Hou and Roos, 2008). The ability of ICP-MS to resolve this tailing effect (termed the abundance sensitivity) is a property of the instrument used. In the case of ICP-SFMS, operating at medium resolution (R= 4,000-4,500, compared to 300 at low resolution) focuses the ion beam over a narrower mass range, and can improve the abundance sensitivity by up to 2 orders of magnitude (Vonderheide et al. 2004, Amr and Abdel-Lateef 2010). For both cold plasma and medium resolution, there is a reduction in instrumental sensitivity, however the improvement in interference removal can improve the detection limit.

The aim of this study is to develop a procedure for low-level detection of ^{90}Sr, focusing on chemical separation and ICP-SFMS quantification. The instrument setup will focus on the impact of cold plasma and medium mass resolution, as well as the sample introduction system, and sample and skimmer cones used. Effective sample introduction can improve analyte sensitivity, as can the sample and skimmer cones used, with an improvement in extraction efficiency achieved through optimisation of the cone design (including external/internal angle, geometry at the tip, and orifice size) (Newman et al. 2009, Hu et al. 2012).

ICP-MS parameter	Zoriy et al. (2005)	Vonderheide et al. (2004)	Amr and Abdel-Lateef (2010)	This study
Sample matrix	Groundwater	Urine	Pottery	Standard solutions
Forward power (W)	650	750	850	650
Cooling gas flow rate (L/min)	18	14	14	16
Auxiliary gas flow rate (L/min)	1.5	0.8	0.3	0.9
Nebuliser gas flow rate (L/min)	1.2	1.0	0.8	1.1
Solution uptake rate (mL/min)	0.3	0.3	-	0.1
Sample and skimmer cones	Nickel	Nickel	Copper	Nickel sample H-skimmer
Focus lens potential (V)	-1100	-1000		-1300
Nebuliser	PFA-100 microconcentric	Micromist	Microconcentric Aridus	PFA-100 Microflow
Mass resolution	4,400	4,450	4,000	300

Table 7.2. Instrument settings for previous measurements of ^{90}Sr by ICP-SFMS

7.2 Experimental

7.2.1 Reagents

Instrumental performance and chemical separation procedures were determined using stable standard element solutions prepared from 1000mg/L elemental stock solutions (Inorganic Ventures) in 0.1% HNO_3 (v/v), other than Zr, which was prepared in Milli-Q water and trace HF. Unless mentioned otherwise, analytical reagent grade HNO_3 (Fisher Chemicals) and high purity de-ionised water (resistivity higher than 18.2 MΩ) produced from a Q-Pod Millipore System (Merck) were used throughout. Calcium oxalate precipitation was carried out using analytical reagent grade ammonia and ammonium oxalate (Fisher Chemicals), and Sr-resin (particle size 100-150μm) was supplied by Triskem International.

7.2.2 Instrumentation

The removal of interfering elements by calcium oxalate precipitation and Sr-resin was initially assessed using a Thermo-Scientific X-series II bench-top quadrupole instrument (ICP-QMS). For non-active sediment samples spiked with a ^{85}Sr tracer, recovery was determined by counting samples for 2 hours using a Canberra well-type HPGe detector. Analysis of the energy spectra and calculation of radionuclide activity was performed using Fitzpeaks software (JF Computing, Stanford in the Vale, UK).

Low-level measurements were acquired using a Thermo Element XR ICP-SFMS. The instrument is fitted with a Guard Electrode between the torch and load coil, which reduces the plasma potential that would otherwise lead to secondary discharge. This reduces the ion energy spread and improves ion transmission, which can minimise the formation of argon-based polyatomic interferences (Jakubowski et al. 1998; Becker and Dietze, 1999; Wollenweber et al. 1999; Amr and Abdel-Lateef 2010). Three sample introduction systems were investigated, all using PFA nebulisers at an uptake rate of ~100 μL/min. Firstly, a PC^3 sample inlet system (Elemental Scientific) is a robust, low maintenance unit incorporating a cyclonic spray chamber with an air-cooled Peltier, which reduces the solvent and water loads entering the plasma (Elemental Scientific, 2014(A)). Secondly, the Apex Q (Elemental Scientific) consists of a heated cyclonic

spray chamber, and three-stage Peltier-cooled desolvation system. The Apex Q has the option of membrane desolvation by the addition of the Actively Cooled Membrane (ACM), which further reduces water vapour loading, reducing the oxide formation rate from ~0.5% to 0.05% (calculated as the cerium oxide/cerium ratio) (Elemental Scientific, 2014(B)). In this study the Apex Q was operated without the ACM attached. Finally, the Aridus II desolvating sample introduction system (Cetac) combines a heated PFA spray chamber with a PTFE membrane desolvator unit, which offers very low hydride and oxide levels (CeO/Ce <0.03%) (Cetac, 2013)

The difference in performance of the H and X-skimmer cone was also investigated. The orifice of the two cones is the same (0.78 mm); however they differ in the shape of the throat, with the X-cone having a more open geometry than the stepped angles of the H-cone (Figure 7.1) (Taylor and Farnsworth, 2012). Operating with the X-cone has been shown to improve sensitivity under hot plasma conditions (Zheng and Yamada, 2006; Newman et al. 2009; Hu et al. 2012; Taylor and Farnsworth, 2012), however the impact of skimmer cone design under cold plasma conditions is not known. The Aridus II was operated in combination with the Jet interface, combining a high capacity dry interface pump and specially designed Jet sample cone, which when combined with the X-skimmer cone can achieve a sensitivity of up to 80,000 counts for a 1 ng/L solution (Chapter 2.3.3. page 37-40) (Thermo Scientific, 2010; Russell et al. 2014(A)). The benefits of the JET sample cone are only achieved in combination with a desolvating sample introduction system; therefore a standard nickel sample cone was used when operating with the PC^3 and Apex Q. The detection limit was calculated as the equivalent concentration of 3 times the standard deviation of the blank at mass 90, divided by the sensitivity for stable Sr standards. The signal to noise ratio, Sr/Zr separation factor and change in instrument sensitivity under cold plasma conditions was also assessed (Appendix G, page 173-175). The abundance sensitivity was calculated by running a 25 µg/L Sr standard solution at low and medium mass resolution using the PC^3 inlet system, and standard nickel sample and H-skimmer cones. The tailing effect was calculated as the signal intensity at mass 90 divided by the intensity at mass 88.

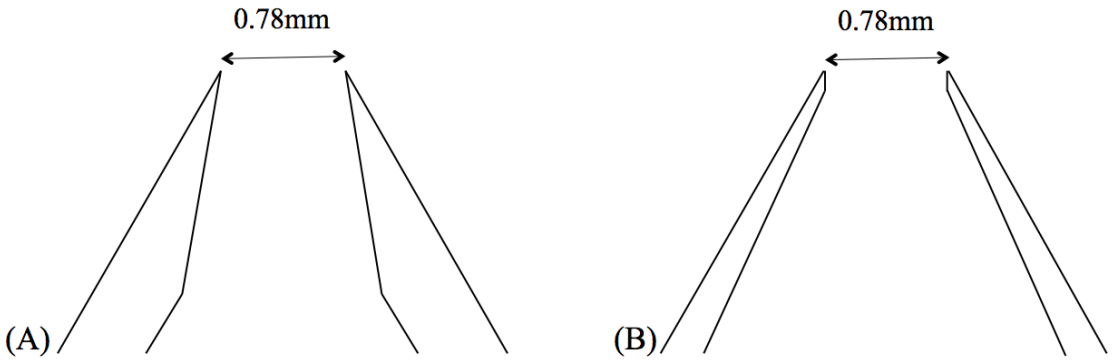

Figure 7.1. Geometry of H-skimmer and X-skimmer cone designs. (A) Finnigan standard cone. (B) Finnigan X (Taylor and Farnsworth, 2012)

7.3 Results and Discussion

7.3.1 Digestion

Sediment samples were dissolved using aqua regia acid leaching (Figure 7.2(A)). The Sr recovery achievable from different digestion methods was not investigated in this study. In previous studies, dissolution using HNO_3 or HCl is commonly applied, and for sample destruction a mixture of acids including hydrofluoric and perchloric acids, and hydrogen peroxide have been effectively used, in some cases using high pressure microwave digestion (Grinberg et al. 2007; Taylor et al. 2007; Feuerstein et al. 2008; Amr and Abdel-Lateef, 2010; Vajda and Kim, 2010).

7.3.2 Chemical separation

Calcium oxalate precipitation was applied as an initial separation procedure for ^{90}Sr (Figure 7.2(B)). Depending on the sample matrix, a Ca carrier solution may be required to form a precipitate. When using standard solutions, 1 mL 2 M CaCl was added to the sample, whereas no carrier was required in the sediment leachate tests, owing to the high Ca content present in the sample. The precipitate formed can also be effectively separated by filtration, however centrifuging was a cleaner and more rapid approach.

The performance of Sr-resin was assessed with regards to decontamination of ^{90}Zr, and polyatomic interferences formed by the reaction of high abundance elements with argon

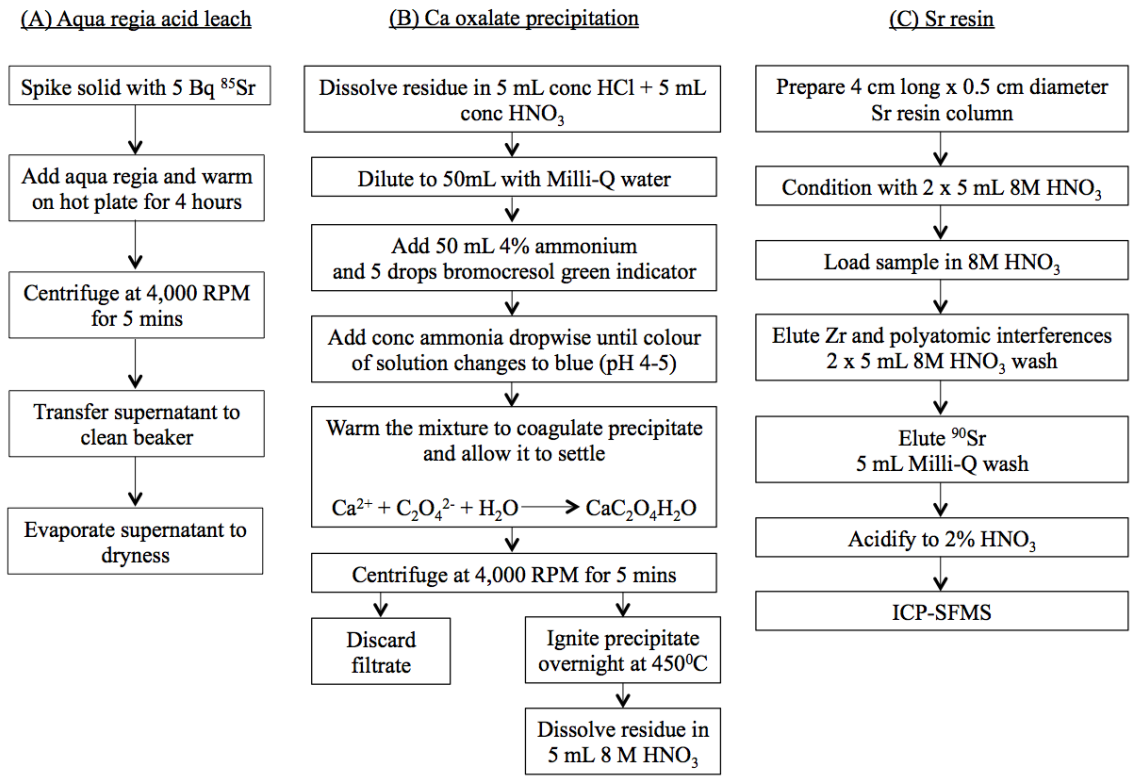

Figure 7.2. Digestion and chemical separation procedure for a sediment leachate sample prior to ^{90}Sr detection by ICP-SFMS, incorporating (A) Aqua regia acid leaching; (B) Calcium oxalate precipitation; (C) Sr-resin extraction chromatography

in the plasma (Table 7.3). A 5 mL 8M HNO_3 solution with 1 mg/L of interfering elements and Sr was loaded onto a 4 cm long x 0.5 cm diameter column, followed by a 10x1 mL 8M HNO_3 wash, and then a 10x1 mL Milli-Q water wash (Figure 7.2(C)). A 100x dilution was applied to each fraction and measured by ICP-QMS. The resulting profile (Figure 7.3) shows effective elution of interfering elements following a 5 mL 8M HNO_3 load and wash, with recoveries ranging from 87±3% (Cr) to 94±4% (Zr). The recovery of Zr in the Milli-Q wash was ≤0.8%, with a maximum for other interferences of 1.8±0.2% (Cr). The result for Zr is in agreement with a previous recovery of 91.4% following a 6 mL 8M HNO_3 wash from a 5 cm long column (Horwitz et al. 1992). Further investigation into the performance of Sr-resin with regards to decontamination of Zr found no significant difference in performance for load and wash concentrations ranging from 1-8 M HNO_3, with a Zr recovery of >90% over this concentration range. Despite the high recovery from 5mL 8M HNO_3, for low level detection of ^{90}Sr, a 10 mL 8M HNO_3 wash is recommended for a 4 cm long x 0.5 cm diameter column to

maximise decontamination of interferences. The loss of Sr in the load and wash fraction was calculated as ≤0.5%.

Interference	Sediment concentration (mg/kg)	Resolution required for separation (m/Δm)
^{90}Zr	260	29,620
$^{52}Cr^{38}Ar$	61	19,987
$^{54}Cr^{36}Ar$		37,855
$^{50}V^{40}Ar$	47	49,894
$^{50}Ti^{40}Ar$	3 450	158,287

Table 7.3. Properties of isobaric and high abundance polyatomic interferences affecting ICP-SFMS detection of ^{90}Sr (Gorindaraju, 1994; Zoriy et al. 2005; EuroGeoSurveys, 2011)

The Sr recovery in the Milli-Q fraction was 103±4%, with the >100% recovery potentially a result of residual Sr present on the resin (Grinberg et al. 2007). This can be removed by washing the column with Milli-Q water prior to 8M HNO_3 conditioning. The uptake of elements onto Sr resin is often measured as the number of free column volumes (FCV) to peak maximum in a chromatographic column (k'), where FCV is a measure of the void volume in the column (Horwitz, 2013). The value for k' peaks at ~90 for Sr at 8M HNO_3, decreasing to <1 at concentrations below 0.05M HNO_3 (Eichrom, 2013). If the the mass of resin added to the column is known, the weight distribiution ratio (D_W) can be calculated (Equation 7.1) and the value divided by a conversion factor (2.0 for Sr resin) to obtain a value for k' (Horwitz, 2013).

$$D_W = \frac{A_0 - A_S}{A_S} \times \frac{mL}{g} \qquad (7.1)$$

Where A_0 - A_s is the activity sorbed onto a known weight of resin (g) and A_s is the activity in a known volume (mL). At 8M HNO_3, the D_W for Sr was calculated as 186 mL/g, corresponding to a k' of 93, decreasing to 0.9 in Milli-Q water. This is in good agreement with the values quoted by the manufacturer (Eichrom 2013). For interfering elements, k' ranged from 2.0 (Zr) to 6.5 (Cr) at 8M HNO_3.

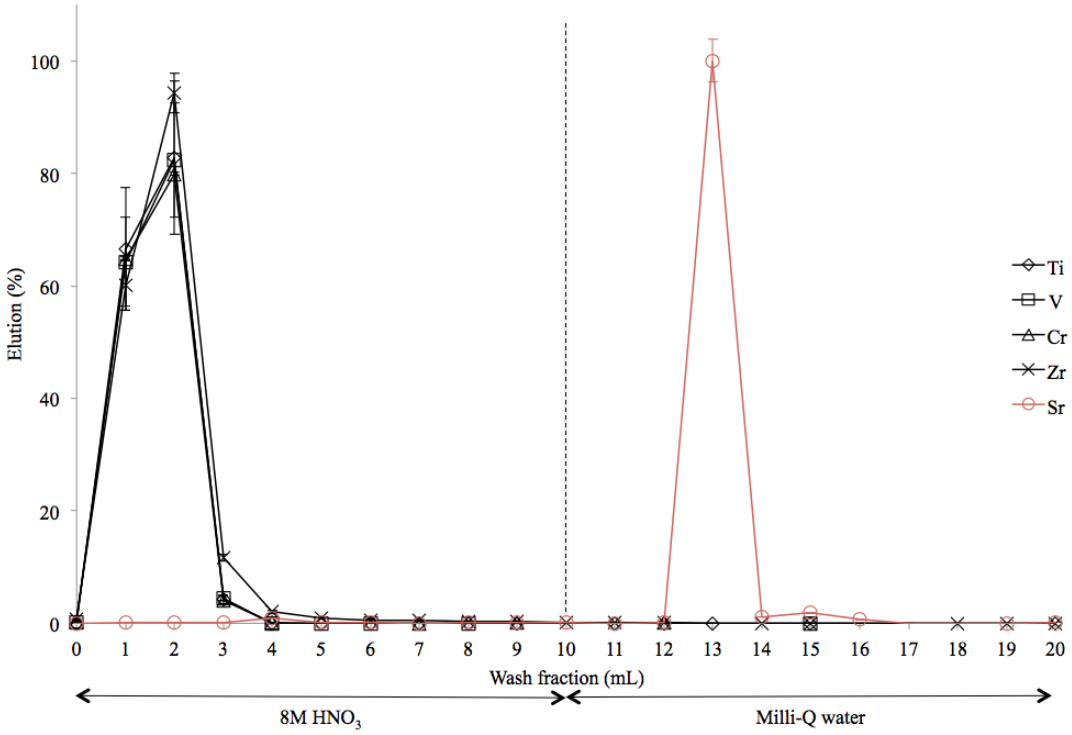

Figure 7.3. Elution profile for Sr and interfering elements from a 4 cm long x 0.5 cm diameter Sr-resin column

Minimising the elution volume will reduce the extent of sample dilution, potentially allowing direct sample introduction and thereby reducing the concentration of interfering elements in the procedural blank as a result of environmental contamination. The volume required to elute Sr from the resin increased with HNO_3 concentration over a range of 0.3-0.6 M. (Figure 7.4). A volume of >10mL was required for all concentrations over this range, compared to a quantitative recovery in 5mL Milli-Q water. This fraction can then be acidified to 2% HNO_3 prior to sample introduction.

Combined calcium oxalate and Sr-resin separation was applied to a non-active sediment leachate sample with a starting Zr concentration of ~2 mg/L. The leachate was spiked with ~5Bq ^{85}Sr, with fractions counted after each separation stage for 2 hours by gamma spectrometry to assess recovery. A separate solution containing ^{85}Sr and no sample was reserved to confirm the activity added to samples. Calcium oxalate precipitation and Sr-

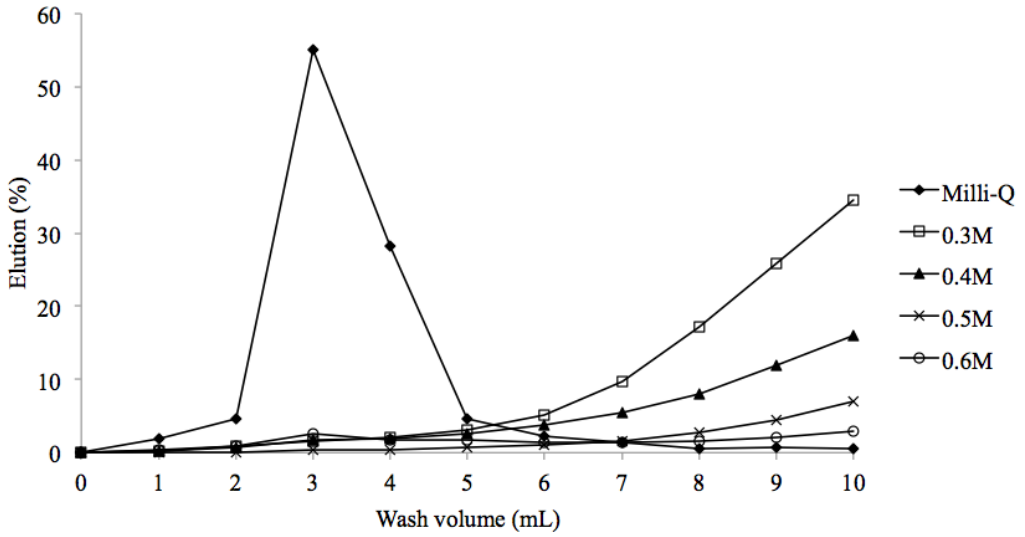

Figure 7.4. Elution volume for Sr at different HNO_3 concentrations for a 4cm long x 0.5cm diameter Sr-resin column

resin achieved an average ^{85}Sr recovery of 91.4±7.4% and 87.8±6.9%, respectively, with a combined recovery of 80.3±6.9%. The Zr decontamination factor was calculated as ~310 and ~3,300 for Ca oxalate and Sr-resin, respectively, giving a combined decontamination factor on the order of 10^5. The procedure described is therefore not sufficient to allow low-level detection of ^{90}Sr, as the ^{90}Zr/^{90}Sr value in environmental samples typically ranges from 10^7-10^{11} depending on the sample matrix (Lariviere et al. 2006). Further chemical and/or instrument-based separation is therefore required.

The average procedural blank Zr concentration was 31.1 ng/L, improving to 10.2 ng/L when the Sr-resin stage was carried out in a class 1000 clean laboratory using Teflon sub boiled HNO_3, and labware subjected to rigorous cleaning procedures prior to use (Appendix C, page 159-164). In the absence of instrument-based separation, further reductions in the procedural blank is critical in achieving low detection limits. This

would require the use of high purity reagents and working under clean laboratory conditions throughout.

7.3.3 Quantification

7.3.3.1 Instrument sensitivity

For all instrumental setups, the Sr sensitivity was optimised with a 25 ng/L standard solution through adjustment of the gas flow, torch and lens positions under 'hot' plasma conditions (RF=1200-1300 W). The highest instrument sensitivity was achieved at an RF value of ~1200 W, with a reduction in sensitivity and signal stability from 1200-1300W (Figure 7.5). Following this, the forward power was reduced to a minimum of 650 W, with tuning files saved at ~100 W intervals over this range. When retuning under cold plasma conditions, a parameter of particular interest was the focus lens voltage, which corrects for the difference in ion kinetic energy, and therefore differs between hot and cold plasma conditions. By reducing the focus lens voltage from -900 V to -1,300 V at 650 W, the sensitivity improved by a factor of up to 2.6 (Figure 7.6). This is in good agreement with a previous study that achieved a two-fold improvement in sensitivity by reducing the focus lens voltage from -850 V to -1,100 V when operating under cold plasma conditions (Zoriy et al. 2005).

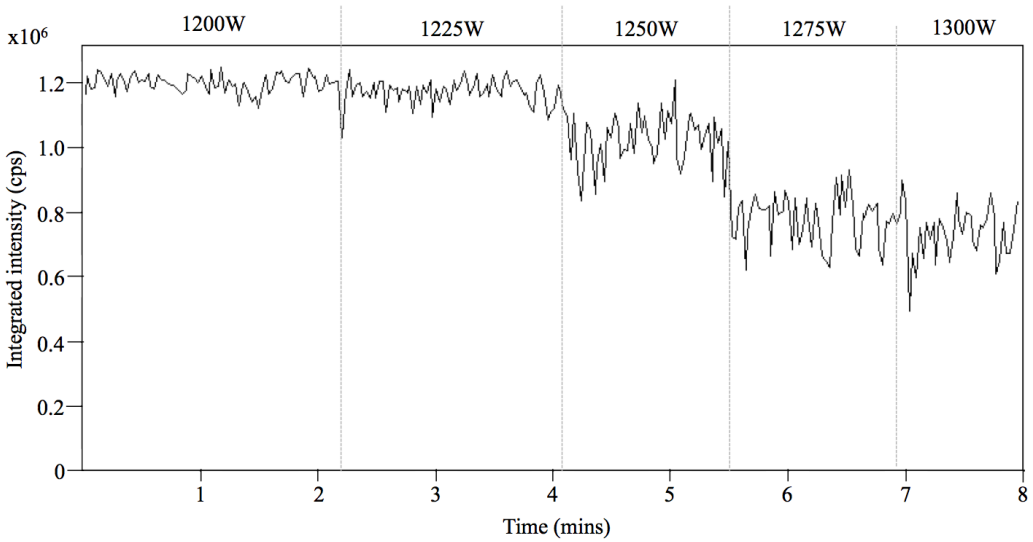

Figure 7.5. Signal sensitivity and stability for a 25ng/L stable Sr solution at 1200-1300W when operating with the Apex Q, standard Ni sample cone and H-skimmer cone

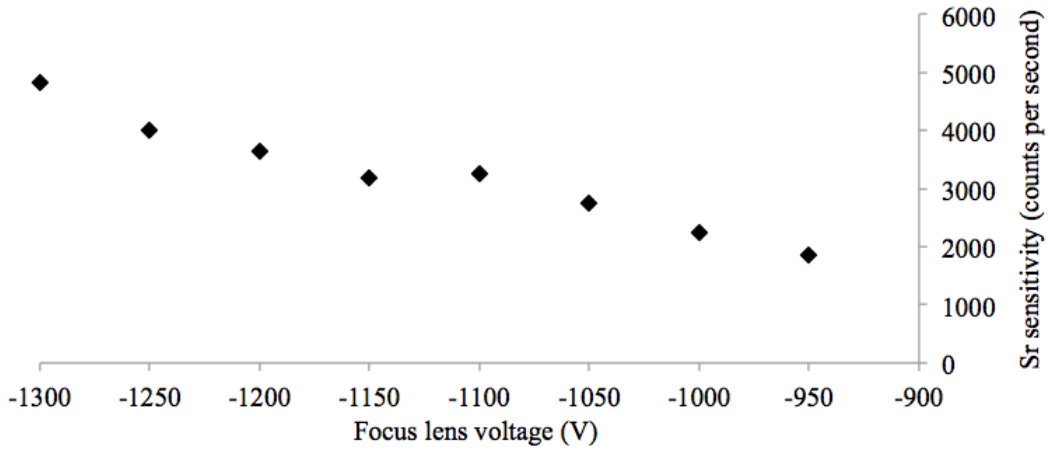

Figure 7.6. Impact of Focus lens voltage on ICP-SFMS sensitivity for a 25 ng/L stable Sr solution at 650W

An increase in nebuliser gas flow rate can improve sensitivity through further cooling of the plasma, reducing argide-based interferences (Kehm et al. 2003; Vonderheide et al. 2004; Zoriy et al. 2005; Feuerstein et al. 2008), however an increase in oxide formation must be considered, which could increase the formation of polyatomic interferences (Table 6.1, page 102). The sample gas and add gas flow rates were adjusted to achieve high analyte sensitivity, without compromising on the rate of oxide formation. For both the PC^3 and Apex Q, the maximum sample gas and add gas flow rates were 0.70 L/min and 0.45 L/min, respectively. For the Aridus II, the maximum argon sweep gas was 7.8 L/min, above which oxide formation rates increased significantly.

It has been assumed that chemical separation and cold plasma conditions will effectively remove elements that can form polyatomic interferences that impact detection of ^{90}Sr. Whilst argon-based interferences are reduced by a combination of cold plasma and the presence of a Guard Electrode (Jakubowski et al. 1998; Jarvis and Williams, 1998; Murphy et al. 2002), an increase in oxide interferences due to the change in the background spectrum must be considered. An increase in polyatomic oxide ions has been noted when using cold plasma conditions (Tanner, 1995; Jarvis and Williams, 1998), whilst a Guard Electrode has been shown to increase the rate of oxide formation under hot plasma conditions (Becker and Dietze, 1999; Appelblad et al. 2000). When tuning the instrument, high Sr sensitivity must be achieved, but not at the expense of high oxide levels. In future it would be beneficial to monitor the elements

known to form oxide interferences to assess the effectiveness of chemical separation, and the likelihood of interference formation.

Following instrument tuning, the impact of forward power was assessed for 0.1-50 ng/L mixed Sr and Zr standards. The highest count rate (30,900 counts per ng/L Sr) was achieved using the Aridus II in combination with the Jet interface and X-skimmer cone, with a detection limit of 15.9pg/L (Table 7.4). The Apex Q returned a sensitivity of 5,400 counts per ng/L when operating with a standard nickel sample and H-skimmer cone, with a detection limit of 62.7 pg/L. The same cone configuration was applied to the PC^3 inlet system, which returned a sensitivity of 1,650 counts per ng/L, and a detection limit of 106.5pg/L. The instrumental sensitivity and detection limits using the Apex Q was superior to the PC^3, therefore the impact of the skimmer cone design was assessed further using this introduction system. The X-skimmer cone improved the sensitivity by a factor of 2.7 compared to the H-cone, with a value of 14,600 counts per ng/L, and a detection limit of 19.9pg/L.

Instrument parameter	PC^3	Aridus II + Jet interface and X-skimmer	Apex Q + H-skimmer	Apex Q + X-skimmer
RF (W)	750	1200	650	900
Sr counts per ng/L	39	**30,865**	110	697
Sr sensitivity loss vs. 1200W	42.6	**0**	49.2	21.0
Sr/Zr separation factor	**1,529**	1.6	235.3	543.4
Signal/noise for 10 ng/L Sr	1.5	**38.0**	2.2	1.3
LOD (pg/L)	24.0	15.9	**4.5**	4.9

Table 7.4. Comparison of instrumental setups based on the RF value that achieved the lowest detection limit. Values in bold show the optimal value for the setups described.

7.3.3.2 Impact of cold plasma and mass resolution

For all instrumental setups, there was a reduction in Sr (and to a greater extent Zr) sensitivity as the RF value decreased from 1200 W to 650 W (Figure 7.7 and Appendix G, page 173-175). The Zr signal decreased to <1 count per ng/L at 650 W-750 W for all setups other than the Aridus II, whereas the Sr sensitivity at 650 W ranged from 25-270 counts per ng/L. This is a good indicator of the effectiveness of cold plasma separation. When operating with the PC^3, the Sr sensitivity increased slightly from 39 counts per ng/L to 46 counts per ng/L, despite the RF value reducing from 750 W to 650 W, however this was not observed for any other instrumental setup.

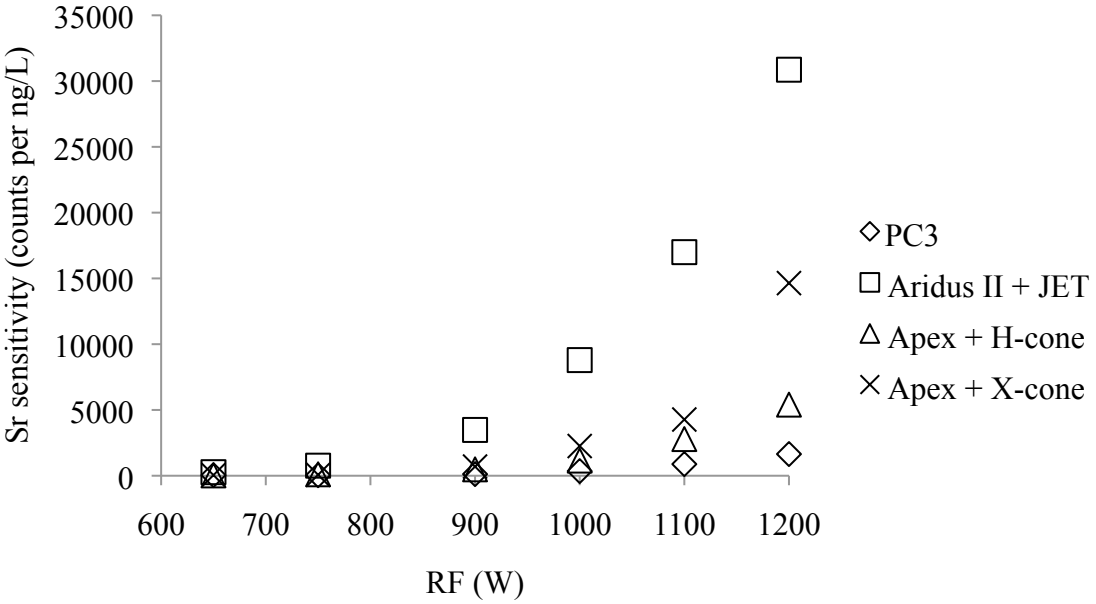

Figure 7.7. Impact of forward power on ICP-SFMS sensitivity for Sr for different instrumental setups

The detection limit increased with a reduction in forward power for the Aridus II, as the rate of Sr sensitivity reduction (compared to the optimal value at 1200 W) was greater than the rate of background reduction, which was not observed for any other instrument setup (Table 7.5). In addition, cold plasma conditions did not significantly impact the Sr/Zr separation factor for the Aridus II, with a maximum value of 2.2 at 750 W, which is lower than the PC^3 (1,529) and Apex Q (235 and 4,551 with the H-cone and X-cone, respectively) at the same RF value. This is a result of desolvation effectively introducing the plasma dry, with no liquid vapour in the sample aerosol to cool the

plasma (Kehm et al. 2003). The Apex Q (without the ACM) is a more desolvating unit than the PC^3, however with a reduction in forward power, the detection limit generally improved for both introduction systems, with the lowest values measured between 650 W and 900 W (Figure 7.8). This suggests that the extent of desolvation for the Apex Q is not sufficient to prevent the formation of cold plasma conditions. It is expected that the Apex Q operating with the ACM in combination with the Jet interface would improve Sr sensitivity compared to the Apex Q without the ACM, however like the Aridus II cold plasma separation would not be applicable.

Sensitivity parameter	PC^3	Aridus II	Apex Q	Apex Q
Sample cone	Ni	Jet	Ni	Ni
Skimmer cone	H	X	H	X
Background reduction	1,600	16	2,500	1,470
Sr sensitivity reduction	36	115	210	310

Table 7.5. Difference in instrument background and sensitivity at 650W compared to 1200W for different instrumental setups

A detection limit of 15.9 pg/L for the Aridus II setup at 1200 W is higher than the optimum values obtained for the Apex Q with the H-skimmer cone (4.5 pg/L at 650 W) and X-skimmer cone (4.9 pg/L at 900 W). However, the sensitivity and signal to noise ratio for the Aridus II at 1200 W is the highest of any setup tested (Table 7.4). The limitation is that cold plasma separation is not possible, and the detection limit achievable is therefore dependent on chemical separation. The Zr procedural blank of 10.2 ng/L from cleanup of the sediment leachate described equates to a method detection limit of 154.3 pg/L. In order to match the instrumental detection limit, a procedural blank concentration of approximately 1.0 ng/L is required, which would necessitate the use of high purity resins and reagents, with procedures carried out under clean laboratory conditions. This increases the procedural time and expense, which can

potentially be offset by using an alternative instrument setup where cold plasma separation is applicable.

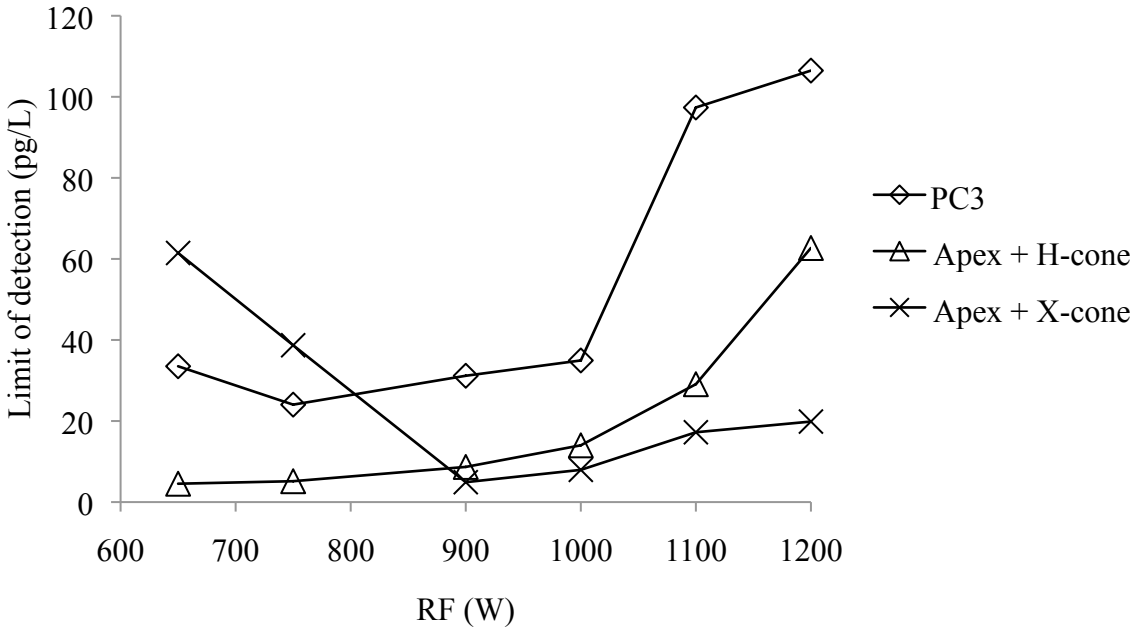

Figure 7.8. Impact of cold plasma conditions on the detection limit for different ICP-SFMS setups

For the Apex Q, the skimmer cone used had a significant impact on sensitivity and the impact of cold plasma conditions. At 900-1200 W, the X-cone achieved a lower detection limit than the H-cone, with a minimum value of 4.9 pg/L at 900 W. However, as the forward power was reduced further, the detection limit increased sharply to 61.5 pg/L at 650 W (Figure 7.8). Whilst the X-cone is more sensitive than the H-cone at RF >900 W, below this value there was greater rate of Sr sensitivity loss. Upon reducing the RF from 900 W to 750 W, the sensitivity dropped by a factor of 9.7 when operating with the Apex Q and X-cone, compared to a factor of 4.4 for the Apex Q and H-cone, and 3.2 for the PC^3. It is possible that the cone was not designed for cold plasma applications, however an alternative is that the X-cone is more vulnerable to the adjustment in plasma conditions than the H-cone, and therefore a more comprehensive retuning of the instrument may be required. Further evidence for the importance of thorough instrument tuning was the increase in detection limit from 24.0 pg/L at 750 W to 33.5 pg/L at 650 W when operating with the PC^3 inlet system.

The lowest detection limit of 4.5 pg/L was measured at 650 W for the Apex Q + H-skimmer cone, which is in good agreement with values achieved in previous studies (Table 7.6) (Vonderheide et al. 2004; Zoriy et al. 2005).

Reference	Instrument	RF power (W)	RF for tuning (W)	Resolution	LOD (pg/L)
Vonderheide (2004)	Element	750	1350	300	17
Vonderheide. (2004)	Element	750	750	300	4
Vonderheide (2004)	Element	750	1350	4,450	5
Vonderheide (2004)	Element	750	750	4,450	3
Zoriy (2005)	Element	650	650	4,400	11
Amr (2010)	JEOL, Plasma X2	850	850	4,000	10
This study	Element XR	650	650	300	5

Table 7.6. Comparison of Sr detection limits by ICP-SFMS. Results for this study are given for the Apex Q and H-skimmer cone setup

Previous investigations have applied medium mass resolution (R= 4,000-4,500) to limit the impact of peak tailing from stable ^{88}Sr, which can improve the detection limit, despite the reduction in instrument sensitivity (Table 7.7) (Vonderheide et al. 2004). The abundance sensitivity of the Element XR improved from $1.1x10^{-5}$ at low resolution, to $1.3x10^{-6}$ at medium resolution, which is lower than an improvement from $2x10^{-5}$ to $6\text{-}7x10^{-7}$ achieved using a Thermo Element ICP-SFMS (Vonderheide et al. 2004).

Resolution	Sensitivity (counts for 1/ng/L Sr)	Detection limit (pg/L)	Abundance sensitivity
Low (300)	1,650	118.3	1.1×10^{-5}
Medium (4000)	70	956.3	1.3×10^{-6}

Table 7.7. Difference in performance of the Element XR at low and medium mass resolution using the PC^3 sample introduction system

Depending on the sample matrix, operating at medium resolution is necessary for low-level detection, as tailing of ^{88}Sr arguably has a more significant impact on the detection limits achievable than isobaric ^{90}Zr. There is no known ICP-SFMS procedure for detection of ^{90}Sr that has operated at low mass resolution. In the case of more complex sample matrices such as soils and sediments, analysis has been performed using an ICP-QMS equipped with a Dynamic Reaction Cell (DRC), with abundance sensitivity values ranging from 3×10^{-9} to $<10^{-10}$ (Grinberg et al. 2007; Taylor et al. 2007; Feuerstein et al. 2008). There is no known ICP-SFMS procedure for detection of ^{90}Sr from a soil or sediment sample matrix, and operating at medium resolution may be insufficient to prevent tailing from high concentrations of stable Sr.

7.4 Conclusions

This study gives a preliminary investigation into low-level detection of ^{90}Sr by ICP-SFMS, focusing on the effectiveness of chemical separation, and instrument setup. The critical factors in achieving low detection limits are the removal of an isobaric interference from ^{90}Zr, polyatomic interferences formed by reactions in the plasma gas, and peak tailing from stable ^{88}Sr. Combined calcium oxalate precipitation and extraction chromatography using Sr-resin can achieve a Zr decontamination factor of $\sim 10^5$, which is insufficient to prevent interference with low-level ^{90}Sr measurement. Whilst there is no known ICP-SFMS procedure for ^{90}Sr that has relied solely on chemical separation for interference removal, this stage is critical in reducing the impact of matrix interferences following sample introduction.

The instrumental setup (specifically the sample introduction system, and sample and skimmer cone design) was investigated for Sr sensitivity, as well as the effectiveness of cold plasma-based separation of Sr from Zr. An Aridus II desolvating introduction system combined with the Jet interface and X-skimmer cone was the most sensitive instrumental setup under 'hot' plasma conditions (~1200 W), with a detection limit of 15.9 pg/L. However, desolvating sample introduction cannot achieve cold plasma conditions, therefore is dependent on chemical separation prior to sample introduction. The Zr procedural blank concentration must be reduced to a value of ~1.0 ng/L in order to achieve the instrumental detection limit. This is one order of magnitude higher than the value achieved in this study, and further reductions require working under clean laboratory conditions using high purity resins and reagents.

The PC^3 and Apex Q introduction systems showed a general reduction in detection limit with a decrease in forward power, with a higher sensitivity achieved using the Apex Q. The skimmer cone design also impacted the instrument sensitivity, and effectiveness of cold plasma separation. At 900-1200 W, the Apex Q combined with a standard nickel sample cone and X-skimmer cone measured up to 2.7 times the sensitivity of the H-skimmer cone, with a minimum detection limit of 4.9 pg/L at 900 W. However, as the forward power decreased below 900 W, the sensitivity of the X-cone setup reduced significantly, leading to an increase in the detection limit. By comparison, when operating with an H-cone, the detection limit continued to decrease to a minimum value of 4.5 pg/L at 650 W. A more comprehensive re-tuning of the instrument under cold plasma conditions is likely to improve the sensitivity further, particularly when operating with the high performance X-skimmer cone, which has been effectively applied to improve sensitivity under 'hot' plasma conditions in multiple applications.

This study demonstrates the flexibility of ICP-SFMS, and the impact of instrumental setup on sensitivity and extent of interference separation. The most sensitive instrumental setup is not necessarily favourable, as chemical separation alone may not be sufficient to enable low-level radionuclide detection. The application of cold plasma conditions can potentially remove the need to carry out sample preparation under clean laboratory conditions in order to achieve low level radionuclide detection, thereby reducing the analytical time and expense. Comprehensive retuning of the instrument under cold plasma conditions should be considered further, particularly when operating with the X-skimmer cone. Furthermore, the improvement in detection limit achievable

by operating at medium mass resolution can be assessed by running samples with high concentrations of stable Sr.

Conclusions and Future Work

This project has thoroughly assessed the capability of the latest generation sector field ICP-MS for analysis of low-level nuclear waste characterisation and measurement of radionuclides in environmental samples. The Thermo Element XR ICP-SFMS was investigated for the ability to measure both medium and long-lived emitters, focusing on the significant fission product radionuclides of caesium (^{135}Cs and ^{137}Cs) and strontium (^{90}Sr). In both cases, the primary issue affecting accurate detection is isobaric interferences arising from stable isotopes of barium (^{135}Ba and ^{137}Ba) and zirconium (^{90}Zr), respectively. Quantification must therefore be combined with efficient and effective sample preparation procedures that achieve both a high analyte recovery, and effective decontamination of interferences.

The project initially investigated the measurement of ^{135}Cs: a long-lived, low abundance radionuclide, which over longer timescales contributes significantly to the long-term nuclear waste repository. Of additional interest is measurement of the ^{135}Cs/^{137}Cs ratio, which varies depending on the source of nuclear contamination, and can therefore be used as a powerful forensic tool in environmental studies. Research then moved to focus on assessment of whether ICP-SFMS is competitive with the sensitivities achievable by existing radiometric techniques for the measurement of shorter-lived radionuclides, focusing on ^{90}Sr. ICP-SFMS offers a significant reduction in the total procedural time compared to radiometric techniques, which can reduce the cleanup time at nuclear facilities, offering significant economic benefits to decommissioning sites.

For digestion of solid samples, lithium metaborate fusion is a relatively rapid and straightforward procedure, achieving a quantitative recovery of ^{137}Cs from clay-rich sediment samples. Acid-leaching-based techniques struggled to liberate Cs from clay minerals, whilst sodium hydroxide sintering could only match the performance of borate fusion if repeat procedures were applied.

Contamination from Ba is a major limitation affecting low-level radiocaesium detection by ICP-SFMS. The concentration of Ba in the reagents used and from general environmental contamination is often greater than the concentration of ^{135}Cs and ^{137}Cs in the final sample; therefore, thorough chemical separation and cleaning procedures

were developed. Experimental work was carried out under clean laboratory conditions using high purity reagents, with the number and volume of reagents used minimised. Extensive cleaning procedures were also developed for all labware. The addition of a final stage chemical cleanup prior to sample introduction further improved Ba decontamination; however, at very low sample activity, it is possible that the contamination introduced by an extra procedural step does not offer a significant improvement.

The addition of calixarene extraction chromatography separation was the most effective approach for minimising Ba concentration in the final sample. A number of exchange materials have been developed for radiocaesium separation; however, these are generally focused on separation of ^{137}Cs from fission products and alkali metals, and struggle to quantitatively recover ^{137}Cs from the exchange material. The straightforward extraction and elution of Cs from the calixarene is well suited to ICP-MS, with the eluted fraction able to be directly loaded into the instrument. Previous calixarene procedures have often been more complex than the one presented in this project with regards to synthesis of the chromatographic material, or through the addition of further reagents to improve Cs recovery. Given the benefits of calixarene separation, future work could develop the material further to improve properties including Cs capacity, Ba decontamination, and radioactivity resistance. This in turn would expand applications from a final stage Ba cleanup, to the point where calixarenes could be applied as the sole separation stage prior to sample introduction.

Chemical separation of ^{90}Sr is critical in both radiometric and ICP-MS applications to eliminate interferences that impact the accuracy of the measured value. A combination of calcium oxalate precipitation and extraction chromatography using commercially available Sr-resin was investigated, with a Zr decontamination factor of 10^5. This is not sufficient to enable low-level detection of ^{90}Sr, which agrees with previous studies that have relied on a combination of chemical and instrument based separation (either a reaction cell or cold plasma conditions) to remove isobaric ^{90}Zr.

A consideration for future work for the radionuclides investigated is a combined extraction chromatography procedure for simultaneous separation of Sr and Cs, with a single column consisting of the extractants in Sr-resin and the calixarene. Previous investigations have focused on simultaneous extraction of ^{90}Sr and ^{137}Cs from nuclear

waste solutions (Todd et al. 2004; Riddle et al. 2004; Riddle et al. 2005), whereas this approach would be applied as a final-stage cleanup for decontamination of isobaric Zr and Ba interferences. A key factor to consider is the impact of combining the two extractants on the effectiveness of Sr and Cs extraction and elution, compared to the performance when separate separation procedures are used.

Given that isobaric interferences are a major limitation in low-level radionuclide detection, future work could investigate the development of coupling chemical separation online with ICP-SFMS. This could further reduce contamination by minimising reagent volumes and analyst exposure. Such separation can be achieved through flow injection of the sample into a carrier stream, or sequential injection of the sample and reagent into a multi-port selection valve. A technique must be developed that can effectively couple the system to the instrument, and it must be considered that the sample throughput is lower than offline separation.

The Element XR demonstrates the high analytical flexibility of ICP-SFMS. A range of instrumental setups were investigated in order to develop optimal protocols that would achieve the highest sensitivity and interference separation. For $^{135}Cs/^{137}Cs$ detection, the maximum sensitivity was achieved using the Jet interface (consisting of a high capacity pump and specially designed JET sample cone). When combined with the CETAC Aridus II desolvating sample introduction system and X-skimmer cone, a sensitivity of up to 80,000 counts for a 1 ng/L solution was achieved, with an instrumental detection limit of 1 pg/L. The extent of Ba contamination determined the detection limit of the method, with a value of 50 pg/L, and a minimum of 10 pg/L following the introduction of calixarene separation. Repeat measurements of $^{135}Cs/^{137}Cs$ from a fission product standard solution were measured over a concentration range representative of environmental samples (0.1-2.5 ng/L), with an increasing uncertainty at lower concentrations as a result of increased Ba contribution to the signal at masses 135 and 137. This was further observed in seawater samples, where the method detection limit must be reduced by an additional order of magnitude to enable quantification of $^{135}Cs/^{137}Cs$ over a concentration range of 10-40 pg/L. This application demonstrated both the high sensitivity of ICP-SFMS, and the significance of Ba contamination at these low level concentrations.

The seawater samples collected from the research cruise, as with a number of other previous studies of $^{135}Cs/^{137}Cs$, represent isotope ratio values at a single point in time. To further determine the ability to use the $^{135}Cs/^{137}Cs$ ratio as a forensic tool, analysis was conducted for a saltmarsh sediment core in close proximity to the Sellafield reprocessing facility. The core collected shows a good chronological record of authorised aqueous radioactive discharges from the site. In this application, peak tailing from the high concentration of ^{133}Cs in the sediment prevented quantification of ^{135}Cs, as opposed to the extent of Ba decontamination. The relatively poor abundance sensitivity of the Element XR can be corrected mathematically; however, when combined with correction for environmental Ba contamination, this leads to a high uncertainty in the measured values.

The highly sensitive JET interface + Aridus II configuration is also applicable to ^{90}Sr; however, unlike with $^{135}Cs/^{137}Cs$, the instrument setup also impacts the extent of Zr interference separation. By operating at a reduced forward power (cold plasma conditions), Sr was separated from Zr based on the difference in ionisation energy of the two elements. Furthermore, the reduction in instrument background led to an improvement in the limit of detection. The sensitivity and extent of separation varies significantly with the instrument setup, and under cold plasma conditions comprehensive retuning is critical in maximising the sensitivity achievable. A combination of cold plasma and medium resolution is recommended for ICP-SFMS procedures to remove isobaric ^{90}Zr and limit the tailing from stable ^{88}Sr. A range of sample matrices including water, vegetation and soils have been subjected to chemical separation and ^{90}Sr determined from radiometric techniques. Further investigations would involve repeating the analysis by ICP-SFMS to determine the effectiveness of the procedure developed.

The methodology developed can be extended to other long-lived, low abundance radionuclides that are difficult to detect by radiometric techniques, but as with ^{135}Cs will contribute to the long-term radiological risk associated with deep geological disposal. Two such examples are nickel-59 and zirconium-93 (activation and fission products, respectively). The key consideration in detection of these radionuclides is removal of stable isobars of cobalt-59 and niobium-93, respectively, both of which have a 100% isotopic abundance.

A significant development in instrumentation during the course of this research is the Agilent 8800 triple quadrupole ICP-MS. This instrument offers some advantages over ICP-SFMS for radionuclide detection. Firstly, the tandem quadrupole arrangement can reach a theoretical abundance sensitivity value of 10^{-14}, which is a significant improvement over any ICP-SFMS instrument (Zheng et al. 2014). Secondly, the octopole reaction cell can separate isobaric and polyatomic interferences as an alternative to final stage chemical cleanup. This instrument has been applied to $^{135}Cs/^{137}Cs$ measurements in environmental samples contaminated by the accident at Fukushima (Ohno and Muramatsu, 2014; Zheng et al. 2014). Additional applications include detection of iodine-129 in soils (Ohno et al. 2013), plutonium in multiple environmental samples (Labrecque et al. 2013), and low-level uranium isotope ratios ($^{236}U/^{238}U$) in multi-element standard solutions (Tanimizu et al. 2013). There has not been an application to detection of ^{90}Sr, however given that the majority of previous applications have used ICP-DRC-MS rather than ICP-SFMS, the instrument seems well-suited to ^{90}Sr detection. The Agilent 8800 cannot match the sensitivities achievable by the Element XR, which highlights that all instruments have relative strengths and limitations.

This project demonstrates the advances in sensitivities achievable by ICP-SFMS, and the importance of interference removal in order to achieve accurate low-level radionuclide detection. In order to benefit from the capabilities of ICP-SFMS, novel chemical separation procedures have been developed, both in terms of the materials used and the cleanliness of the reagents and laboratory conditions. This project is significant with regards to both environmental monitoring and low level waste characterisation, as the instrumental flexibility and capabilities have been demonstrated for both medium and long-lived emitters. Furthermore, the importance of effective digestion and chemical separation prior to sample introduction have also been assessed, with the methodology developed applicable to other medium and long-lived radionuclides.

Chapter 8. Appendices

A. Impact of Inert Support Material on AMP Performance

The impact of support material on AMP performance was compared for ammonium molybdophosphate impregnated on silica gel support (ASG resin) prepared using the method from Baker (1975), and AMP prepared using the same method with no support material. One hundred milligrams of each material was added to a 10 mL 1 M HNO_3 solution spiked with ~10 Bq ^{137}Cs (AEA Technology QSA). A 0.5mL aliquot was taken at regular intervals over 1 hour and syringe filtered through a 0.45 µm PTFE syringe filter unit. The filtrate was collected in a 22 mL polythene scintillation vial, diluted to 20mL with Milli-Q water and counted for 2 hours using a Canberra well-type HPGe detector. The recovery was calculated from the activity in the filtrate compared to that in the starting solution.

ASG filtered effectively, however for unsupported AMP there was a build up of pressure in the syringe and breakthrough of AMP through a 0.45µm filter, and to a lesser extent through a 0.22 µm filter. Filtering was achieved by repeated syringing through 0.22 µm filters, with several cartridges required for a 10mL solution. When observed during preparation of the material, and on the filter paper following separation, the heterogeneous particle size of unsupported AMP was evident, compared to the uniform nature of ASG resin. Despite the difficulty in filtration, the ^{137}Cs recovery was similar for AMP and ASG (Table A.1).

The test was repeated to compare the performance of two ASG batches (prepared in 2002 and 2013) to AMP with a polyacrylonitrile support (PAN), (Triskem International) (Figure A.1). PAN support is inexpensive, easy to prepare and can be shaped into grains, fibers or membranes (Miller et al. 1995), with no uptake ability for Cs, and no impact on uptake kinetics (Šebesta and Štefula, 1990; Nilchi et al. 2006; Bombard et al. 2013). Embedding an ion exchanger in an a PAN matrix controls properties including particle size, topography, porosity, hydrophilicity, cross-linking of resin matrix and the amount of exchanger embedded in the resin {Triskem product guide}.

Reaction time (minutes)	Uptake (%)	
	ASG	AMP
1	95.4±2.6	92.5±1.8
10	95.9±2.7	96.3±2.5
20	96.6±2.8	95.2±2.1
30	97.4±3.4	94.4±1.9
40	97.1±2.9	94.5±1.9
50	97.6±3.1	94.7±1.9
60	97.6±3.0	93.4±2.3

Table A.1. Uptake of ^{137}Cs from a 1M HNO_3 solution by ASG resin and AMP with no support material

After a reaction time of one hour, a Cs uptake of 94.6 %, 98.6 % and 80.3 % was achieved by AMP-PAN, 2002 ASG and 2013 ASG, respectively. There was a difference in the rate of uptake between the materials, with AMP-PAN recovering 18.3 % Cs after one minute, compared to 97.1 % and 74.1 % for 2002 ASG and 2013 ASG, respectively. An advantage to AMP-PAN was that separation of the material from the sample solution could be achieved by centrifuging, where as filtration was necessary for both ASG batches. In addition, chromatographic separation was effective using AMP-PAN, where as the elution rate for ASG batches was very slow, with breakthrough of the exchange material in some tests. Pumping the sample through the resin column, rather than relying on the gravitational flow rate could improve this. Aside from the support material used, the difference in behaviour may be because AMP-PAN arrives in the form of a slurry, where as ASG is prepared as a dry powder. Despite being prepared by the same procedure, the difference in performance between the two ASG batches is a further argument in favour of using industry-prepared AMP-PAN.

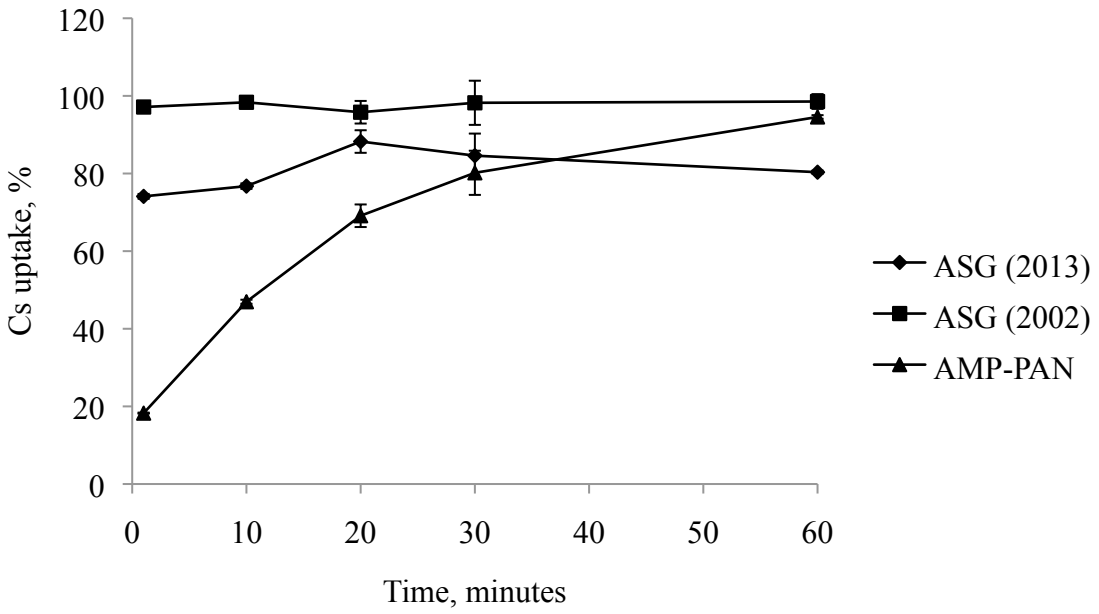

Figure A.1. Caesium uptake onto AMP-PAN and ASG from a 1M HNO_3 solution

B. Comparison of KNiFC-PAN and AMP-PAN for Chemical Separation of $^{135}Cs/^{137}Cs$ prior to ICP-MS Quantification

B.1. Introduction

A number of inorganic ion exchangers have been applied to separation of ^{137}Cs from nuclear waste solutions, however the only such exchanger to be applied to $^{135}Cs/^{137}Cs$ separation prior to ICP-MS measurement has been ammonium molybdophosphate (AMP) (Taylor et al. 2008; Russell et al. 2014(A); Zheng et al. 2014). A second group that is potentially applicable is insoluble hexacyannoferrates, specifically potassium nickel hexacyanoferrate (KNiFC). This material has been applied to ^{137}Cs separation from a range of waste solutions (Ismail et al. 1998; (Mimura et al. 1999(B); Nilchi et al. 2006), and offers a higher distribution coefficient (K_d) than a number of natural and synthetic ion exchangers, including AMP (Table 1.7, page 17) (Ismail et al. 1998; Kamenik and Ŝebesta, 2003). The effectiveness of KNiFC in ICP-MS procedures is dependent on decontamination of isobaric barium interferences ^{135}Ba and ^{137}Ba that interfere with $^{135}Cs/^{137}Cs$ detection, as well as being able to quantitatively elute Cs sorbed onto the material.

KNiFC has a face centered cubic structure (FCC) (Lehto et al. 1992; Mimura et al. 1997(B)), with Fe and Ni located at corners of these cubes, cyano (CN) groups at the edges, and exchangeable K^+ at the body centre (Mimura et al. 1997(B). KNiFC shows good resistance to acidic conditions, remaining stable in the presence of up to 8 M HCl or 8M HNO_3, with a K_d for Cs of ~10^4 mL/g (Mimura et al. 1997(C)). The highest chemical and thermal stability has been reported in solutions of pH1-5.5 (Ismail et al. 1998), and in the case of chromatographic separation, neutral to slightly acidic sample loading conditions have been recommended (Bombard et al. 2013). High Na concentrations (>1 M) have been shown to reduce the K_d for Cs, due to hydrolysis of Ni and release of Fe as $Fe(CN)_6^{4-}$ ions (Mimura et al. 1997(C)). However, separate studies have shown the K_d to remain almost constant at Na concentrations from 10^{-4} M - 5M (Mimura et al. 1997(B)). A decrease in K_d has been reported for increasing K and NH_4 concentrations (Mimura et al. 1997(B); Du et al. 2013), with a linear decrease in K_d at increasing NH_4 concentrations >0.1 M suggesting uptake is determined by a cation exchange reaction (Mimura, Lehto et al. 1997(B)). The exchange reaction of Cs with K^+

ions located at the centre of the cubic structure is thermodynamically favourable, with a Gibbs free-energy value calculated as -15.4±1.4 kJ/mol (Mimura et al. 1997(B)). The order of K_d for Cs in the presence of coexisting cations follows the order NH_4> K>Na, closely resembling the order of size of hydrated cations (Mimura et al. 1997(B)). This suggests concentrated NH_4-based solutions can effectively elute Cs from KNiFC.

For batch separations, approximately 100 mg of KNiFC has been added to 10-140 mL of aqueous solution (Lehto et al. 1992; Mimura et al. 1997(A); Mimura et al. 1999(A); Kamenik and Ŝebesta, 2003; Nilchi et al. 2006; Du, Jia et al. 2013), with contact times of up to 7 days (Mimura et al. 1999(B), although equilibrium conditions have been reached in 1-2 hours (Nilchi et al. 2006). Chromatographic separation has been successfully applied to waste water (Ismail et al. 1998), urine and milk samples (Bombard et al. 2013), with a chemical yield of ~95 % Cs for both milk and urine, based on gamma spectrometry of the dried resin (Bombard et al. 2013).

The most common preparation technique for hexacyannoferrates is formation of a precipitate by reacting a solution of transition metal salt with a solution of alkali metal (commonly K^+ or Na^+) salts and ferrocyanic acid. A slurry is formed that is then filtered, dried and ground (Ismail et al. 1998; Mimura et al. 1999(B); Nilchi et al. 2006; Du et al. 2013). The mechanical properties and chemical behaviour of the material formed depend on the preparation method used, with variables including the concentration of solutions, precipitation and drying temperatures, pH, ageing time and impact of a mechanical carrier (Ismail et al. 1998; Nilchi et al. 2006). KNiFC is often bound to an inert support material for both batch and chromatographic separation, with colloidal silica and Polyacrylonitrile (PAN) successfully used (Ismail et al. 1998; Mimura et al. 1999(B); Nilchi et al. 2006; Bombard et al. 2013; Du et al. 2013). The structure of KNiFC has been assessed using X-ray diffraction (XRD) (Moon et al. 2004; Mimura et al. 1999(B)), with loading and chemical composition determined from electron probe micro analysis (EPMA), and surface morphology examined using scanning electron microscopy (SEM) (Mimura et al. 1999(B); Nilchi et al. 2006).

The aim is to determine if KNiFC is an alternative to AMP as an initial chemical separation stage prior to ICP-MS measurement of $^{135}Cs/^{137}Cs$, by investigating uptake of Cs and interfering Ba, as well as the ease of recovering Cs sorbed onto the exchange material.

B.2. Experimental

The effectiveness of batch separation was compared for KNiFC and AMP bound to PAN inert support material (Triskem International) in Milli-Q water, 0.1 M HNO_3 and 1 M HNO_3 solutions, prepared using a Q-Pod Millipore System (Merck) and analytical reagent grade HNO_3 (Fisher Chemicals). Uptake was investigated by mixing 100 mg of exchanger with a 30 mL solution spiked with 100 µg/L stable Cs and Ba (prepared from 1000 mg/L elemental stock solutions (Inorganic Ventures)) for a total of 4 hours. The sample was mixed using a Luckham Multimix Major. At regular intervals a 1mL aliquot was syringe filtered through a 0.45 µm PTFE filter, diluted up to 10 mL with 2 % (v/v) HNO_3 and measured using a Thermo Scientific X-series II bench-top quadrupole ICP-MS. Retention on KNiFC-PAN and AMP-PAN was calculated as the concentration of Cs and Ba in the filtrate compared to the starting solution.

Selectivity was further investigated by repeating the procedure for a solution spiked with multiple gamma-emitting radionuclides (Table B.1). For dissolution, ammonia-based solutions have been effectively applied to AMP (Pibida et al. 2004; Taylor et al. 2008; Delmore et al. 2011; Russell et al. 2014(A); Zheng et al. 2014), and are theoretically suitable for KNiFC (Mimura et al. 1997(B)), therefore recovery of sorbed ^{137}Cs was initially investigated using 25% (v/v) NH_4OH. The recovery was calculated as the activity in the filtrate and ammonia solution compared to the starting solution. Samples were counted for 2 hours using a Canberra well-type HPGe detector with an efficiency of 10 % at 662 keV (corresponding to the gamma photopeak energy for $^{137}Cs/^{137m}Ba$). Analysis of the energy spectra and calculation of radionuclide activity was performed using Fitzpeaks software (JF Computing, Stanford in the Vale, UK).

B.3. Results

A high Cs recovery was achieved for both materials in all solutions (Figure B.1), with an average uptake of 99.4±4.3 % for KNiFC after one-hour contact time, compared to 94.3±2.3 % for AMP-PAN, which increased to 98.6±1.7 % after 2 hours. The rate of uptake was higher for KNiFC, with Cs uptake ranging from 80.6-99.3 % after 20 minutes contact time, compared to 61.4-71.9 % for AMP-PAN. Equilibrium conditions were established after one hour for KNiFC-PAN, and 2 hours for AMP-PAN, with no evidence of Cs desorption or degradation of either material after a contact time of 4

hours.

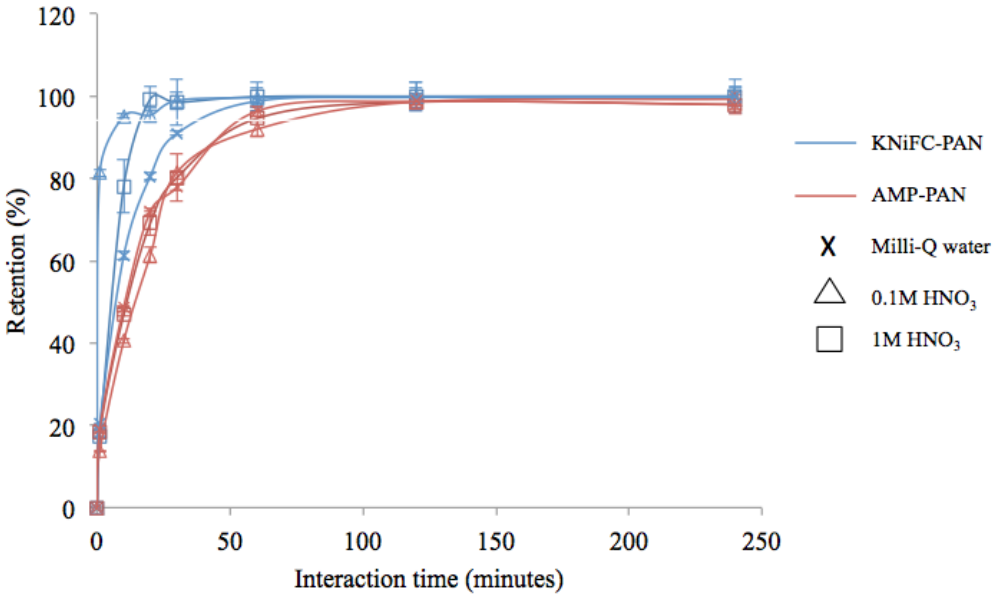

Figure B.1. Uptake of stable ^{133}Cs by AMP-PAN (red line) and KNiFC-PAN (blue line) in Milli-Q water, 0.1M HNO_3 and 1M HNO_3 solutions

Both exchangers showed a higher Cs selectivity over Ba with increasing HNO_3 concentration (Figure B.2(A) and (B)). For a one-hour contact time, Ba uptake onto KNiFC was 5.2±0.1 % in Milli-Q water, compared to 1.5± <0.1 % in 1M HNO_3. Over a 4 hour reaction time, the Ba retention on KNiFC did not exceed 2.37±0.1 % in a 1 M HNO_3 solution, compared to a maximum of 3.47±0.2 % and 8.68±0.2 % in 0.1 M HNO_3 and Milli-Q water, respectively. The impact of increased acidity on Cs selectivity was more extreme for AMP-PAN, with a Ba recovery of 89.4±1.5 % in Milli-Q water after 2 hours contact time, compared to 6.1±0.1 % in 1M HNO_3. Under acidic conditions, AMP has been proven to be highly selective, as only monovalent cations (particularly Cs) can stably pack into the molybdophosphoric acid lattice and form an insoluble compound. In weaker acid and neutral conditions, AMP acts as a generic ion exchanger (Chapter 2.3.2. page 35) (Morgan and Arkell, 1963; Smit and Robb, 1964; Russell et al. 2014(A)). With regards to Cs recovery and Ba decontamination, under the conditions tested KNiFC-PAN can be considered a superior material to AMP-PAN.

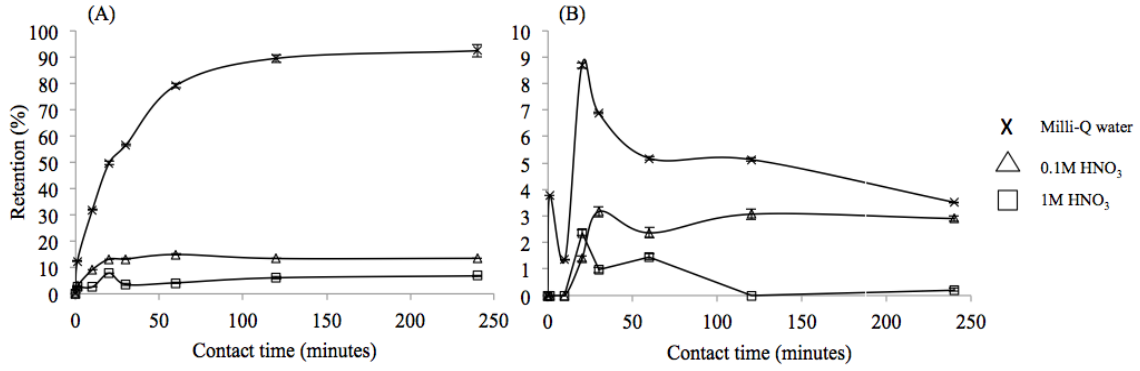

Figure B.2. Uptake of stable ^{137}Ba by (A) AMP-PAN and (B) KNiFC-PAN in Milli-Q water, 0.1 M HNO_3 and 1 M HNO_3 solutions

Following results from stable Cs and Ba solutions, 100 mg KNiFC-PAN and AMP-PAN was mixed with a 1 M HNO_3 solution containing multiple gamma-emitting radionuclides for one hour (Table B.1). AMP achieved a ^{137}Cs recovery of 93.4±7.0 %, with the activity of other radionuclides falling below the detection limit after a 2-hour count time (limit of detection ranged from 3 to 5 % of the activity in the starting solution). The ^{137}Cs uptake by KNiFC (94.0±6.0 %) was similar to AMP, however the material also showed uptake of other radionuclides, with the highest values for ^{113}Sn (91.1±10.8 %), ^{65}Zn (67.2±7.1 %), and ^{60}Co (12.6±0.8 %). The partial retention of Co agrees with results from previous studies (Ismail et al. 1998; Nilchi et al. 2006), whilst an investigation of ^{137}Cs separation from seawater using potassium cobalt hexacyannoferrate (KCFC) also showed sorption of radionuclides other than ^{137}Cs, including ^{144}Ce (34 %), ^{60}Co (29 %) and ^{65}Zn (26 %) (Baker, 1975).

The dissolution of KNiFC and AMP and recovery of ^{137}Cs was tested using 25 % (v/v) NH_4OH. The alkali solution was slowly syringe filtered through the material in 5 mL aliquots. KNiFC recovered 28.5±2.7 % of ^{137}Cs following a 100 mL NH_4OH wash. The recovery of other radionuclides was >90%, other than those that showed higher uptake onto the material, with recoveries of 48.0±3.9 % (^{113}Sn), 75.9±4.2 % (^{65}Zn), and 93.5±4.5 % (^{60}Co). By comparison, AMP was effectively dissolved in 10 mL NH_4OH, with a ^{137}Cs recovery of 85.0±6.5 %. Therefore, despite the high recovery of Cs and low uptake of Ba, the difficulty in dissolving KNiFC in alkali solution and recovering ^{137}Cs from the material is a limitation to ICP-Ms procedures.

Nuclide	Retention by KNiFC (%)	Total recovery from KNiFC following 100 mL 25 % (v/v) NH_4OH wash (%)
^{137}Cs	94.0±6.0	28.5±2.7
^{113}Sn	91.1±10.8	48.0±3.9
^{65}Zn	67.2±7.1	75.9±4.2
^{60}Co	12.6±0.8	93.5±4.5
^{85}Sr	7.8±0.9	92.2±3.8
^{54}Mn	7.7±0.5	93.5±2.8
^{88}Y	5.2±0.7	94.8±3.2
^{109}Cd	4.9±0.6	99.9±5.6
^{139}Ce	4.1±0.4	95.9±4.0

Table B.1. Uptake of gamma-emitting radionuclides onto KNiFC-PAN in a 20 mL 1 M HNO_3 solution following a contact time of 2 hours

B.4. Discussion

The results suggest a difference in Cs uptake mechanism between the two materials. Retention on AMP in neutral and acidic conditions is the result of exchange of Cs^+ with NH_4^+ ions located between molybdophosphate spheres, with effective dissolution of AMP and recovery of bound Cs achievable using alkali solutions. For KNiFC, the difficulty in eluting Cs suggests a strong retention in the KNiFC structure. Ismail et al. (1998) compared the infrared spectra of KNiFC, Cs-loaded KNiFC and Co-loaded KNiFC. Infrared spectroscopy exploits the theory that molecules absorb wavelength frequencies that are specific to their structure. In this case, the spectra focused on the cyano group (C≡N), with a band in the region 2,000-2,100 cm^{-1} (Ismail et al. 1998; Nilchi et al. 2006; Mimura et al. 1999(B)), as well as absorption bands at 3,500 cm^{-1} and

1,610 cm^{-1}, characteristic of water stretching vibration and water in the crystal lattice of the compound, respectively (Ismail et al. 1998). When loaded with Cs, the KNiFC spectra showed a shift in the C≡N band, and a new band at 1,385 cm^{-1}, indicative of the presence of a C-N bond. By comparison, there was no evidence of structural change on the infrared spectra of KNiFC loaded with Co, which shows a lower retention on the material (Lehto et al. 1992; Ismail et al. 1998). This change in structure may account for the difficulty in recovering Cs from KNiFC. It is likely that a higher concentration alkali solution will improve recovery. Alternatively, hot, concentrated sulphuric acid has been successfully used for potassium cobalt hexacyannoferrate (KCFC) dissolution following ^{137}Cs separation from seawater, however the process was slow, with high amounts of cyanide fumes produced (Baker, 1975). Application of a more concentrated alkali solution will also result in a more hazardous procedure, and may impact the performance of subsequent separation stages (commonly ion exchange) prior to quantification. By comparison, 25 % NH_4OH has been effectively loaded onto a cation exchange column without impacting the performance with regards to Cs recovery or Ba decontamination (Russell et al. 2014(A) (Chapter 2.3.2. page 35-37).

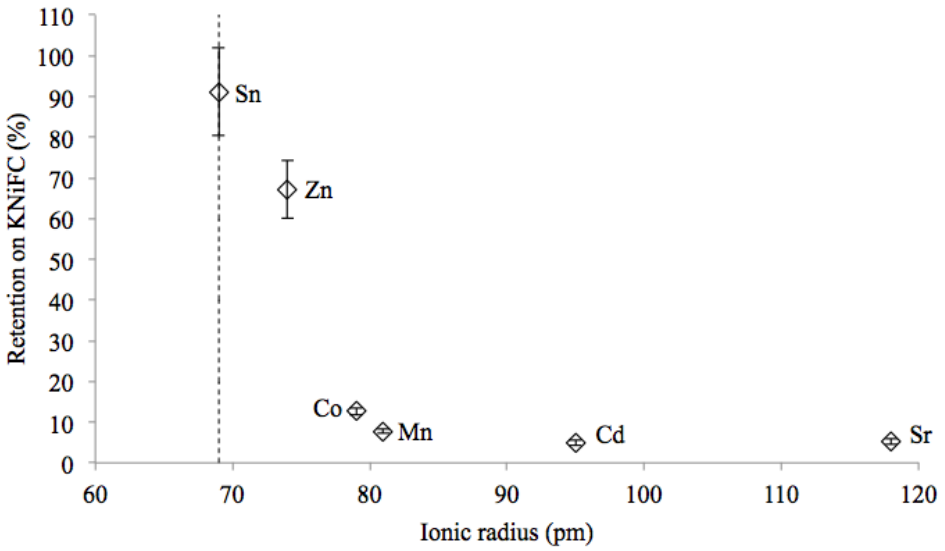

Figure B.3. Correlation between ionic radius and uptake onto KNiFC for radionuclides present as divalent cations in 1 M HNO_3 solution. The dashed line is the ionic radius of Ni^{2+} (69pm)

Ion exchange with Ni^{2+} ions in the KNiFC structure may account for the uptake of other

radionuclides from the mixed gamma solution. For radionuclides present as divalent cations in acidic solution, there is a correlation between uptake and similarity of the ionic radius to that of Ni^{2+} (69 picometres) (Figure B.3). The highest uptake is observed for ^{113}Sn, which is usually present as Sn^{4+} in aqueous solution, however can exist as a divalent cation in acidic solutions (Nervik, 1960).

B.5. Conclusions

A number of inorganic ion exchangers have been proven to show a high uptake of ^{137}Cs. However, AMP is the only such material to be applied to an ICP-MS based procedure to enable detection of both ^{137}Cs and long-lived ^{135}Cs. KNiFC is an inorganic ion exchanger commonly applied to separation of ^{137}Cs from environmental and nuclear waste solutions, and has been investigated as an alternative exchange material to AMP for ICP-MS procedures. The critical factors are selectivity towards Cs, decontamination of isobaric Ba interferences, and the ability to remove Cs bound to the material to enable further separation and quantification.

Both KNiFC and AMP bound to inert polyacrylonitrile (PAN) support material can recover >90 % Cs from Milli-Q water, 0.1 M HNO_3 and 1M HNO_3 solutions. The rate of uptake was higher for KNiFC, with equilibrium conditions established in 1 hour, compared to 2 hours for AMP. In addition, sorption of Ba was lower for KNiFC under the conditions tested, particularly under neutral conditions, where AMP behaves as a generic ion exchanger and shows a low Cs selectivity. The exchange materials were further assessed in a 1 M HNO_3 solution containing multiple gamma-emitting radionuclides. AMP showed a high selectivity towards ^{137}Cs, however for KNiFC there was retention of multiple other radionuclides, potentially as a result of ion exchange reactions with Ni in the KNiFC lattice.

AMP was effectively dissolved in 10 mL 25 % (v/v) NH_4OH, with a ^{137}Cs recovery of 85.0±6.5 %. By comparison, a 100mL wash recovered 28.5±2.7 % ^{137}Cs from KNiFC. The poor recovery is likely a result of strong retention of Cs in the KNiFC structure. Whilst this is beneficial in the immobilisation of Cs and cleanup of contaminated sites, it presents a limitation to ICP-MS applications, which requires recovery of Cs for further separation. Despite the limited conditions investigated, for $^{135}Cs/^{137}Cs$ detection by ICP-MS, AMP is favoured over KNiFC as an initial chemical separation stage, primarily because of the comparative simplicity in recovering Cs bound to the material.

C. Barium Procedural Blank Reduction and Summary of Cleaning Procedures

Given the importance of the Ba procedural blank in the accuracy of $^{135}Cs/^{137}Cs$ values, a number of factors were taken into consideration during method development, including the decontamination factor of interferences required, minimising the number of procedural steps and labware used, maintaining a clean laboratory environment throughout, developing cleaning routines for labware (Table C.1), using the highest purity reagents (Table C.2), and implicating a dedicated instrument setup. The major factors under consideration when minimising the procedural blank are given in Figure C.1.

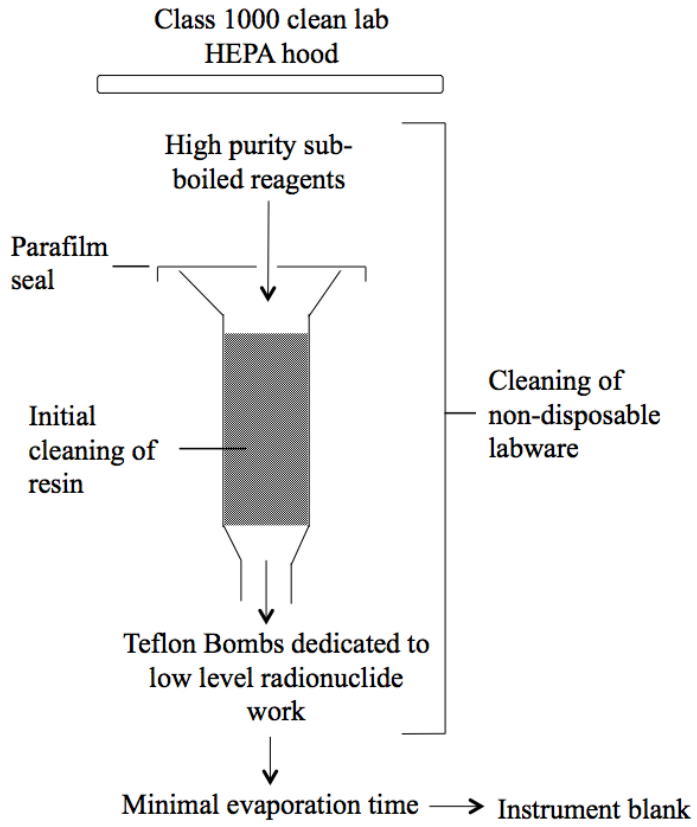

Figure C.1. Steps taken to minimise Ba contamination for chromatographic separation procedures

Equipment	Cleaning procedure
Pipette tips, scintillation vials, columns	1. 10 % HNO_3 (24 hours)
	2. 10 % HCl (24 hours)
	3. Left in 10 % HNO_3 until needed
Teflon bombs	1. Heated in 50 % HNO_3 (24 hours)
	2. Heated in 50 % HCl (24 hours)

Table C.1. Summary of cleaning procedure for labware

The AMP+cation exchange procedure was initially run with no consideration of cleanliness, with a Ba procedural blank concentration of approximately 500 ng/L. The lowest procedural blanks were achieved in a class 1000 clean laboratory, with initial values of ~40-50 ng/L, improving to 5-20 ng/L, and a minimum value of 2 ng/L following further steps to reduce Ba decontamination. When operating in the clean laboratory, no samples from other analyses were present, and the surfaces cleaned with Milli-Q water prior to use. Hot plates were also cleared of other samples during evaporation, prior to making up in 2 % HNO_3 for sample introduction.

Reagent	Sub-boiled HNO_3	Sub-boiled HCl	Milli-Q	2 % HNO_3
Minimum (ng/L)	1.9±0.12	1.7±0.18	1.0±0.10	0.3±0.04
Maximum (ng/L)	6.4±0.49	6.2±0.79	4.1±0.29	3.1±0.24

Table C.2.Range of Ba concentrations in reagents

Blank concentrations were lower when operating under a high efficiency particulate air (HEPA) filter than the fume hood, as determined by leaving open-topped scintillation vials containing 2 % HNO_3 around the clean laboratory over a 3-4 week period (Figure C.2). A mobile high efficiency particulate air (HEPA) unit achieved a procedural blank of 55 ng/L, which is an improvement of one order of magnitude over the laboratory the

unit was located in. A well-designed and maintained HEPA hood is therefore applicable to certain applications, and is also a significantly cheaper option than fitting of a class 1000 clean laboratory.

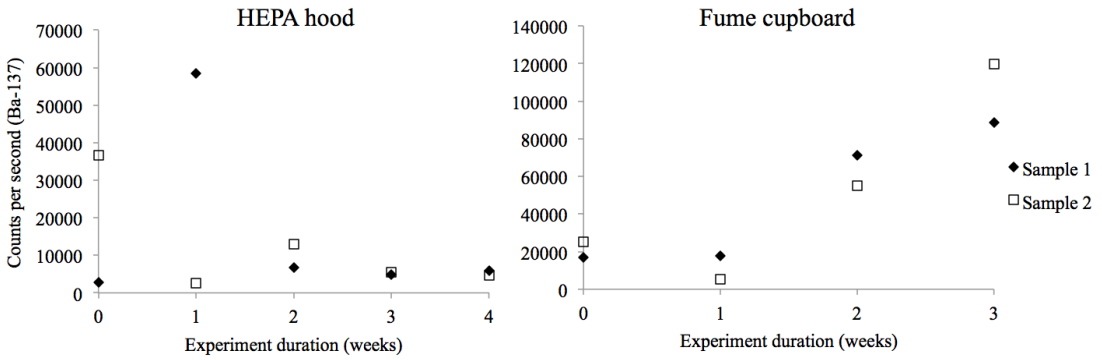

Figure C.2. Example of environmental Ba contamination when a 10mL 2% HNO_3 solution is left in a HEPA hood and fume cupboard of a class 1000 clean laboratory

Repeated use of columns can also act as a source of Ba decontamination, with a range of Ba concentrations measured after passing a Ba-free solution through a number of columns (Figure C.3). The Ba concentration measured up to 15-20 ng/L as a result of Ba build up on the column frit (Figure C.4). The frits and columns were effectively cleaned overnight in 8 M HNO_3 at 60^0C, with the columns labelled and their applications recorded.

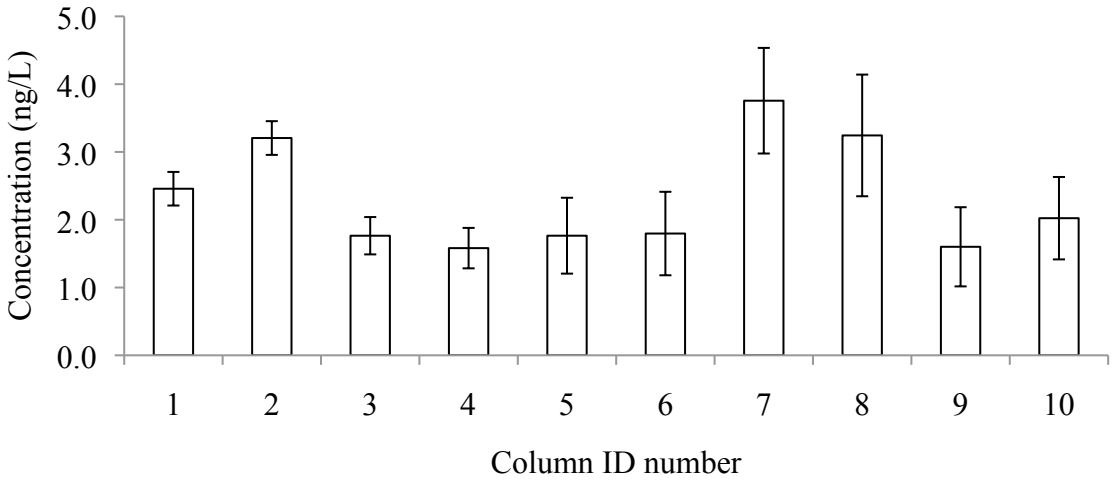

Figure C.3. Variation in Ba concentration in 0.5 cm diameter columns following repeated and unmonitored use

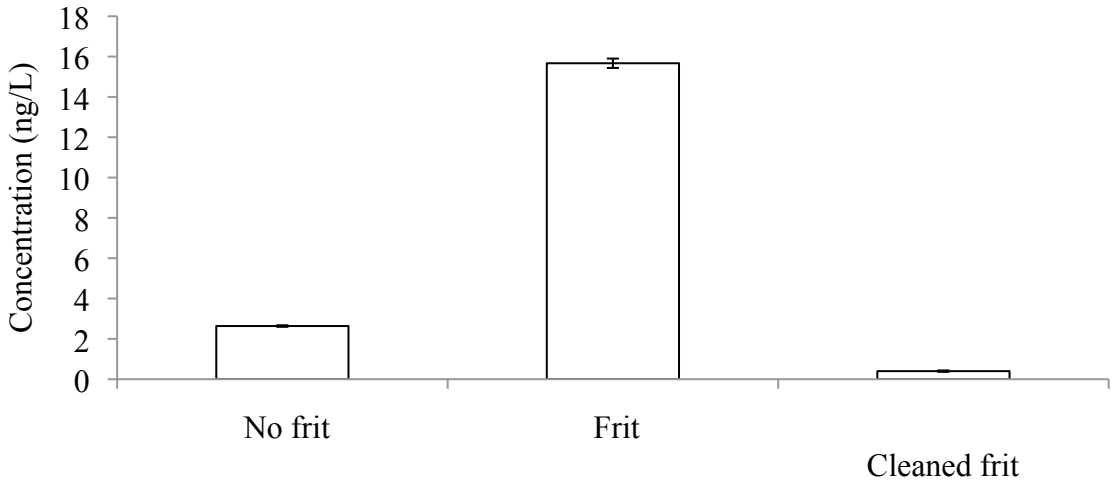

Figure C.4. Average Ba contamination in the three contaminated columns. The contamination reduces considerably following cleaning of the frit in 8 M HNO_3

Evaporation of eluted fractions prior to ICP-MS increased the procedural blank compared to non-evaporated samples (Table C.3), which was minimised by using a wider diameter Teflon bomb, and the introduction of a final stage calixarene cleanup.

Sample treatment	Ba concentration (ng/L)
Evaporated	3.8±0.5
Non-evaporated	1.7±0.2

Table C.3. Difference in Ba concentration in 2% HNO_3 solution for samples evaporated to dryness overnight, compared to non-evaporated samples (n=10)

The variation in Ba concentration in 2 % HNO_3 used for instrument blanks and standard preparation was monitored (Figure C.5), with a target ^{137}Ba value of ~3,000 cps.

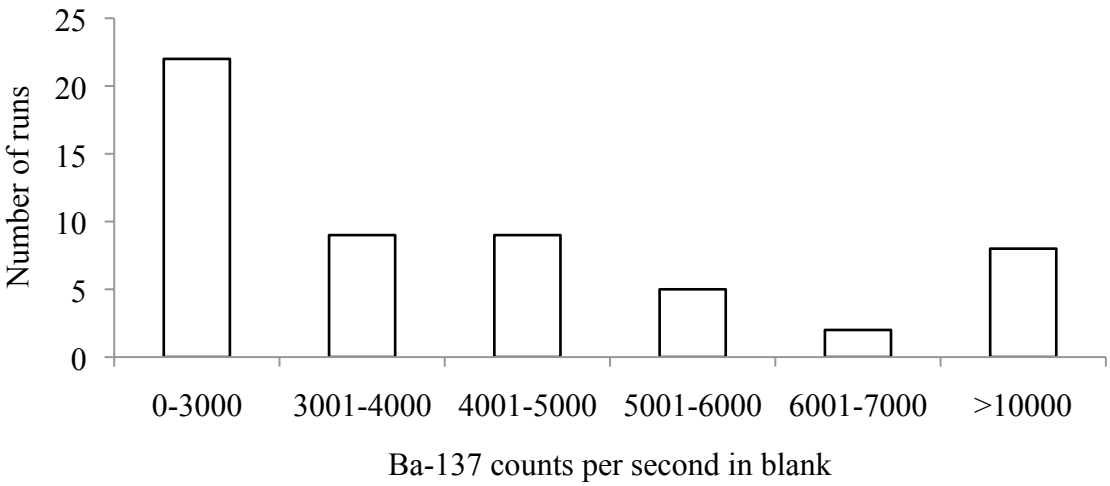

Figure C.5. Range of Ba concentrations in 2% HNO_3 blank

D. Preparation of Ammonium Molybdophosphate Coated Silica (ASG)

1. Dissolve 100g of ammonium molybdate and 6g of ammonium monohydrogen phosphate in 400ml Milli-Q water in a 5-litre borosilicate glass beaker.
2. Stir in 250g of chromatographic grade silica (60A) to produce a slurry, and allowed to stand for three days. Dry the mixture overnight at 110^0C.
3. Dissolve 10g ammonium nitrate in 300ml 3M HNO_3 and mix this into the dried material.
4. Warm the material at 80^0C on a hotplate. Leave the mixture to stand for 3 hours with regular stirring, during which time a bright yellow material is produced.
5. Decant the supernatant liquid, and then add 3,000mL Milli-Q water to form a slurry. Allow the solid to settle and decant the supernatant liquid.
6. Repeat the slurrying and settling procedure until the supernatant is relatively clear.
7. Transfer the solid ASG resin to a dish and dry overnight at 110^0C.
8. Test the material by adding 10ml of 0.2M HNO_3 containing ^{137}Cs to approximately 0.1g of ASG. Shake the mixture for one hour and then filter through a 0.22μm membrane filter. Measure the residual ^{137}Cs activity in an aliquot of the filtrate. The distribution coefficient should exceed 10^4.

E. Barium Interference Correction

E.1. Instrumental mass bias

The instrument is naturally bias towards the heavier isotope, in this case ^{138}Ba. Simply dividing the ^{138}Ba signal by the true ^{135}Ba /^{138}Ba ratio will not account for instrumental bias, and to calculate this the ^{138}Ba signal must be divided by the measured ^{135}Ba/^{138}Ba value. The combination of natural abundance and mass bias correction should then give a value of 0 at mass 135 in the absence of ^{135}Cs. In order to determine the instrumental mass bias, standards were run for isobaric interferences ^{135}Ba and ^{137}Ba during each run, and the mass bias factor calculated using both the linear and exponential equation (Equations E1 and E2). Corrections were applied using repeat measurements of a 10ng/L standard Ba concentration.

Linear:

$$R_t = R_m \times (1+\Delta m f) \qquad \text{(E1)}$$

$$f = (R_t/R_m - 1) / \Delta m$$

Where t is the true ratio, m is the measured ratio, and f is the correction factor

Exponential:

$$R_t = R_m(M_B/M_A)^{\beta} \qquad \text{(E2)}$$

$$\beta = \ln(R_m/R_t)/\ln(M_A/M_B)$$

Where R_t is the true ratio, R_m is the measured ratio, M is the expected mass of isotopes A and B, and β is the mass bias coefficient.

Because a large fraction of the signal at mass 135 is from Ba rather than Cs, the error within the correction is important. It can be assumed that the mass bias is constant with time, however there is likely to be some instrumental drift during the course of the measurement. The Element software can measure isotope ratios in each run, which is

more reliable than taking the average calculated value when processing the data manually. Barium also has a slight interference at mass 138 from ^{138}Ce (0.25% abundance) and ^{138}La (0.09% abundance), which can be corrected at ^{139}La (99.91%) and ^{138}Ce (88.45%). These elements are not expected to be a concern, however given the low concentrations aimed for, accurate correction for interferences is critical in obtaining accurate results.

E.2. Correcting for Ba interferences in measured values

A mass spectrometric interference must also be applied as a result of Ba contamination, which was estimated from the ^{138}Ba signal (Equation E3):

$$(^{135}\text{Ba and } ^{137}\text{Ba})_c = {}^{138}\text{Ba}_m \text{ x } (^{135}\text{Ba and } ^{137}\text{Ba})/{}^{138}\text{Ba}_t \qquad \text{(E3)}$$

Where $(^{135}\text{Ba and } ^{137}\text{Ba})_c$ is the calculated value, $^{38}\text{Ba}_m$ is the measured value, and $(^{135}\text{Ba and } ^{137}\text{Ba})/{}^{138}\text{Ba}_t$ is the true isotope ratio based on isotopic abundances.

The impact of the combined uncertainty from mass bias correction and mass spectrometric interference correction is shown in Figure 2.4, page 40. For the same ^{135}Cs or ^{137}Cs concentration, a higher Ba concentration will lead to a higher uncertainty in the measured values, with Ba contributing to a larger fraction of the signal.

F. Additional calixarene information

F.1. Structure

The calixarene structure consists of phenolic units (C_6H_5OH) surrounded by methylene groups. Nomenclature is based on the number of repeating units i.e. calix[4]arene, calix[6]arene, with rotation around the methylene group leading to a number of possible conformations, and therefore selectivity towards different ions (Figure F.1) (Asfari et al. 1995; Casnati et al. 1995; Ikeda and Shinkai, 1997; Theury et al. 2000). Of these, the 1,3 alternate conformation shows the highest selectivity towards Cs, as rather than 4 phenolic oxygens interacting with one metal cation, it offers 2 independent binding sites, each with 2 phenolic oxygens and 2 benzene rings (Ikeda and Shinkai, 1994).

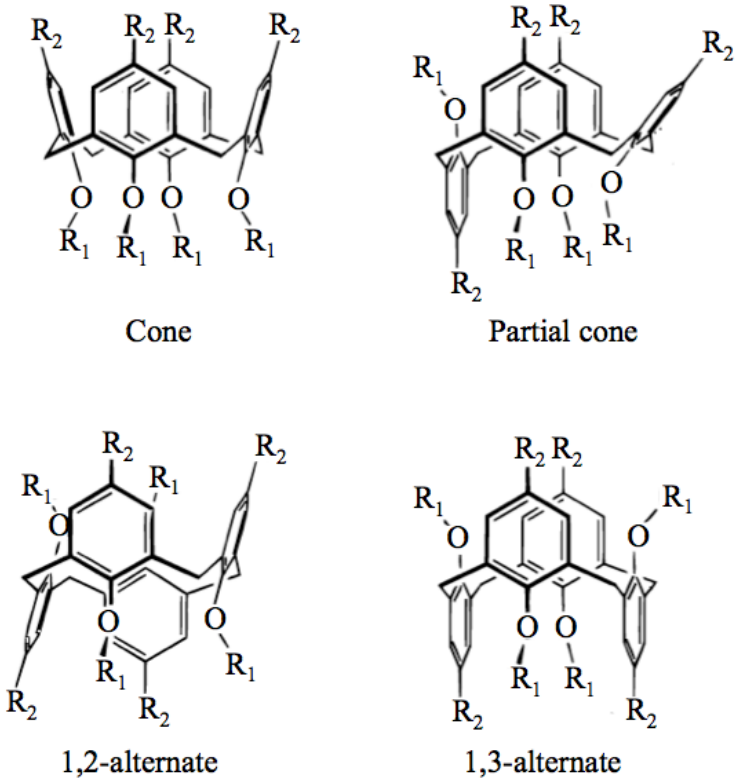

Figure F.1. Four stable calixarene conformations. From Ikeda and Shinkai (1997)

Additional groups can improve Cs selectivity by altering the calixarene structure. In the case of BOBCalixC6 (calix[4]arene-bis-tert-octylbenzo-crown-6), the presence of substituent benzene groups changes the complex stabilisation by rigidification of the structure. Given that the crown-6 ether is slightly larger than the Cs cation, this rigidification reduces extraction, however this structural change has a greater impact on smaller Na and K ions, thus improving selectivity (Lamare et al. 1999). The presence of two crown-6 groups means there are two potential Cs binding sites (Asfari et al. 1995), although electrostatic repulsion of the first Cs ion may prevent formation of a second complex (Asfari et al. 1995). Other studies have shown that binding of a second ion is possible (Thuery et al. 2000); however this can be weak and only expected under high Cs loading conditions (Bonnesen et al. 1998). Finally, The inclusion of lipophilic octyl groups can enhance the solubility of calixarenes in organic solvents, which has been reported as a problem (Zhou et al. 2013).

F.2. Addition of modifiers to improve performance

Multiple reagents have been combined with HNO_3 in order to improve the calixarene performance, commonly to improve stripping of ^{137}Cs from the extractant. For example, Bonnesen et al. (1998) found successive stripping with dilute HNO_3 to have limited success, however addition of non-radioactive $CsNO_3$ improved decontamination, at a ratio of $1x10^{-4}$M $CsNO_3$ to $5x10^{-4}$M HNO_3. Organic-phase Cs is held constant by the $CsNO_3$ addition, so decontamination can be seen as isotopic dilution. As stripping continues, ^{137}Cs:^{133}Cs in solvent decreases until sufficient decontamination is achieved.

The addition of a small concentration (~10^{-5}-10^{-3}M) of extractant such as alkylamine or trioctylamine (TOA) can improve the stripping performance, without impacting the extraction efficiency for Cs (Bonnesen et al. 1998; Leonard et al. 2001; Riddle et al. 2005). These extractants act as a nitrate buffer to suppress ion-pair dissociation, as well as nullifying the adverse impacts of anionic impurities that impair stripping of ^{137}Cs. This approach is more economical than using $CsNO_3$, but more importantly the Cs distribution ratio is lowered by a factor of at least 2 compared to stripping with $CsNO_3$ (Bonnesen et al. 1998).

F.3. Diluents

A number of non-polar and polar diluents have been successfully combined with calixarenes (Table 3.1, page 48). Non-polar diluents e.g. alkanes and chloroform have a low dielectric constant and give behaviour that conforms to complete ion pairing (Equation F1), whilst polar diluents such as nitrobenzene have a high dielectric constant that conforms to organic-phase ionic species (Equation F2). Those with an intermediate dielectric constant (~5-20) e.g. octanol can result in partial ion pairing (Bonnesen et al. 1998).

$$Cs^+ (aq) + NO_3^- (aq) + X (org) = CsXNO_3 (org) \quad (F1)$$

$$Cs^+ (aq) + NO_3^- (aq) + X (org) = CsX^+ (org) + NO_3^- (org) \quad (F2)$$

Where X is the calixarene.

F.4. Chromatographic Separation

Chromatographic separation offers increased efficiency over batch separation because of theoretical plate theory. This supposes a chromatographic column is made up of a large number of separate layers (theoretical plates), within which equilibration between the stationary and mobile phase occurs. The analyte moves down the column by transfer of equilibrated mobile phase from one plate to the next. A column with a higher number of theoretical plates is considered to have higher column efficiency. The height equivalent to a theoretical plate (HETP) is a further measure of column efficiency, usually reported in millimetres. A shorter plate indicates higher efficiency, as more theoretical plates are contained in a given length of column.

F.4.1. Summary of previous calixarene preparation procedures

F.4.1.1. Dietz et al. (2006)

Methanol was poured over the Amberlite CG-71 support material and allowed to percolate through, before drying residual methanol by vacuum filtration. The process was repeated twice more until the final methanol wash was clear. The resin was then

transferred to a round-bottomed flask containing methanol, which was removed in vacuo at a controlled temperature using a rotary evaporator, yielding a purified resin. This was slurried with methanol, and the calixarene added. The slurry was stirred, and then the solvent concentrated in vacuo at a controlled temperature to a constant weight, providing a loaded resin.

F.4.1.1. Zhang and Hu (2010)

SiO_2-P particles were initially treated with methanol and acetone to improve the surface activity of the support. The calixarene and methyloctyl-2-di-methyl-butanemide (MODB) modifier were dissolved in dichloromethane, and SiO_2-P particles added under shaking. The mixture formed was transferred to a temperature-controlled silicon oil bath and stirred at a constant temperature, with the purpose of impregnating calixarene and MODB onto the silica particles. The final stage was vacuum drying the mixture to form a colourless composite. A similar procedure was applied by Zhang et al. (2009) except with n-octanol rather than MOD-B impregnated onto SiO_2-P support particles. The properties of calixarene chromatographic materials are summarised in Table F.1.

Ref	Calixarene	Diluent	Support material	Modifier	Sample matrix	Load [HNO_3]	Cs elution [HNO_3]
Dietz (2006)	BCB*	1,2 dichloro-ethane	XAD-7	-	Multiple elements	0.5M	6M
Zhang (2009)	Calix[4]arene -R14**	Octanol	SiO_2-P	-	HLW fission products	4M	Water
Zhang (2010)	Calix[4]arene -R14	Chloro-methane	SiO_2-P	Methyloctyl-2-di-methy-lbutanemide (MODB)	HLW fission and non-fission products	3M	Water

Table F.1. Summary of previous chromatographic calixarene separation procedures
***BCB-1,3-calix[4]bis-*o*-benzo-crown-6.**
****Calix[4]arene-R14- 1,3-[(2,4-diethylheptylethoxyoxy]-2,4-crown-6-calix[4]arene**

G. Data tables: ICP-SFMS measurement of Sr under cold plasma conditions

RF (W)	Counts per ng/L		Sensitivity loss vs. 1200W		Sr/Zr separation factor	LOD (pg/L)	Signal/noise (10ng/L Sr)
	Sr	Zr	Sr	Zr			
650	46.0	0.002	35.8	745,346.6	17,379.8	33.5	1.0
750	38.7	0.03	42.6	77,872	1,529.0	24.0	1.5
900	123.8	2.7	13.3	735.5	46.2	31.2	3.5
1000	351.6	46.8	4.7	42.1	7.5	34.9	5.6
1100	883.0	581.7	1.9	3.4	1.5	97.4	6.7
1200	1,647.3	1,971.0			0.8	106.5	6.5

Table G.1. PC^3 inlet system, Ni sample cone, H-skimmer cone

RF (W)	Counts per ng/L		Sensitivity loss compared to 1200W		Sr/Zr separation factor	LOD (pg/L)	Signal/noise for 10ng/L Sr
	Sr	Zr	Sr	Zr			
650	270.7	123.9	114.0	151.7	2.2	92.1	1.2
750	765.6	374.4	40.3	54.1	2.2	97.1	5.5
900	3480.9	1,657.9	8.9	11.3	2.1	28.6	9.3

Table G.2. Aridus II, Jet interface, and X-skimmer cone)

RF (W)	Counts per ng/L		Sensitivity loss compared to 1200W		Sr/Zr separation factor	LOD (pg/L)	Signal/noise for 10ng/L Sr
	Sr	Zr	Sr	Zr			
1100	16,996.6	9,684.9	1.8	1.9	1.8	16.4	24.7
1200	30,864.6	18,799.7			1.6	15.9	38.0

Table G.2. Continued

RF (W)	Counts per ng/L		Sensitivity loss compared to 1200W		Sr/Zr separation factor	LOD (pg/L)	Signal/noise for 10ng/L Sr
	Sr	Zr	Sr	Zr			
650	25.4	0.3	212.8	6250.6	81.7	4.5	1.5
750	109.8	0.5	49.2	4167.1	235.3	5.2	2.17
900	486.3	6.5	11.1	299.4	74.9	8.7	3.24
1000	1,151.5	52.6	4.7	37.0	21.9	14.0	5.56
1100	2,787.4	356.3	1.9	5.5	7.8	29.1	8.67
1200	5,405.8	1,943.8			2.8	62.7	9.98

Table G.3. Apex Q, Ni sample cone and H-skimmer cone

RF (W)	Counts per ng/L		Sensitivity loss compared to 1200W		Sr/Zr separation factor	LOD (pg/L)	Signal/noise for 10ng/L Sr
	Sr	Zr	Sr	Zr			
650	47.4	0.03	308.7	126,640	1907.1	61.5	0.1
750	71.7	0.02	204.4	200,123	4,551.2	38.7	0.2
900	697.0	1.3	21.0	2456.1	543.4	4.9	1.3
1000	2,258.5	10.5	6.5	301.3	216.0	8.0	4.4
1100	4,273.2	451.7	3.4	7.0	9.5	17.2	24.8
1200	14,644.0	3,150.6			4.7	19.9	24.9

Table G.4. Apex Q, Ni sample cone and X-skimmer cone

List of References

Aarkrog, A., L. Botter-Jensen, L., Jiang, C.Q., Dahlgaard, H. and H. Hansen (1988). Environmental radioactivity in Denmark in 1986. Riso National Laboratory, Denmark

Aarkrog, A. (1994). Radioactivity in polar regions-Main sources. Journal of Environmental Radioactivity 25 (1-2), 21-35

Aarkrog, A., Dahlgaard, H. and S.P. Nielsen (1999). Marine radioactivity in the Arctic: a retrospect of environmental studies in Greenland waters with emphasis on transport of ^{90}Sr and ^{137}Cs with the East Greenland Current. The Science of the Total Environment 237, 143-151

Agatemor, C. and D. Beauchemin (2011). Matrix effects in inductively coupled plasma mass spectrometry: A review. Analytica Chimica Acta 706 (1), 66-83

Agilent Technologies (2012). http://www.chem.agilent.com/Library/Support/Documents/f39250232446.pdf

Alonso, J.I.G., Sena, F., Arbore, P., Betti, M. and L. Koch (1995). Determination of fission products and actinides in spent nuclear fuels by isotope dilution ion chromatography inductively coupled plasma mass spectrometry. Journal of Analytical and Atomic Spectrometry 10 (5), 381-393

Amr, M. and A. Abdel-Lateef (2010). Comparing the Capability of Collision/Reaction Cell Quadrupole and Sector Field Inductively Coupled Plasma Mass Spectrometers for Interference Removal from ^{90}Sr; ^{137}Cs; and ^{226}Ra. International Journal of Mass Spectrometry 299, 184-190

Aoyama, M., Hirose, K., Miyao, T. and Y. Igarashi (2000). Low level ^{137}Cs measurements in deep seawater samples. Applied Radiation and Isotopes 53 (1-2), 159-162

Appelblad, P., Rodushkin, I. and D.C. Baxter (2000). The use of Pt guard electrode in inductively coupled plasma sector field mass spectrometry: advantages and limitations. Journal of Analytical Atomic Spectrometry 15 (4), 359-364

Asfari, Z., Bressot, C., Vicens, J., Hill, C., Dozol, J.F., Rouquette, H., Eymard, S., Lamare, V. and B.Tournois (1995). Doubly crowned calix [4] arenes in the 1, 3-alternate conformation as cesium-selective carriers in supported liquid membranes. Analytical Chemistry 67 (18), 3133-3139

Bailly du Bois, P., Laguionie, P., Boust, D., Korsakissok, I., Diddier, D. and B. Fiévet, (2012). Estimation of marine source-term following Fukushima Dai-ichi accident. Journal of Environmental Radioactivity 114, p. 2-9

Baker, C. (1975). The Determination of Radiocaesium in Sea and Fresh Water. Fisheries Research Technical Report no. 16, Ministry of Agriculture, Fisheries and Food, Directorate of Fisheries Research

Becker, J. S. and H. J. Dietze, (1999). Application of double-focusing sector field ICP mass spectrometry with shielded torch using different nebulizers for ultratrace and precise isotope analysis of long-lived radionuclides. Journal of Analytical Atomic Spectrometry 14 (9), 1493-1500

Becker, J.S. (2005). Recent developments in isotope analysis by advanced mass spectrometric techniques Plenary lecture. Journal of Analytical Atomic Spectrometry 20 (11), 1173-1184

Betti, M., Giannarelli, S., Hiernaut, T., Rasmussen, G. and L. Koch (1996). Detection of trace radioisotopes in soil, sediment and vegetation by glow discharge mass spectrometry. Frensius' Journal of Analytical Chemistry 355 (5), 642-646

Betti, M. (1997). Use of ion chromatography for the determination of fission products and actinides in nuclear applications. Journal of Chromatography A 789 (1-2), 369-379

Boll, R., Schweitzer, G. and R. Garber (1997). An improved actinide separation method for environmental samples. Journal of Radioanalytical and Nuclear Chemistry 220 (2), 201-206

Bombard, A., Happel, S. and F. Sebesta (2013). Cesium radioisotopes separation in environmental and waste samples: use of inorganic/organic composite absorbers AMP-PAN, KNiFC-PAN. Presented at the Coordinating Group on Environmental Radioactivity conference

Bonnesen, P.V., Delmau, L.H., Haverlock, T.J. and B.A. Moyer (1998). Alkaline-Side Extraction of Cesium from Savannah River Tank Waste Using a Calixarene-Crown Ether Extractant. http://web.ornl.gov/sci/csd/pdfs/cs_TM13704.pdf. Prepared by the Oak Ridge National Laboratory for the US Department of Energy

Bostick, B.C., Vairavamurthy, M.A., Karthikeyan, K.G. and J.Chorover (2002). Cesium adsorption on clay minerals: An EXAFS spectroscopic investigation. Environmental Science & Technology 36 (12), 2670-2676

Boulyga, S.F., Becker, J.S., Matusevich, J.L. and H-J. Dietze (2000). Isotope ratio measurements of spent reactor uranium in environmental samples by using inductively coupled plasma mass spectrometry. International Journal of Mass Spectrometry 203 (1), 143-154

Boulyga, S.F., Matusevich, J.L., Mironov, V.P., Kudrjashov, V.P., Halicz, L., Segal, I., McLean, J.A., Montaser, A. and J.S. Becker (2002). Determination of $^{236}U/^{238}U$ isotope ratio in contaminated environmental samples using different ICP-Ms instruments. Journal of Analytical and Atomic Spectrometry 17 (8), 958-964

Boulyga, S.F., Klötzil, U. and T. Prohaska (2006). Improved abundance sensitivity in MC-ICP-MS for determination of $^{236}U/^{238}U$ isotope ratios in the 10^{-7} to 10^{-8} range. Journal of Analytical and Atomic Spectrometry 21 (12), 1427-1430

Bowen, V. T., Noshkin, V.E., Livingston, H.D. and K.M. Wong (1974). Cesium-137 to strontium-90 ratios in the Atlantic Ocean 1966 through 1972. Limnology Oceanography 19, 670-681

Braun, T. and G. Ghersini (1975). Extraction chromatography. Journal of Chromatography Library 2, 56-65

Brun, S., Bessac, S., Uridat, D. and B. Boursier (2002). Rapid method for the determination of radiostrontium in milk. Journal of Radioanalytical and Nuclear Chemistry 253 (2), 191-197

Buesseler, K., M. Aoyama, and M. Fukasawa (2011). Impacts of the Fukushima nuclear power plants on marine radioactivity. Environmental Science & Technology 45 (23), 9931-9935

Buesseler, K. O., Jayne, S.R., Fisher, N.S., Rypina, I.I., Baumann, H., Baumann, Z., Breier, C.F., Douglass, E.M., George, J. and A.M. Macdonald (2012). Fukushima-derived radionuclides in the ocean and biota off Japan. Proceedings of the National Academy of Sciences 109 (16), 5984-5988

Casnati, A., Pochini, A., Ungaro, R., Ugozzoli, F., Arnaud, F., Fanni, S., Schwing, M.J., Egberink, R.J.M., De Jong, F. and D.N. Reinhoudt (1995). Synthesis, complexation, and membrane transport studies of 1, 3-alternate calix [4] arene-crown-6 conformers: a new class of cesium selective ionophores. Journal of the American Chemical Society 117 (10), 2767-2777

Cetac (2013). Aridus II desolvating sample introduction system http://www.cetac.com/pdfs/Brochure_Aridus_II.pdf.

Chao, J.H. and C.L. Tseng (1996). Determination of ^{135}Cs by neutron activation analysis. Nuclear Instruments and Methods in Physics Research Section A: Accelerators, Spectrometers, Detectors and Associated Equipment 372 (1-2), 275-279

Chen, Q., Hou, X., Yu, Y., Dahlgaard, H. and S.P. Nielsen, (2002). Separation of Sr from Ca, Ba and Ra by means of $Ca(OH)_2$ and $Ba(Ra)Cl_2$ or $Ba(Ra)SO_4$ for the determination of radiostrontium. Analytica Chimica Acta 466 (1), 109-116

Chen, H-W., Lee, T., Ku T-L. and J.P. Das (2008). Production Ratio of Nuclear Fallout $^{137}Cs/^{135}Cs$. Chinese Journal of Physics 46, 560-569

Charles, M. and J. Harrison (2007). Hot particle dosimetry and radiobiology past and present. Journal of Radiological Protection 27, A97-A109

Chu, N-C., Taylor, R.N., Chavagnac, V., Nesbitt, R.W., Boella, R.M., Milton, J.A., German, C.R., Bayon, G. and K. Burton (2002). Hf isotope ratio analysis using multi-collector inductively coupled plasma mass spectrometry: an evaluation of isobaric interference corrections. Jounral of Analytical and Atomic Spectrometry 17 (12), 1567-1574

Clearfield, A. (2000). Inorganic ion exchangers, past, present, and future. Solvent Extraction and Ion Exchange 18 (4), 655-678

Cochran, J. K., Hirschberg, D.J., Livingston, H.D., Buesseler, K.O. and R.M. Key (1995). Natural and anthropogenic radionuclide distributions in the Nansen Basin, Arctic Ocean: Scavenging rates and circulation timescales. Deep Sea Research (Part II, Topical Studies in Oceanography) 42 (6),1495-1517

Croudace, I.W. and S. Marshall (1991). Determination of rare earth elements and yttrium in nine geochemical reference samples using a novel group separation procedure involving mixed-acid elution ion-exchange chromatography. Geostandards Newsletter 15,139-144

Croudace, I., Warwick, P., Taylor, R., and S.Dee (1998). Rapid procedure for plutonium and uranium determination in soils using a borate fusion followed by ion-exchange and extraction chromatography. Analytica Chimica Acta 371, 217-225

Dahlgaard, H. (1995). Transfer of European coastal pollution to the Arctic: radioactive tracers. Marine Pollution Bulletin 31(1-3), 3-7

Dahlgaard, H., Eriksson, M., Nielsen, S.P. and H.P. Joensen (2004). Levels and trends of radioactive contaminants in the Greenland environment. Science of the total environment, 331(1), 53-67

Delmore, J.E., Snyder, D.C., Tranter, T. and N.R. Mann (2011). Cesium isotope ratios as indicators of nuclear power plant operations. Journal of Environmental Radioactivity 102 (11), 1008-1011

Dennis, F., G. Morgan, and F. Henderson (2007). Dounreay hot particles: the story so far. Journal of Radiological Protection 27, A3-A11

Dietz, M.L., Ensor, D.D., Harmon, B. and S. Seekamp (2006). Separation and preconcentration of cesium from acidic media by extraction chromatography. Separation Science and Technology 41 (10), 2183-2204

Dozol, J.F., Simon, N., Lamare, V., Rouquette, H., Eymard, S., Tournois, B., De Marc, D. and R.M. Macias (1999). A solution for cesium removal from high-salinity acidic or alkaline liquid waste: the crown calix[4]arenes: Separation Science and Technology 34 (6-7), 877-909

Du, Z., Jia, M. and X. Wang (2013). Cesium removal from solution using PAN-based potassium nickel hexacyanoferrate (II) composite spheres. Journal of Radioanalytical and Nuclear Chemistry 298 (1), 167-177

Eichrom Industries (2013). Sr Resin. www.eichrom.com/products/info/sr_resin.aspx

Eliades, J., Zhao, X-L., Litherand, A.E. and W.E. Kieser (2013). On-line ion chemistry for the AMS analysis of ^{90}Sr and ^{135,137}Cs. Nuclear Instruments and Methods in Physics Research Section B: Beam Interactions with Materials and Atoms 294, 361-363

Elemental Scientific (2014(A)). PC^3 sample introduction system. http://www.icpms.com/pdf/PC3-ESI.pdf.

Elemental Scientific (2014(B)). Apex Q sample introduction system. http://www.icpms.com/pdf/ApexQ-ESI.pdf.

Epov, V.N., Taylor, V., Lariviere, D., Evans, R.D. and R.J. Cornett (2003). Collision cell chemistry for the analysis of radioisotopes by inductively coupled plasma mass spectrometry. Journal of Radioanalytical and Nuclear Chemistry 258 (3), 473-480

EuroGeoSurveys (2011). http://www.eurogeosurveys.org/foregs.html.

Favre, G., Brennetot, R., Chartier, F. and P. Vitorge (2007). Understanding reactions with O_2 for ^{90}Sr measurements by ICP-MS with collision-reaction cell. International Journal of Mass Spectrometry 265 (1), 15-22

Feuerstein, J., Boulyga, S.F., Galler, P., Stingeder, G. and T. Prohaska (2008). Determination of ^{90}Sr in soil samples using inductively coupled plasma mass spectrometry equipped with dynamic reaction cell (ICP-DRC-MS). Journal of Environmental Radioactivity 99 (11), 1764-1769

Finegan, P., Vintrò, L.L., Mitchell, P.I., Boust, D., Gouzy, A., Kershaw, P.J. and J.A. Lucey (2009). Accumulation, solid partitioning and remobilisation of ^{99}Tc in subtidal intertidal sediments in the Irish Sea. Continental Shelf Research 29(16), 1995-2010

Gaur, S. (1996). Determination of Cs-137 in environmental water by ion-exchange chromatography. Journal of Chromatography A 733 (1-2), 57-71

Govindaraju, K. (1994). Composition of the average shale and its related materials. Geostandards Newsletter XVIII (0150 5505)

Granet, M., Nonell, A., Favre, G., Chartier, F., Isnard, H., Moureau, J., Caussignac, C. and B. Tran (2008). Cs-Ba separation using N_2O as a reactant gas in a Multiple Collector-Inductively Coupled Plasma Mass Spectrometer collision-reaction cell: Application to the measurements of Cs isotopes in spent nuclear fuel samples. Spectrochimica Acta Part B: Atomic Spectroscopy 63 (11), 1309-1314

Granfors M. and J. Low (2013). Isotope dilution analysis of Sr-90 with dynamic reaction cell ICP-MS. 2nd NKS-B Workshop on Radioanalytical Chemistry, Roskilde, Denmark

Gray, J., Jones, S. and A. Smith (1995). Discharges to the environment from the Sellafield site. Journal of Radiological Protection 15 (2), 99-131

Grinberg, P., Willie, S. and R.E. Sturgeon (2007). Determination of natural Sr and ^{90}Sr in environmental samples by ETV-ICP-MS. Journal of Analytical Atomic Spectrometry 22 (11), 1409-1414

Grunder, M., Dozol, J.F., Asfari, Z. and J. Vicens (1999). Simultaneous removal of technetium and cesium by functionalized calixarenes from acidic liquid waste. Journal of Radioanalytical and Nuclear Chemistry 241 (1), 59-67

Hakem, N., Apps, J.A., Moridis, G.J. and I. Al Mahamid (2004). Sorption of fission product radionuclides, ^{137}Cs and ^{90}Sr, by Savannah River Site sediments impregnated with colloidal silica. Radiochimica Acta/International Journal for Chemical Aspects of Nuclear Science and Technology 92 (7), 419-432

Happel, S. (2008). Determination of Sr-89 and Sr-90 in environmental and biological samples. Madrid UGM presentation.

Haverlock, T.J., Bonnesen, P.V., Sachleben, R.A. and B.A. Moyer (2000). Analysis of Equilibria in the Extraction of Cesium Nitrate by Calix [4] arene-bis (t-

octylbenzo-crown-6) in 1, 2-Dichloroethane. Journal of Inclusion Phenomena and Macrocyclic Chemistry 36 (1), 21-37.

Heldal, H.E. and P. Varskog (2002). Distribution of selected anthropogenic radionuclides (^{137}Cs, ^{238}Pu, ^{239,240} Pu and ^{241}Am) in marine sediments with emphasis on the Spitsbergen-Bear Island area. Science of the Total Environment, 293 (1-3), 233-245

Horwitz, E.P., Dietz, M.L. and D.E. Fisher (1991). Separation and preconcentration of strontium from biological, environmental, and nuclear waste samples by extraction chromatography using a crown ether. Analytical chemistry 63 (5), 522-525

Horwitz, E. P., Chiarizia, R. and M.L. Dietz (1992). A novel strontium-selective extraction chromatographic resin. Solvent Extraction and Ion Exchange 10 (2), 313-336

Horwitz, E.P., Dietz, M.L. and M.P. Jensen (1996). A combined cesium-strontium extraction/recovery process. Presented at International Solvent Extraction Conference

Horwitz, E. (2013). Extraction chromatography of actinides and selected fission products: Principles and achievement of selectivity. http://www.eichrom.com/products/extraction.aspx.

Hou, X. and P. Roos (2008). Critical comparison of radiometric and mass spectrometric methods for the determination of radionuclides in environmental, biological and nuclear waste samples. Analytica Chimica Acta 608 (2), 105-139

Hu, Q.H., Weng, J.Q. and J.S. Wang (2010). Sources of anthropogenic radionuclides in the environment: a review. Journal of environmental radioactivity 101 (6), 426-437

Hu, Z., Liu, Y., Gao, S., Liu, W., Zhang, W., Tong, X., Lin, L., Zong, K., Li, M. and H. Chen (2012). Improved in situ Hf isotope ratio analysis of zircon using newly designed X skimmer cone and Jet sample cone in combination with the addition of nitrogen by laser ablation multiple collector ICP-MS. Journal of Analytical Atomic Spectrometry 27 (9), 1391-1399

Hunt, J., Leonard, K. and L. Hughes (2013). Artificial radionuclides in the Irish Sea from Sellafield: remobilisation revisited. Journal of Radiological Protection 33 (2), 261-279

Ikeda, A. and S. Shinkai (1994). On the Origin of High Ionophoricity of 1, 3-Alternate Calix [4] arenes:. pi.-donor Participation in Complexation of Cations and Evidence for Metal-Tunneling through the Calix [4] arene Cavity. Journal of the American Chemical Society 116 (7), 3102-3110

Ikeda, A. and S. Shinkai (1997). Novel cavity design using calix [n] arene skeletons: toward molecular recognition and metal binding. Chemical Reviews 97 (5), 1713-1734

Ismail, I., El-Sourougy, M.R., Moneim, N.A. and H.F. Aly (1998). Preparation, characterization, and utilization of potassium nickel hexacyanoferrate for the separation of cesium and cobalt from contaminated waste water. Journal of Radioanalytical and Nuclear Chemistry 237 (1), 97-103

Isnard, H., Aubert, M., Blanchet, P., Brennetot, R., Chartier, F., Geertsen, V. and F. Manuguerra (2006). Determination of $^{90}Sr/^{238}U$ ratio by double isotope dilution inductively coupled plasma mass spectrometer with multiple collection in spent nuclear fuel samples with in situ $^{90}Sr/^{90}Zr$ separation in a collision-reaction cell. Spectrochimica Acta Part B: Atomic Spectroscopy 61(2), 150-156

Isnard, H., Granet, M., Caussignac, C., Ducarme, E., Nonell, A., Tran, B. and F. Chartier (2009). Comparison of thermal ionization mass spectrometry and Multiple Collector Inductively Coupled Plasma Mass Spectrometry for cesium isotope ratio measurements. Spectrochimica Acta Part B: Atomic Spectroscopy 64 (11-12), 1280-1286

Jäggi, M. and J. Eikenberg (2009). Separation of ^{90}Sr from radioactive waste matrices-Microwave versus fusion decomposition. Applied Radiation and Isotopes 67 (5), 765-769

Jakopi , R. and L. Benedik (2005). Tracer studies on Sr resin and determination of ^{90}Sr in environmental samples. Acta Chimica Slovenica 52, 297-302

Jakubowski, N., Moens, L. and F. Vanhaecke, 1998. Sector field mass spectrometers in ICP-MS. Spectrochimica Acta Part B: Atomic Spectroscopy 53 (13), 1739-1763

Jarvis, K. E. and J. G. Williams (1998). Critical assessment of the effects of skimmer cone geometry on spectroscopic and non-spectroscopic interference in inductively coupled plasma mass spectrometry. Journal of Analytical Atomic Spectrometry 13 (8), 689-696

Jefferies, D., Preston, A. and A. Steele (1973). Distribution of caesium-137 in British coastal waters. Marine Pollution Bulletin 4 (8), 118-122

Johnson, A. C. J. H., Greenwood, P., Hagström, M., Abbas, Z. and S. Wall (2008). Aggregation of nanosized colloidal silica in the presence of various alkali cations investigated by the electrospray technique. Langmuir 24 (22), 12798-12806

Kamenik, J. and F. Ŝebesta (2003). Comparison of some commercial and laboratory prepared caesium ion-exchangers. Czechoslovak Journal of Physics 53 (1), A571-A576

Kamenik, J., Dulaiova, H., Buesseler, K.O., Pike, S.M. and K. Ŝt'astná (2013). Cesium-134 and 137 activities in the central North Pacific Ocean after the Fukushima Dai-ichi nuclear power plant accident. Biogeosciences Discussions 10 (3), 5223-5244

Karam, L., Pibida, L. and C. McMahon (2002). Use of resonance ionization mass spectrometry for determination of Cs ratios in solid samples. Applied Radiation and Isotopes 56 (1-2), 369-374

Kehm, K., Hauri, E.H., Alexander, C.M. and R.W. Carlson (2003). High precision iron isotope measurements of meteoritic material by cold plasma ICP-MS. Geochimica et Cosmochimica Acta 67 (15), 2879-2891

Kershaw, P. and A. Baxter (1995). The transfer of reprocessing wastes from north-west Europe to the Arctic. Deep Sea Research Part II: Topical Studies in Oceanography 42 (6) 1413-1448

Kershaw, P., Sampson, K.E., McCarthy, W. and R.D. Scott (1995). The measurement of the isotopic composition of plutonium in an Irish Sea sediment by mass spectrometry. Journal of Radioanalytical and Nuclear Chemistry 198 (1), 113-124

Kershaw, P., Gurbutt, P., Woodhead, D., Leonard, K. and J. Rees (1997). Estimates of fluxes of ^{137}Cs in northern waters from recent measurements. Science of the Total Environment 202 (1), 211-223

Ketterer, M. and S. Szechenyi (2008). Determination of plutonium and other transuranic elements by inductively coupled plasma mass spectrometry: A historical perspective and new frontiers in the environmental sciences. Spectrochimica Acta Part B: Atomic Spectroscopy 63 (7), 719-737

Kim, J.S., Suh, I.H., Kim, J.K. and M.H. Cho (1998). Selective sensing of caesium ions by novel calix [4] arene bis (dibenzocrown) ethers in an aqueous environment. Journal of the Chemical Society, Perkin Transactions 1, (15), 2307-2312

Kutschera, W. (2013). Applications of accelerator mass spectrometry. International Journal of Mass Spectrometry 349, 203-218

Lamare, V., Dozol, J.F., Fuangswasdi, S., Arnaud-Neu, F., Thuery, P., Nierlich, M., Asfari, Z. and J.Vicens (1999). A new calix [4] arene-bis (crown ether) derivative displaying an improved caesium over sodium selectivity: molecular dynamics and experimental investigation of alkali-metal ion complexation. Journal of the Chemical Society, Perkin Transactions 2 (2), 271-284

Labrecque, C., Whitty-Léveillé, L. and D. Lariviere (2014). Cloud Point Extraction of Plutonium in Environmental Matrixes Coupled to ICP-MS and α Spectrometry in Highly Acidic Conditions. Analytical Chemistry 85, 10549-10555

Lavrov, V.V., Blagojevic, V., Koyanagi, G.K., Orlova, G. and D.K. Bohme (2004). Gas-phase oxidation and nitration of first-, second-, and third-row atomic cations in reactions with nitrous oxide: Periodicities in reactivity. The Journal of Physical Chemistry A, 108 (26), 5610-5624

Lariviere, D., Taylor, V.F., Evans, R.D. and R.J. Cornett (2006). Radionuclide determination in environmental samples by inductively coupled plasma mass

spectrometry. Spectrochimica Acta Part B: Atomic Spectroscopy 61 (8), 877-904

Lee, T., The-Lung, K., Hsiao-Ling, L. and C. Ju-Chin (1993). First detection of fallout Cs-135 and potential applications of ratios. Geochimica et Cosmochimica Acta 57 (14), 3493-3497

Lehto, J., Paajanen, R. and R. Harjula (1992). Selectivity of potassium cobalt hexacyanoferrate (II) for alkali and alkaline earth metal ions. Journal of Radioanalytical and Nuclear Chemistry 164 (1), 39-46

Leonard, R.A., Conner, C., Liberatore, M.W., Sedlet, J., Aase, S.B., Vandegrift, G.F., Delmau, L.H., Bonnesen, P.V. and B.A.Moyer (2001). Development of a solvent extraction process for cesium removal from SRS tank waste. Separation Science and Technology 36 (5-6), 743-766

Liezers, M., Farmer, O.T. and M. Thomas (2009). Low level detection of ^{135}Cs and ^{137}Cs in environmental samples by ICP-MS. Journal of Radioanalytical and Nuclear Chemistry 282 (1), 309-313

Lindahl, P., Keith-Roach, M., Worsfold, P., Choi, M.S., Shin, H.S. and S.H. Lee (2010). Ultra-trace determination of plutonium in marine samples using multi-collector inductively coupled plasma mass spectrometry. Analytica Chimica Acta 671 (1), 61-69

Livens, F. and P. Loveland (1988). The influence of soil properties on the environmental mobility of caesium in Cumbria. Soil Use and Management 4 (3), 69-75

Livingston, H. D., Kupferman, S.L., Bowen, V.T. and R.M. Moore (1984). Vertical profile of artificial radionuclide concentrations in the central Arctic Ocean. Geochimica et Cosmochimica Acta 48 (11), 2195-2203

Lo, L., Shen, C.C., Lu, C-J., Chen, Y-C., Chang, C-C., Wei, K-Y., Qu, D. and M.K. Gagan (2014). Determination of element/Ca ratios in foraminifera and corals using cold-and hot-plasma techniques in inductively coupled plasma sector field mass spectrometry. Journal of Asian Earth Sciences 81, 115-122

Mardan, A., Ajaz, R., Mehmood, A., Raza, S.M. and A. Ghaffar (1999). Preparation of silica potassium cobalt hexacyanoferrate composite ion exchanger and its uptake behavior for cesium. Separation and Purification Technology 16 (2), 147-158

Marsh, S.F., Svitra, Z.V. and S.M. Bowen (1994). Distributions of 14 Elements on 63 Absorbers from Three Simulant Solutions (Acid-Dissolved Sludge, Acidified Supernate, and Alkaline Supernate) for Hanford HLW Tank 102-SY. Report LA-12654, Los Alamos National Laboratory

Maxwell, S. L., Culligan, B.K. and G.W. Noyes (2010). Rapid separation of actinides and radiostrontium in vegetation samples. Journal of Radioanalytical and Nuclear Chemistry 286 (1), 273-282

Meeks, A., Giaquinto, J. and J. Keller (1998). Application of ICP-MS radionuclide analysis to Real World samples of department of Energy radioactive waste. Journal of Radioanalytical and Nuclear Chemistry 234 (1), 131-136.

Merz, S., Steinhauser, G. and N. Hamada (2013). Anthropogenic radionuclides in Japanese food: environmental and legal implications. Environmental science & technology 47, 1248-1256

Miller, C.J., Olson, A.L. and C.K. Johnson (1997). Cesium absorption from acidic Solutions using ammonium molybdophosphate on a polyacrylonitrile support (AMP PAN). Separation Science and Technology 32, 37-50

Mimura, H., Lehto, J. and R. Harjula (1997(A)). Selective removal of cesium from simulated high-level liquid wastes by insoluble ferrocyanides. Journal of Nuclear Science and Technology 34 (6), 607-609

Mimura, H., Lehto, J. and R. Harjula (1997(B)) Ion exchange of cesium on potassium nickel hexacyanoferrate (II) s. Journal of Nuclear Science and Technology 34 (5), 484-489

Mimura, H., Lehto, J. and R. Harjula (1997(C)). Chemical and thermal stability of potassium nickel hexacyanoferrate (II). Journal of Nuclear Science and Technology 34 (6), 582-587

Mimura, H., Kimura, M., Akiba, K. and Y. Onodera (1999(A)). Separation of Cesium and Strontium by Potassium Nickel: Hexacyanoferrate (II)-Loaded Zeolite A. Journal of Nuclear Science and Technology 36 (3), 307-310

Mimura, H., Kimura, M., Akiba, K. and Y. Onodera (1999(B)). Selective removal of cesium from highly concentrated sodium nitrate neutral solutions by potassium nickel hexacyanoferrate (II)-loaded silica gels. Solvent Extraction and Ion Exchange 17 (2), 403-417

Mimura, H., Saito, M., Akiba, K. and Y. Onodera (2001). Selective Uptake Of Cesium by ammonium molybdophosphate (AMP)-calcium alginate composites. Solvent Extraction and Ion Exchange 18 (5) 1015-1027

Mohapatra, P., Ansari, S.A., Sarkar, A., Bhattacharyya, A. and V.K. Manchanda (2006). Evaluation of calix-crown ionophores for selective separation of radio-cesium from acidic nuclear waste solution. Analytica Chimica Acta 571 (2), 308-314

Molero, J., Sanchez-Cabeza, J.A., Merino, J., Pujol, L., Mitchell, P.I. and A. Vidal-Quadras (1995). Vertical distribution of radiocaesium, plutonium and americium in the Catalan Sea (Northwestern Mediterranean). Journal of environmental radioactivity 26 (3), 205-216

Moon, J.-K., Lee, E-H. and H.-T. Kim (2004). Ion exchange of Cs ion in acid solution with potassium cobalt hexacyanoferrate. Korean Journal of Chemical Engineering 21 (5), 1026-1031

Moreno, J.M.B., Betti, M. and G. Nicolaou (1999). Determination of caesium and its isotopic composition in nuclear samples using isotope dilution-ion chromatography-inductively coupled plasma mass spectrometry. Journal of Analytical and Atomic Spectrometry 14 (5), 875-879

Morgan, A. and G. Arkell (1963). A method for the determination of caesium-137 in sea water. Health Physics 9 (8), 857

Morris, K., Butterworth, J.C. and F.R. Livens (2000). Evidence for the remobilisation of Sellafield waste radionuclides in an intertidal salt marsh, West Cumbria, UK. Estuarine, Coastal and Shelf Science 51 (5), 613-625

Murphy, K. E., Long, S.E., Rearick, M.S. and Ö.S. Ertas (2002). The accurate determination of potassium and calcium using isotope dilution inductively coupled "cold" plasma mass spectrometry. Journal of Analytical Atomic Spectrometry 17 (5), 469-477

Nervik, W. E. (1960). The Radiochemistry of Tin. National Academy of Science, Nuclear Science Series, 2-6

Newman, K., Freedman, P.A., Williams, J., Belshaw, N.S. and A.N. Halliday (2009). High sensitivity skimmers and non-linear mass dependent fractionation in ICP-MS. Journal of Analytical Atomic Spectrometry 24 (6), 742-751

Nies, H., Harms, I.H., Karcher, M.J., Dethleff, D. and C. Bahe (1999). Anthropogenic radioactivity in the Arctic Ocean- review of the results from the joint German project. Science of the Total Environment 237-238, 181-191

Nilchi, A., Khanchi, A., Atashi, H., Bagheri, A. and L. Nematollahi (2006). The application and properties of composite sorbents of inorganic ion exchangers and polyacrylonitrile binding matrix. Journal of Hazardous Materials 137 (3), 1271-1276

Niu, H. and R. Houk (1996). Fundamental aspects of ion extraction in inductively coupled plasma mass spectrometry. Spectrochimica Acta Part B: Atomic Spectroscopy 51 (8), 779-815

Noell, A. L., Thompson, J.L., Corapcioglu, M.Y. and I.R. Triay (1998). The role of silica colloids on facilitated cesium transport through glass bead columns and modeling. Journal of Contaminant Hydrology 31 (1), 23-56

Ohno, T., Muramatsu, Y., Shikamori, Y., Toyama, C., Okabe, N. and H. Matsuzaki (2013). Determination of ultratrace ^{129}I in soil samples by Triple Quadrupole ICP-MS and its application to Fukushima soil samples. Journal of Analytical and Atomic Spectrometry 28, 1283-1287

Ohno, T. and Y. Muramatsu (2014). Determination of radioactive cesium isotope ratios by triple quadrupole ICP-MS and its application to rainwater following the Fukushima Daiichi Nuclear Power Plant accident. Journal of Analytical Atomic Spectrometry 29 (2), 347-351

Okamura, Y., Fujiwara, K., Ishihara, R., Sugo, T., Kojima, T., Umeno, D. and K. Saito (2014). Cesium removal in freshwater using potassium cobalt hexacyanoferrate-impregnated fibers. Radiation Physics and Chemistry 94, 119-122

Owens, P.N., Walling, D.E. and Q. He (1996). The behaviour of bomb-derived caesium-137 fallout in catchment soils. Journal of Environmental Radioactivity 32 (3), 169-191

Paul, M., Berkovits, D., Cecil, L.D., Feldstein, H., Hershkowitz, A., Kashiv, Y. and S. Vogt (1997). Environmental ^{90}Sr measurements. Nuclear Instruments and Methods in Physics Research Section B: Beam Interactions with Materials and Atoms 123 (1), 394-399

Perkin Elmer (2004). Elan II DRC Brochure. https://www.esc.cam.ac.uk/esc/files/Department/facilities/icp-ms/drcii-b.pdf. Accessed 2/4/14

Pibida, L., McMahon, C. and B.A. Bushaw (2004). Laser resonance ionization mass spectrometry measurements of cesium in nuclear burn-up and sediment samples. Applied Radiation and Isotopes 60 (2-4), 567-570

Pike, S.M., Buesseler, K.O., Breier, C.F., Dulaiova, H., Stastna, K. and F. Sebesta (2013). Extraction of cesium in seawater off Japan using AMP-PAN resin and quantification via gamma spectroscopy and inductively coupled mass spectrometry. Journal of Radioanalytical and Nuclear Chemistry 296 (1), 369-374

Pitois, A., Heras, L.A.L. and M. Betti (2008). Determination of fission products in nuclear samples by capillary electrophoresis-inductively coupled plasma mass spectrometry (CE-ICP-MS). International Journal of Mass Spectrometry 270 (3), 118-126

Quemet, A., Brennetot, R., Chevalier, E., Prian, E., Laridon, A-L., Mariet, C., Fichet, P., Laszak, I. and F. Goutelard (2012). Analysis of twenty five impurities in uranium matrix by ICP-MS with iron measurement optimized by using reaction collision cell, cold plasma or medium resolution. Talanta 99, 207-212

Ramendik, G., Fatyushina, E.V., Stepanov, A.I. and V.S. Sevast'yanov (2001). New approach to the calculation of relative sensitivity factors in inductively coupled plasma mass spectrometry. Journal of Analytical Chemistry 56 (6), 500-506

Resano, M., Vanhaecke, F. and M.T.C. De Loos-Vollebregt (2008). Electrothermal vaporization for sample introduction in atomic absorption, atomic emission and plasma mass spectrometry, a critical review with focus on solid sampling and slurry analysis. Journal of Analytical Atomic Spectrometry 23 (11), 1450-1475

Riddle, C.L., Baker, C.L., Law, J.D, McGrath, C.A., Meikrantz, D.H., Mincher, B.J., Peterman, D.R. and T.A. Todd (2004). Development of a Novel Solvent for the Simultaneous Separation of Strontium and Cesium from Dissolved Spent Nuclear Fuel Solutions. Idaho National Engineering and Environmental Laboratory. America's Nuclear Energy Symposium 2004.

Riddle, C.L., Baker, C.L., Law, J.D, McGrath, C.A., Meikrantz, D.H., Mincher, B.J., Peterman, D.R. and T.A. Todd (2005). Fission Product Extraction (FPEX): Development of a novel solvent for the simultaneous separation of strontium and cesium from acidic solutions. Solvent Extraction and Ion Exchange 23 (3), 449-461

Rodriguez, M., Suarez, J.A. and A.G. Espartero (1996). Separation of radioactive strontium by extraction using chromatographic resin. Nuclear Instruments and Methods in Physics Research Section A: Accelerators, Spectrometers, Detectors and Associated Equipment 369 (2-3), 348-352

Russell, B.C., Croudace, I.W. Warwick, P.E. and J.A. Milton (2014(A)). Determination of precise $^{135}Cs/^{137}Cs$ in environmental samples using sector field inductively coupled plasma mass spectrometry. Analytical Chemistry 86 (17), 8719-8726

Russell, B. C., Warwick, P.E. and I.W. Croudace (2014(B)). Calixarene-based extraction chromatographic separation of ^{135}Cs and ^{137}Cs in environmental and waste samples prior to sector field ICP-MS analysis. Analytical Chemistry 86 (23), 11890-11896

Sachleben, R.A., Bonnesen, P.V., Descazeaud, T.J., Urvoas, A. and B.A. Moyer (1999). Surveying the extraction of cesium nitrate by 1,3-alternate calix[4]arene crown-6

ethers in 1,2-dichloroethane. Solvent Extraction and Ion Exchange 17 (6), 1445-1459

Sakama, M., Nagano, Y., Saze, T., Higaki, S., Kitade, T., Izawa, N., Shikino, O. and S. Nakayama (2013). Application of ICP-DRC-MS to screening test of strontium and plutonium in environmental samples at Fukushima. Applied radiation and isotopes 81, 201-207

Šebesta, F. and V. Štefula (1990). Composite ion exchanger with ammonium molybdophosphate and its properties. Journal of Radioanalytical and Nuclear Chemistry 140 (1) 15-21

Scottish Environment Protection Agency (SEPA), Radioactivity in Food and the Environment (RIFE) reports. http://www.sepa.org.uk/radioactive_substances/publications/rife_reports.aspx

Shiho, A., Hanzawa, Y., Okumura, K., Shinohara, N., Inagawa, J., Hotoku, S., Suzuki, K. and S.Kaneko (2011). Determination of ^{79}Se and ^{135}Cs in Spent Nuclear Fuel for Inventory Estimation of High-Level Radioactive Wastes. Journal of Nuclear Science and Technology (2011). 48 (5), 851-854

Smit, J.R. and W. Robb (1964). Ion exchange on ammonium molybdophosphate-II: Bivalent and trivalent ions. Journal of Inorganic and Nuclear Chemistry 26 (4), 509-518

Smith, J.N., Ellis, K.M. and E.P. Jones (1990). Cesium 137 transport into the Arctic Ocean through Fram Strait. Journal of Geophysical Research 95 (C2), 1693-1701

Song, M., Probst, T.U. and N.G. Berryman (2001). Rapid and sensitive determination of radiocesium (Cs-135, Cs-137) in the presence of excess barium by electrothermal vaporization-inductively coupled plasma-mass spectrometry (ETV-ICP-MS) with potassium thiocyanate as modifier. Fresenius' Journal of Analytical Chemistry 370 (6), 744-751

Snyder, D.C., Delmore, J.E., Tranter, T., Mann, N.R., Abbott, M.L. and J.E. Olson (2012). Radioactive cesium isotope ratios as a tool for determining dispersal and

re-dispersal mechanisms downwind from the Nevada Nuclear Security Site. Journal of Environmental Radioactivity 110, 46-52

Spry, N., Parry, S. and S. Jerome (2000). The development of a sequential method for the determination of actinides and ^{90}Sr in power station effluent using extraction chromatography. Applied Radiation and Isotopes 53 (1-2), 163-171

Stamm, H. (1973). Determination of ^{135}Cs in sodium from an in-pile loop by activation analysis. Journal of Radioanalytical and Nuclear Chemistry 14 (2), 367-373

Stohl, A., Seibert, P., Wotawa, G., Arnold, D., Burkhart, J.F., Eckhardt, S., Tapia, C., Vargas, A. and T.J. Yasunari (2012). Xenon-133 and caesium-137 releases into the atmosphere from the Fukushima Dai-ichi nuclear power plant: determination of the source term, atmospheric dispersion, and deposition. Atmospheric Chemistry and Physics 12 (5), 2313-2343

Suomela, J., Wallber, L. and J. Melin (1993). Method for determination of ^{90}Sr in food and environmental samples by Cerenkov counting. Swedish Radiation Protection Institute, SSI-Rapport 93 (1), 19

Sunderman, D. N. and C. W. Townley (1960). The radiochemistry of barium, calcium and strontium. National Academy of Science Report number NAS-NS 3010, 1960

Takagai, Y., Furukawa, M., Kameo, Y. and K. Suzuki (2014). Sequential inductively coupled plasma quadrupole mass-spectrometric quantification of radioactive strontium-90 incorporating cascade separation steps for radioactive contamination rapid survey. Analytical Methods 6 (2), 355-362

Tanimizu, M., Sugiyama, N., Ponzevera, E. and G. Bayon (2014). Determination of ultra-low ^{236}U/^{238}U isotope ratios by tandem quadrupole ICP-MS/MS. Journal of Analytical and Atomic Spectrometry 28, 1372-1376

Tanner, S. D. (1995). Characterization of ionization and matrix suppression in inductively coupled cold plasma mass spectrometry. Journal of Analytical and Atomic Spectrometry 10 (11), 905-921

Taylor, V., Evans, R.D. and R.J. Cornett (2007). Determination of ^{90}Sr in contaminated environmental samples by tuneable bandpass dynamic reaction cell ICP-MS. Analytical and Bioanalytical Chemistry 387 (1), 343-350

Taylor, V., Evans, R. and R. Cornett (2008). Preliminary evaluation of $^{135}Cs/^{137}Cs$ as a forensic tool for identifying source of radioactive contamination. Journal of Environmental Radioactivity 99 (1), 109-118

Taylor, N. and P. B. Farnsworth (2012). Experimental characterization of the effect of skimmer cone design on shock formation and ion transmission efficiency in the vacuum interface of an inductively coupled plasma mass spectrometer. Spectrochimica Acta Part B: Atomic Spectroscopy 69, 2-8

Thermo Scientific (2008). Element 2 & Element XR High performance high resolution ICP-MS. www.thermo.com/eThermo/CMA/PDFs/Product/productPDF_23502.pdf

Thermo Scientific (2010). Jet Interface Element 2/Element XR ICP Mass Spectrometers. http://www.thermoscientific.de/eThermo/CMA/PDFs/Product/productPDF_56336.pdf

Thermo Scientific (2011). Neptune Plus Multicollector ICPMS. http://www.thermoscientific.fr/eThermo/CMA/PDFs/Product/productPDF_59110.PDF

Thirlwall, M. (2001). Inappropriate tail corrections can cause large inaccuracy in isotope ratio determination by MC-ICP-MS. Journal of Analytical and Atomic Spectrometry 16 (10), 1121-1125

Thomson, J., Dyer, F.M. and I.W. Croudace (2002). Records of radionuclide deposition in two salt marshes in the United Kingdom with contrasting redox and accumulation conditions. Geochemica et Cosmochimica Acta 66 (6), 1011-1023

Thuery, P., Nierlich, M., Lamare, V., Dozol, J.F., Asfari, Z. and J.Vicens (2000). Bis (crown ether) and azobenzocrown derivatives of calix [4] arene. A review of structural information from crystallographic and modelling studies. Journal of Inclusion Phenomena and Macrocyclic Chemistry 36 (4), 375-408

Todd, T.A., Mann, N.R., Tranter, T.J., Sebesta, F., John, J. and A. Motl (2002). Cesium sorption from concentrated acidic tank wastes using ammonium molybdophosphate-polyacrylonitrile composite sorbents. Journal of Radioanalytical and Nuclear Chemistry 254 (1), 47-52

Todd, T.A., Batcheller, T.A., Law, J.D. and R.S. Herbst (2004). Cesium and Strontium Separation Technologies Literature Review. Idaho National Engineering and Environmental Laboratory

Tovedal, A., Nygren, U. and H. Ramebäck (2008). Determination of ^{90}Sr in preparedness: Optimization of total analysis time for multiple samples. Journal of Radioanalytical and Nuclear Chemistry 276 (2), 357-362

Tranter, T., Herbst R.S., Todd, T.A., Olson A.L. and H.B. Eldbredge (2002). Evaluation of ammonium molybdophosphate-polyacrylonitrile (AMP-PAN) as a cesium selective sorbent for the removal of ^{137}Cs from acidic nuclear waste solutions. Advances in Environmental Research 6, 107-121

Triskem International (2012). Sr Resin Product Sheet. www.triskeminternational.com/iso_album/ft_resine_sr_en_121219.pdf Accessed 10/4/12

Tumey, S. J., Brown, T.A., Hamilton, T.E. and D.J. Hillegonds (2008). Accelerator mass spectrometry of strontium-90 for homeland security, environmental monitoring and human health. Nuclear Instruments and Methods in Physics Research Section B: Beam Interactions with Materials and Atoms 266 (10), 2242-2245

United Nations Scientific Committee on the Effects of Atomic Radiation (UNSCEAR) (2000). Annex J: Exposures and effects of the Chernobyl accident, 453-566.

Vajda, N. and C. Kim, 2010. Determination of radiostrontium isotopes: A review of analytical methodology. Applied Radiation and Isotopes 68 (12), 2306-2326

Vonderheide, A. P., Zoriy, M.V., Izmer, A.V., Pickhardt, C., Caruso, J.A., Ostapczuk, P., Hille, R. and J.S. Becker (2004). Determination of ^{90}Sr at ultratrace levels in urine by ICP-MS. Journal of Analytical Atomic Spectrometry 19 (5), 675-680

Warneke, T., High-precision isotope ratio measurements of uranium and plutonium in the environment (2002). University of Southampton PhD thesis, Faculty of Science, School of Ocean and Earth Science, Southampton Oceanography Centre, 60-78

Warneke, T., Croudace, I.W., Warwick, P.E. and R.N. Taylor (2002). A new ground-level fallout record of uranium and plutonium isotopes for northern temperate latitudes. Earth and Planetary Science Letters 203 (3-4), 1047-1057

Warwick, P.E. (1999). The determination of pure beta emitters and their behaviour in a salt-marsh environment, 2002. University of Southampton PhD thesis, Faculty of Science, School of Ocean and Earth Science, Southampton Oceanography Centre

Warwick, P. and I. Croudace (2006). Isolation and quantification of ^{55}Fe and ^{63}Ni in reactor effluents using extraction chromatography and liquid scintillation analysis. Analytica Chimica acta 567 (2), 277-285

Watari, K., Kiyoko, I. and M. Izawa (1967). Isolation of ^{137}Cs with Copper Ferrocyanide-Anion Exchange Resin. Journal of Nuclear Science and Technology 4 (4), 190-194

Wendt, K., Bhowmick, G.K., Bushaw, B.A., Hermann, G., Kratz, J.V., Lantzsch, J., Müller, P., Nörtershäuser, W., Otten, E-W., Schwalbach, R., Seibert, U-A., Trautmann, N. and A. Waldek (1997). Rapid trace analysis of $^{89,90}Sr$ in environmental samples by collinear laser resonance ionization mass spectrometry. Radiochimica Acta 79 (3), 183-190

Wigley, F. (2000). Mechanisms for accumulation and migration of technitium-99 in saltmarsh sediments. University of Southampton PhD thesis, Faculty of Science, School of Ocean and Earth Science, Southampton Oceanography Centre

Wollenweber, D., Straßburg, S. and G. Wünsch (1999). Determination of Li, Na, Mg, K, Ca and Fe with ICP-MS using cold plasma conditions. Fresenius' journal of Analytical Chemistry 364 (5), 433-437

Xiao, C., Zhang, A. and Z. Chai (2014). Synthesis and Characterization of Novel Macroporous Silica-Polymer-Calixcrown Hybrid Supramolecular Recognition

Materials for Effective Separation of Cesium. Journal of Hazardous Materials 267 (28), 109-118

Zhang, A., Xiao, C., Xue, W. and Z. Chai (2009). Chromatographic separation of cesium by a macroporous silica-based supramolecular recognition agent impregnated material. Separation and Purification Technology 66 (3), 541-548

Zhang, A. and Q. Hu (2010). Adsorption of cesium and some typical coexistent elements onto a modified macroporous silica-based supramolecular recognition material. Chemical Engineering Journal 159 (1), 58-66

Zheng, J. and M. Yamada, 2006. Inductively coupled plasma-sector field mass spectrometry with a high-efficiency sample introduction system for the determination of Pu isotopes in settling particles at femtogram levels. Talanta 69 (5), 1246-1253

Zhou, H., Connery, K.E., Bartsh, R.A., Moyer, B.A., Haverlock, T.J. and L.H. Delmau (2013). Lipophilic, Mono-ionizable, Calix [4] arene-bis (benzocrown-6) Compounds for Solvent Extraction of Cesium from Nuclear Wastes: Synthesis and Evaluation. Solvent Extraction and Ion Exchange 31 (7), 683-696

Zimmer, K., Stenner, J., Kluge, H-J., Lantzsch, J., Monz, L., Otten, E.W., Passler, G., Schwalbach, R., Schwarz, M. and H. Stevens (1994). Determination of ^{90}Sr in environmental samples with resonance ionization spectroscopy in collinear geometry. Applied Physics B 59 (2), 117-121

Zoriy, M.V., Ostapczuk, P., Halicz, L., Hille, R. and J.S. Becker (2005). Determination of ^{90}Sr and Pu isotopes in contaminated groundwater samples by inductively coupled plasma mass spectrometry. International Journal of Mass Spectrometry 242 (2-3), 203-209

Zheng, J., Tagami, K., Bu, W., Uchida, S., Watanabe, Y., Kubota, Y., Fuma, S. and S. Ihara (2014). ^{135}Cs/^{137}Cs Isotopic Ratio as a New Tracer of Radiocesium Released from the Fukushima Nuclear Accident. Environmental Science and Technology. Just accepted